

THE PREPARATION AND USE OF METAL SALEN COMPLEXES DERIVED FROM  
CYCLOBUTANE DIAMINE

by

SMITA S. PATIL

B. Tech., University of Mumbai, 2005

M. Tech., University of Mumbai, 2007

AN ABSTRACT OF A DISSERTATION

Submitted in partial fulfillment of the requirements for the degree

DOCTOR OF PHILOSOPHY

Department of Chemistry  
College of Arts and Sciences

KANSAS STATE UNIVERSITY

Manhattan, Kansas

2014

## Abstract

The helix is an important chiral motif in nature, there is increasing development in field of helical transition metal complexes and related supramolecular structures. Hence, the goals of this work are to apply the principles of helicity in order to produce metal complexes with predictable molecular shapes and to study their properties as asymmetric catalysts.

Computational studies suggest that the (1*R*,2*R*)-cyclobutyldiamine unit can produce highly twisted salen complexes with a large energy barrier between the *M* and *P* helical forms. To test this prediction, the tartrate salt of (1*R*,2*R*)-cyclobutyldiamine was synthesized and condensed with a series of salicylaldehydes to produce novel salen ligands. The salicylaldehydes chosen have extended phenanthryl or benz[*a*]anthryl sidearms to encourage formation of helical coordination complexes. These ligands were metallated with zinc, iron and manganese salts to produce salen metal complexes which were characterized by NMR analysis, high-resolution mass spectrometry, and IR spectroscopy.

A second ligand type, neutral bis(pyridine-imine) has also been synthesized from (1*R*,2*R*)-cyclobutyldiamine and quinolylaldehydes. The synthesis of bis(pyridine-imine) ligands was conducted using greener method, solvent assisted grinding. These ligands, in-situ with nickel metal salts, showed good catalytic activity for asymmetric Diels-Alder reactions.

The third ligand type studied was chiral acid-functionalized Schiff-base ligands. These were synthesized by the condensation of 3-formyl-5-methyl salicylic acid and (1*R*,2*R*)-cyclobutyldiamine. With this type of ligand, there is possibility of producing both mono and dinuclear metal complexes. In our studies, we were only able to synthesize mononuclear complexes. These were tested as catalysts for asymmetric direct Mannich-type reaction, but were found to be ineffective.

THE PREPARATION AND USE OF METAL SALEN COMPLEXES DERIVED FROM  
CYCLOBUTANE DIAMINE

by  
SMITA PATIL

B. Tech., University of Mumbai, 2005

M. Tech., University of Mumbai, 2007

A DISSERTATION

submitted in partial fulfillment of the requirements for the degree

DOCTOR OF PHILOSOPHY

Department of Chemistry

College of Arts and Sciences

KANSAS STATE UNIVERSITY

Manhattan, Kansas

2014

Approved by:

Major Professor

Dr. Christopher J. Levy

# **Copyright**

SMITA PATIL

2014

## Abstract

The helix is an important chiral motif in nature, there is increasing development in field of helical transition metal complexes and related supramolecular structures. Hence, the goals of this work are to apply the principles of helicity in order to produce metal complexes with predictable molecular shapes and to study their properties as asymmetric catalysts.

Computational studies suggest that the (1*R*,2*R*)-cyclobutyldiamine unit can produce highly twisted salen complexes with a large energy barrier between the *M* and *P* helical forms. To test this prediction, the tartrate salt of (1*R*,2*R*)-cyclobutyldiamine was synthesized and condensed with a series of salicylaldehydes to produce novel salen ligands. The salicylaldehydes chosen have extended phenanthryl or benz[*a*]anthryl sidearms to encourage formation of helical coordination complexes. These ligands were metallated with zinc, iron and manganese salts to produce salen metal complexes which were characterized by NMR analysis, high-resolution mass spectrometry, and IR spectroscopy.

A second ligand type, neutral bis(pyridine-imine) has also been synthesized from (1*R*,2*R*)-cyclobutyldiamine and quinolylaldehydes. The synthesis of bis(pyridine-imine) ligands was conducted using greener method, solvent assisted grinding. These ligands, in-situ with nickel metal salts, showed good catalytic activity for asymmetric Diels-Alder reactions.

The third ligand type studied was chiral acid-functionalized Schiff-base ligands. These were synthesized by the condensation of 3-formyl-5-methyl salicylic acid and (1*R*,2*R*)-cyclobutyldiamine. With this type of ligand, there is possibility of producing both mono and dinuclear metal complexes. In our studies, we were only able to synthesize mononuclear complexes. These were tested as catalysts for asymmetric direct Mannich-type reaction, but were found to be ineffective.

## Table of Contents.

List of Figures .....	ix
List of Tables .....	xii
Acknowledgements .....	xiii
Dedication .....	xiv
Chapter 1 - Introduction .....	1
1.1 Schiff base ligands .....	1
1.2 Preparation of Schiff-bases .....	1
1.3 Salen ligands .....	3
1.3.1 Background of salen metal complexes.....	4
1.3.2 Conformational effects in Salen Catalyst .....	6
1.4 Helical Complexes .....	10
1.4.1 Monohelices and Helicates .....	10
1.4.2 Types of Single-Stranded Monohelices .....	12
1.5 Design of new ligand system .....	14
Chapter 2 - Selection and synthesis of (+)- <i>trans</i> -Cyclobutane-1,2-diamine backbone .....	17
2.1 Introduction.....	17
2.1.1 Design of New Chiral Ligands: Chiral Backbones.....	17
2.1.2 Design of New Chiral Ligands: Sidearm .....	18
2.1.3 Design of New Chiral Ligands: Metal .....	18
2.1.4 Previous studies .....	19
2.2 Cyclobutyl backbone .....	19
2.2.1 Selection criteria .....	19
2.2.2 Synthesis .....	20
2.2 Experimental .....	21
2.2.1 Synthesis .....	21
2.2.2 Calculations.....	27
2.3 Results & Discussion .....	30
2.4 Conclusion .....	31
Chapter 3 - Synthesis and characterization of novel ligands with (1 <i>R</i> ,2 <i>R</i> )-cyclobutyl backbone	33

3.1 Introduction.....	33
3.2 Experimental.....	34
3.2.1 Synthesis .....	34
3.2.2 Synthesis of ligands .....	37
3.2.2.1 2,2'-[(1 <i>R</i> ,2 <i>R</i> )-1,2-Cyclobutanediylbis(nitrilomethylidyne)]bisbenz [a] anthracen-1-ol, (( <i>R</i> , <i>R</i> )-20).....	37
3.2.2.2 3,3'-[(1 <i>R</i> ,2 <i>R</i> )-1,2-Cyclobutanediylbis(nitrilomethylidyne)]bis-4- phenanthrenol, (( <i>R</i> , <i>R</i> )-21) .....	38
3.2.2.3 (1 <i>R</i> ,2 <i>R</i> )- <i>N,N'</i> -Bis[(2-benzoquinolyl)methylene]-1,2-cyclobutanediamine, (( <i>R</i> , <i>R</i> )-22) .....	39
3.2.2.4 (1 <i>R</i> ,2 <i>R</i> )- <i>N,N'</i> -Bis[(2-quinoliny)methylene]-1,2-cyclobutanediamine), (( <i>R</i> , <i>R</i> )-23) .....	40
3.2.2.5 3,3'-[(1 <i>R</i> ,2 <i>R</i> )-1,2-cyclobutanediylbis(nitrilomethylidyne)]bis[2- hydroxybenzoic acid], (( <i>R</i> , <i>R</i> )-24a) .....	40
3.2.2.6 3,3'-[(1 <i>R</i> ,2 <i>R</i> )-1,2-cyclobutanediylbis(nitrilomethylidyne)]bis[2- hydroxybenzoic acid], (( <i>R</i> , <i>R</i> )-24b) .....	41
3.3 Results & Discussion .....	42
3.3.1 NMR spectroscopy.....	45
3.3.1.1 NMR spectroscopy of ligands ( <i>R</i> , <i>R</i> )-20 and ( <i>R</i> , <i>R</i> )-21 .....	45
3.3.1.2 NMR spectroscopy of ligands ( <i>R</i> , <i>R</i> )-22 and ( <i>R</i> , <i>R</i> )-23 .....	48
3.3.1.3 NMR spectroscopy of acid functionalized ligand, ( <i>R</i> , <i>R</i> )-24.....	51
3.3.2 Electronic and infrared spectra .....	54
3.3.3 Mass spectral analysis.....	55
3.4 Conclusion .....	62
Chapter 4 - Synthesis and characterization of complexes with cyclobutyl backbone .....	63
4.1 Introduction.....	63
4.2 Synthesis .....	63
4.2 Experimental.....	66
4.2.1 Synthesis .....	66
4.2.1.1 Zn(II)-( <i>R</i> , <i>R</i> )-20-complex, (( <i>R</i> , <i>R</i> )-25).....	67
4.2.1.2 Mn(IV)-( <i>R</i> , <i>R</i> )-20-complex, (( <i>R</i> , <i>R</i> )-26) .....	67

4.2.1.3 Zn(II)-( <i>R,R</i> )-21-complex, (( <i>R,R</i> )-27).....	68
4.2.1.4 Fe(III)-( <i>R,R</i> )-21-complex, (( <i>R,R</i> )-28).....	69
4.2.1.5 Ni(II)-( <i>R,R</i> )-24-complex, (( <i>R,R</i> )-29).....	69
4.3 Results and discussion .....	70
4.3.1 NMR spectroscopy.....	70
4.3.2 Electronic and infrared spectra .....	72
4.3.3 Mass spectra analysis.....	76
4.4 Conclusion .....	79
Chapter 5 - Catalytic study of complexes with cyclobutyl backbone.....	81
5.1 Introduction.....	81
5.1.2 Catalysis.....	82
5.1.2.1 Diels-Alder reaction.....	82
5.1.2.1 Mannich-type reaction .....	82
5.2 Experimental.....	83
5.2.1 Synthesis .....	83
5.2.1.1 <i>t</i> -butyl 2-bromo-propanoate, 31 .....	83
5.2.1.2 <i>t</i> -butyl 2-nitro-propanoate, 32.....	84
5.2.1.3 $\alpha$ -sulfonyl amine, 34 .....	84
5.2.1.4 <i>N</i> -Boc imine, 35 .....	85
5.2.1.5 3-acryl-2-oxazolidinone, 38.....	86
5.2.1.6 3-(Bicyclo[2.2.1]hept-5-en-2-ylcarbonyl)-2-oxazolidinone, 39.....	86
5.3 Results & Discussion.....	87
5.3.1 Diels–Alder reactions with bis-imine catalyst.....	87
5.3.2 Mannich-type reactions with acid fictionalized catalyst.....	90
5.4 Conclusion .....	91
Chapter 6 - Overall conclusion and future work.....	92
Appendix A – $^1\text{H}$ and $^{13}\text{C}$ NMR .....	93

## List of Figures

Figure 1.1 Synthesis of Schiff-base ligand by the condensation of diamine and aldehyde.....	1
Figure 1.2 Preparation of salicylaldehydes and their condensation to form Schiff-bases and salens.3.....	2
Figure 1.3 Different Salen ligands and M(II) Salencomplexes.3 .....	3
Figure 1.4 Chiral Mn-salen complex and metalloporphyrins.....	4
Figure 1.5 Jacobsen and Katsuki's catalysts for epoxidation.....	5
Figure 1.6 Different approaches of Substrate to Jacobsen's catalyst. <sup>20</sup> .....	6
Figure 1.7 Diaxial and diequatorial conformers in a salen catalyst.....	7
Figure 1.8 Approach of the substrates to the manganese complex by different pathways. <sup>25</sup> .....	8
Figure 1.9 Stereoselectivities based on steric role of cis- and trans-alkenes.....	9
Figure 1.10 General design of monohelical metal complex with a chiral backbone.....	9
Figure 1.11 <i>M</i> and <i>P</i> configurations of heptahelicene. <sup>29</sup> .....	10
Figure 1.12 Examples of monohelices with single, double, and triple-strands.....	11
Figure 1.13 Double and triple stranded helicates.....	12
Figure 1.14 Morphologies for single-stranded monohelices of octahedral .....	13
Figure 1.15 Salen ligands with phenanthryl and benz[a]anthryl siderams.....	14
Figure 2.1 General design of salen metal complex.....	17
Figure 2.2 Extended planar polyaromatic ring systems for producing monohelical complexes.	18
Figure 2.3 Illustration of the N-C-C-N dihedral angle.2 .....	20
Figure 2.4 Synthesis of <i>trans</i> -cyclobutane-1,2-diamine backbone.....	21
Figure 2.5 Results of Semi-empirical AM1 calculation for <i>P</i> -type of Zn complexes with 4-ring sidearm.....	28
Figure 2.6 Results of Semi-empirical AM1 for <i>M</i> -type of Zn complexes with 4-ring sidearm.	28
Figure 2.7 Results of Semi-empirical AM1 calculation for <i>P</i> -type of Zn complexes with 3-ring sidearm.....	29
Figure 2.8 Results of Semi-empirical AM1 calculation for <i>M</i> -type of Zn complexes with 3-ring sidearm.....	29
Figure 2.9 Energy difference between <i>P</i> and <i>M</i> conformer with respective backbone.....	30
Figure 3.1 General scheme of tetradentate Schiff-base ligand formation from 1,2-diamines.....	33

Figure 3.2	Some previously synthesized ligand with cyclobutyl backbone. ....	34
Figure 3.3	The precursors for ligand synthesis. ....	42
Figure 3.4	Synthetic scheme for ligands ( <i>R,R</i> )-20 and ( <i>R,R</i> )-21. ....	43
Figure 3.5	Synthetic scheme for ligands ( <i>R,R</i> )-22 and ( <i>R,R</i> )-23 by solvent-assisted grinding. ...	44
Figure 3.6	Synthetic scheme for ligands ( <i>R,R</i> )-24 and ( <i>R,R</i> )-25. ....	45
Figure 3.7	The <sup>1</sup> H NMR spectrum of ( <i>R,R</i> )-20 with specific assignments.....	46
Figure 3.8	The <sup>1</sup> H NMR spectrum of ( <i>R,R</i> )-21 with specific assignments.....	47
Figure 3.9	The <sup>1</sup> H- <sup>1</sup> H COSY NMR spectrum of ligand ( <i>R,R</i> )-20. ....	48
Figure 3.10	The <sup>1</sup> H NMR spectrum of ( <i>R,R</i> )-22 with specific assignments.....	49
Figure 3.11	The <sup>1</sup> H NMR spectrum of ( <i>R,R</i> )-23 with specific assignments.....	50
Figure 3.12	The <sup>1</sup> H- <sup>1</sup> H COSY NMR spectrum of ligand ( <i>R,R</i> )-22. ....	51
Figure 3.13	The <sup>1</sup> H NMR spectrum of ( <i>R,R</i> )-24 with specific assignments.....	52
Figure 3.14	The hydrogen bonding between the phenolic hydrogens, the imine nitrogens and the carboxylate oxygens.....	53
Figure 3.15	The <sup>1</sup> H- <sup>1</sup> H COSY NMR spectrum of ligand ( <i>R,R</i> )-24. ....	54
Figure 3.16	The simulated isotopic pattern (top) and observed mass spectrum of ligand ( <i>R,R</i> )-20 (bottom).....	56
Figure 3.17	The simulated isotopic pattern (top) and observed mass spectrum of ligand ( <i>R,R</i> )-21 (bottom).....	57
Figure 3.18	The simulated isotopic pattern (top) and observed mass spectrum of ligand ( <i>R,R</i> )-22 (bottom).....	58
Figure 3.19	The simulated isotopic pattern (top) and observed mass spectrum of ligand ( <i>R,R</i> )-23 (bottom).....	59
Figure 3.20	The simulated isotopic pattern (top) and observed mass spectrum of ligand ( <i>R,R</i> )-24 (bottom).....	60
Figure 3.21	The simulated isotopic pattern (top) and observed mass spectrum of ligand ( <i>R,R</i> )-20 (bottom).....	61
Figure 4.1	Synthetic scheme for metallosalen complex. <sup>5</sup> ....	63
Figure 4.2	Synthetic scheme for complex ( <i>R,R</i> )-25 and ( <i>R,R</i> )-26. ....	64
Figure 4.3	Synthetic scheme for complex ( <i>R,R</i> )-27 and ( <i>R,R</i> )-28. ....	65
Figure 4.4	Synthetic scheme for nickel complex ( <i>R,R</i> )-29. ....	66

Figure 4.5 The $^1\text{H}$ NMR spectrum of complex ( <i>R,R</i> )-25 with specific assignments.....	71
Figure 4.6 The $^1\text{H}$ NMR spectrum of complex ( <i>R,R</i> )-27 with specific assignments.....	72
Figure 4.7 The IR spectra of ligand ( <i>R,R</i> )-20. ....	73
Figure 4.8 The IR spectra of Zn complex ( <i>R,R</i> )-25. ....	73
Figure 4.9 The IR spectra of ligand ( <i>R,R</i> )-21. ....	74
Figure 4.10 The IR spectra of Zn complex ( <i>R,R</i> )-27. ....	74
Figure 4.11 The IR spectra of ligand ( <i>R,R</i> )-24a.....	75
Figure 4.12 The IR spectra of Ni complex ( <i>R,R</i> )-27.....	75
Figure 4.13 Observed mass spectrum (top) for Zn salen complex ( <i>R,R</i> )-25 with simulated isotopic pattern (bottom).....	76
Figure 4.14 Observed mass spectrum (top) for Zn salen complex ( <i>R,R</i> )-27 with simulated isotopic pattern (bottom).....	77
Figure 4.15 Observed mass spectrum for Ni salen complex ( <i>R,R</i> )-29 by negative ESI. ....	78
Figure 4.16 Observed mass spectrum for Ni salen complex ( <i>R,R</i> )-29 indicating absence of dinuclear complex. ....	79
Figure 5.1 Enantiomers of chiral drug Thalidomide. <sup>3</sup> ....	81
Figure 5.2 Diels–Alder reactions of cyclopentadiene with 3-alkenoyl-2-oxazolidinones.....	82
Figure 5.3 Mannich-type reactions of <i>N</i> -Boc imines and $\alpha$ -substituted nitroacetates. ....	83
Figure 5.4 $^1\text{H}$ -NMR spectra of 3-alkenoyl-2-oxazolidinones (top) and H-NMR spectra of Diels–Alder reactions of cyclopentadiene with 3-alkenoyl-2-oxazolidinones without catalyst. (* shows peak indicating conversion) .....	88
Figure 5.5 Ligand used in catalyst preparation (top) and $^1\text{H}$ -NMR spectra of Diels–Alder reactions of cyclopentadiene with 3-alkenoyl-2-oxazolidinones with catalyst. (* shows peak indicating conversion).....	89
Figure 5.6 $^1\text{H}$ -NMR spectra of Mannich-type reactions of <i>N</i> -Boc imines and $\alpha$ -substituted nitroacetates. ....	90

## List of Tables

<b>Table 3.1</b> Characteristic UV-vis absorption bands for ligands. ....	55
<b>Table 3.2</b> Characteristic IR absorption bands for ligands. ....	55
<b>Table 4.1</b> Ligand and Zn(II) complex <sup>1</sup> H NMR chemical shifts.....	70

## Acknowledgements

Foremost, I would like to thank my advisor Dr. Christopher J. Levy for his advice, support, encouragement and his patience, whilst a member of his research group. I've taken great leaps as a chemist under his supervision.

I would like to thank my committee members, Professors Eric Maatta, Daniel Higgins, Bret Flanders, and Anna Zolkiewska for fitting me into their busy schedules. Thank you for being on my committee and so accommodating with scheduling of the final defense.

Thanks to the various people from Department of Chemistry for their assistance, especially, Jim Hodgson, Tobe Eggers, Earline Dikeman, Yasmin Patel, Mary Dooley and Kim Ross. Thanks to Leila Maurmann for NMR and HPLC training. You were a great help and I have a much better understanding about NMR and HPLC instruments now, than I had before. Special thanks to Ron Jackson for being there to fix things from lab and NMR room.

Thanks to all of my friends at Kansas State who have made my time here so memorable. Very special thanks to Dhanushi for helping me in completing all required formality of graduate school in my absence.

I would also like to thank my family and friends for all the support throughout my life. Especially, my parents, for treasured memories and loving support throughout my education.

Most importantly, I'd like to thank my husband; none of this would be possible without him. His undying love, support and motivation over the past few years has allowed me to achieve my goals and further my career as a chemist.

Last, but certainly not least, I would like to thank my son for making me laugh! SO MUCH!! Your hysterical take on life is so refreshing.

## **Dedication**

*To my son, husband and parents for their love and support.*

# Chapter 1 - Introduction

## 1.1 Schiff base ligands

In 1864, Hugo Schiff described the condensation between an aldehyde and an amine leading to a Schiff base, Figure 1.1.<sup>1</sup> Schiff base ligands have the capacity to coordinate metals through their imine nitrogen and are often key components of chelating ligands. Schiff base ligands are considered “privileged ligands” due to easy synthesis by the condensation between aldehydes and amines and the fact that stereogenic centres, planes or axes can be readily introduced in the synthetic design.<sup>2</sup> Many thousands of chiral ligands have been prepared in recent decades but only a handful, the so-called privileged ligands; have found wide applicability and effectiveness in asymmetric catalysis. Most privileged ligands have  $C_2$  symmetry, which limits the number of possible reaction pathways and often leads to enhanced selectivity. Schiff-base ligands can coordinate to many different metals, and stabilize a variety of oxidation states, allowing the use of Schiff-base metal complexes for a large number of useful catalytic transformations. Chiral Schiff-base complexes have proven to be effective asymmetric catalysts for producing nonracemic products, yet the scaffold is so versatile that there remain many avenues of exploration available to exploit.<sup>3</sup>

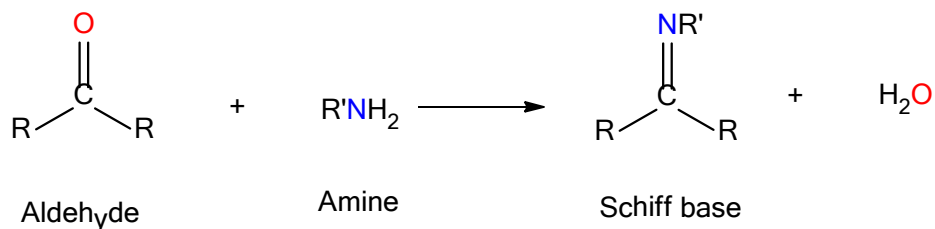


**Figure 1.1** Synthesis of Schiff-base ligand by the condensation of diamine and aldehyde.

## 1.2 Preparation of Schiff-bases

The condensation between aldehydes and amines can be carried out under a variety of reaction conditions, and in many different solvents. The presence of dehydrating agents usually favors the formation of Schiff-bases. The water produced when reactions are run in low polarity solvents such as toluene can be removed by using a Dean Stark apparatus or by placing agents such as 3Å or 4Å molecular sieves in the reaction mixture. Ethanol is an effective solvent for the preparation of Schiff bases either at room temperature or under reflux conditions. Decomposition

of the Schiff-bases can occur during purification. For example, chromatography of Schiff bases on silica gel can cause some degree of decomposition through hydrolysis due to the acidic nature of silica. In such cases purification by recrystallization is preferred. The Schiff bases are usually insoluble in hexane or cyclohexane, therefore they can be purified by stirring the crude reaction mixture in these solvents, sometimes adding a small portion of a more polar solvent such as (Et<sub>2</sub>O, CH<sub>2</sub>Cl<sub>2</sub>), in order to extract impurities. Usually, Schiff bases are stable compounds and can be stored without much precaution.<sup>3</sup>

Salicylaldehydes bearing different substituents are obtained by the introduction of a formyl group, using a simple and well established reaction, into the corresponding phenol derivative, Figure 1.2. The combinatorial approach to the discovery of new catalysts is an innovative and exciting area of research. Schiff bases are suitable ligands for the preparation of libraries due to the easy reaction conditions and the variety of chiral amines and aldehydes used as precursors.<sup>4</sup>

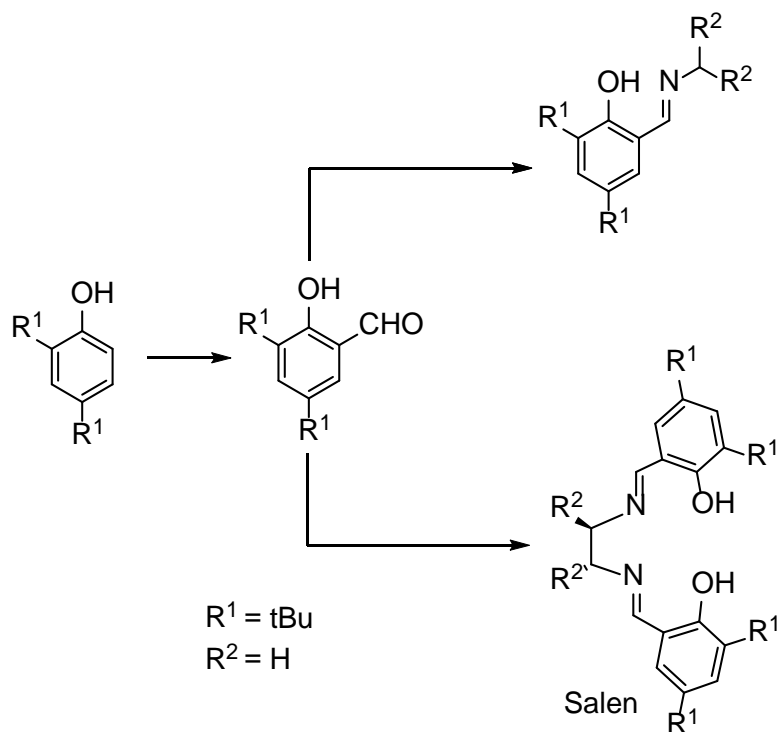


**Figure 1.2** Preparation of salicylaldehydes and their condensation to form Schiff-bases and salens.

### 1.3 Salen ligands

Condensation of salicylaldehydes or salicylaldehyde derivatives with 1,2-diamines leads to the formation of one extremely important class of ligands, known as “Salens”. The ligand has four coordinating sites and, when coordinated to an octahedral metal center, leaves two sites (often axial) open to ancillary ligands, substrates, or reactants. This parallels the coordination properties of porphyrins, but salen ligands have the distinct advantage of being synthetically more accessible. Although the term salen (a contraction of the salicylaldehyde and ethylenediamine) was used formerly only to describe the tetradentate Schiff-bases derived from ethylenediamine, the more general term Salen-type is used in the literature to describe the class of [O,N,N,O] tetradentate bis(Schiff-base) ligands, Figure 1.3. The condensation of the  $C_2$ -symmetric *trans*-1,2-diaminocyclohexane with 3,5-di-*tert*-butylsalicylaldehyde gives a chiral salen ligand that forms complexes with many metal ions. Among these, complexes with  $Cr^{3+}$ ,  $Mn^{3+}$ ,  $Co^{3+}$ , and  $Al^{3+}$  have proven particularly useful for asymmetric transformations.

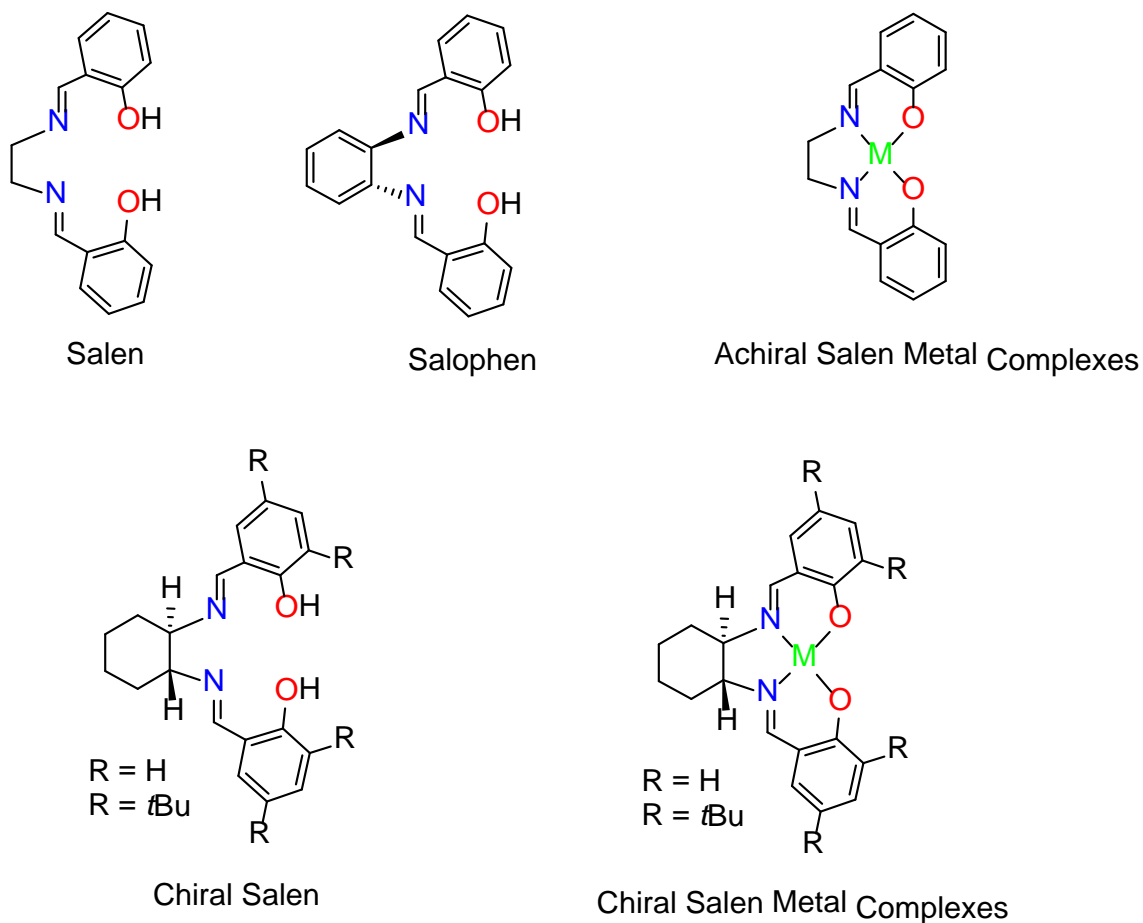


**Figure 1.3** Different Salen ligands and M(II) Salencomplexes.<sup>3</sup>

### 1.3.1 Background of salen metal complexes

Some of the most important synthetic ligand systems, especially in the context of asymmetric catalysis, are the tetradentate Schiff bases known as salen (*N,N*-bis(salicylaldehyde)ethylenediamine). In 1889, while studying the effect of diamines on diketones, Combes prepared the first salen ligand and its copper(II) complex.<sup>5</sup> Since then, salen derivatives and their metal complexes have been synthesized and characterized and gradually their value as catalysts has become recognized.<sup>6</sup> With the growth in interest in enantiomerically pure compounds for the pharmaceutical and agrochemical industries, it is perhaps not surprising that in the last few decades attention has focused on chiral salen ligands, and in particular on the use of their optically pure metal complexes as asymmetric catalysts. Applications have grown rapidly and a broad range of asymmetric catalysis have now been described including oxidations, additions and reductions.<sup>7</sup>

The first reports on the stoichiometric epoxidation of unfunctionalized olefins using achiral Cr(III)(salen) complex were published by Kochi *et al.* in 1985 and by Burrows *et al.* three years later.<sup>8,9,10</sup> In contrast to metalloporphyrins, salen complexes are non-planar, a property that could explain the stereoselection obtained using these systems.<sup>11,12,13</sup> Houk and his group observed a twisting of the two salen's aromatic rings. The dihedral angle arising between the aromatic rings ( $\phi$ ) is  $73^\circ$ . This twisting of aromatic ring might be the source of the chiral induction in these catalysts, Figure 1.4.<sup>14</sup>

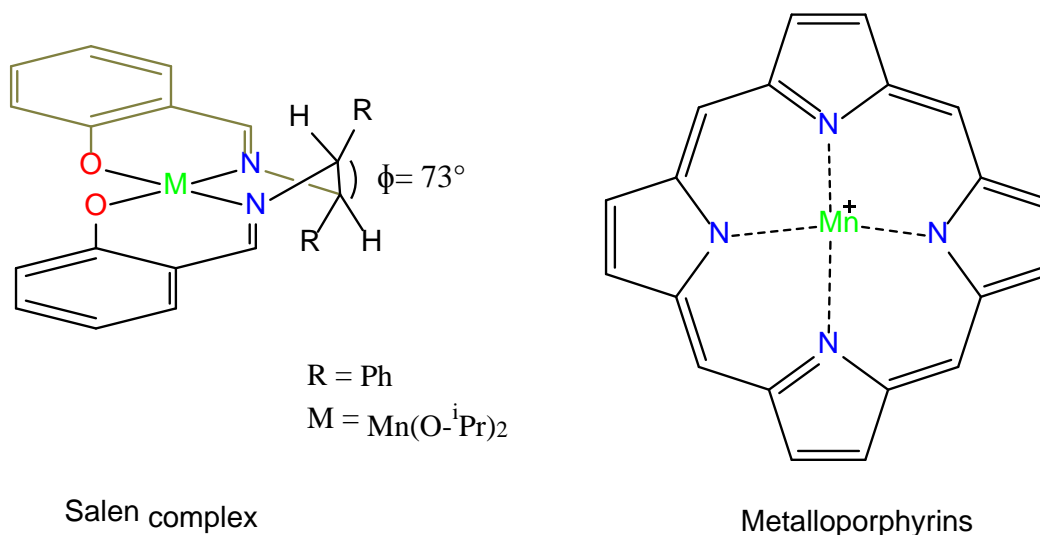


**Figure 1.4** Chiral Mn-salen complex and metalloporphyrins.

In further studies Kochi and coworkers found that Mn(salen)s can also catalyze alkene epoxidation.<sup>15</sup> In contrast to their Cr(salen) systems, Mn(salen)s were able to epoxidize unfunctionalized acyclic alkenes more efficiently. Enhanced reactivities and a greater substrate scope were also demonstrated. Due to the fleeting nature of the intermediate the active species was not directly observed, but was postulated to be an O=Mn(V)(salen)<sup>+</sup> complex. This work set the stage for the development of chiral salen catalysts independently by Jacobsen and Katsuki.<sup>16,17</sup> The main differences between their systems lie in the presence of four stereogenic centers in the Katsuki catalysts and in the replacements of the stereocenters at C3 and C3' with bulky *t*-butyl groups in the Jacobsen complexes.<sup>18,19</sup> Katsuki's catalysts exhibit similar enantioselectivities for *cis* olefins compared to Jacobsen's but afford greater enantioselectivities in the epoxidation of *trans*-alkenes (66% vs 25-33% ee for *trans*-stilbene oxide).

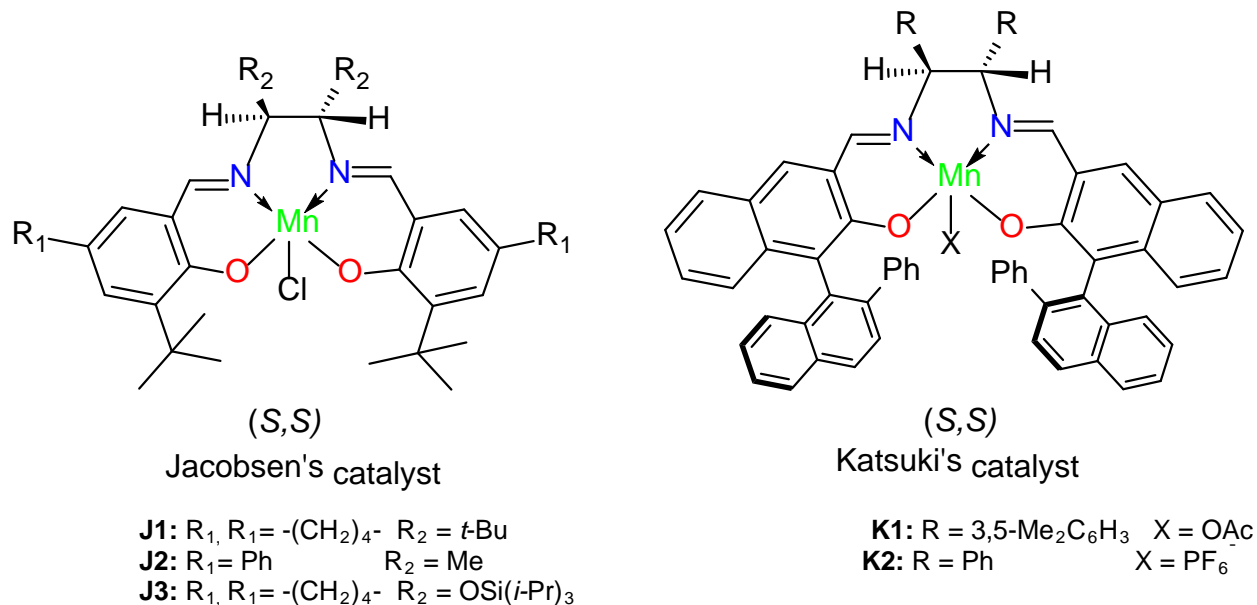


**Figure 1.5** Jacobsen and Katsuki's catalysts for epoxidation.

Following this initial work, reports detailing metallo-salens containing various substituent groups at the 3-5 and 8 positions were published. In one of these, the well-known Jacobsen's catalyst, Figure 1.6 was first described, wherein, the inclusion of *t*-butyl groups at the 3,3' and 5,5' positions markedly improved enantioselectivities. It was suggested that the effect of the *t*-butyl groups was steric in nature. It is determined that while the 3,3' *t*-butyl groups play mainly a steric role, the effect of those at the 5,5' positions is principally electronic.<sup>20</sup>

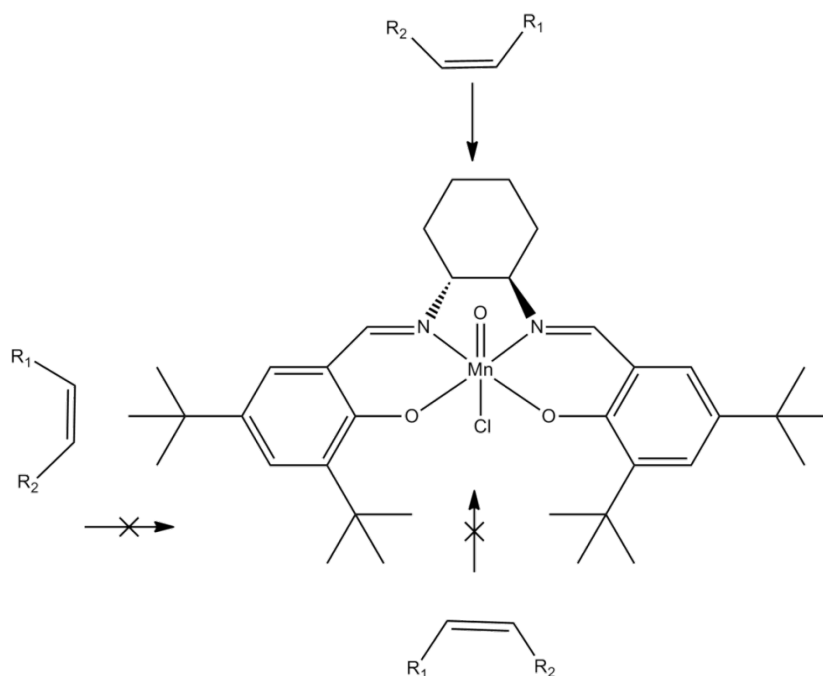


**Figure 1.6** Different approaches of Substrate to Jacobsen's catalyst.

### ***1.3.2 Conformational effects in Salen Catalyst***

The stereoselectivity of a catalyst often depends on its conformation, and this is very true in the case of salen-type ligands.<sup>21</sup> The incorporation a flexible *trans* substituted ethylene bridge into the backbone of the salen molecule allows a substantial degree of conformational mobility. The flexibility and chirality of this ethylene bridge results in two ‘stepped’ conformations, Figure 1.7. Between these two, steric factors favor the diequatorial structure, although in solution an equilibrating diaxial-diequatorial mixture can exist.<sup>22</sup> The conformation of salen catalyst can be easily altered by changing the metal, its oxidation state and/or counter ion. Conformational control of the metallo-salen is necessary in order to achieve high levels of stereochemical induction in catalysis.

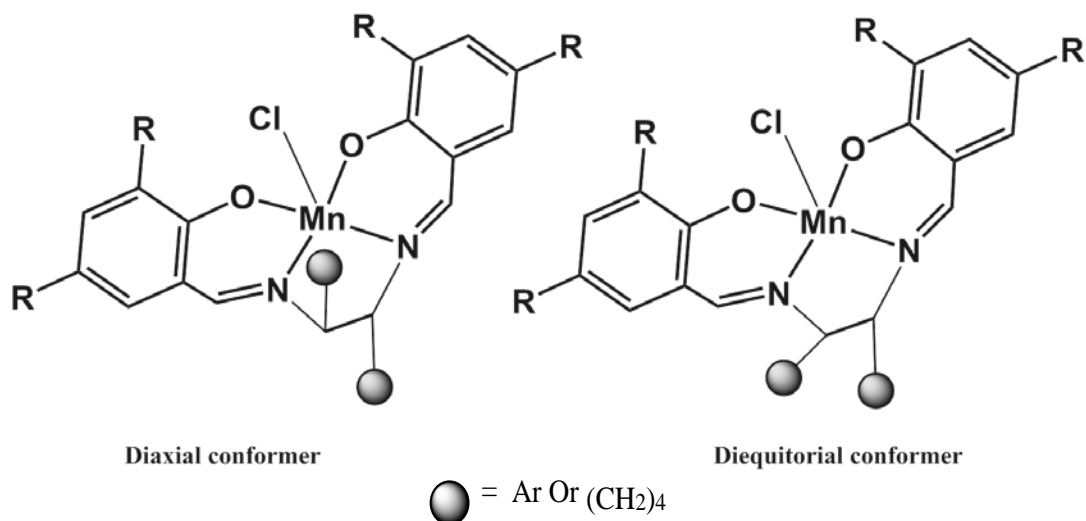


**Figure 1.7** Di axial and diequatorial conformers in a salen catalyst.

There are some critical factors for highly-stereoselective atomic transfers reactions such as olefin epoxidation - i) the selection of central metal ions that are suitable for the formation of reactive intermediates after reaction with transfer reagent and ii) the suitable design of salen ligands that takes into consideration the structures of the intermediates. In 1986, Fujita *et al.* reported the asymmetric oxidation of sulfides using optically active vanadyl salen complex as the catalyst.<sup>23</sup> In 1990, Jacobsen *et al.* reported on asymmetric epoxidation using manganese complexes, which revealed the usefulness of salen ligands bearing bulky constituents at the 3-position, Figure 1.8.<sup>24</sup> These studies explained the initiation of asymmetric oxidation using metallosalen complexes. The stereoselectivity of the reactions like epoxidation are dependent on the direction from which the oxo species are approached by the substrate and the orientation of the substrate during this process, Figure 1.8. In other words, high-stereoselectivity can be achieved during the reaction by controlling the direction of approach and the orientation. Oxo compounds, MO(salen) can adopt the stepped conformation as suggested by the experimental results of asymmetric epoxidation using achiral salen complexes. This assumption is supported by the calculated results. In the case where bulky substituents ( $R_1$ ) exist at the 3,3'-positions, olefins approach the oxo compound along the N-M bond axis near to the downward-bent benzene ring, thereby directing the bulkier substituent ( $R_L$ ) away from the bulky 3- or 3'-substituents ( $R_1$ ), Figure 1.8. The alternative approach pathway along the N-M bond axis is

considered to be less effective due to a repulsive interaction with the upward-bent benzene ring. With a bulky substituent ( $R_2$ ) at the 5-position, an approach from the direction of the upwardly-bent benzene ring becomes even less effective, and thus the enantioselectivity of the reactions improves.<sup>25</sup>

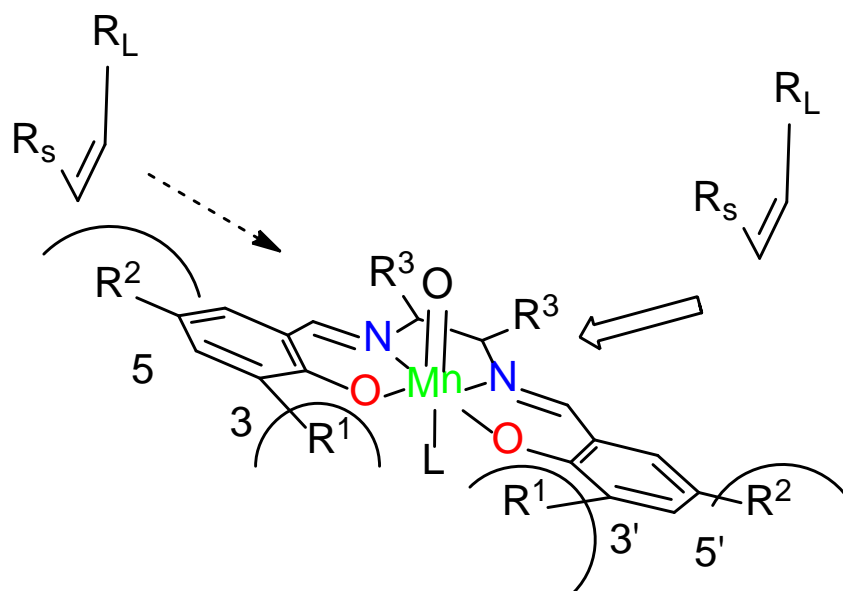


**Figure 1.8** Approach of the substrates to the manganese complex by different pathways.

The steric role of the alkene and its attached substituents must also be considered. With the related porphyrin systems the incoming alkene is thought to orientate  $\sim 90^\circ$  to the  $M=O$  bond to allow favorable orbital overlap.<sup>26</sup> The same general orientation of approach is predicted in salens also. For a *trans* alkene (I), this would necessitate one of the substituents being directed downwards into the salen ligand; an unfavorable interaction, Figure 1.9. Differentiation due to sterics therefore is expected between the stereoselectivities of *cis*- and *trans*-alkenes, and this is indeed the case. *Cis*-alkenes (II) are in general observed to give higher ee's than corresponding *trans*-alkenes. However, if the salen were 'deeply twisted' or 'stepped' steric repulsion for *trans*-alkenes (III) is minimized, allowing the preferred direction of approach. Higher ee's would therefore be expected, and in a few instances this has been observed.<sup>27,28</sup>

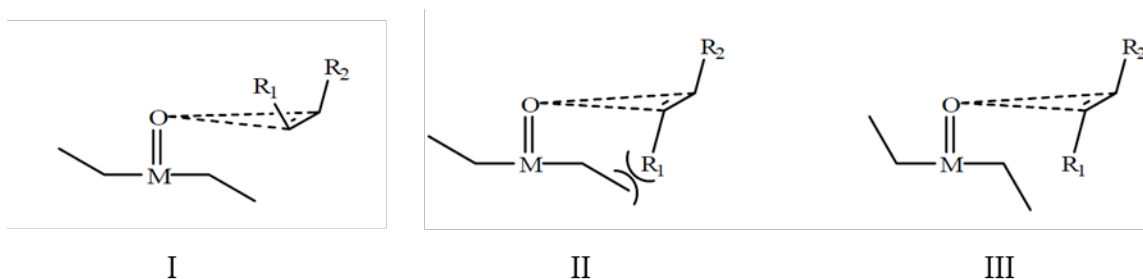


**Figure 1.9** Stereoselectivities based on steric role of cis- and trans-alkenes.

As mentioned above, there are various factors that can affect stereochemical outcome. Nonetheless, the salen with ‘deeply stepped’ conformation is one of them which can have a major impact on stereoselectivity. A helical molecule can be thought of as adopting this single ‘locked’ conformation. It would only be necessary to extend the ligand arms in order to obtain a true helix. Interconversion between conformers would be restricted, Figure 1.10, and a ‘deeply stepped’ structure is likely to result from steric repulsion between the overlapping ligand arms.

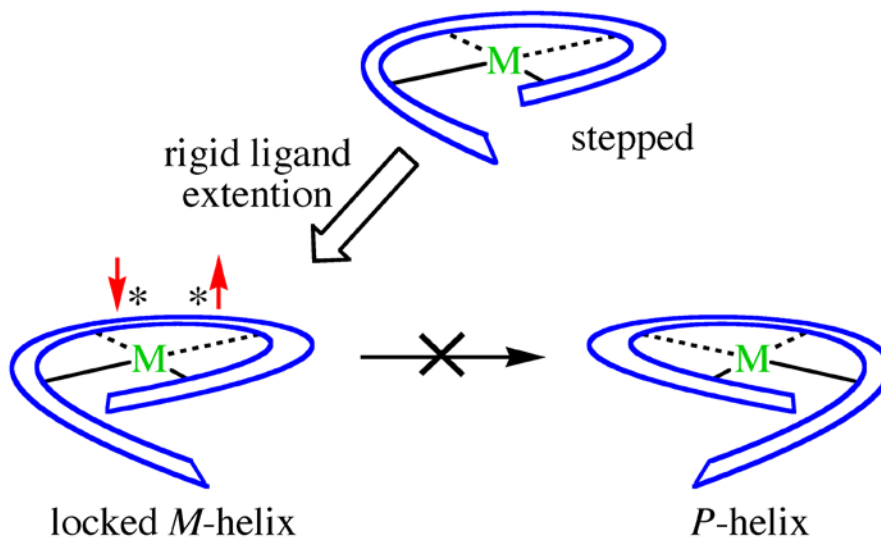


**Figure 1.10** General design of monohelical metal complex with a chiral backbone.

The other notable advantage of a helical ‘deeply stepped’ structure is that it has potential to be efficient and stereoselective for epoxidizing *trans*-alkenes. The chirality at C-8 and C-8’

positions predetermines the conformation of this helix, where the chirality is transferred and amplified throughout the metallo-salen. The use of, (*R,R*) stereochemistry in backbone biases the free ligand toward formation of the *M*-helix, thus, only one helical type is expected to form. However, creation of a limited quantity of the minor helical type cannot be ruled out.

## 1.4 Helical Complexes

A helix is defined as a twisted shape like a coil spring or spiral staircase. Helices are important in biology, as the DNA molecule is formed as two intertwined helices, and many proteins have helical substructures. For the classification of absolute configuration of helices the (*P,M* nomenclature) is used. *P* (plus) is a right-handed helix, where *M* (minus) is a left-handed helix. The *P/M* terminology is used particularly for molecules that actually resemble a helix, such as hexahelicene, Figure 1.11. Control of absolute helicity in metal salen complexes is of great interest since metal complexes serve as exceptionally useful asymmetric catalyst in many organic reactions.<sup>29</sup>

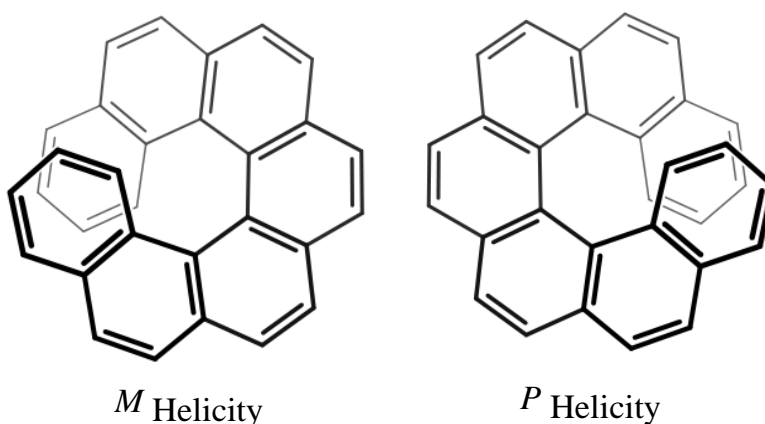


**Figure 1.11** *M* and *P* configurations of heptahelicene.

### 1.4.1 Monohelices and Helicates

Molecular complexes of transition metals can be classified into two general groups, monohelices and helicates. Monohelices complexes contain a single metal ion and can have single, double, or triple strands depending on the nature of the ligand. Examples of these complexes are shown in Figure 1.12. A single stranded monohelix can be formed when a single

multidentate ligand wraps around a single metal center, as for the europium complex shown.<sup>30</sup> A double stranded helix is made when two chelating ligands coordinate to the same metal, as for the platinum complex.<sup>31</sup> Triple-stranded monohelices can be formed when three chelating ligands coordinate to a single metal center such as  $[\text{Co}(\text{en})]^{3+}$ . Double and triple stranded monohelices resemble two and three-bladed propellers, respectively.

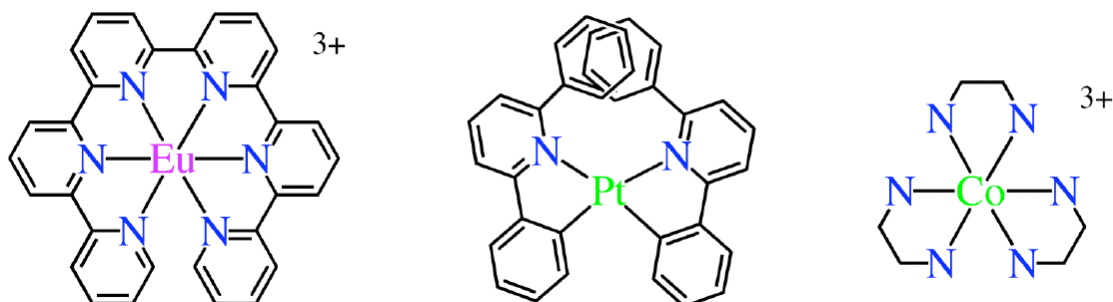


**Figure 1.12** Examples of monohelices with single, double, and triple-strands.

The term helicate was introduced by Lehn and coworkers in 1987 for the description of a polymetallic helical double-stranded complex, in effect a metal containing helix.<sup>32</sup> This original definition has been expanded to include all helical complexes with two or more metal centers. There is a wide array of different helicates, but some of the most common forms are double and triple stranded dihelicates produced when ligands with two chelating sections coordinate to two metal centers, Figure 1.13.

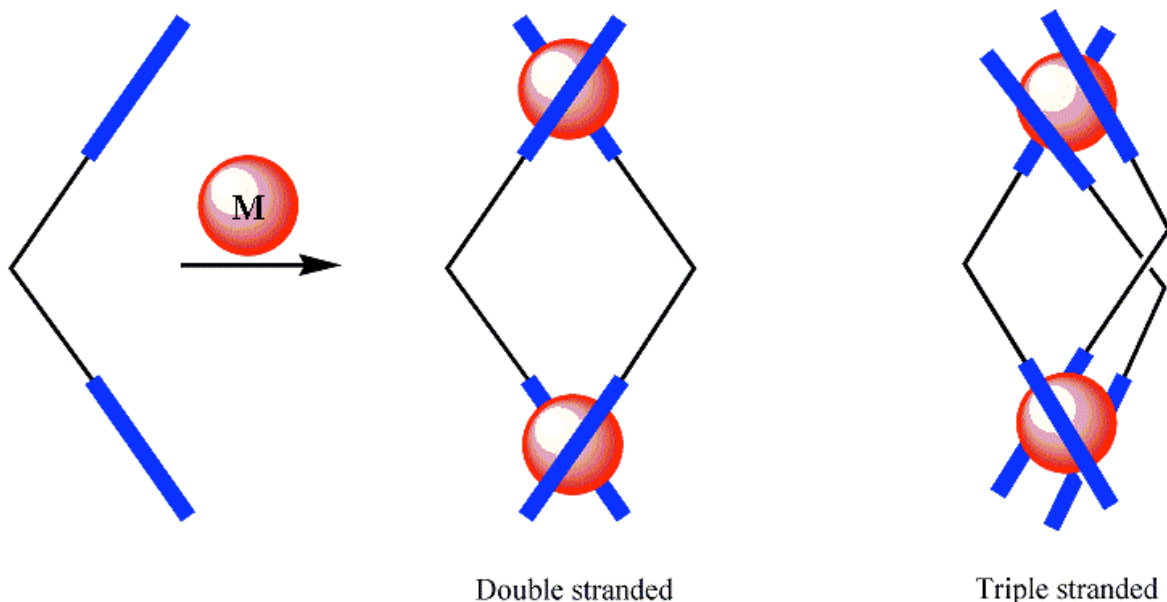


**Figure 1.13** Double and triple stranded helicates.

#### ***1.4.2 Types of Single-Stranded Monohelices***

A primary goal of the research presented in this thesis is the production of transition metal complexes of predetermined shapes. Our particular focus has been on producing small molecules with helical shapes that can be used as asymmetric catalysts. In order for these complexes to be useful as catalysts, they should have two labile coordination sites. One way of achieving this, is to coordinate a tetradentate ligand to an octahedral metal center, therefore there remain two reactive positions. There are three different morphologies; trans,  $\alpha$ -cis and  $\beta$ -cis, Figure 1.14. Of these complexes, trans-complexes have been widely used as catalysts for various asymmetric reactions. The different arrangements are likely to lead to complexes that exhibit very different selectivities and catalytic activity. For four coordinate metal centers there is no distinction between these, since the tetradentate ligand coordinates to all available coordination sites.<sup>33</sup>

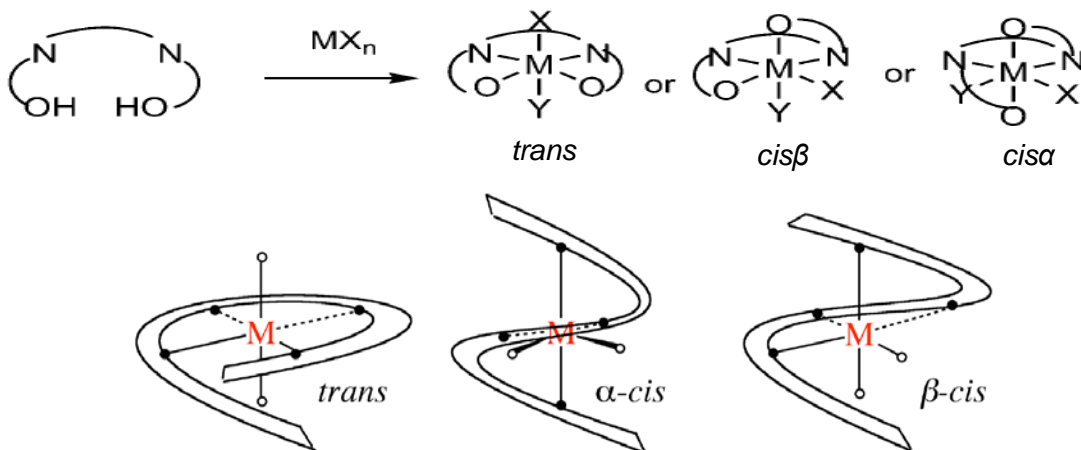


**Figure 1.14** Morphologies for single-stranded monohelices of octahedral metals ions

Single-stranded monohelices are very important as asymmetric catalysts because of their well-defined reaction centers and their deeply stepped conformations. In order to be suitable as catalysts a complex should exist in a single helical type (*M* or *P*). Predetermination of helical chirality around a metal center can be achieved if ligands themselves are chiral. The chirality can be introduced in the central section of the ligand i.e. the backbone, or at the ends of the ligand i.e. the sidearms. The metal complexes to be studied in this work will include chiral elements in the central section of the ligand (backbone). Below is an example where chiral cyclohexyl backbones are utilized in salen type ligands. A series of monohelical salen Fe(II) and Zn(II) complexes have been synthesized previously in the Levy group.<sup>3435</sup> Ligands bearing phenanthryl and benz[*a*]anthryl siderams attached to a binaphthyl or cyclohexyl backbone bridging groups were utilized, Figure 1.15.

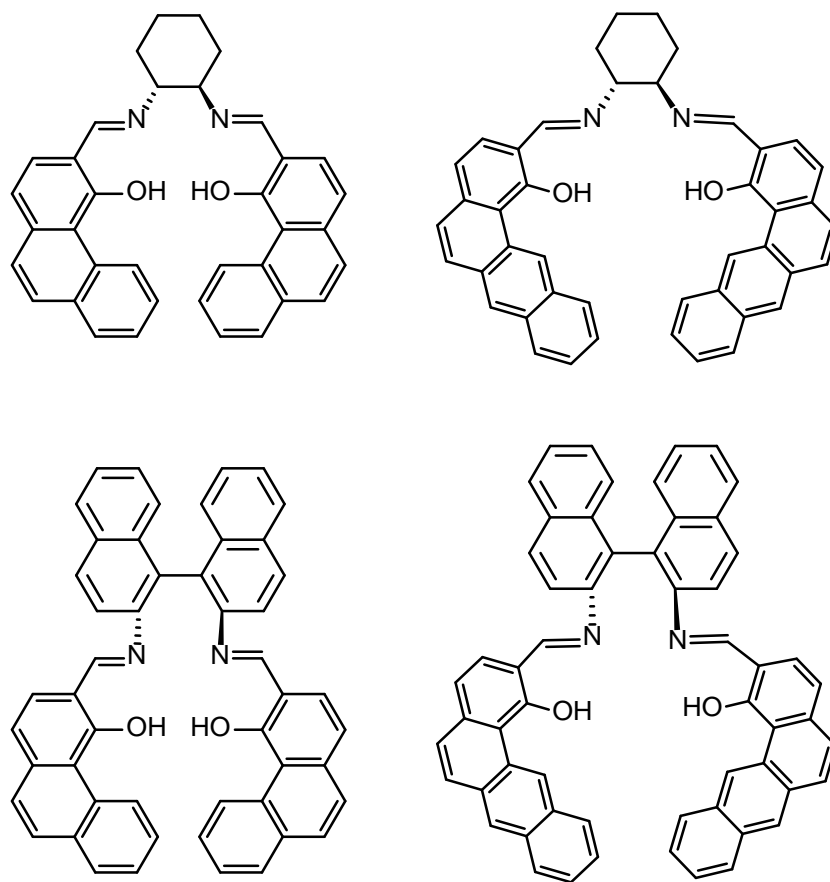


**Figure 1.15** Salen ligands with phenanthryl and benz[a]anthryl siderams.

### 1.5 Design of new ligand system

The innovation of new asymmetric catalysts requires the development of new ligands, which should have the capacity to support the central metal ions and give the required enantioselectivity in asymmetric reactions. The development of ligands is the collective effect of rational design, perception, trial and error. Successful ligand design/synthesis/test cycles are greatly assisted by the following controlling principles.<sup>36</sup>

- (1) Proposed synthesis should be by modular means; it should be possible to produce many different members of a ligand family using the same reaction simply by varying the combination of starting materials.

- (2) Ligands should be easy to synthesize in very few steps, and the diversification step should be placed as close as possible to the end of the synthetic route.
- (3) Simple, high-yielding reactions should be used whenever possible.
- (4) It should be possible to install multiple stereocentres that are independently variable. This in turn should allow for trivial expansion of ligand families.
- (5) Basic ligand frameworks should be easily modifiable to allow production of “next generation” ligands of higher complexity.

In this thesis, we are going to present the development of asymmetric catalysis by metal complexes of chiral tetra- and polydentate nitrogen-donor ligands. We describe various strategies for the design and synthesis of a number of different types of ligands, asymmetric catalytic applications, structure and bonding in coordination complexes, and limitations and future challenges.

## References

- 
- <sup>1</sup> Schiff, H., *Ann. Suppl.*, **1864**, 3, 343.
  - <sup>2</sup> Yoon, T.; Jacobsen, E., *Science*, **2003**, 299, 1691.
  - <sup>3</sup> Cozzi, P., *Chem. Soc. Rev.*, **2004**, 410-412.
  - <sup>4</sup> Gennari, C.; Piarulli, U., *Chem. Rev.*, **2003**, 103, 3071.
  - <sup>5</sup> Combes, A., *C. R. Acad. Fr.*, **1889**, 108, 1252.
  - <sup>6</sup> Sheldon, R.; Kochi, J., *Metal Catalysed Oxidations of Organic Compounds*, Academic Press, New York, **1981**, 102-105.
  - <sup>7</sup> Canali, L.; Sherrington D., *Chem. Soc. Rev.*, **1999**, 28, 85-93.
  - <sup>8</sup> Srinivasan, K.; Michaud, P.; Kochi, J. K. *J. Am. Chem. Soc.*, **1986**, 108, 2309.
  - <sup>9</sup> Samel, E. G.; Srinivasan, K.; Kochi, J. K. *J. Am. Chem. Soc.* **1985**, 107, 7606.
  - <sup>10</sup> Yoon, H.; Borrows, C. J. *J. Am. Chem. Soc.* **1988**, 110, 4087.
  - <sup>11</sup> Daly, A. ; Dalton, C.; Renehan, M.; Gilheany, D. *Tetrahedron Lett.* **1999**, 40, 3617.
  - <sup>12</sup> Hamada, T.; Fukuda, T.; Imanishi, H.; Katsuki, T. *Tetrahedron* **1996**, 52, 515.
  - <sup>13</sup> Daly, A.; Gilheany, D. *Tetrahedron: Asymmetry* **2003**, 14, 127.
  - <sup>14</sup> Strassner, T.; Houk, K. *Org. Lett.* **1999**, 1, 419.
  - <sup>15</sup> Srinivasan, K.; Michaud, P.; Kochi, J. *J. Am. Chem. Soc.* **1986**, 108, 2309.
  - <sup>16</sup> Zhang, W.; Loebach, J.; Wilson, S.; Jacobsen, E. *J. Am. Chem. Soc.* **1990**, 112, 2801.

- 
- <sup>17</sup> Irie, R.; Noka, K.; Ito, Y.; Matsumoto, N.; Katsuki, T. *Tetrahedron Lett.* **1990**, 31, 7345.
- <sup>18</sup> Katsuki, T. *J. Mol. Cata. A* **1996**, 113, 87
- <sup>19</sup> Jacobsen, E. *Catalytic Asymmetric Synthesis*; Ojima, I. Ed.; VCH: New York, **1993**, 159.
- <sup>20</sup> Jacobsen, E. *Catalytic Asymmetric Synthesis*, Ed. Ojima, I. VCH Publisher Inc. **1993**, 166.
- <sup>21</sup> Samsel, E.; Srinivasan, K.; Kochi, J. *J. Am. Chem. Soc.* **1985**, 107, 7606.
- <sup>22</sup> Katsuki, T. *Adv. Synth. Catal.* **2002**, 344, 131.
- <sup>23</sup> K. Nakajima, M. Kojima, J. Fujita, *Chem. Lett.*, **1986**, 1483.
- <sup>24</sup> Zhang, W.; Loebach, J.; Wilson, S.; Jacobsen, E. *J. Am. Chem. Soc.*, **1990**, 112, 2801.
- <sup>25</sup> Jacobsen, E.; Zhang, W.; Muci, L.; Ecker, J.; Deng, L. *J. Am. Chem. Soc.*, **1991**, 113, 7063.
- <sup>26</sup> Hamada, T.; Fukuda, T.; Imanishi, H.; Katsuki, T. *Tetrahedron* **1996**, 52, 515.
- <sup>27</sup> Nishikori, H.; Ohta, C.; Katsuki, T. *Synlett* **2000**, 1557.
- <sup>28</sup> O'Mahony, C.; McGarrigle, E.; Renehan, M.; Ryan, K.; Kerrigan, N.; Bousquet, C.; Gilheany, D. *Org. Lett.* **2001**, 3, 3435.
- <sup>29</sup> VLU: Additional Chirality Elements – Chemgapedia.
- <sup>30</sup> Constable, E.; Chotalia, R.; Tocher, T. *J. Chem. Soc. Chem. Commun.* **1992**, 771.
- <sup>31</sup> Cornioley, C.; Stoeckli-Evans, H.; Zelewsky, A. *J. Chem. Soc. Chem. Commun.* **1990**, 121.
- <sup>32</sup> Lehn, J.; Rigault, A.; Siegel, J.; Harrowfield, J.; Chevrier, B.; Moras, D. *Proc. Natl. Acad. Sci. U.S.A.* **1987**, 84, 25.
- <sup>33</sup> Katsuki, T. *Chem. Soc. Rev.*, **2004**, 33, 437-4444.
- <sup>34</sup> Wiznycia, A.; Desper, J.; Levy C. *Dalton Trans.* **2007**, 1520–1527
- <sup>35</sup> Wiznycia, A.; Desper, J.; Levy C. *Chem. Commun.* **2005**, 4693–4695.
- <sup>36</sup> Caputo, C.; Jones, N. *Dalton Trans.*, **2007**, 4627–4640.

## Chapter 2 - Selection and synthesis of (+)-*trans*-Cyclobutane-1,2-diamine backbone

### 2.1 Introduction

For the preparation of a monohelical salen or related complex it is desirable that certain criteria be met. New catalyst with desirable properties can be achieved with the modification of backbone, sidearm and central metal atom of existing salen, Figure 2.1.

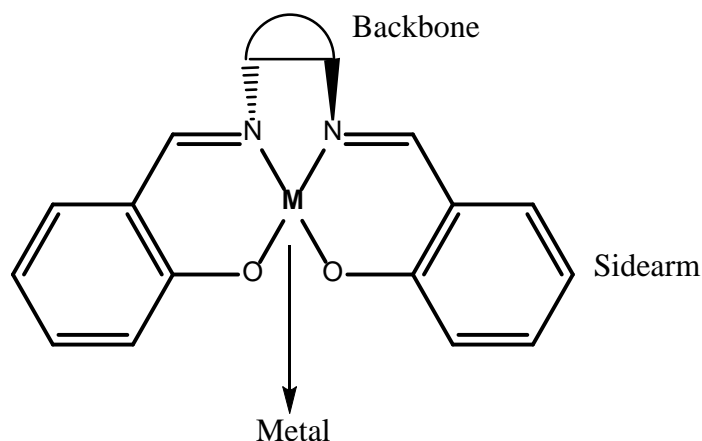


**Figure 2.1** General design of salen metal complex.

#### 2.1.1 Design of New Chiral Ligands: Chiral Backbones

Chirality must be incorporated into any new ligand system in order to produce monohelical complexes of only one conformation (*P* or *M*). It has been shown that the chiral components can either be located at the ends of the ligand (sidearm) or in the central portion (backbone). Primarily, the ligand should incorporate groups that influence the structure towards helix formation. This requirement can be partially fulfilled through the use of a chiral directing backbone, to provide a sense of 'handedness' or 'twist'. Locating the chirality in the backbone section of the ligands allows the ligands arms to be roughly planar and avoid unfavorable steric interactions that would prevent the ligand wrapping around the metal. If at the same time the backbone group is relatively inflexible, the probability that unwanted arrangements and geometries form is decreased.<sup>1</sup>

### 2.1.2 Design of New Chiral Ligands: Sidearm

In order to obtain monohelical complexes, the ligand sidearms should be rigid and have relatively low steric bulk so that they do not interact strongly upon wrapping and overlap. It is also desirable that sterically large ligand arms be employed, so as to yield slightly over one helical turn, in effect 'locking' the structure. Aryl rings typically comprise the arms of salen complexes; consequently this objective can be accomplished through either replacement with extended polyaromatic ring systems, and/or by appending on the appropriate substituents. Saturated rings are unattractive for use in this respect due to their flexibility, and to the conformational mobility that subsequently results. Modeling studies indicate that both methodologies are feasible and that for polyaromatic arms, nonlinear, i.e curved polyaromatics, are required for the adoption of a 'locked' helix, Figure 2.2. Additionally, if the second approach is to be followed, the appended substituents must be positioned on the inward side of the ligand arms close to the donor atoms, for 'locking' to take place.<sup>2</sup>

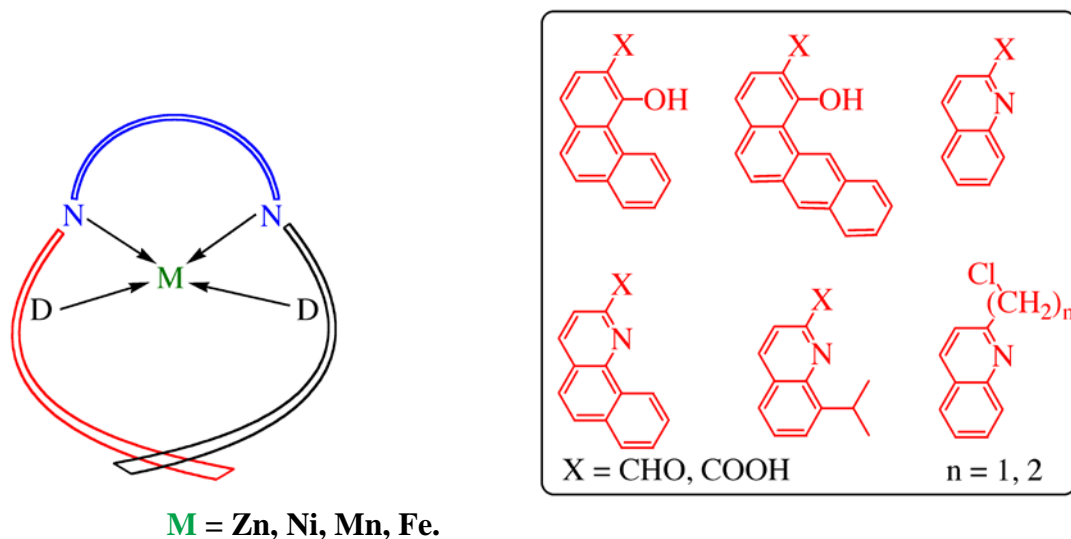


**Figure 2.2** Extended planar polyaromatic ring systems for producing monohelical complexes.

### 2.1.3 Design of New Chiral Ligands: Metal

In addition to the ligand, the metal must also be carefully selected. In this work there are three main considerations for the choice of metal; ease of characterization, ease of handling, and

potential for high catalytic activity. Zinc(II) complexes are diamagnetic and so can be readily characterized via NMR spectroscopy. Furthermore, they are typically stable to air and consequently meet the second requirement also. For high catalytic activity potential metals include cobalt, iron, and manganese, where, in the context of salen and pyridyl-imine catalysis iron is the least studied. For metals in the 2+ oxidation state no counterions are present when two anionic donors are employed, as in M(salen) and M(binap-salen) complexes.

#### ***2.1.4 Previous studies***

Different helical tetradentate salen ligands with cyclohexyl and binaphthyl backbones and phenanthryl and benz[*a*]anthryl side arms were synthesized and characterized in our group.<sup>3</sup> These ligands possess unique stepped helical conformations. Vanadium (IV) complexes of these ligands with cyclohexyl backbones adopt *M* helical conformations in the solution as observed from the CD spectra of these complexes. However, in the solid state these complexes form 1:1 mixtures of both *M* and *P* conformations. Asymmetric sulfoxidations by these complexes showed moderate ee. We concluded that chiral cyclohexyl diamine is a weak director of chirality and this hypothesis was previously presented by Fox et al.<sup>4</sup>

## **2.2 Cyclobutyl backbone**

### ***2.2.1 Selection criteria***

The non-planarity in the salen ligands arises as a result of the  $sp^3$  centres on the diimine bridge.<sup>5</sup> Thus, the N-C-C-N dihedral angle between the two nitrogen atoms of the ligand is a measure of the resultant twist or step in the complex, Figure 2.3. For complexes derived from *trans*-cyclohexane-1,2-diamine the rigid nature of the cyclohexane ring, with a set N-C-C-N dihedral angle, is a major influence on the complex conformation. It has been previously suggested that salen complexes facilitate selective epoxidation of alkenes by their stepped nature. Smaller ring diamines might lead to more enantioselective epoxidation catalysts by increasing the N-C-C-N dihedral angle and thus altering the ligand conformation in a favorable manner.<sup>6</sup>

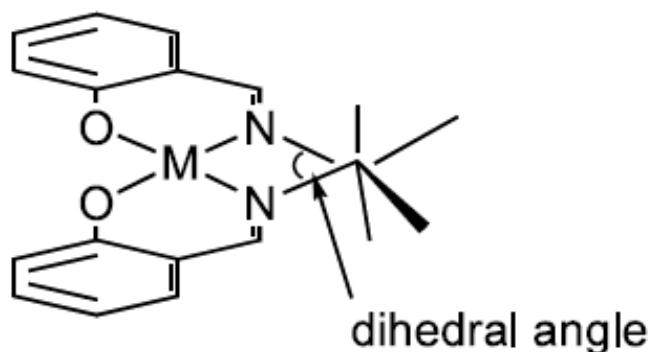


**Figure 2.3** Illustration of the N-C-C-N dihedral angle.<sup>6</sup>

### *2.2.2 Synthesis*

There are two routes reported for the synthesis of *trans*-cyclobutane-1,2-diamine; one with iminonitrile as starting material and other with adipic acid as starting material. The process with adipic acid was recently revised by the Gilheany group.<sup>6</sup> We have followed the same procedure with required modification as mentioned in the experimental section. The general scheme of this synthesis includes the conversion of adipic acid **1** into the dibromo-dimethyl ester **2** of adipic acid. Then the ring-closure step was carried out using potassium cyanide on the dibromo-dimethyl ester **2**. In this manner a mixture of the two isomers of nitrile diester **3** was obtained. The mixture of isomers was directly used for subsequent hydrolysis to get triacid **4**, heating of which at 180°C yields cyclobutane-1,2-diacid **5** as a mixture of *trans*- and *cis*-isomers. The mixture of isomers was equilibrated by heating in 12 M HCl at 120°C for 6 days. Subsequent cooling leads to crystallisation of pure *trans*-isomer **6**. This *trans*-isomer was then converted into the foul smelling diacid chloride **7** using thionyl chloride. The di(acid chloride) was then converted into the diamine dihydrochloride **8** using sodium azide in a one pot reaction. Finally the resolution of *trans*-cyclobutane-1,2-diamine was done using the ‘Dutch resolution’ technique.<sup>6</sup>

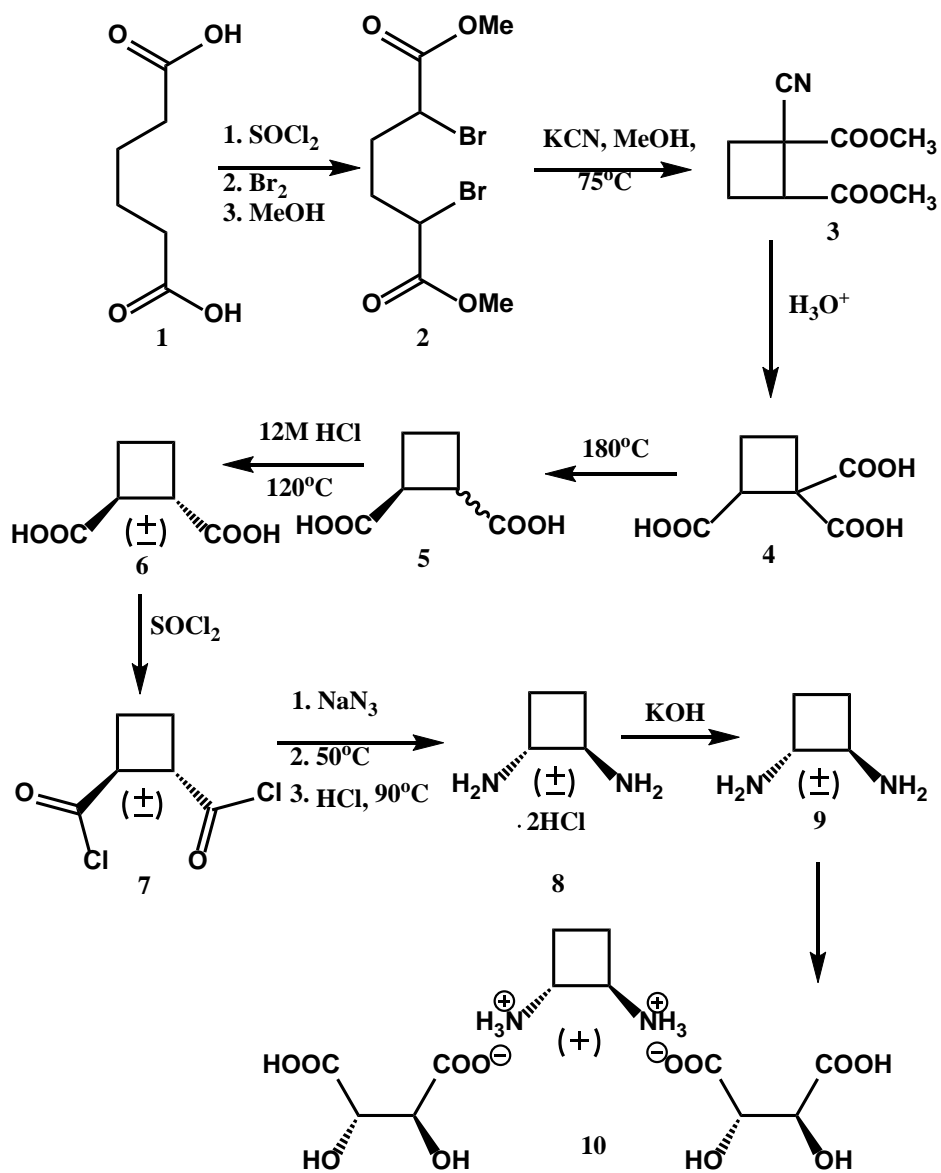


**Figure 2.4** Synthesis of *trans*-cyclobutane-1,2-diamine backbone.

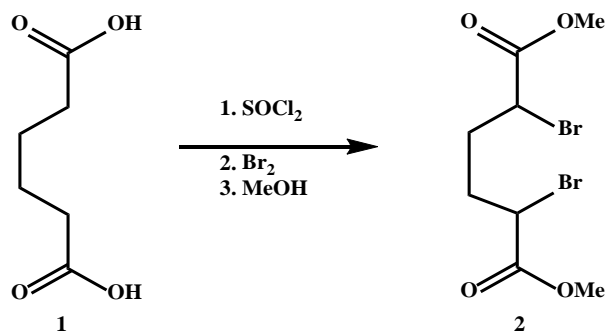
## 2.2 Experimental

### 2.2.1 Synthesis

$^1\text{H}$  and  $^{13}\text{C}$  NMR spectra were recorded on a Varian Unity plus 400 MHz or 200 MHz spectrometer in  $\text{CDCl}_3$  or  $\text{D}_2\text{O}$ . Data is expressed in parts per million (ppm) downfield shift from

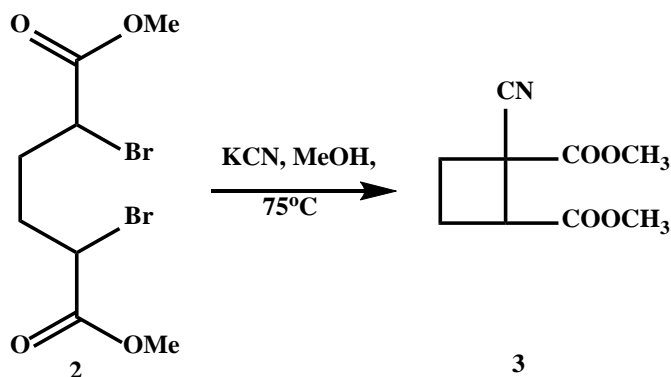
tetramethylsilane or residual protiosolvent as internal reference and are reported as position (in ppm), multiplicity (s = singlet, d = doublet, t = triplet, m = multiplet), coupling constant ( $J$  in Hz) and integration (number of protons). Infrared spectroscopy (IR) was done on neat sample using Nicolet 380 FT-IR .

### 2.2.1.1 *meso*-Dimethyl 2,5-dibromohexane-1,6-dioate, 2 6



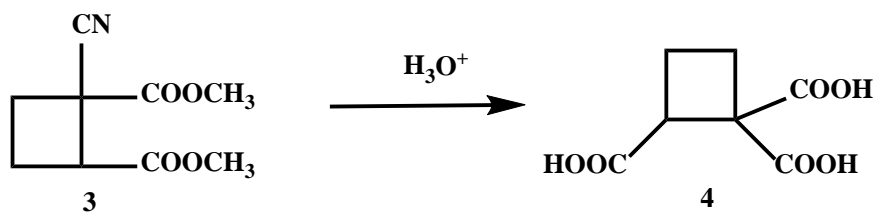
Thionyl chloride (32.3 g, 0.271 mol) was added in 7 mL portions over 2 hrs to adipic acid (19.7 g, 0.135 mol) heated at 80°C in a two-neck 250 mL round bottom flask equipped with a reflux condenser and a pressure equalized dropping funnel. On heating, after some time gas evolution ceased, some solid (adipic acid) still remained in the reaction. Therefore, additional 10 mL of thionyl chloride was added and heating continued until gas evolution ceased completely. The addition took 7 hrs in total. Following this, bromine (47.3 g, 0.290 mol) was added dropwise to the pale yellow hot reaction mixture over 12 hrs and heating was then continued for a further 3 h. After cooling to rt, N<sub>2</sub> was passed through the reaction for removal of excess bromine. The resulting brown reaction mixture was added dropwise to MeOH (27.5 mL) in a 250 mL round bottom flask cooled in an ice bath. A white precipitate formed during the addition and this was filtered as soon as addition was complete and recrystallised from MeOH (20.1 g, 45.0 %). On further standing precipitate formed in the mother liquor which was also recrystallised from MeOH (5.2 g, 12%) <sup>1</sup>H NMR (400 MHz, CDCl<sub>3</sub>) δ 4.28–4.25 (m, 2H, CHBr), 3.81 (s, 6H, OCH<sub>3</sub>), 2.33–2.30 (m, 2H, CH-CBr), 2.09–2.05 (m, 2H, CH-CBr); <sup>13</sup>C NMR (100 MHz, CDCl<sub>3</sub>) δ 169.69, 53.21, 44.34, 32.49.

### 2.2.1.2 1-Cyano-cyclobutane-1,2-dicarboxylic acid dimethyl ester, 3 6



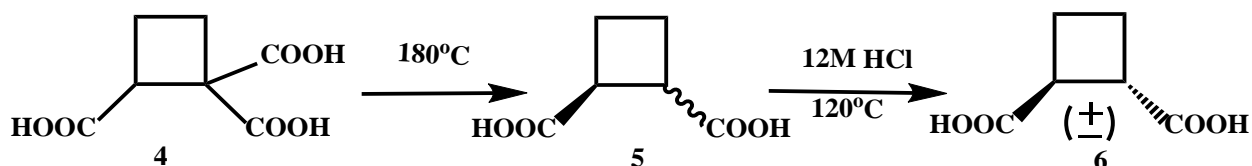
*meso*-Dimethyl 2,5-dibromohexane-1,6-dioate (20 g, 0.060 mol) and potassium cyanide (8.83 g, 0.136 mol) were added to a 250 mL round bottom flask containing MeOH (40 mL). The reaction mixture was heated at 75 °C for 56 hrs. After cooling to rt, methanol was distilled at atmospheric pressure and the residue was flushed through a pad of silica with CH<sub>2</sub>Cl<sub>2</sub>. The solvent was removed in vacuo to yield a yellow liquid (8.41 g, 71.0 %). <sup>1</sup>H NMR indicated this to be a mixture of the two isomers of the product. The mixture of isomers was used for the next step without purification. <sup>1</sup>H NMR (400 MHz, CDCl<sub>3</sub>) δ 3.85 (s, 3H, OCH<sub>3</sub>), 3.79–3.72 (m, 1H, cyclobutyl-H), 3.72 (s, 3H, OCH<sub>3</sub>), 2.75–2.53 (m, 3H, cyclobutyl-H), 2.42–2.26 (m, 1H, cyclobutyl-H); liquid isomer <sup>1</sup>H NMR (270 MHz, CDCl<sub>3</sub>) δ 3.88 (s, 3H, OCH<sub>3</sub>), 3.83–3.76 (m, 1H, cyclobutyl-H), 3.80 (s, 3H, OCH<sub>3</sub>), 2.69–2.53 (m, 3H, cyclobutyl-H), 2.35–2.27 (m, 1H, cyclobutyl-H); <sup>13</sup>C NMR (400 MHz, CDCl<sub>3</sub>) δ 170.26, 169.93, 167.89, 118.72, 117.52, 54.09, 53.80, 52.65, 52.42, 45.36, 43.99, 43.73, 42.27, 29.08, 28.53, 21.44, 20.23.

### 2.2.1.3 Cyclobutane-1,2-dicarboxylic acid, 4 6



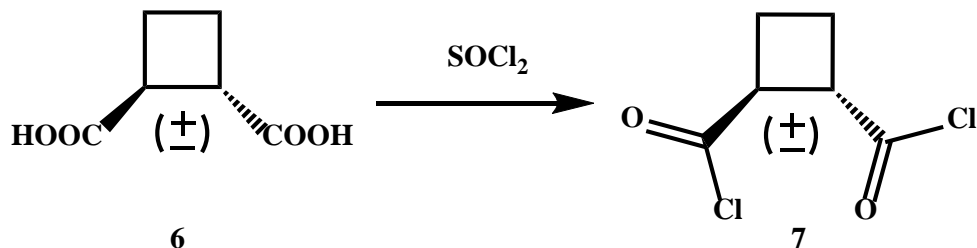
A mixture of the two isomers of 1-cyano-cyclobutane-1,2-dicarboxylic acid dimethyl ester (4.63 g, 0.0234 mol) and 6 M HCl (11.7 mL) were refluxed for 12 hrs. The mixture was concentrated in vacuo until a white solid precipitated. Et<sub>2</sub>O (20 mL) was added to the residue and the mixture was filtered. The filtrate was washed with water (3 x 50 mL), dried over Na<sub>2</sub>SO<sub>4</sub> and the solvent was removed in vacuo to yield a pale yellow liquid (3.34 g). This liquid was heated at 180°C under vacuum (water pump) until gas evolution ceased (~2.5 hrs). On cooling, a brown solid was formed (2.10 g, 62%). <sup>1</sup>H NMR indicated this to be a mixture of the *trans* and *cis* diacids: <sup>1</sup>H NMR (400 MHz, D<sub>2</sub>O) δ (*trans* isomer) 3.37–3.34 (m, 2H, CHCO), 2.07–2.09 (m, 4H, cyclobutyl-H); <sup>1</sup>H NMR (400 MHz, D<sub>2</sub>O) δ (*cis* isomer) 3.45–3.47 (m, 2H, CHCO), 2.16–2.18 (m, 4H, cyclobutyl-H).

#### 2.2.1.4 *trans*-Cyclobutane-1,2-dicarboxylic acid, 6<sup>7</sup>



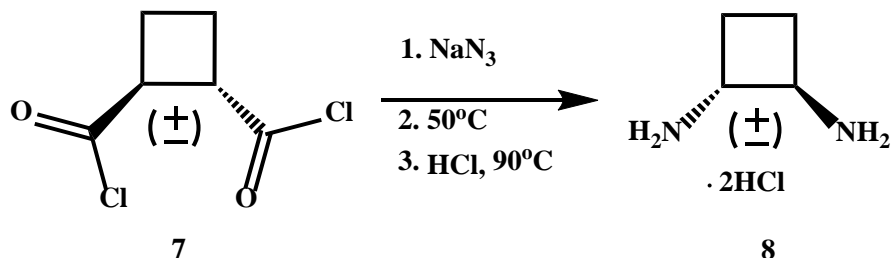
The mixture of *cis*- and *trans*-cyclobutane-1,2-dicarboxylic acid (1.890 g, 0.0131 mol) was placed in 100 mL, round-bottom flask. 12M HCl (4 mL) is added and the mixture is heated at 120°C for 160 hrs. It was then cooled down slowly (overnight), giving a white crystal which was filtered from the brownish mother liquor, washed quickly with ice cold 12M HCl (1 mL) and dried under vacuum overnight to afford grey crystal of pure *trans*-diacid (1.0 g, 54%). <sup>1</sup>H (400 MHz, D<sub>2</sub>O) δ 3.46–3.42 (m, 2H, CHCO), 2.18–2.16 (m, 4H, cyclobutyl-H); <sup>13</sup>C NMR (400 MHz, D<sub>2</sub>O) δ 178.02, 40.11, 21.36.

### 2.2.1.5 *trans*-Cyclobutane-1,2-dicarbonyl dichloride, 7



*trans*-Cyclobutane-1,2-dicarboxylic acid (7.99 g, 55.4 mmol) and <http://onlinelibrary.wiley.com/doi/10.1002/anie.201305549/abstract> thionyl chloride (15.0 mL, 206 mmol) were heated at 70°C in benzene (35 mL) for 24 hrs. Benzene and excess thionyl chloride were distilled off and the brown residue dried under water pressure and purified by Kugelrohr distillation to yield a colorless liquid (9.41 g, 94.0 %). <sup>1</sup>H NMR (400 MHz, CDCl<sub>3</sub>) δ 3.94–3.90 (m, 2H, CHCO), 2.44–2.34 (m, 4H, cyclobutyl-H); <sup>13</sup>C NMR (400 MHz, CDCl<sub>3</sub>) δ 173.45, 77.48, 77.16, 76.84, 50.57, 22.12.

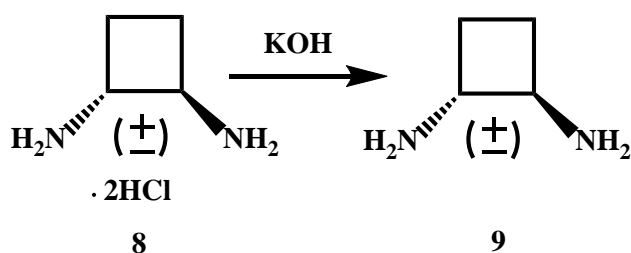
### 2.2.1.6 *trans*-Cyclobutane-1,2-diamine dihydrochloride, 8



A solution of *trans*-cyclobutane-1,2-dicarbonyl dichloride (9.50 g, 52.5 mmol) in benzene (60 mL) was added dropwise over 5 min to a solution of sodium azide (11.9 g, 184 mmol) in water (60 mL) cooled to 0°C. The resulting two phase mixture was stirred vigorously for 2 hrs after which time the phases were separated and the organic phase was washed with 5% NaHCO<sub>3</sub> (20 mL), water (20 mL) and dried over CaCl<sub>2</sub>. This benzene solution of diacyl azide (CAUTION: explosion risk) was decanted into a fresh flask equipped with a reflux condenser and oil bubbler and heated slowly to 50°C. Initial slow evolution of gas became vigorous at ~ 40°C, so heating was stopped. After gas evolution had ceased, the reaction mixture was heated at 50°C for 1 hour. After cooling to rt 20% HCl (20 mL) was added and the reaction heated to 90°C

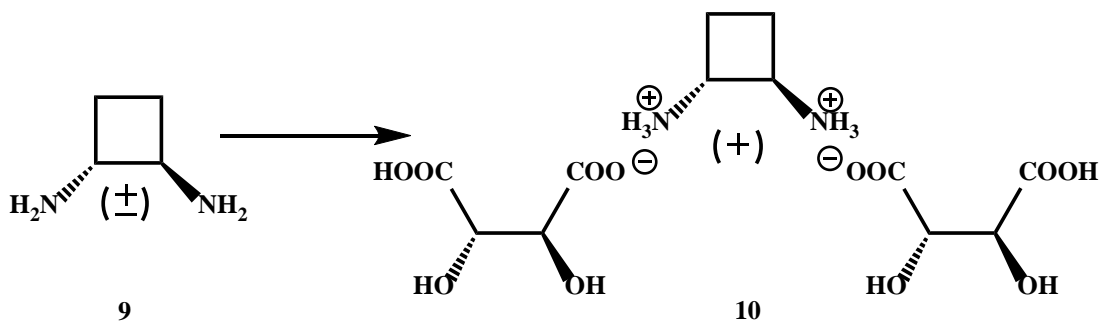
for 4 h, then allowed to cool to rt overnight. The benzene layer was separated and washed with water (50 mL). The aqueous layers were combined and washed with benzene (100 mL). Water was removed in vacuo to yield a brown solid which was recrystallised from MeOH/Et<sub>2</sub>O to give a white solid (6.29 g, 46%). <sup>1</sup>H NMR (400 MHz, D<sub>2</sub>O) δ 3.82–3.76 (m, 2H, CHN), 2.17–2.14 (m, 2H, cyclobutyl-H), 1.82–1.80 (m, 2H, cyclobutyl-H); <sup>13</sup>C NMR (400 MHz, D<sub>2</sub>O) δ 48.38, 20.59.

### 2.2.1.7 (±)-*trans*-Cyclobutane-1,2-diamine, 9



*trans*-Cyclobutane-1,2-diamine dihydrochloride (1.22 g, 7.67 mmol) was dissolved in water (3 mL) and added to a separatory funnel containing freshly ground KOH (1.72 g, 30.7 mmol). The mixture was shaken vigorously and then extracted with CHCl<sub>3</sub> (4×10 mL). The CHCl<sub>3</sub> extracts were dried over Na<sub>2</sub>SO<sub>4</sub> and the solvent was removed in vacuo to a pale yellow liquid (612 mg, 93%). <sup>1</sup>H NMR (400 MHz, CDCl<sub>3</sub>) δ 2.86–2.82 (m, 2H, CHN), 2.04–2.00 (m, 2H, cyclobutyl-H), 1.82 (br s, 4H, NH<sub>2</sub>), 1.22–1.17 (m, 2H, cyclobutyl-H); <sup>13</sup>C NMR (400 MHz, CDCl<sub>3</sub>) δ 59.25, 25.73.

### 2.2.1.8 Resolution of *trans*-cyclobutane-1,2-diamine, 10<sup>8</sup>



(±)-*trans*-Cyclobutane-1,2-diamine (2.11 g, 24.5 mmol) was added to a solution (+)-tartaric (8.64 g, 57.6 mmol) acid and 1 mL of methanol in 7 mL of water. At 40°C, 12 mL of methanol was filtered, washed with 10 mL of methanol and dried in air to give a white precipitate (1.95 g, containing a 2:1 ratio of (+)-tartaric acid and *trans*-cyclobutane-1,2-diamine: <sup>1</sup>H NMR (400 MHz, D<sub>2</sub>O) δ 4.47 (s, 4H), 3.96–3.93 (m, 2H), 2.32–2.29 (m, 2H), 1.97–1.95 (m, 2H); Three recrystallisations of this material from MeOH/H<sub>2</sub>O (1:1) gave white crystals (961 mg, 10%); [α]<sub>D</sub><sup>20</sup> = +32.0 (c 1, H<sub>2</sub>O); <sup>13</sup>C NMR (400MHz, D<sub>2</sub>O) δ 179.10, 75.53, 51.06, 23.25.

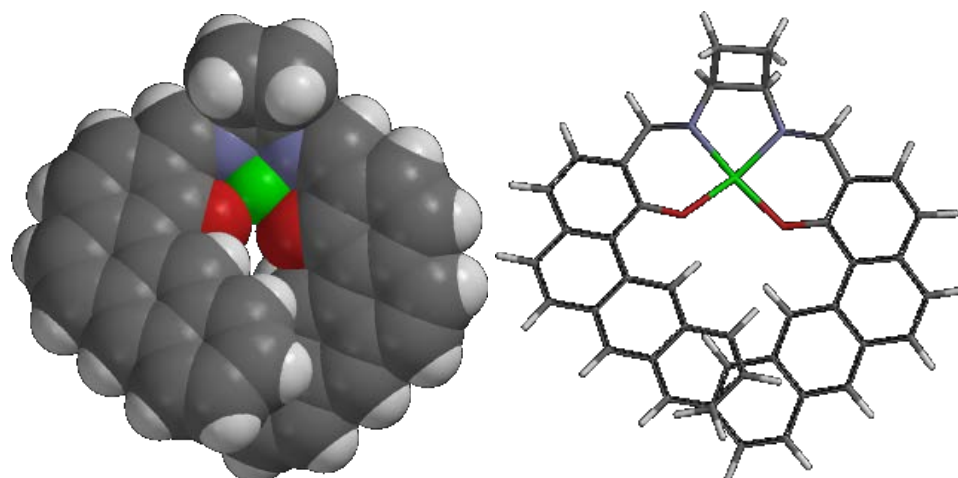
### 2.2.2 Calculations

Semi empirical calculations have been the best in predicting the geometric properties and vibrational frequencies of transition and organometallic metal complexes.<sup>9</sup> Therefore we have used this method for the salen conformer.

The molecular structures were constructed using Spartan '08 (Wavefunction, Inc. Irvine, CA). For construction of structure, we have used teradented Zn metal. In the following structures,

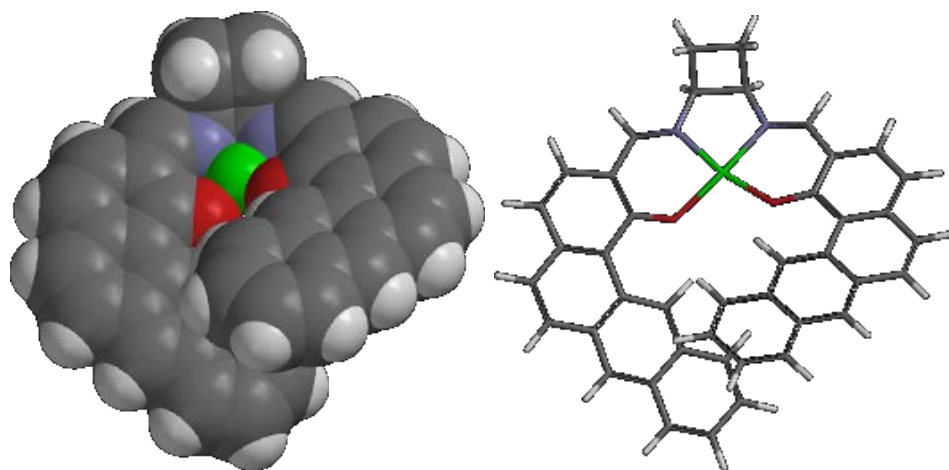
<b>Color</b>	<b>Atom</b>
<b>Grey</b>	Carbon
<b>White</b>	Hydrogen
<b>Blue</b>	Nitrogen
<b>Red</b>	Oxygen
<b>Green</b>	Zn metal

We have calculated the heat of formation (E) for following transition metal complexes in their *M* and *P* forms using semi-empirical AM1 calculations. The obtained results are as follows,



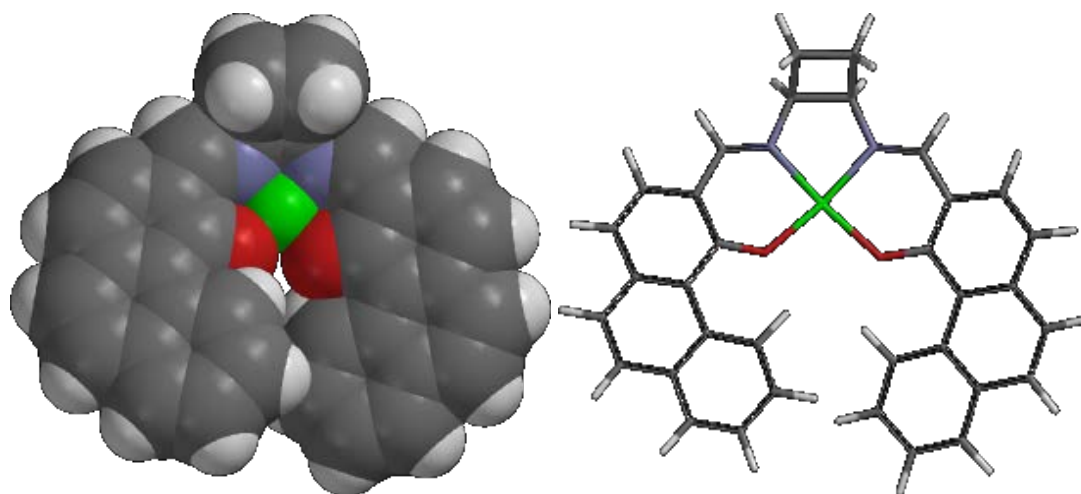
*P*-type complexes,  $E= 912.555$  kJ/mol

**Figure 2.5** Results of Semi-empirical AM1 calculation for *P*-type of Zn complexes with 4-ring sidearm.



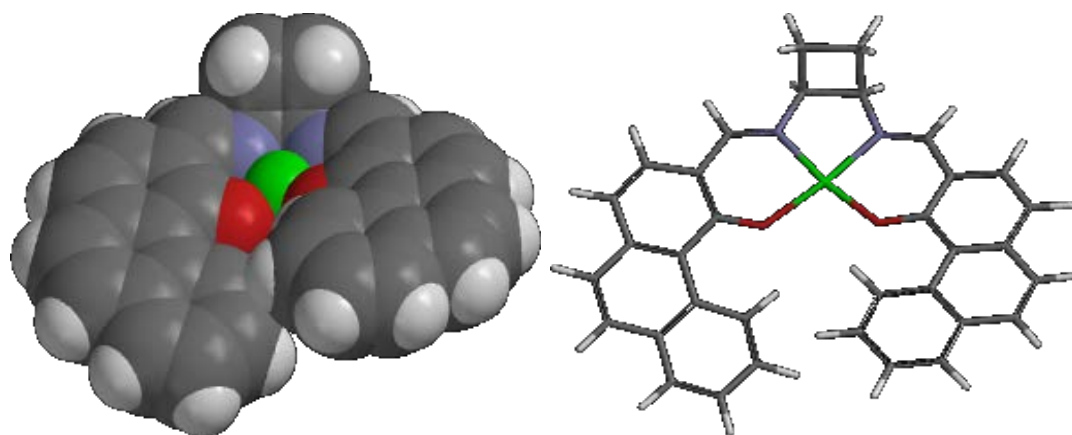
*M*-type complexes,  $E= 923.348$  kJ/mol

**Figure 2.6** Results of Semi-empirical AM1 for *M*-type of Zn complexes with 4-ring sidearm.



P-type complexes,  $E= 1573.029$  kJ/mol

**Figure 2.7** Results of Semi-empirical AM1 calculation for *P*-type of Zn complexes with 3-ring sidearm.



*M*-type complexes,  $E= 1598.190$  kJ/mol

**Figure 2.8** Results of Semi-empirical AM1 calculation for *M*-type of Zn complexes with 3-ring sidearm.

## 2.3 Results & Discussion

As previously mentioned, it is important to have conformational control of catalysts in order to achieve high enantioselectivity in asymmetric catalysis. We have used the Spartan '08 program to perform semi-empirical AM1 calculations, with the primary aim of geometry optimization and single-point energy determination. Using this method we have calculated the energy difference between *P* and *M* conformers of complexes with different backbones and sidearms. The energy differences reported in Figure 2.9 show that in case of the 1,2-cyclobutyl backbone, we can expect a significant difference ( $> 10 \text{ kJ mol}^{-1}$ ) in the helical conformers. In case of a backbone with bigger rings, we predict lower energy differences between helical conformers and also have more flexibility. For the cyclopropyl backbone, it is possible to have inconvertible conformer due to high energy difference between *P* and *M* conformer's nevertheless high flexibility of cyclopropyl ring might affect its ability to bind metals.

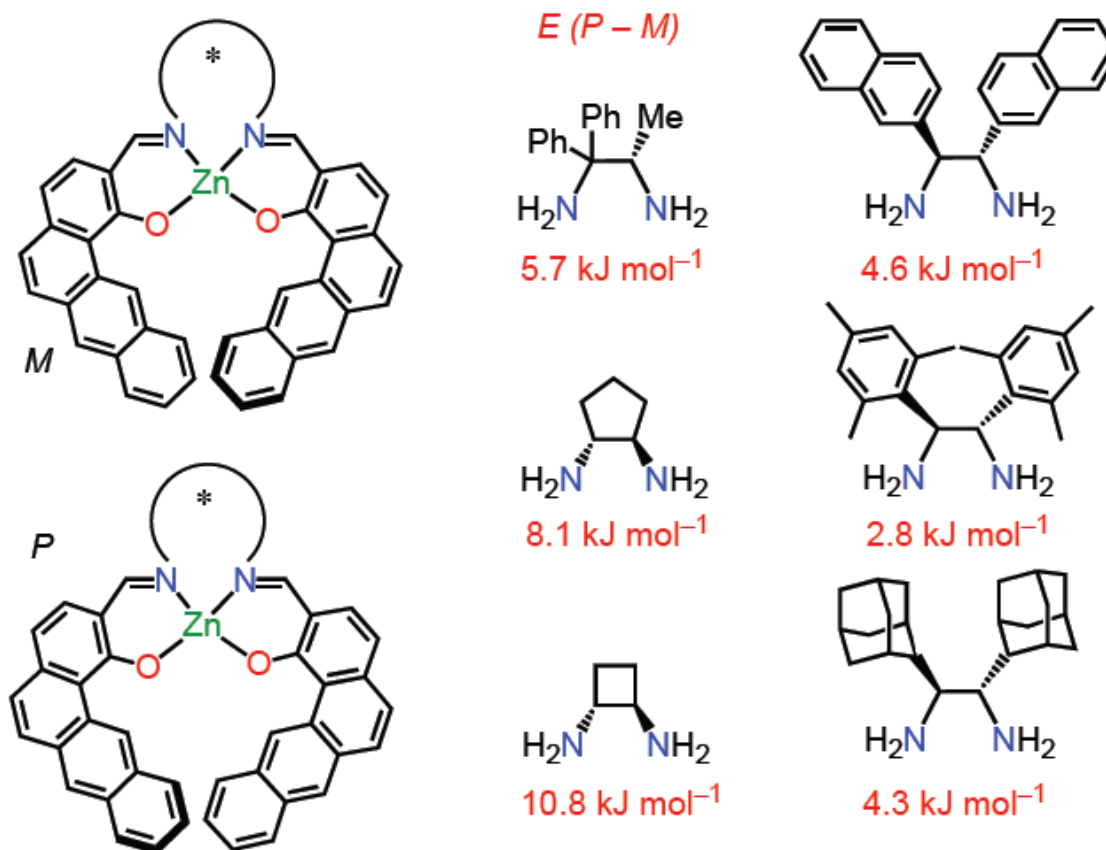


**Figure 2.9** Energy difference between *P* and *M* conformer with respective backbone.

For the synthesis of *trans*-cyclobutane 1,2-diamines, we have mainly used literature procedures with following modifications :

- 1) In step two, 1-cyano-cyclobutane-1,2-dicarboxylic acid dimethyl ester, was prepared from *meso*-dimethyl 2,5-dibromohexane-1,6-dioate and KCN using methanol as the solvent. The reaction was carried out for 67 h. After addition of water, the product was extracted in ethyl acetate and the solvent was removed using vacuum. The obtained product was directly used for next step without further purification.
- 2) Instead of converting tartrate salt to pure diamine, the ligand synthesis was carried out using the tartrate salt of *trans*-cyclobutane-1,2-diamine to avoid yield loss during conversion.

We have measured the specific rotation of the bis(tartrate) salt of *trans*-cyclobutane-1,2-diamine by using polarimeter. Observed data as follow;

$$[\alpha]_D^{20} = 100\alpha/l * C$$

$$(\alpha = +0.32, l= 1 \text{ dm}, C=1.09 \text{ g/100 ml})$$

$$[\alpha]_D^{20} = +31.19 (c 1, \text{H}_2\text{O})$$

The specific rotation value ( $[\alpha]_D^{20}$ ) indicates that the formed enantiomer is dextrorotary enantiomer. In literature, the specific rotation value for the bis(tartrate) salt of *trans*-cyclobutane-1,2-diamine is  $[\alpha]_D^{20} = +28$  with this result they have reported presence of only one enantiomer of the diamine derivative<sup>6</sup> Therefore in our case also we expect to have single enantiomer i.e.(*R*)-enantiomer.

## 2.4 Conclusion

In conclusion, the modeling and the calculations presented us the opportunity to take a critical look at this novel salen complex. On the basis of our computational study of various backbone for salen ligand and also the literature study shows that the cyclobutyl ring could be good replacement for cyclohexyl backbone. To synthesize monohelical salen complexes, we have chose *trans*-cyclobutane-1,2-diamine as the source of chirality and we were able to synthesize

*trans*-cyclobutane-1,2-diamine with few modification to the literature procedure. The analysis of synthesized tartrate salt of diamine confirms formation of enantiopure product and the formed salt will be directly used for ligand synthesis explained in coming chapter.

## References

---

- <sup>1</sup> Wiznycia, A., Desper J.; Levy, C. *Chem. Commun.*, **2005**, 4693.
- <sup>2</sup> Wiznycia, A.; Desper, J; Levy, C. *Inorg. Chem.*, **2006**, 45, 10034.
- <sup>3</sup> Barman, S.; Patil, S.; Desper, J.; Aikens, C.; Levy, C. *Eur. J. Inorg. Chem.* **2013**, 5708–5717.
- <sup>4</sup> Dong, Z.; Karpowicz, R; Bai, S.; Yap, G.; Fox, J., *J. Am. Chem. Soc.* **2006**. 128, 14242-14243.
- <sup>5</sup> Houk, K.; DeMello, N.; Condroski, K.; Fennen, J.; Kasuga, T. *Origins of Stereoselectivity in Jacobsen Epoxidations, at Electronic Conference on Heterocyclic Chemistry, ECHET96*; Rzepa, H. S., Snyder, J. P.; Leach, C., Eds., London, 24/6–22/7, **1996**; (<http://www.ch.ic.ac.uk/ectoc/echet96/>).
- <http://www.ch.ic.ac.uk/ectoc/echet96>.
- <sup>6</sup> Daly, M.; Gilheany, D. *Tetrahedron: Asymmetry* ,**2003**, 14, 127–137
- Brunet, J.-J.; Herbowski, A.; Neibecker, D. *Synth. Commun.***1996**, 26, 483–493.
- <sup>8</sup> Toftlund, H.; Pedersen, E. *Acta Chem. Scand.* **1972**, 26, 4019–4030.
- <sup>9</sup> Hehre W. *A guide to molecular mechanics and Quantum Chemical calculations in Spartan*. Wavefunction, Inc. ISBN 1-890661-18-X, **2003**.

# Chapter 3 - Synthesis and characterization of novel ligands with (1*R*,2*R*)-cyclobutyl backbone

## 3.1 Introduction

Chiral tetradentate Schiff-base ligands have numerous attractive features that constitute the basis for their effectiveness in asymmetric reactions. Salens are a type of tetradentate Schiff-base ligand which commonly prepared by the condensation of two equivalents of a salicylaldehyde derivative with a 1,2-diamine. Chiral versions of this tetradentate bis(imine) ligand are prepared simply by using chiral 1,2-diamines, although ligands derived from other diamines (1,3-, 1,4-, etc.) are often included in this class. Related tetradentate Schiff-base ligands with neutral pyridine-type donors can be produced by condensing a diamine with a pyridine aldehyde. These ligands are overall neutral in their binding to metal ions. The condensation to generate the tetradentate Schiff-base ligands generally proceeds in nearly quantitative yield (Figure 3.1).

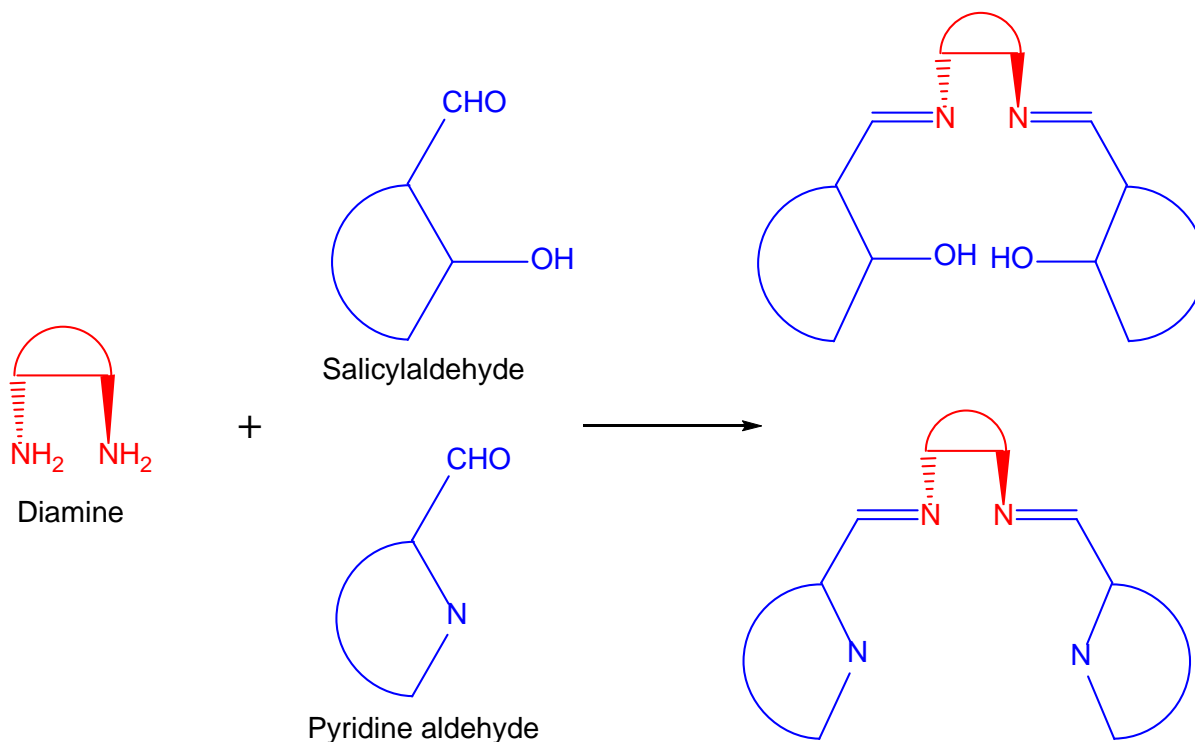


**Figure 3.1** General scheme of tetradentate Schiff-base ligand formation from 1,2-diamines.

Metal complexes of above mentioned salen ligands are readily prepared from a variety of first row and second row transition metal salts as well as main group metals, with the ligand being dianionic after the loss of phenoxy protons. Once the suitable metal for the preferred reactivity has been identified, the modularity of synthesis of ligands permits the systematic tuning of catalyst steric and electronic properties by alteration of the metal counterion, the chiral diamine or the salicylaldehyde components.<sup>1</sup> It is striking that salen ligand has often been found to be the optimum ligand for a broad range of reactions catalyzed by several different metals.<sup>2</sup>

Figure 3.2 shows a few examples of ligands available with a 1,2-cyclobutyl backbone that have been prepared for previous studies.<sup>3,4</sup>

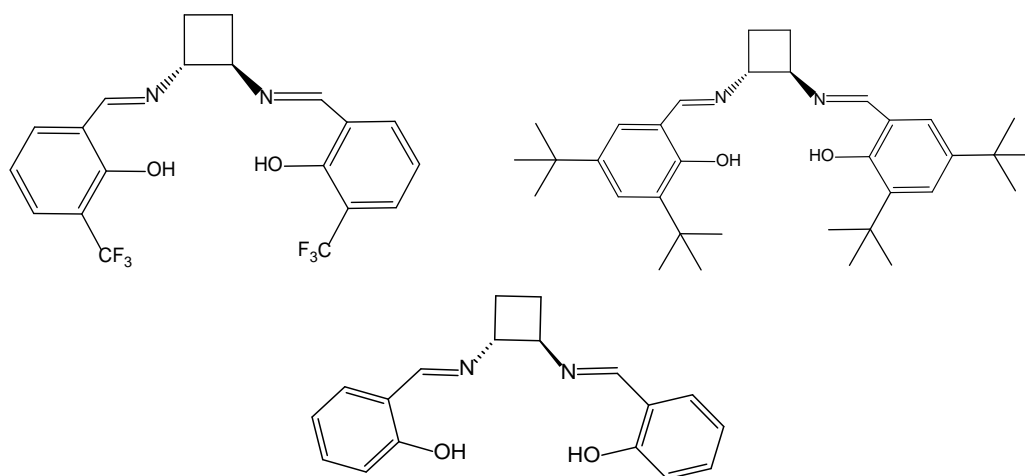


**Figure 3.2** Some previously synthesized ligand with cyclobutyl backbone.

In this chapter, we will be discussing synthesis and characterization of novel ligand bearing cyclobutyl backbone. For synthesis of these ligands, We have used three different types of sidearm according to their functional advantages in asymmetric catalysis.

## 3.2 Experimental

### 3.2.1 Synthesis

<sup>1</sup>H, 2D and <sup>13</sup>C NMR spectra were recorded on a Varian Unity plus 400 MHz or 200 MHz spectrometer in CDCl<sub>3</sub> or DMSO-*d*<sub>6</sub>. Data is expressed in parts per million (ppm) downfield shift from tetramethylsilane or residual protiosolvent as internal reference and are

reported as position (in ppm), multiplicity (s = singlet, d = doublet, t = triplet, m = multiplet), coupling constant ( $J$  in Hz) and integration (number of protons). IR spectra were collected on neat sample using Nicolet 380 FT-IR (Thermo Scientific, Madison MN) at room temperature. UV-Vis spectra were obtained on a Varian Cary 500 scan UV-Vis-NIR spectrophotometer (Agilent Technologies) in tetrahydrofuran (THF). The solution samples for UV-Vis were prepared at room temperature, with the concentrations ranging between  $1.5$  and  $2.5 \times 10^{-5}$  M. A  $1.00$  cm path length quartz cell was employed for analyses. High resolution electrospray ionization (HR-ESI) mass spectra were acquired on a LCT Premier (Waters Corp., Milford MA) time of flight mass spectrometer.

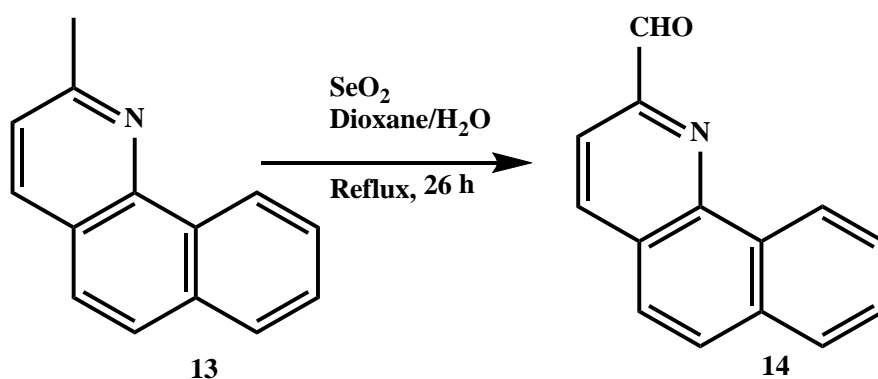
### 3.2.1.1 1-Hydroxybenz[*a*]anthracene-2-carboxaldehyde, 11<sup>5</sup>

Synthesis was carried out using literature procedures<sup>5</sup> and  $^1\text{H}$  NMR data collected for the pure material was consistent with literature.

### 3.2.1.2 4-Hydroxy-3-phenanthrenecarboxaldehyde, 12<sup>6</sup>

Synthesis was carried out using reported procedures and  $^1\text{H}$  NMR data collected for the pure material was consistent with literature.

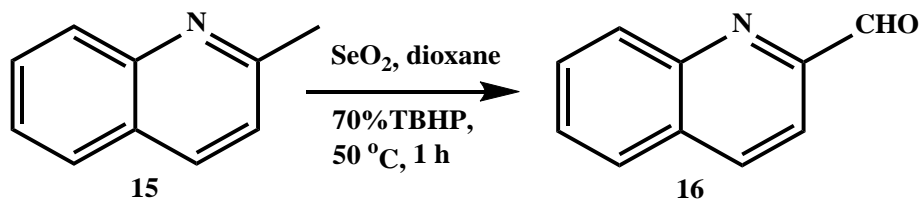
### 3.2.1.3 2-Formylbenzoquinoline, 14<sup>7</sup>



Synthesis was carried out using literature procedures except purification the crude material was achieved by sublimation.  $^1\text{H}$  NMR ( $\text{CDCl}_3$ , 400 MHz):  $\delta$  7.75 (d, 1 H, CH), 7.79 (t, 1 H, CH), 7.84 (t, 1 H, CH), 7.95 (d, 1 H, CH), 7.97 (d, 1 H, CH), 8.19 (d, 1 H, CH), 8.34 (d, 1 H,

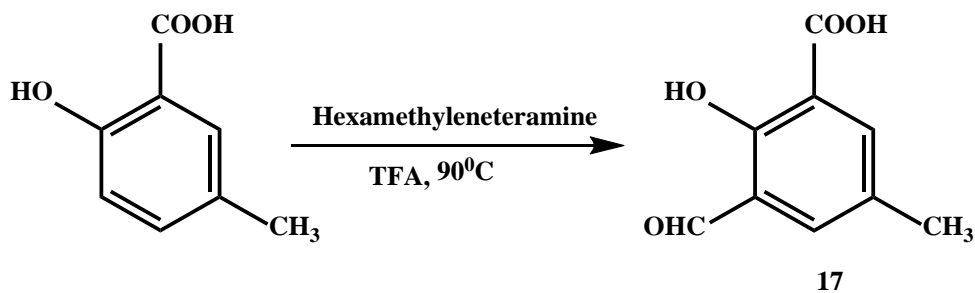
CH), 9.44 (d, 1 H, CH), 10.37 (s, 1 H, CH).  $^{13}\text{C}$  NMR ( $\text{CDCl}_3$ , 100 MHz):  $\delta$  194.21, 151.29, 146.57, 136.93, 133.91, 131.63, 130.83, 129.12, 129.04, 128.17, 127.94, 125.04, 124.69, 118.60.

### 3.2.1.4 2-Formylquinoline, **16**<sup>8</sup>



To a solution of  $\text{SeO}_2$  (2.55 g, 23.0 mmol) in dioxane (20 mL) was added dropwise 70% TBHP (10 mmol) and the mixture was stirred for 0.5 h at room temperature to form the complex. After the quinoline **15** (1.43 g, 10.0 mmol) was added to the mixture, the resulting solution was heated for 1 h at 50°C. The reaction mixture was filtered and the solvent was evaporated to give the residue which was, after addition of a little amount of water, extracted with  $\text{CHCl}_3$ . The  $\text{CHCl}_3$  fraction was evaporated. The residue is purified by sublimation to afford white crystalline product **16** (1.25 g, 80%).  $^1\text{H}$  NMR ( $\text{CDCl}_3$ , 400 MHz):  $\delta$  7.70 (t, 1 H, CH), 7.83 (t, 1 H, CH), 7.92 (d, 1 H, CH), 8.04 (d, 1 H, CH), 8.26 (d, 1 H, CH), 8.32 (d, 1 H, CH), 10.24 (s, 1 H, CH).  $^{13}\text{C}$  NMR (100 MHz)  $\delta$  193.92, 152.53, 147.84, 137.28, 130.60, 130.54, 129.31, 127.97, 77.48, 77.16, 76.84, 28.45.

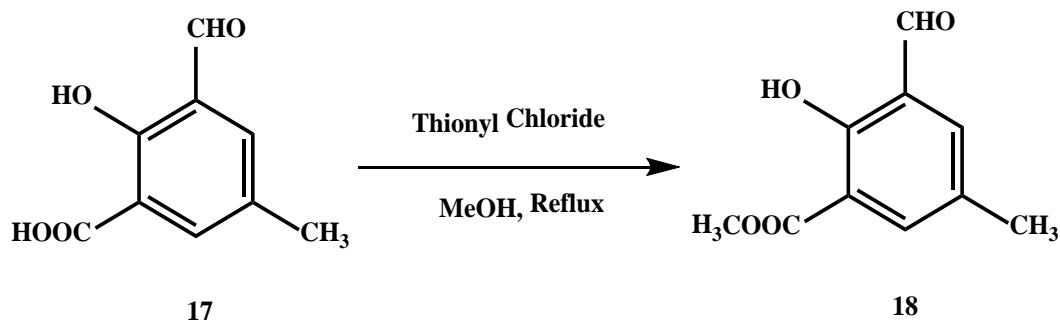
### 3.2.1.5 5-methyl-3-formyl Salicylic acid, **17**<sup>9</sup>



A solution of 5-methylsalicylic acid (5.0 g, 33 mmol) and hexamethylenetetramine (22 g, 150 mmol) in TFA was warmed to 90 °C and stirred for 14 h. The orange solution that resulted was poured into dilute hydrochloric acid (1 M, 500 mL) and the solution was stirred for a further

6 h. The white precipitate that resulted was filtered and then dried in a vacuum desiccator for 2 days. 5-methyl-3-formyl salicylic acid **17** (5.7 g, 97 %) was obtained as a damp off-white solid.  $^1\text{H}$  NMR (DMSO, 400 MHz):  $\delta$  2.20 (s, 3 H,  $\text{CH}_3$ ), 7.61 (d, 1 H, CH), 7.81 (d, 1 H, CH), 10.22 (s, 1 H, CH).  $^{13}\text{C}$  NMR (100 MHz, DMSO)  $\delta$  189.43, 172.08, 162.06, 137.55, 134.35, 128.76, 123.84, 115.00, 20.19.

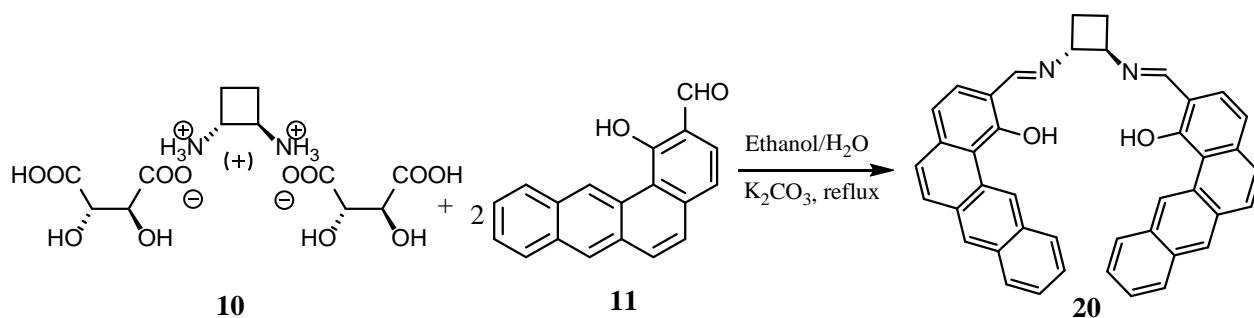
### 3.2.1.6 5-methyl-3-formyl salicylic ester, **18**<sup>10</sup>



The 5-methyl-2-formyl salicylic acid (193 g, 1.07 mol) **17** was dissolved in methanol, thionyl chloride (150 mL) was added and the mixture was refluxed till NMR showed absence of starting material peaks. After cooling, the precipitate was collected by filtration and dried to obtain methyl 5-methyl-3-formyl salicylic ester **19** (190 g, 91%).  $^1\text{H}$  NMR (400 MHz,  $\text{CDCl}_3$ ):  $\delta$  2.33 (s, 3 H,  $\text{CH}_3$ ), 3.98 (s, 3 H,  $\text{OCH}_3$ ), 7.83 (s, 1H, CH), 7.91 (s, 1H, CH), 10.47 (s, 1H, CHO), 11.31 (s, 1H, OH).  $^{13}\text{C}$  NMR (100 MHz,  $\text{CDCl}_3$ )  $\delta$  189.39, 169.95, 161.94, 136.86, 135.11, 128.67, 124.12, 113.97, 52.75, 20.33.

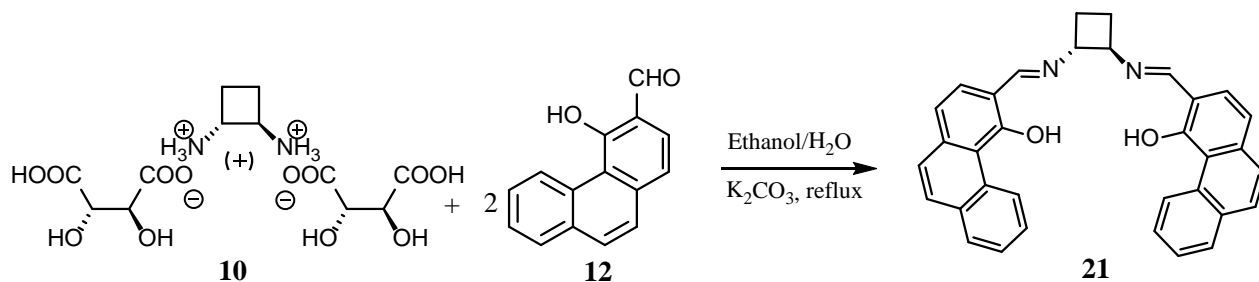
## 3.2.2 Synthesis of ligands

### 3.2.2.1 2,2'-[(1R,2R)-1,2-Cyclobutanediylbis(nitrilomethylidene)]bisbenz[a]anthracen-1-ol, ((R,R)-**20**)



To a solution of (*R,R*)-1,2-dimmoniumcyclobutane bis-(+)-tartrate salt (**10**, 418 mg, 1.08 mmol) in 100 mL of EtOH and 5 mL of H<sub>2</sub>O was added K<sub>2</sub>CO<sub>3</sub> (543 mg, 3.93 mmol). The mixture was heated at 70°C for 10 min. To this solution was added 1-hydroxybenz[*a*]anthracene-2-carboxaldehyde (**11**, 554 g, 2.16 mmol) and the resulting yellow mixture was heated at reflux for 30 min. The reaction was cooled to room temperature, and the volume reduced to approximately 50 mL. At that point, H<sub>2</sub>O (200 mL) was added to induce the precipitation of the title compound. The yellow precipitate was filtered and redissolved in 120 mL of CH<sub>2</sub>Cl<sub>2</sub>, and washed with 100 mL of brine followed by 100 mL of distilled water. The solution was then dried over anhydrous Na<sub>2</sub>SO<sub>4</sub> and filtered. The solvent was removed *in vacuo* to give the ligand (*R,R*)-**20** (610 mg, 95.0 % yield) as a powder. <sup>1</sup>H NMR (400 MHz, CDCl<sub>3</sub>) δ 2.27–2.26 (m, 2 H, CH), 2.48–2.47 (m, 2 H, CH), 3.34–3.32 (m, 2 H, CH), 7.24 (d, 2 H, CH), 7.38 (d, 2H, CH), 7.52 (d, 2 H, CH), 7.57–7.55 (m, 4 H, CH), 7.90 (d, 2 H, CH), 8.05–8.02 (m, 2 H, CH), 8.25–8.23 (m, 2 H, CH), 8.36 (s, 2 H, CH), 8.42 (s, 2 H, N=CH), 10.66 (s, 2 H, CH), 15.72 (s, 2 H, OH). <sup>13</sup>C NMR (100 MHz, CDCl<sub>3</sub>) δ 165.74, 164.25, 137.31, 132.87, 131.31, 131.27, 131.15, 129.88, 129.61, 129.28, 128.14, 127.51, 127.21, 126.67, 125.99, 125.60, 120.21, 118.74, 115.30, 68.10, 24.34. ESI-MS (MeOH) *m/z*: Calc M+H = C<sub>42</sub>H<sub>31</sub>N<sub>2</sub>O<sub>2</sub> = 595.2386, 3.2 ppm; found 595.2405, Calc M+Na = C<sub>42</sub>H<sub>30</sub>N<sub>2</sub>O<sub>2</sub>Na = 617.2205, 4.1 ppm; found 617.2230.

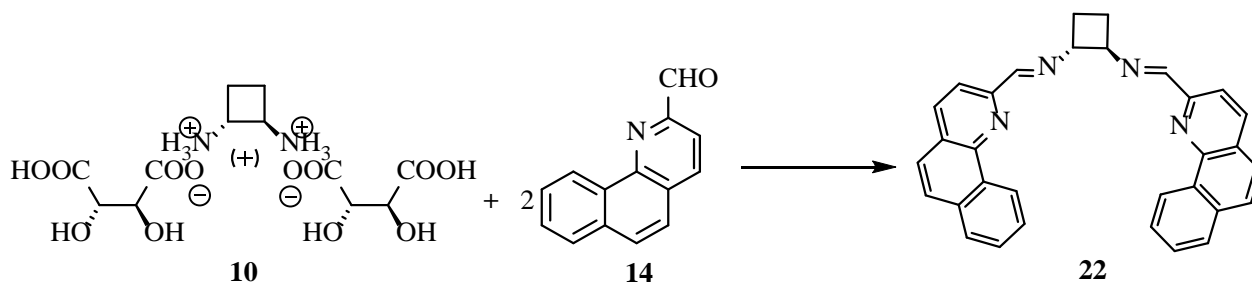
### 3.2.2.2 3,3'-[(1*R*,2*R*)-1,2-Cyclobutanediylbis(nitrilomethylidene)]bis-4-phenanthrenol, ((*R,R*)-**21**)



To a solution of (*R,R*)-1,2-diammoniumcyclobutane bis-(+)-tartrate salt (**10**, 418 mg, 1.08 mmol) in 100 mL of EtOH and 5 mL of H<sub>2</sub>O was added K<sub>2</sub>CO<sub>3</sub> (543 mg, 3.93 mmol). The mixture was heated at 70°C for 10 min. To this solution was added 4-Hydroxy-3-

phenanthrenecarboxaldehyde (**12**, 484 mg, 2.16 mmol) the resulting yellow mixture was heated at reflux for 30 min. The reaction was cooled to room temperature, and the volume was reduced to approximately 50 mL. At that point, H<sub>2</sub>O (200 mL) was added to induce the precipitation of the title compound. The yellow precipitate was redissolved in 120 mL of CH<sub>2</sub>Cl<sub>2</sub>, and washed with 100 mL of brine followed by 100 mL of distilled water. The solution was then dried over anhydrous Na<sub>2</sub>SO<sub>4</sub> and filtered. The solvent was removed *in vacuo* to give the ligand (*R,R*)-**21** (512 mg, 96.0 % yield) as a powder. <sup>1</sup>H NMR (400 MHz, CDCl<sub>3</sub>) δ 2.22–2.21 (m, 2 H, CH), 2.46–2.45 (m, 2 H, CH), 4.28–4.26 (m, 2 H, CH), 7.22 (d, 2 H, CH), 7.31 (d, 2 H, CH), 7.63–7.56 (m, 4 H, CH), 7.73–7.69 (m, 2 H, CH), 7.87 (d, 2 H, CH), 7.89 (dd, 2 H, CH), 8.33 (s, 2 H, N=CH), 10.11 (d, 2 H, CH), 15.45 (s, 2 H, OH). <sup>13</sup>C NMR (100 MHz, CDCl<sub>3</sub>) δ 168.28, 163.68, 137.37, 132.47, 131.71, 130.93, 129.20, 128.47, 128.23, 127.44, 127.02, 126.00, 121.06, 118.25, 113.93, 67.37, 24.29. ESI-MS (MeOH) *m/z*: Calc M+H = C<sub>34</sub>H<sub>27</sub>N<sub>2</sub>O<sub>2</sub> = 495.2073, 4.4 ppm; found 495.2052, Calc M+Na = C<sub>34</sub>H<sub>26</sub>N<sub>2</sub>O<sub>2</sub>Na = 517.1892, 0.6 ppm; found 517.1895.

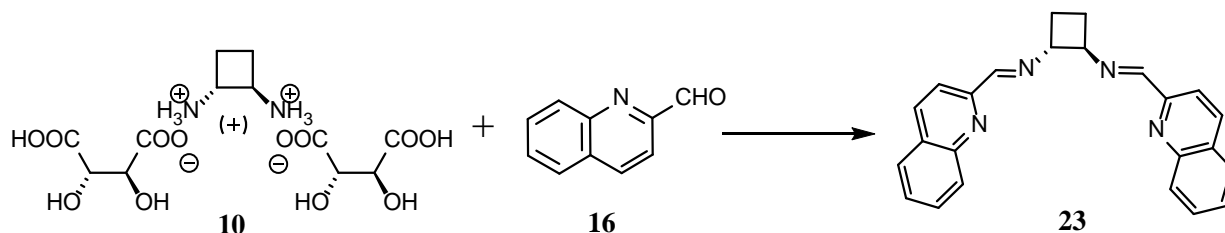
### 3.2.2.3 (*1R,2R*)-*N,N'*-Bis[(2-benzoquinolyl)methylene]-1,2-cyclobutanediamine, ((*R,R*)-**22**)



2-Formylbenzoquinoline (**14**, 25.0 mg, 0.125 mmol), *trans*-cyclobutane-1,2-diamine (**10**, 22 mg, 0.075 mmol) and sodium methoxide (15.0 mg, 0.375 mmol) were added in a porcelain mortar and pestle. To this mixture 4-5 drops of ethanol were added and the mixture was ground at room temperature for 5 minutes. The product was then extracted in chloroform and vacuum dried to give pure product **22** in (33 mg, 98%) in high yield. <sup>1</sup>H NMR (400 MHz, CDCl<sub>3</sub>) δ 2.23–2.21 (m, 2 H, CH), 2.43–2.42 (m, 2 H, CH), 4.53–4.51 (m, 2 H, CH), 7.67 (d, 2 H, CH), 7.69 (t, 2 H, CH), 7.71 (t, 2 H, CH), 7.82 (d, 2 H, CH), 7.91 (d, 2 H, CH), 8.22 (d, 2 H, CH), 8.36 (d, 2 H, CH), 8.74 (s, 2 H, N=CH), 9.35 (d, 2H, CH). <sup>13</sup>C NMR (100 MHz, CDCl<sub>3</sub>) δ 161.81, 153.68,

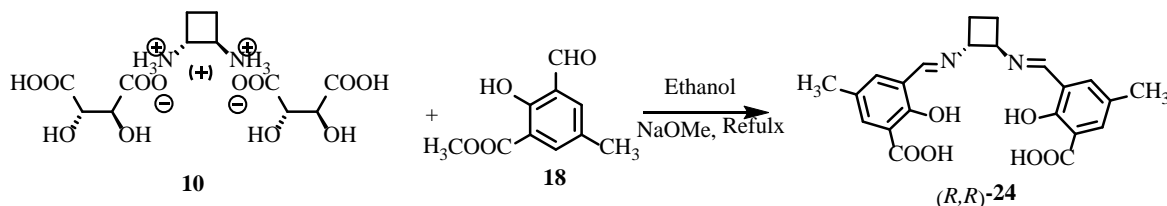
146.15, 136.36, 133.86, 131.66, 128.77, 128.41, 128.00, 127.35, 127.21, 125.33, 124.56, 119.20, 69.87, 23.94. Calc M+H = C<sub>32</sub>H<sub>25</sub>N<sub>4</sub> = 465.2079, 2.8 ppm; found 465.2066.

### 3.2.2.4 (1*R*,2*R*)-*N,N'*-Bis[(2-quinolinyl)methylene]-1,2-cyclobutanediamine), ((*R,R*)-23)



2-Formylquinoline (**16**, 17.0 mg, 0.125 mmol), *trans*-cyclobutane-1,2-diamine (**10**, 22 mg, 0.075 mmol) and sodium methoxide (15 mg, 0.75 mmol) were combined in a porcelain mortar and pestle. To this mixture 4-5 drops of ethanol were added and ground at room temperature for 5 minutes. The product was then extracted in chloroform and vacuum dried to give a pure product in high yield (27 mg, 99%). <sup>1</sup>H NMR (400 MHz, CDCl<sub>3</sub>) δ 2.18-2.16 (m, 2 H, CH), 2.40-2.38 (m, 2 H, CH), 4.48-4.45 (m, 2 H, CH), δ 7.60-7.56 (m, 2H, CH), 7.75-7.72 (m, 2 H,CH), 7.86-7.82 (m, 2 H,CH)8.12 (d, 2 H, CH), 8.22 (d, 2H, CH), 8.32 (d, 1 H, CH), 8.59 (s, 1 H, N=CH). <sup>13</sup>C NMR (100 MHz, CDCl<sub>3</sub>) δ 161.25, 155.06, 147.97, 136.65, 129.92, 129.75, 128.96, 127.88, 127.56, 118.63, 69.74, 23.85, 0.15. Calc M+H = C<sub>24</sub>H<sub>21</sub>N<sub>4</sub> = 365.1766, 2.8 ppm; found 365.1725.

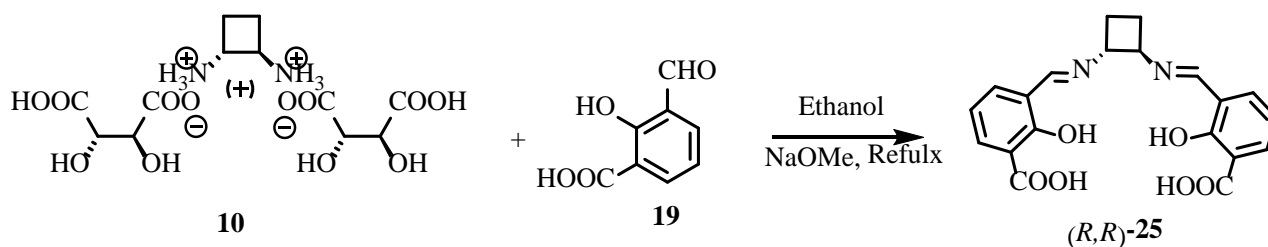
### 3.2.2.5 3,3'-[(1*R*,2*R*)-1,2-cyclobutanediylbis(nitrilomethylidene)]bis[2-hydroxybenzoic acid], ((*R,R*)-24*a*)



To a solution of (*R,R*)-1,2-diammoniumcyclobutane *bis*-(+)-tartrate salt (**10**, 192 mg , 5.00 mmol) in 100 mL of dry EtOH was added NaOMe (216 mg, 40.0 mmol). The mixture was

heated at 70°C for 10 min. To this solution was added 3-formylsalicylic acid ester (**18**, 180 mg, 10 mmol) and the resulting yellow mixture was heated at reflux overnight. The reaction was cooled to room temperature, and the volume reduced to approximately 50 mL. The yellow precipitate was filtered and washed with CH<sub>3</sub>Cl to remove unreacted sidearm. Finally (161 mg, 79.0 %) of yellow product, (*R,R*)-**24**, was obtained. <sup>1</sup>H NMR (400 MHz, DMSO) δ 1.88-1.86 (m, 2 H, CH), 2.28 (s, 3 H, CH<sub>3</sub>), 4.06-4.04 (m, 2 H, CH), 7.58 (s, 4H, CH), 8.58 (s, 2H, N=CH), 17.25 (s, 2 H, COOH). <sup>13</sup>C NMR (100 MHz, DMSO) δ 171.39, 161.81, 155.11, 133.22, 128.66, 123.59, 122.01, 120.71, 70.39, 40.26, 40.05, 39.84, 39.42, 39.21, 39.00, 23.57, 20.26. (One backbone signal overlap with side arm methyl signal), Calc M+H = C<sub>22</sub>H<sub>23</sub>N<sub>2</sub>O<sub>6</sub> = 411.1556, 2.4 ppm; found 411.1546, Calc (M+Na)<sup>+</sup> = C<sub>22</sub>H<sub>22</sub>N<sub>2</sub>O<sub>6</sub>Na = 433.1376; found 433.1349.

### 3.2.2.6 3,3'-[*(1R,2R)*-1,2-cyclobutanediylbis(nitrilomethylidene)]bis[2-hydroxybenzoic acid], (*R,R*)-**24b**)



To a solution of (*R,R*)-1,2-diammoniumcyclobutane *bis*-(+)-tartrate salt (**10**, 192 mg , 5.00 mmol) in 100 mL of dry EtOH was added NaOMe (216 mg, 40.0 mmol). The mixture heated at 70°C for 10 min. To this solution was added 3-formylsalicylic acid (**19**, 180 mg, 10 mmol) the resulting yellow mixture was heated at reflux overnight. The reaction was cooled to room temperature, and the volume reduced to approximately 50 mL. The yellow precipitate was filtered and washed with CH<sub>3</sub>Cl to remove unreacted sidearm. Finally (161 mg, 79.0 %) yellow product, (*R,R*)-**25**, was obtained. <sup>1</sup>H NMR (400 MHz, DMSO) δ 1.88-1.86 (m, 2 H, CH), 2.28 (s, 3 H, CH<sub>3</sub>), 4.06-4.04 (m, 2 H, CH), 7.58 (s, 4H, CH), 8.58 (s, 2H, N=CH), 17.25 (s, 2 H, COOH). <sup>13</sup>C NMR (100 MHz, DMSO) δ 171.39, 161.81, 155.11, 133.22, 128.66, 123.59, 122.01, 120.71, 70.39, 40.26, 40.05, 39.84, 39.42, 39.21, 39.00, 23.57, 20.26. Calc M-H = C<sub>20</sub>H<sub>17</sub>N<sub>2</sub>O<sub>6</sub> = 381.1087; found 381.1077, 2.5 ppm.

### 3.3 Results & Discussion

The precursors for the ligand synthesis are prepared first (Figure 3.3). The chiral diamine salt, *trans*-cyclobutane-1,2-diamine, **10** was prepared by the procedure outlined in chapter 2.

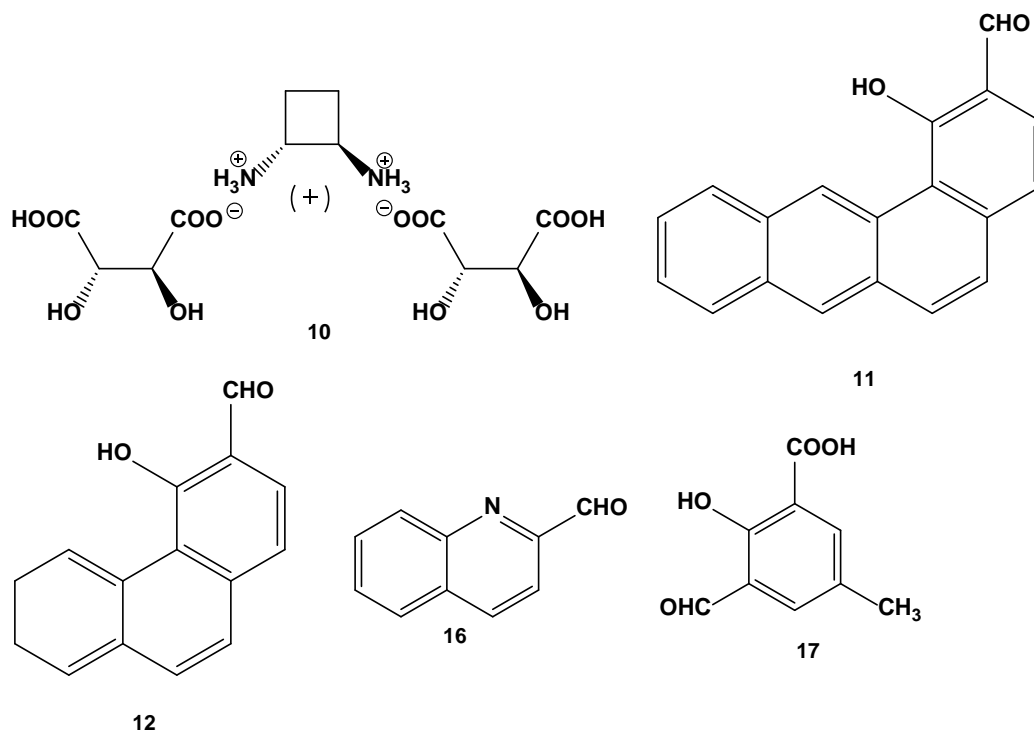


**Figure 3.3** The precursors for ligand synthesis.

Synthesis of ligands (*R,R*)-**20** and (*R,R*)-**21** involves a simple Schiff base condensation reaction of **10** with the appropriate sidearm, **11** or **12** respectively, Figure 3.4. The neutral diamine is subject to oxidation, so we have used the tartaric acid salt of the diamine instead, to avoid yield loss during conversion. First the diamine salt was stirred with base ( $\text{K}_2\text{CO}_3$ ) for *in situ* conversion into diamine and then the respective sidearm was added in the same pot. After reaction completion, water was added to induce preprecipitate formation. Further product was redissolved and washed with brine to afford pure product. Synthesis of ligands was carried out without using inert conditions, however subsequent analysis ( $^1\text{H}/^{13}\text{C}$  NMR) required the use of dry solvent as there is facile decomposition in solution via hydrolysis of the imine bond. As solids, the ligands are stable to decomposition from atmospheric moisture.

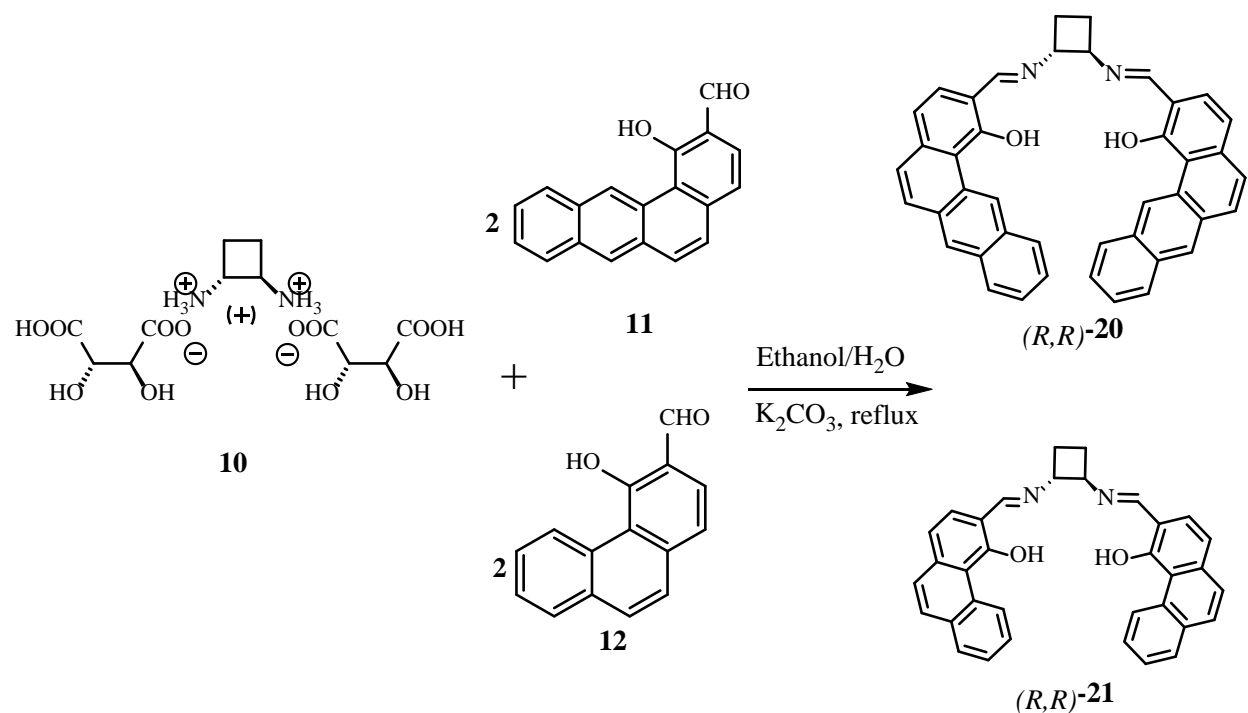


**Figure 3.4** Synthetic scheme for ligands **(R,R)-20** and **(R,R)-21**.

The ligands **(R,R)-22** and **(R,R)-23** were synthesized by solvent assisted grinding. Initially, we tried the condensation reaction using ethanol as the solvent, but this resulted in low yields and impure product. Solvent assisted grinding is a 'greener' process, which also gives very high yields and pure products for these ligands. In this method, the diamine salt **10** is ground with the appropriate sidearm, **14** or **16**, respectively in presence of base and few drops of solvent (Figure 3.5). The ( $^1\text{H}/^{13}\text{C}$  NMR) analysis required the use of dry solvent due to facile decomposition of the imine bond *via* hydrolysis. The ligands are stored under an inert atmosphere to avoid decomposition from atmospheric moisture.

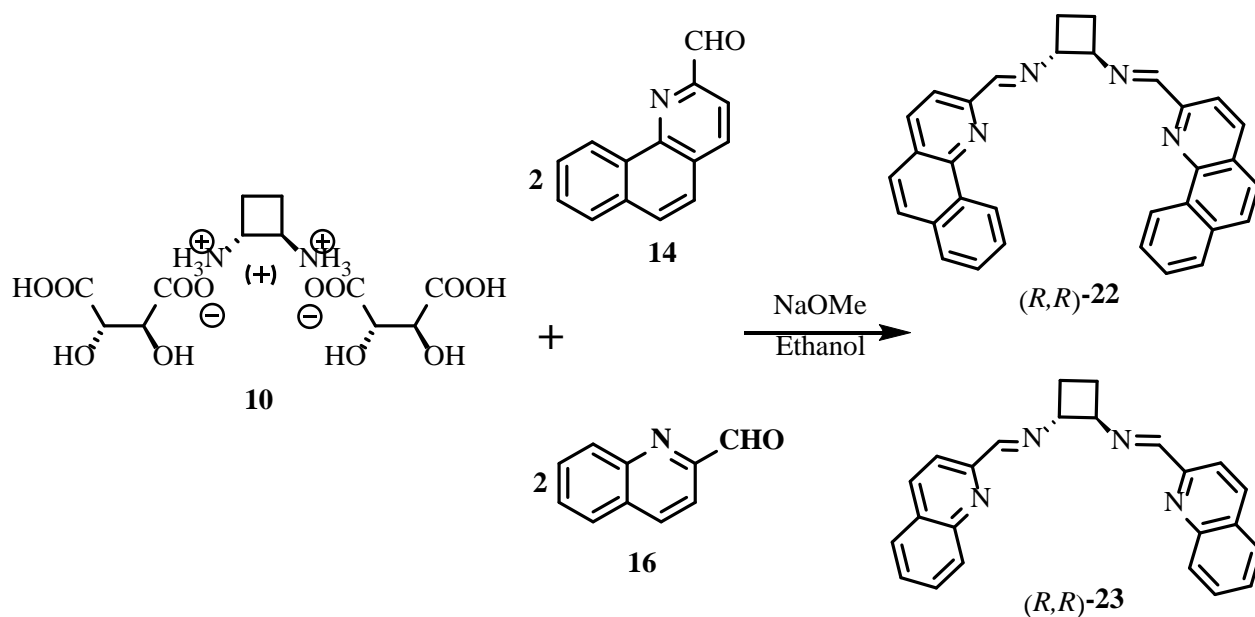


**Figure 3.5** Synthetic scheme for ligands *(R,R)*-22 and *(R,R)*-23 by solvent-assisted grinding.

Synthesis of ligands *(R,R)*-24 and *(R,R)*-25 is accomplished by Schiff-base condensation reactions of the diamine salt **10** with sidearm **18** or **19** (Figure 3.6). The reaction involves conversion of the diamine salt into the free diamine using sodium methoxide as base and then in the same reaction mixture the respective sidearm was added. After completion of the reaction the solid product was purified by chloroform washing. Synthesis of ligands was carried out without using inert conditions, however subsequent analysis ( $^1\text{H}/^{13}\text{C}$  NMR) required the use of dry solvent as there is facile decomposition via hydrolysis of the imine bond. As solids, the ligands are stable to decomposition from atmospheric moisture.

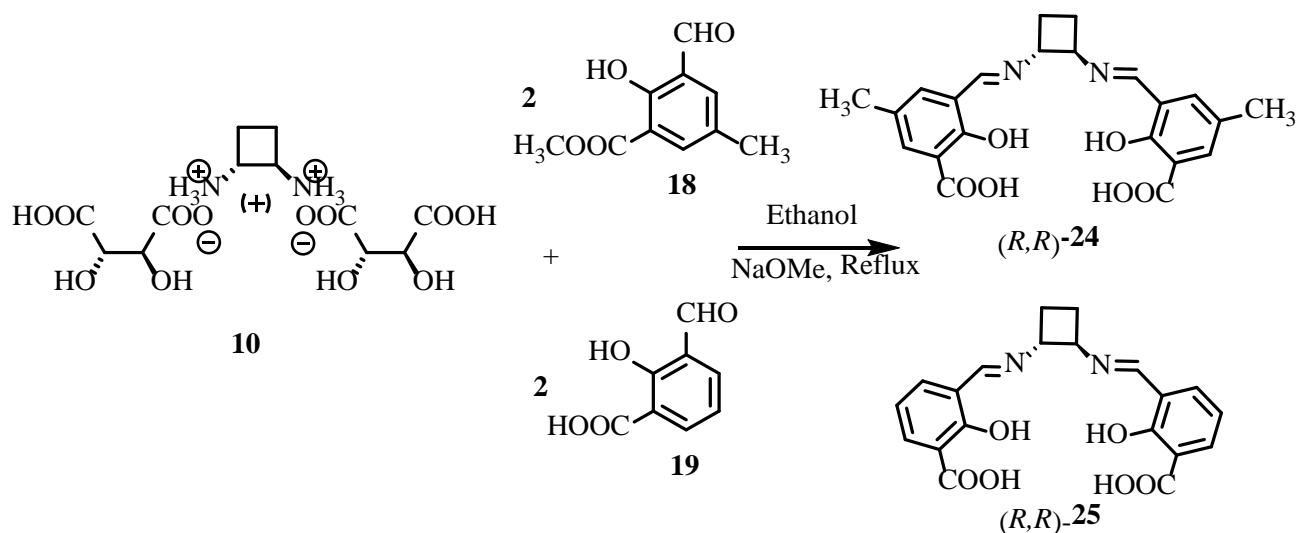


**Figure 3.6** Synthetic scheme for ligands *(R,R)*-24 and *(R,R)*-25.

### 3.3.1 NMR spectroscopy

#### 3.3.1.1 NMR spectroscopy of ligands *(R,R)*-20 and *(R,R)*-21

A similar 1D and 2D NMR analysis was undertaken of the ligand, *(R,R)*-20. The  $^1\text{H}$  NMR spectrum of *(R,R)*-20 with specific assignments is shown in Figure 3.7. Complete assignment of the cyclobutyl backbone was not attempted due to the appearance of broad multiplet peaks in the aliphatic region. This is likely due to fluctuation of the ring and second order effects, not to the presence of multiple conformers. The total number of resonances is half of that possible since the molecule is  $C_2$  symmetric. The imine proton is unique in that it appears as a singlet peak at 8.42 ppm. The doublet peak at 10.66 is also easily assigned as there is a characteristic upfield shift due to a ring current effect in the bay region of the molecule.

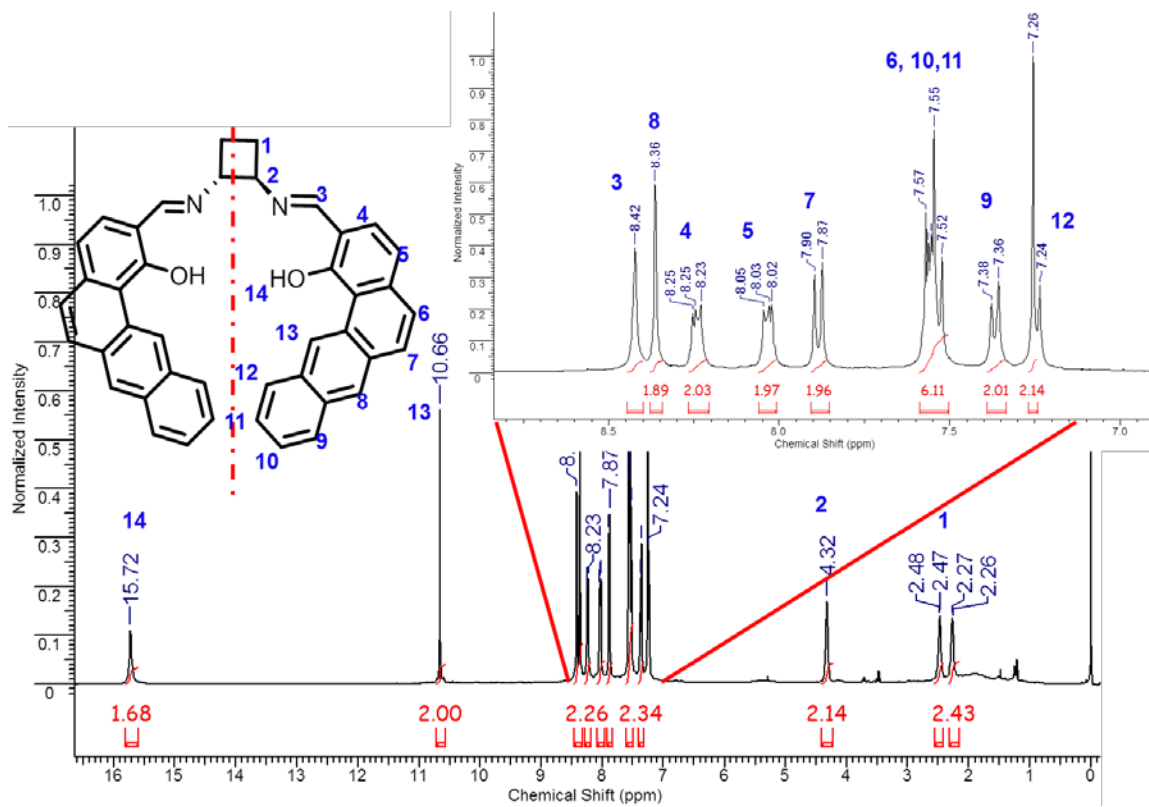


**Figure 3.7** The  $^1\text{H}$  NMR spectrum of  $(R,R)$ -**20** with specific assignments.

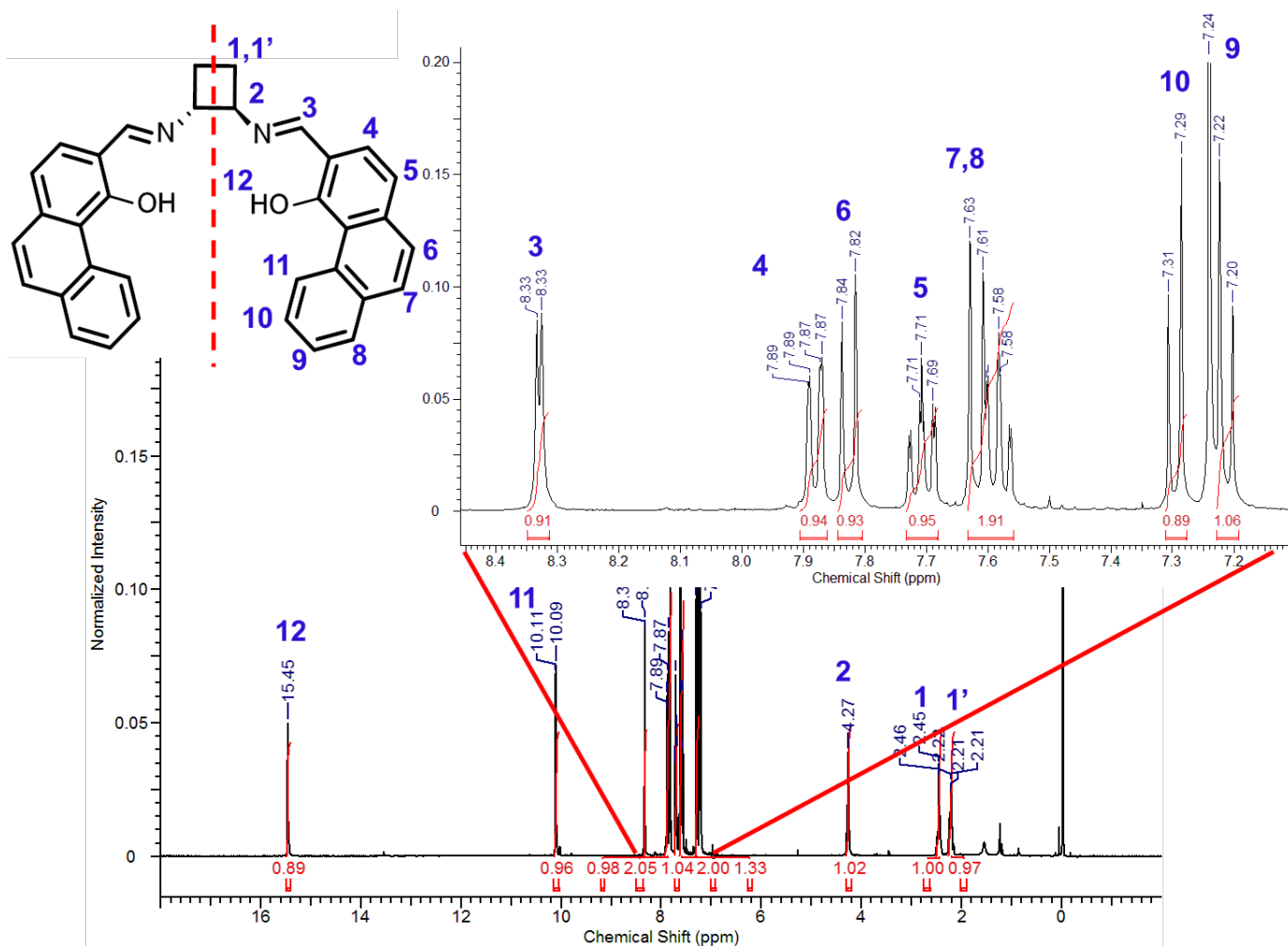


**Figure 3.8** The  $^1\text{H}$  NMR spectrum of  $(R,R)$ -**21** with specific assignments.

The assignments described above for ligand  $(R,R)$ -**20** are also based on 2D COSY NMR spectroscopy. The distinct aromatic bay proton doublet at 10.66 ppm allows for a convenient starting point to assign the remaining aromatic protons of the molecule using the COSY spectra (Figure 3.9). A correlation between the imine proton and the phenolic hydrogen at 15.45 ppm was observed in the COSY. The COSY spectra also allowed the general assignment of signals corresponding to the protons of the cyclobutyl backbone.

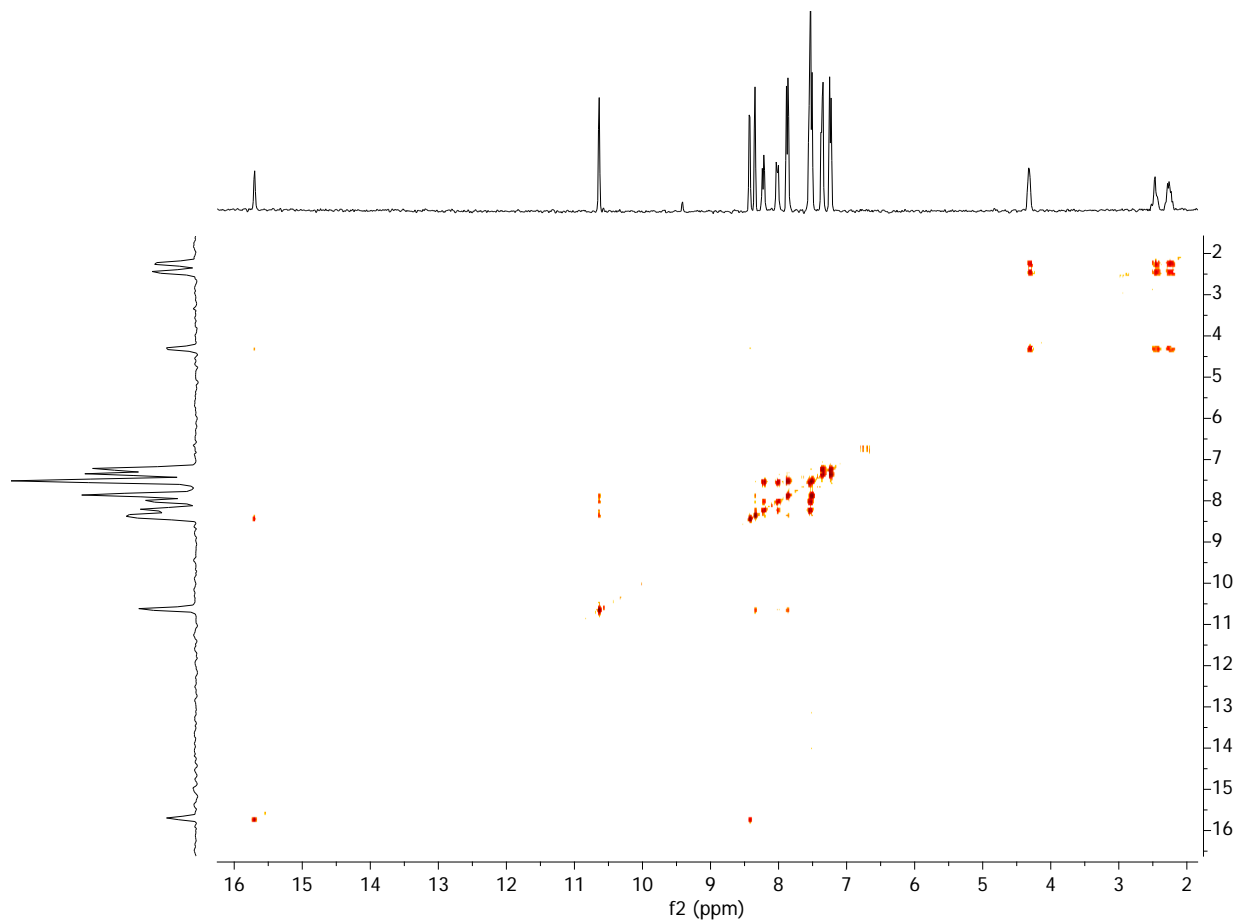


**Figure 3.9** The  $^1\text{H}$ - $^1\text{H}$  COSY NMR spectrum of ligand (*R,R*)-**20**.

### 3.3.1.2 NMR spectroscopy of ligands (*R,R*)-**22** and (*R,R*)-**23**

A similar 1D and 2D NMR analysis was undertaken of the ligand, (*R,R*)-**22**. The  $^1\text{H}$  NMR spectrum of (*R,R*)-**22** with specific assignments is shown in Figure 3.10. Complete assignment of the cyclobutyl backbone was not attempted due to the appearance of broad multiplet peaks in the aliphatic region. This is likely due to fluctuation of the ring and second order effects, not to the presence of multiple conformers. The total number of resonances is half of that possible since the molecule is  $C_2$  symmetric. The imine proton is unique in that it appears as a singlet peak at 8.74 ppm. The doublet peak at 9.33 is also easily assigned as there is a characteristic upfield shift due to a ring current effect in the bay region of the molecule.

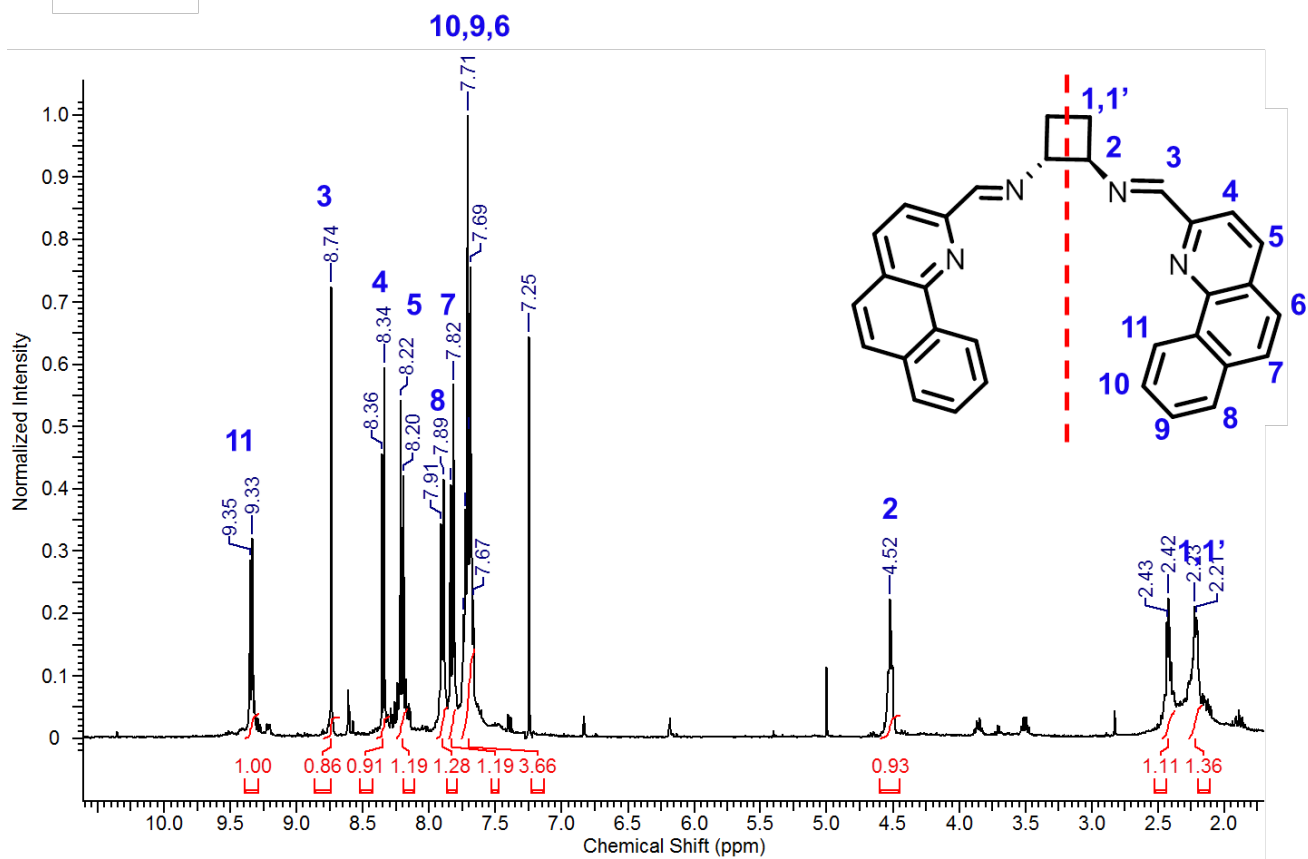


**Figure 3.10** The  $^1\text{H}$  NMR spectrum of  $(R,R)$ -**22** with specific assignments.

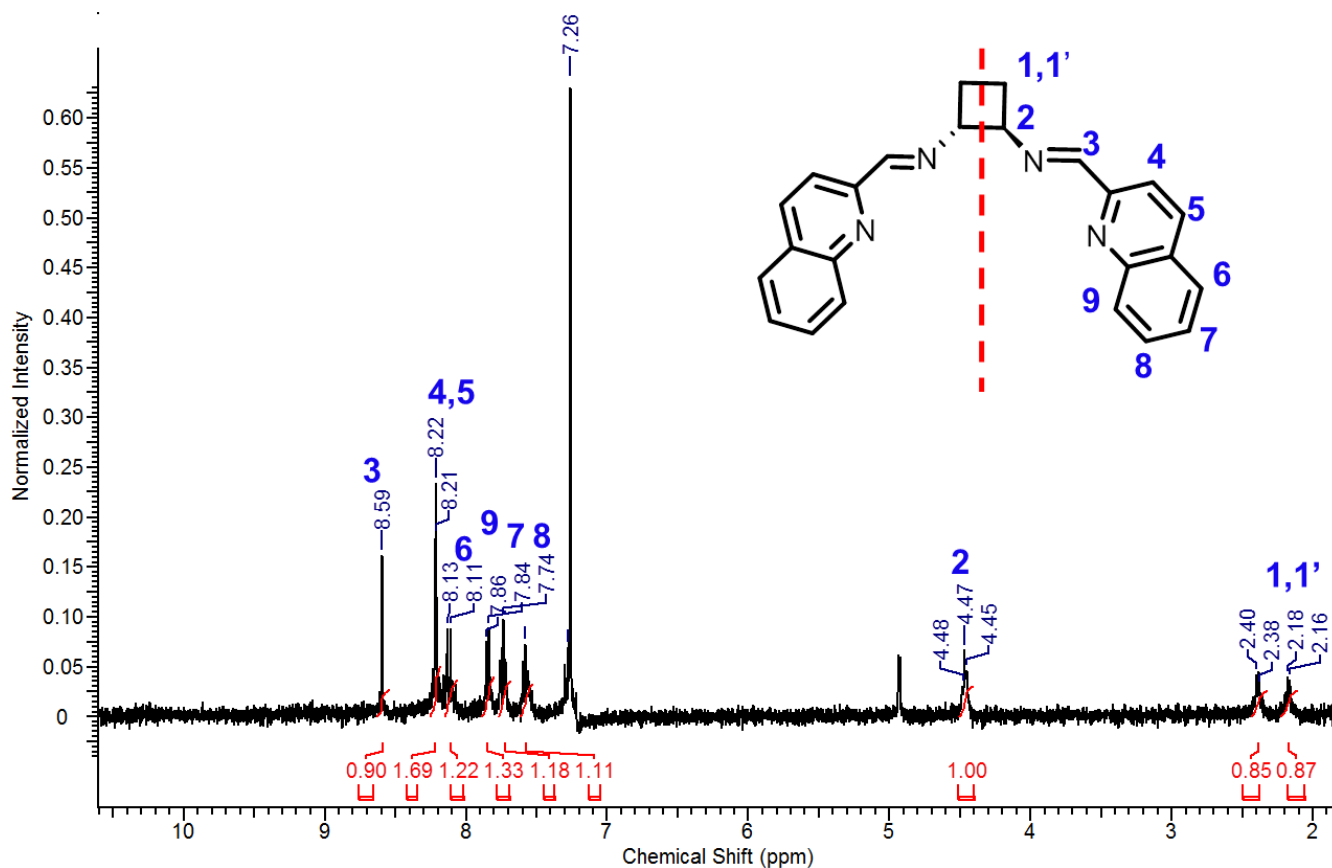


**Figure 3.11** The <sup>1</sup>H NMR spectrum of (*R,R*)-**23** with specific assignments.

For ligand (*R,R*)-**22**, the assignments described above and the distinct resonances of the bay proton (9.33 ppm) to the nearest aromatic proton allows for a convenient starting point to assign the remaining aromatic protons of the molecule using the COSY spectra (Figure 3.12). For example there is a COSY correlation between the doublet resonance at 8.35 ppm and the doublet at 8.21 ppm.

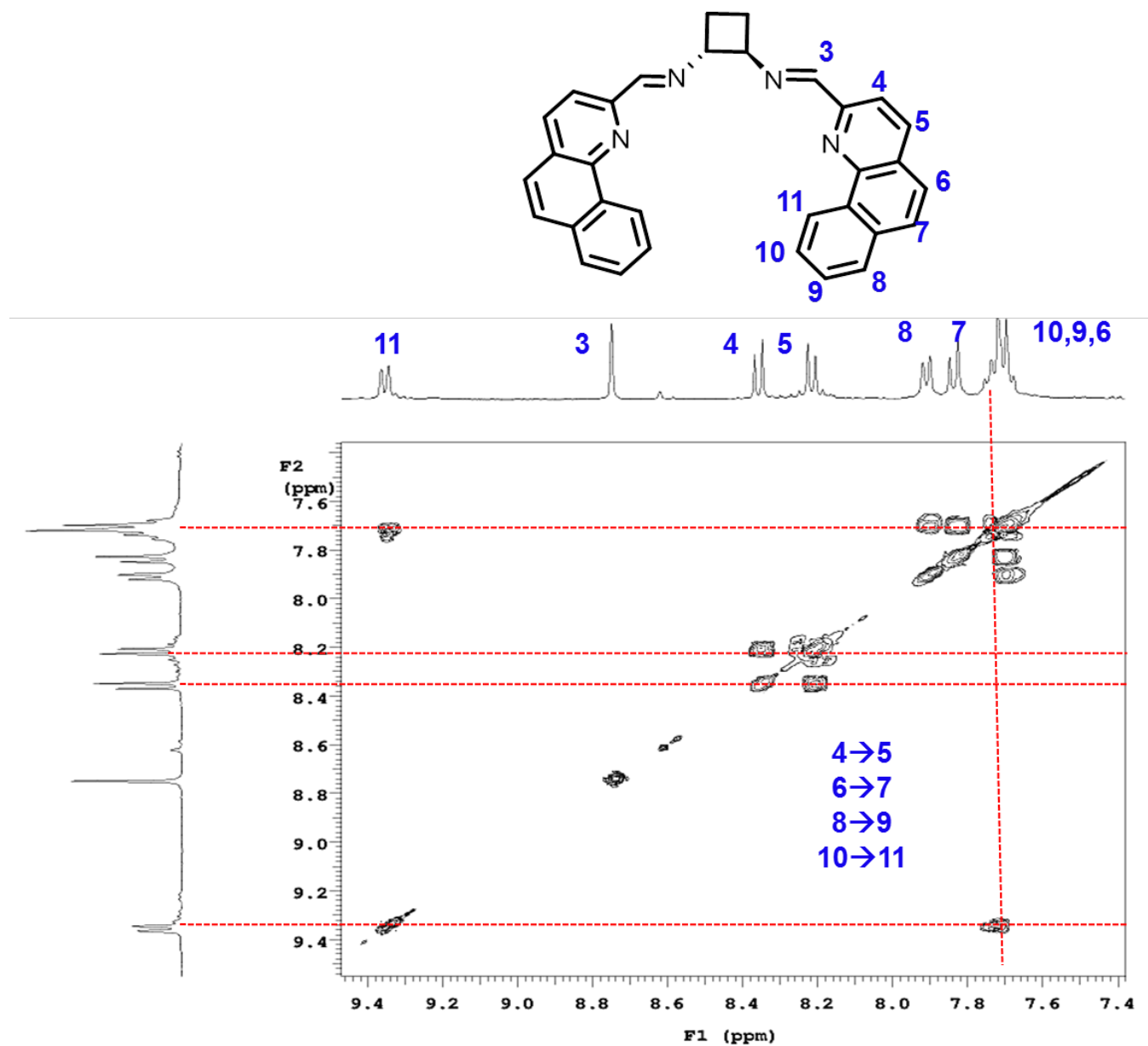
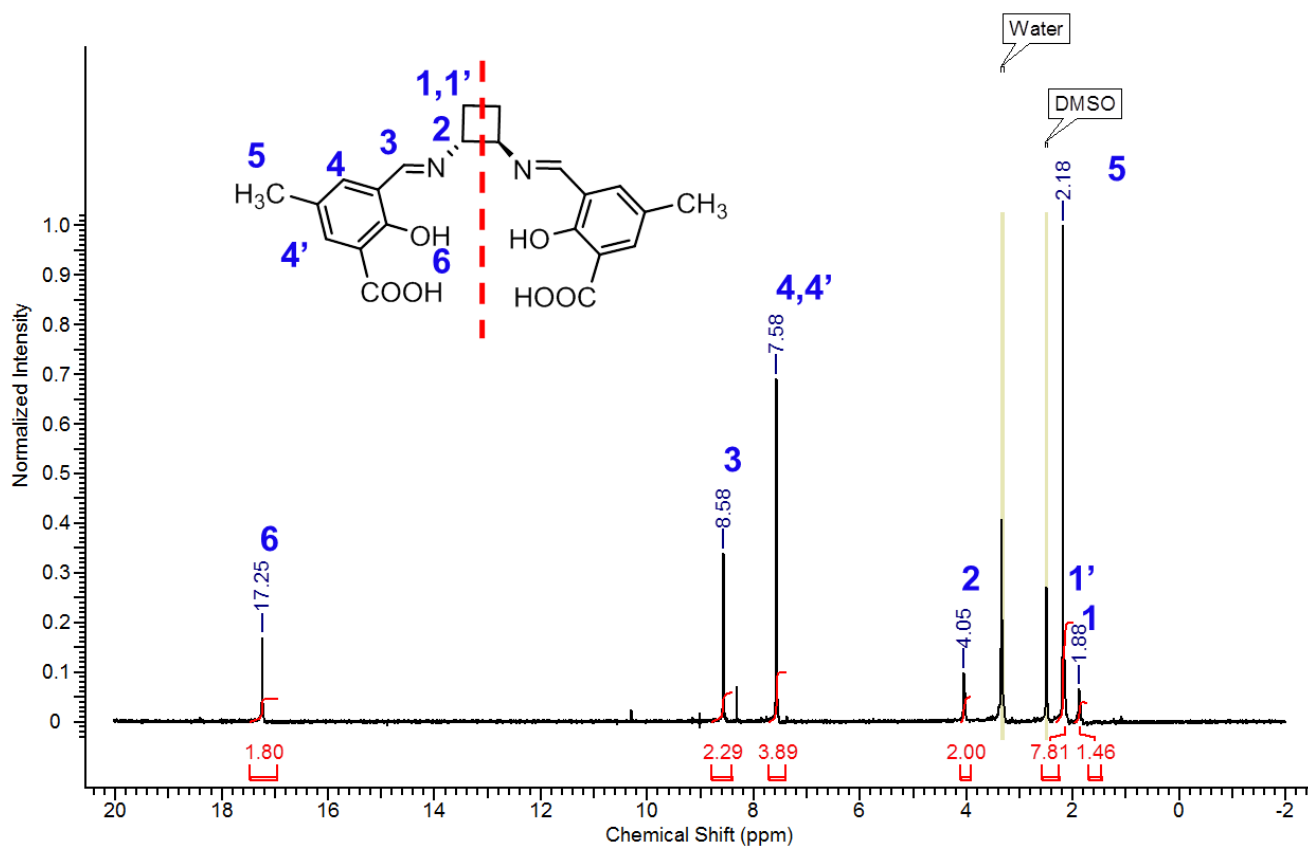


**Figure 3.12** The <sup>1</sup>H-<sup>1</sup>H COSY NMR spectrum of ligand (R,R)-22.

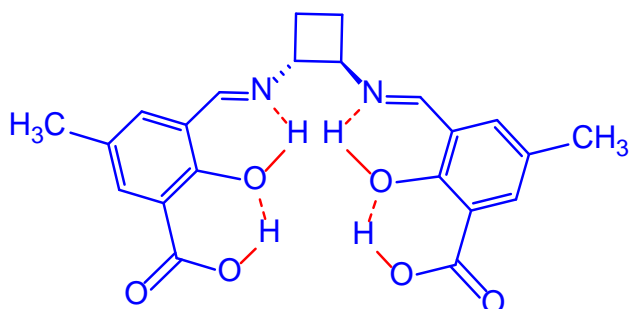
### 3.3.1.3 NMR spectroscopy of acid functionalized ligand, (R,R)-24

Figure 3.13 shows the 1D-<sup>1</sup>H-NMR spectrum of (R,R)-24 along with the specific peak assignments. The number of peaks depicted in the NMR spectra is half the number of possible resonances, indicating the presence of a C<sub>2</sub>-symmetrical molecule. The imine peak appears at 8.58 ppm as a singlet, corresponding to two hydrogens. The two benzyl hydrogens appeared as

singlet at 7.58 ppm. The cyclobutyl backbone hydrogens appear as broadened multiple peaks in the aliphatic region and one backbone peak is under the methyl proton signal at 2.18 ppm. Due to the rapid hydrogen exchange processes between the phenol and a carboxylic acid with the solvent deuterons we just see one sharp singlet at 17.25 ppm for phenol.



**Figure 3.13** The <sup>1</sup>H NMR spectrum of (R,R)-24 with specific assignments.



**Figure 3.14** The hydrogen bonding between the phenolic hydrogens, the imine nitrogens and the carboxylate oxygens.

The molecule is set up for facile hydrogen bonding between the phenolic hydrogens, the imine nitrogens and the carboxylate oxygens, Figure 3.14. Hydrogen bonded phenols/carboxylates usually appear as sharp signals in the  $^1\text{H}$  NMR spectrum as the proton exchange process is restricted in the presence of such bonding. We observed one sharp peak at 17.25 ppm which is significantly sharper than a regular phenol peak, indicating the presence of hydrogen-bonding between phenol and the imine group. We also expect to have hydrogen bonding between the acid protons and the phenol oxygen, but this signal is not present due to H/D exchange.

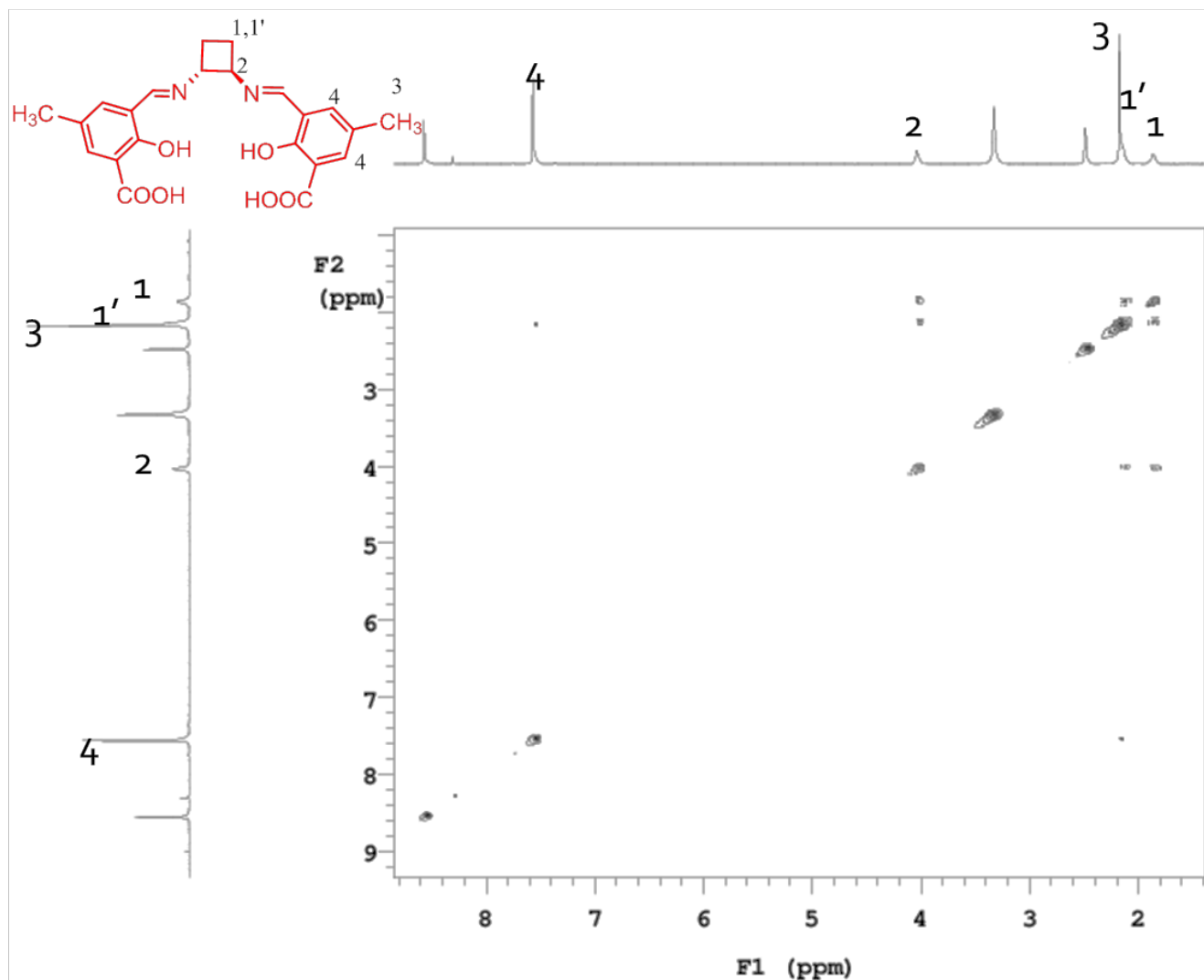


**Figure 3.15** The  $^1\text{H}$ - $^1\text{H}$  COSY NMR spectrum of ligand (*R,R*)-**24**.

### 3.3.2 Electronic and infrared spectra

Most absorption spectroscopy of organic compounds is based on transitions of  $n$  or  $\pi$  electrons to the  $\pi^*$  excited state. This is because the absorption peaks for these transitions fall in an experimentally convenient region of the spectrum (200 - 700 nm). In our case, UV-vis spectra of the ligands were collected on THF solutions. The ligands ((*R,R*)-**20** to (*R,R*)-**24**) exhibit absorption bands in a range of 265 nm and 335 nm, Table 3.1. The band at 265 nm has been assigned to the benzene ring and the one at 335 nm, to the imino groups.

IR spectra of ligand samples were collected on neat samples. The presence of the imine bond band for Schiff-base ligands ((*R,R*)-**20** to (*R,R*)-**24**) in the frequency range of 1690-1590

cm<sup>-1</sup> confirms their formation, Table 3.2.<sup>11</sup> The ligands (*R,R*)-**20**, (*R,R*)-**21** and (*R,R*)-**24** showed characteristic C–O stretching vibrations of the phenolic OH group which are expected to shift at higher frequency after metalation.

**Table 3.1** Characteristic UV-vis absorption bands for ligands.

Compound	Benzene ring	Imino group
( <i>R,R</i> )- <b>20</b>	265	334
( <i>R,R</i> )- <b>21</b>	248	335
( <i>R,R</i> )- <b>22</b>	220	347
( <i>R,R</i> )- <b>23</b>	241	316
( <i>R,R</i> )- <b>24</b>	234	318

**Table 3.2** Characteristic IR absorption bands for ligands.

Compound	$\nu(\text{C=N})/\text{cm}^{-1}$	$\nu(\text{C-O phenolate})/\text{cm}^{-1}$
( <i>R,R</i> )- <b>20</b>	1591	1297
( <i>R,R</i> )- <b>21</b>	1625	1264
( <i>R,R</i> )- <b>22</b>	1615	-
( <i>R,R</i> )- <b>23</b>	1613	-
( <i>R,R</i> )- <b>24</b>	1629	1252

### 3.3.3 Mass spectral analysis

The mass spectra of ligands provided valuable information concerning ligand compositions and structures. Structural information can be provided from the mass peaks in the molecular ion cluster and from the isotope patterns which are matched to those calculated for particular chemical compositions. The MALDI-TOF mass spectra of these ligands showed the expected molecular ion peaks that compared with the simulated values to fourth decimal places. The molecular ion peak for all the ligands (both calculated and found) and the isotopic pattern peak numbers are shown in the experimental section. The isotopic pattern also matches well with the simulated isotopic pattern. This is strong evidence that we have successfully synthesized the described ligands with the cyclobutyl backbone. The mass spectra of the ligands are shown in Figure 3.16 to Figure 3.21.

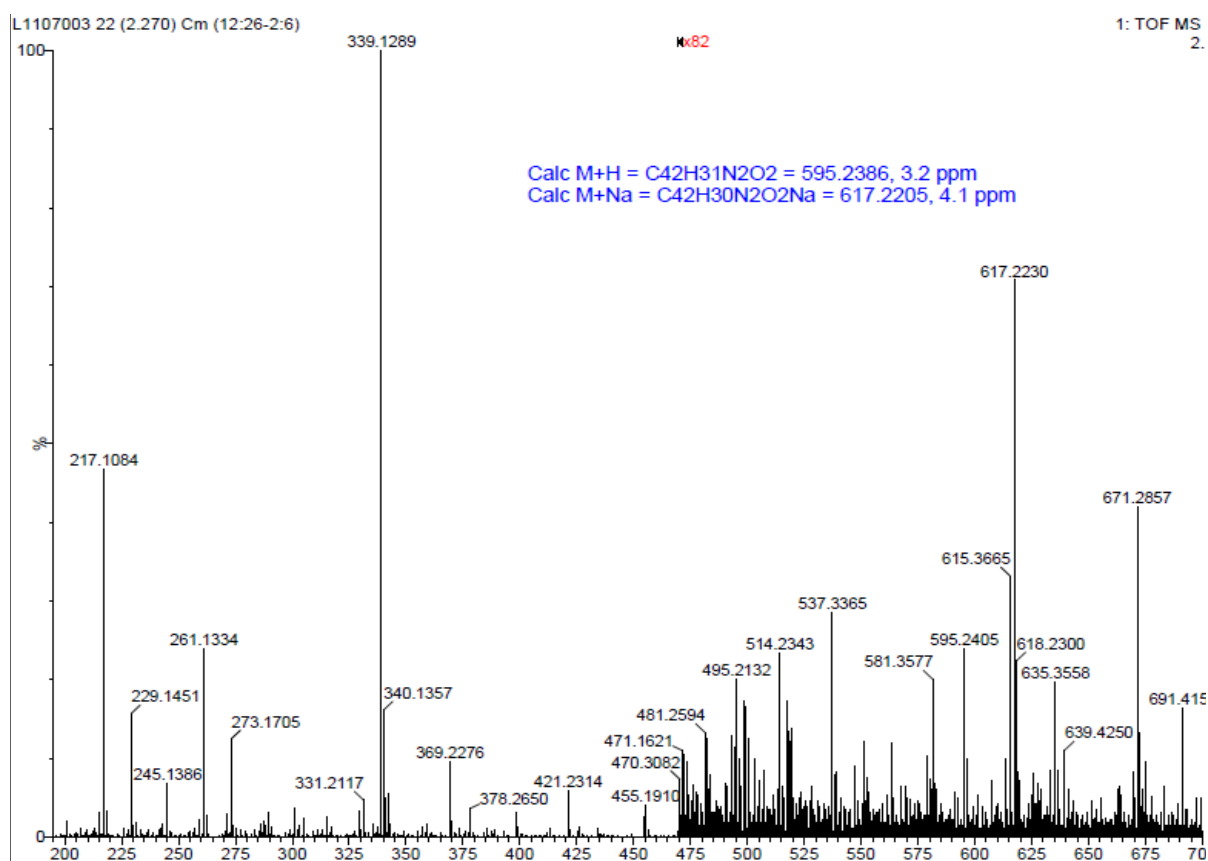
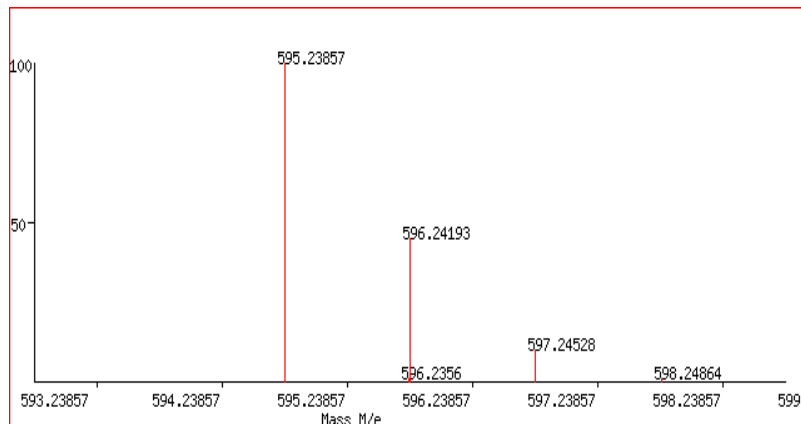
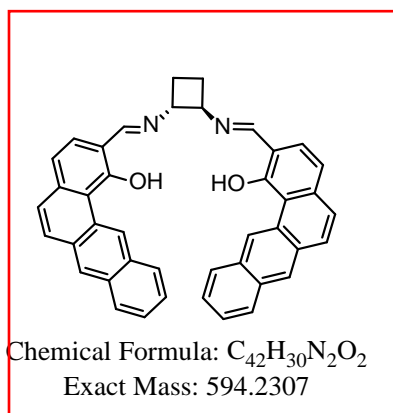


**Figure 3.16** The simulated isotopic pattern (top) and observed mass spectrum of ligand (*R,R*)-**20** (bottom).

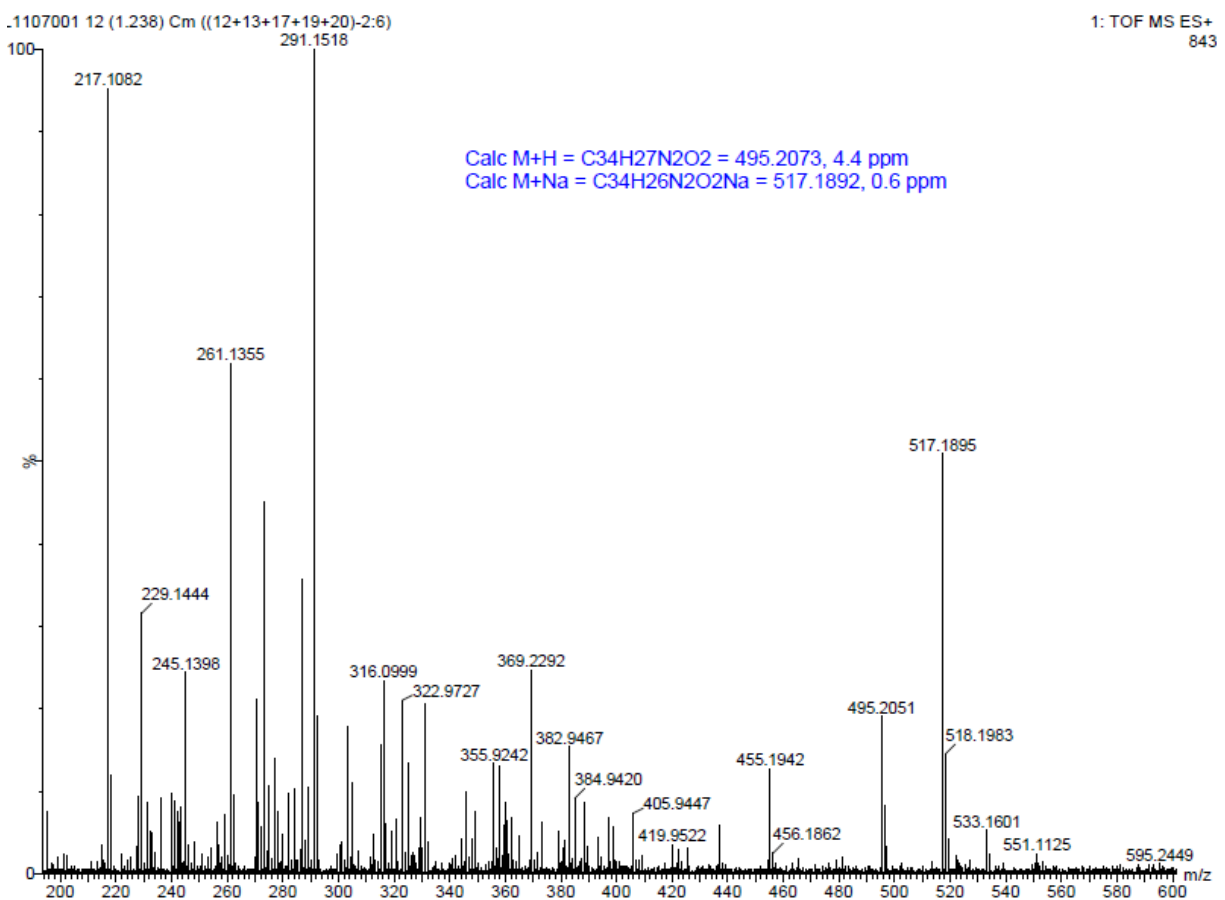
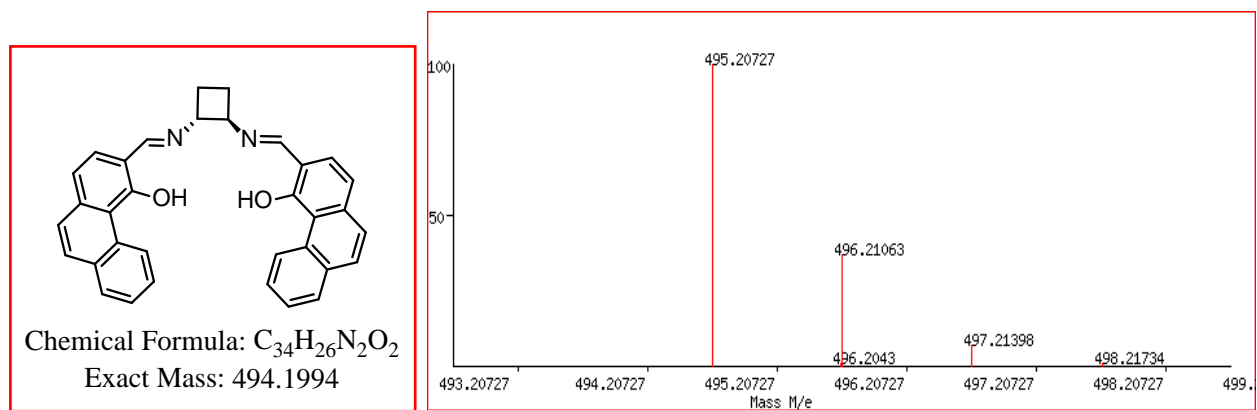


**Figure 3.17** The simulated isotopic pattern (top) and observed mass spectrum of ligand (*R,R*)-**21** (bottom).

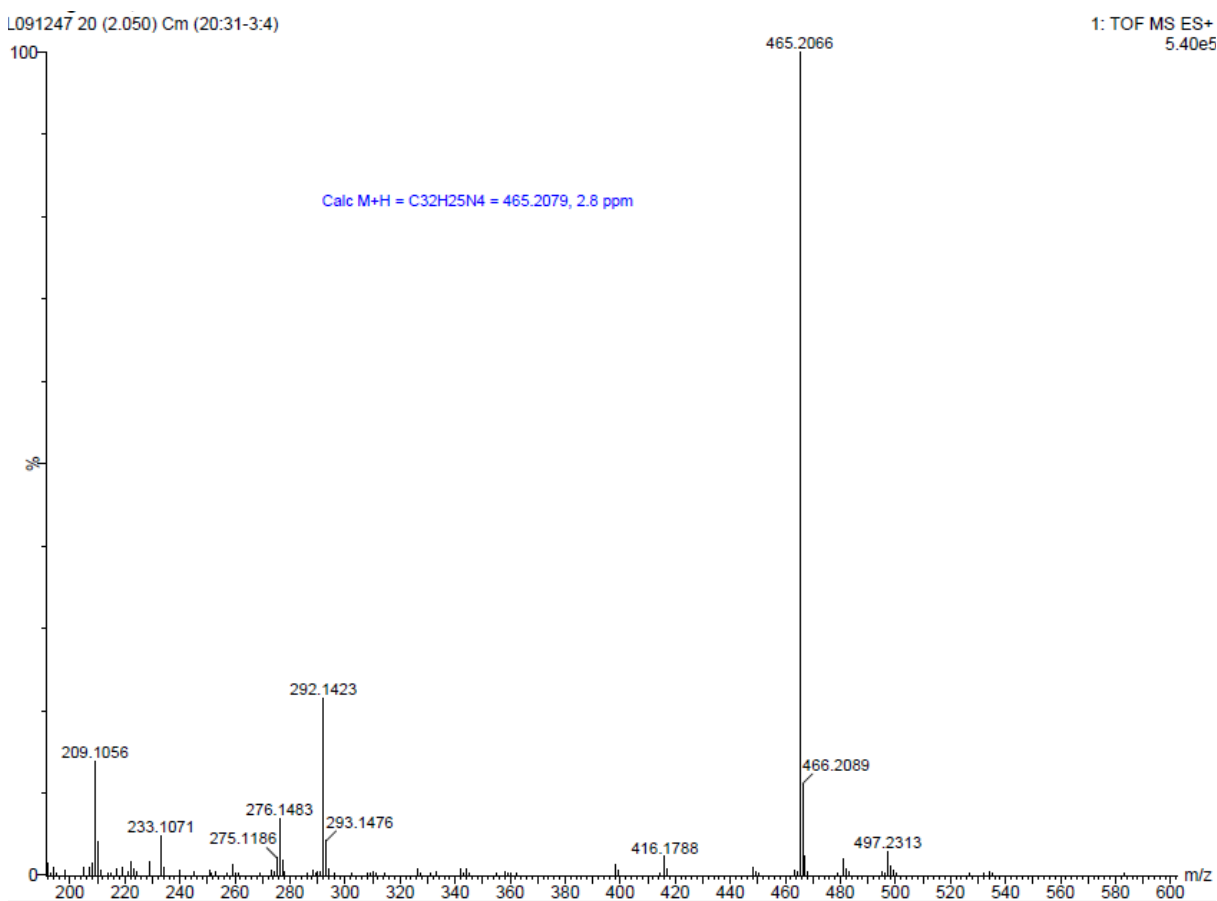
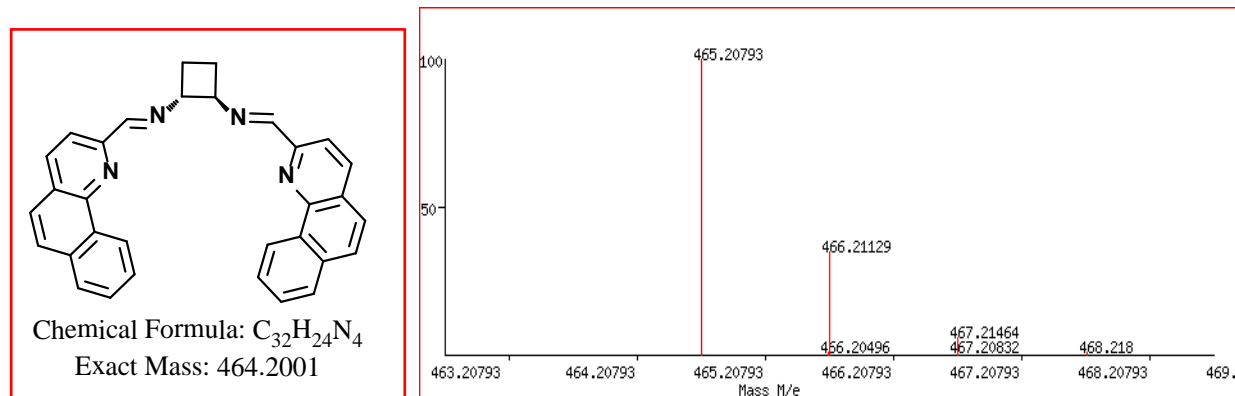


**Figure 3.18** The simulated isotopic pattern (top) and observed mass spectrum of ligand (*R,R*)-**22** (bottom).

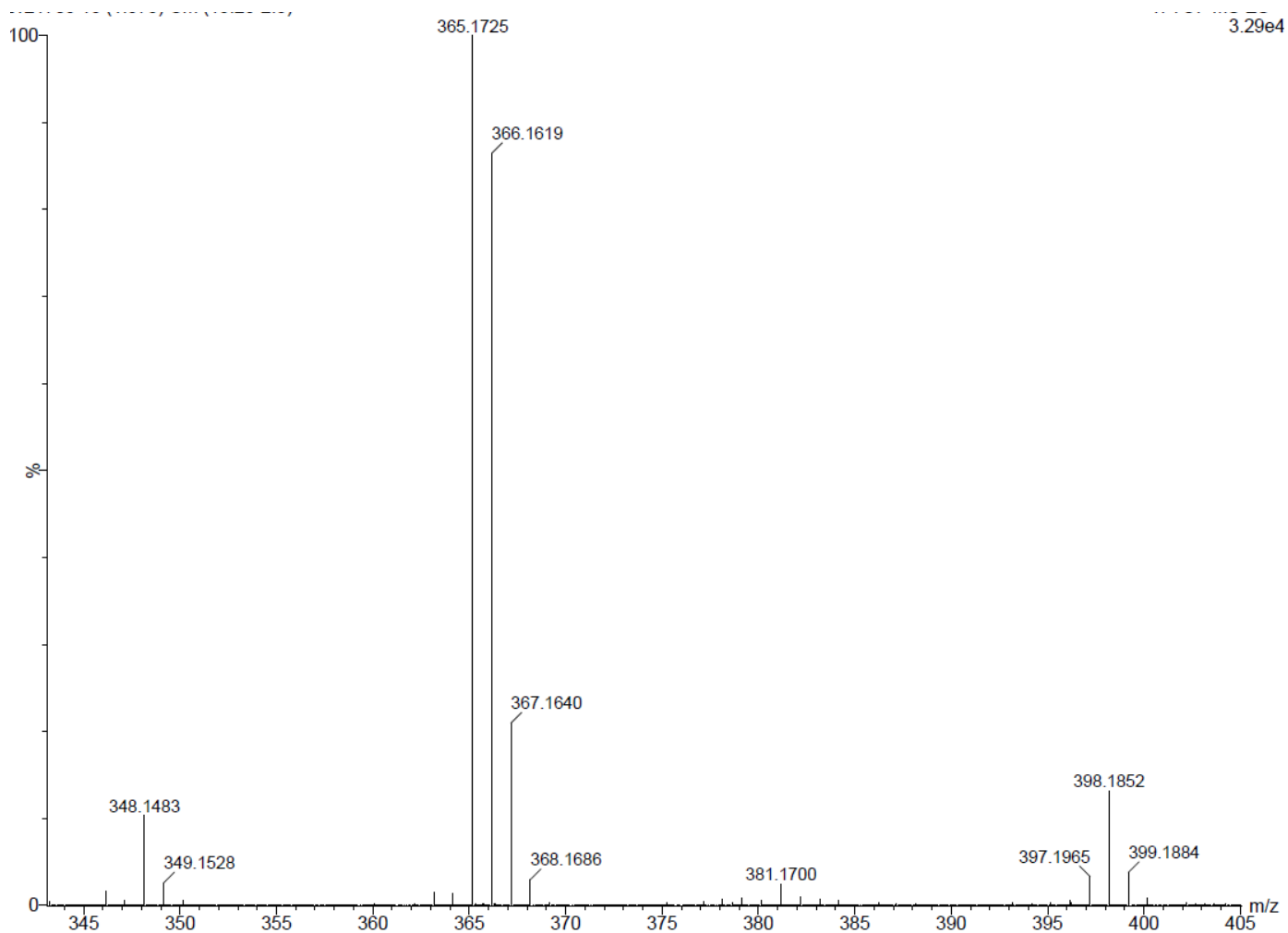
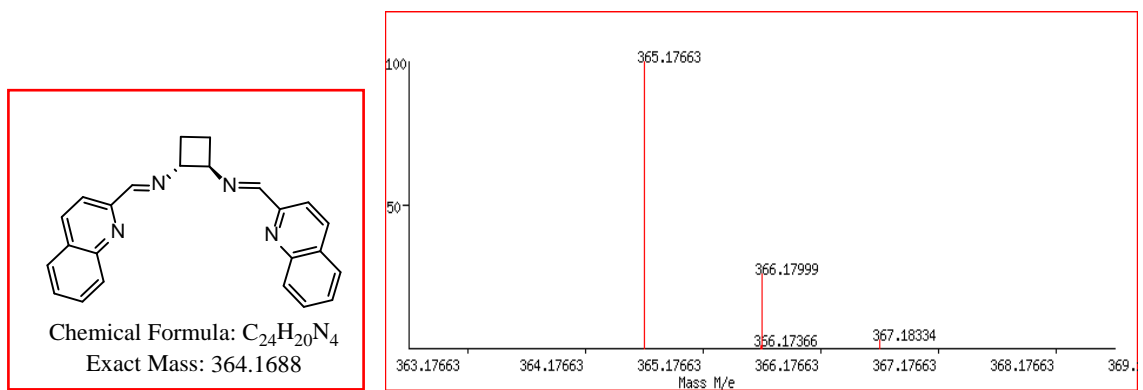


**Figure 3.19** The simulated isotopic pattern (top) and observed mass spectrum of ligand *(R,R)*-**23** (bottom).

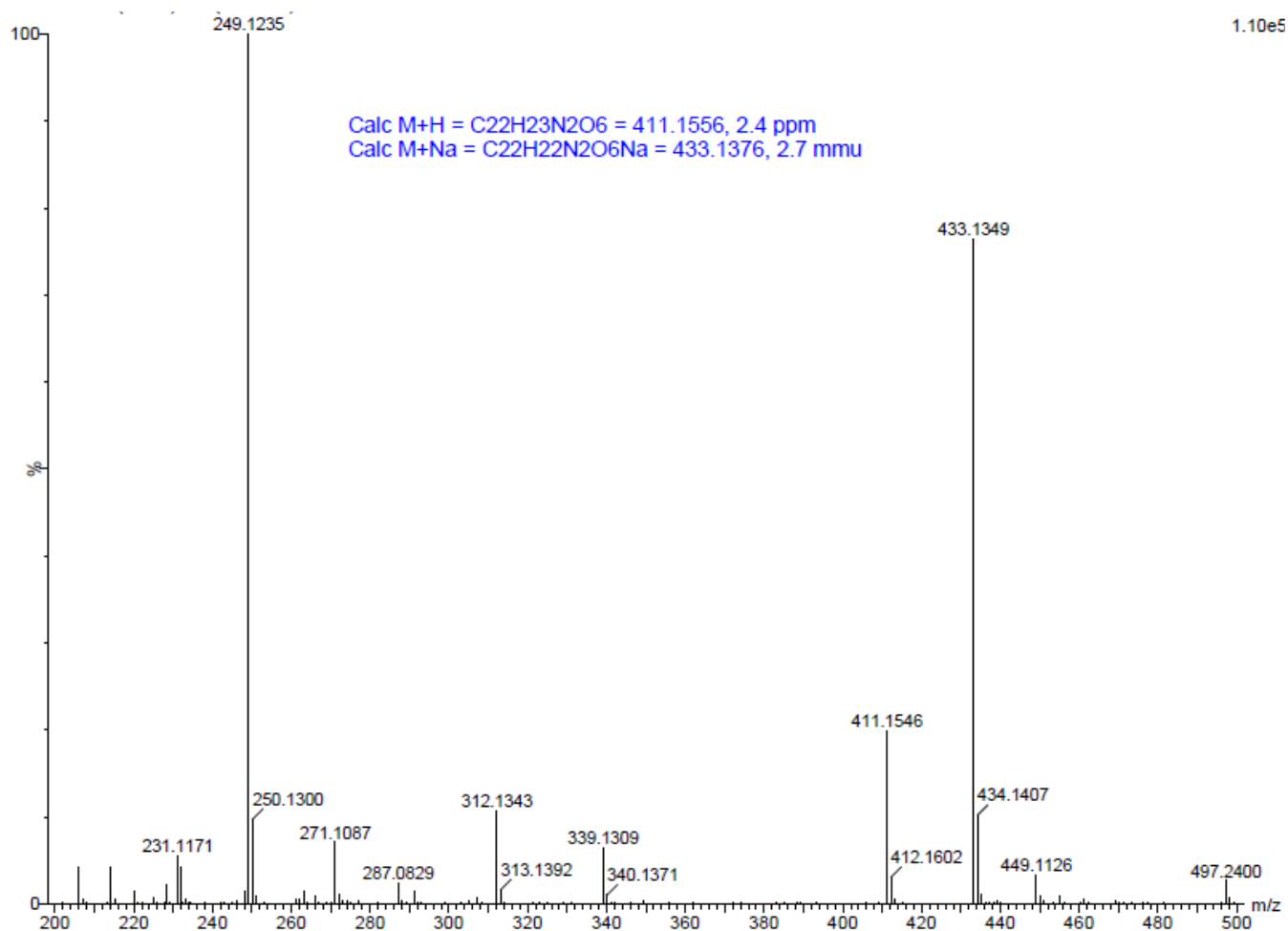
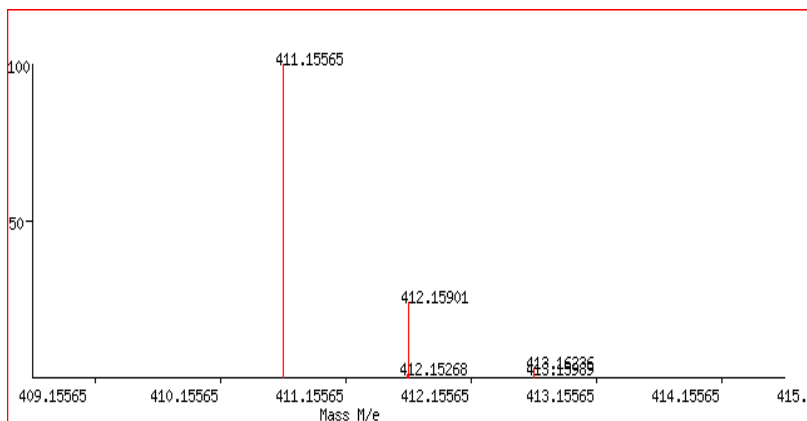
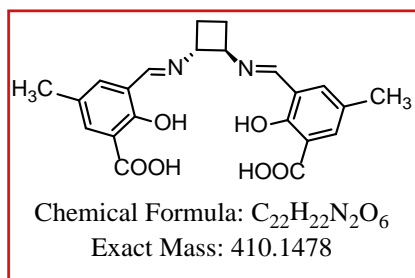


**Figure 3.20** The simulated isotopic pattern (top) and observed mass spectrum of ligand (*R,R*)-**24** (bottom).

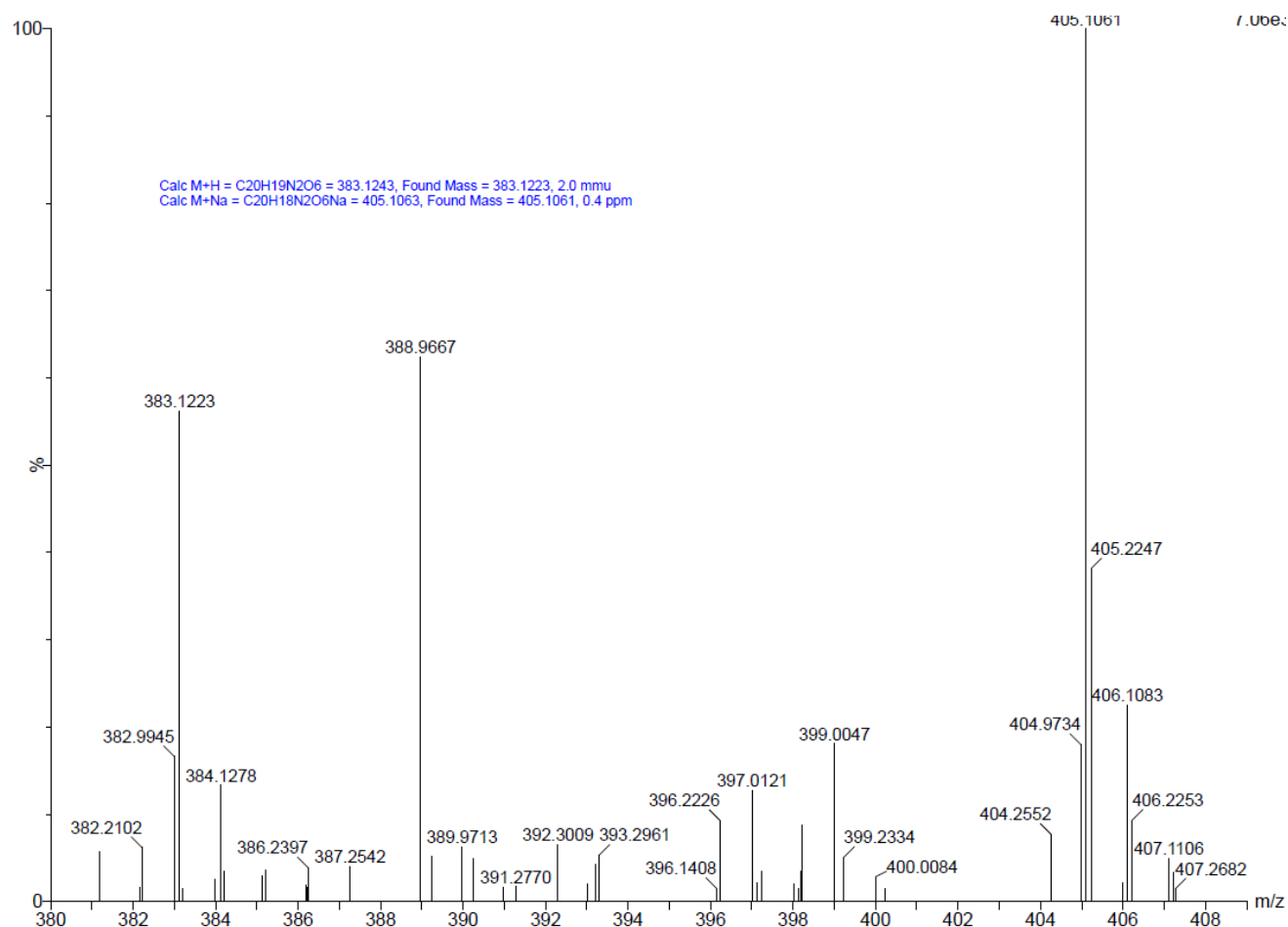
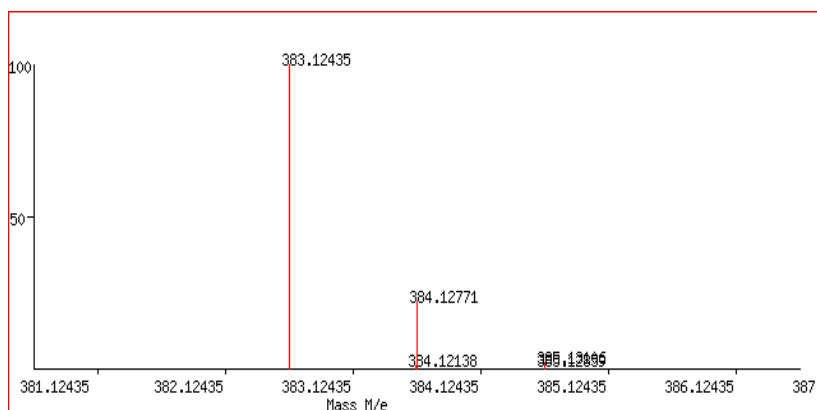
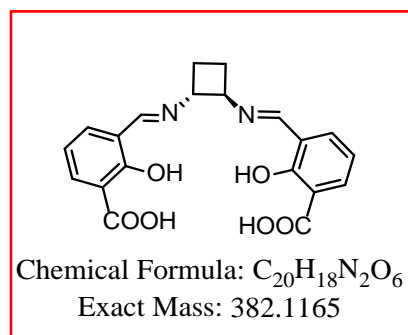


**Figure 3.21** The simulated isotopic pattern (top) and observed mass spectrum of ligand *(R,R)*-**20** (bottom).

### 3.4 Conclusion

We have synthesized and characterized Schiff-base ligand with cyclobutyl backbone incorporating three different types of sidearms. Also, we have explored a new method i.e. solvent assisted grinding for the synthesis of ligand with bis(imine-pyridine) sidearm, which allows us greener synthesis with minimal use of organic solvents. All synthesized ligands showed half number of  $^1\text{H}$  NMR signals which indicate  $C_2$  symmetry. The 1*R*,2*R*-cyclobutyl derived ligands are stable in air therefore can be store without much precaution. We were unable to crystallize ligands, always ending up with powdery or sticky product. In coming chapters, we will be discussing complexation and applications as catalyst of cyclobutyl derived ligands.

### References

- 
- <sup>1</sup> Jacobsen, E.; Zhang, W.; Güler, M. *J Am Chem Soc*, **1991**, 113, 6703.
  - <sup>2</sup> Larrow, J.; Jacobsen E. *Topics Organomet Chem* **2004**, 6, 123–152.
  - <sup>3</sup> Daly, A.; Gilheany, D. *Tetrahedron: Asymmetry* **2003**, 14, 127–137.
  - <sup>4</sup> Northa, M.; Steed J. *Tetrahedron* **2004**, 60, 3191–3204.
  - <sup>5</sup> Wiznycia, A.; Desper J.; Levy C. *Dalton Trans.* **2007**, 1520–1527.
  - <sup>6</sup> Wiznycia, A.; Desper J.; Levy C. *Chem. Commun.* **2005**, 4693–4695.
  - <sup>7</sup> Prema, D.; Wiznycia, A.; Desper J.; Levy C. *Dalton Trans.* **2007**, 4788–479.
  - <sup>8</sup> Tagawa, Y.; Yamashita, K. *Hetrocycles*, Vol. 60, No. 4, **2003**, 953 - 957
  - <sup>9</sup> Ghosh; S. *et al*, Ligands of adenine nucleotide translocase (ant) and compositions and methods related thereto, USP20060194825, August 31, **2006**
  - <sup>10</sup> Iijima, K. *et al*, Benzofuran derivative and processes for preparing the same, USP4882340, November 21, **1989**.
  - <sup>11</sup> Interpretation of Infrared Spectra, A Practical Approach, John Coates, John Wiley & Sons Ltd, Chichester, 2000.

# Chapter 4 - Synthesis and characterization of complexes with cyclobutyl backbone

## 4.1 Introduction

Over the past decade, the number of applications for metal salen complexes has grown rapidly to incorporate an extremely broad range of chemical transformations, containing the asymmetric ring-opening of epoxides, aziridination, cyclopropanation, and the epoxidation of olefins.<sup>1</sup> This versatility in chemical reactivity and selectivity is a result of the ability of salen-type ligands to complex a variety of metals with a large number of oxidation states in an easily tunable chiral environment. As such, there has been considerable interest in the synthesis of new salen-type complexes of transition and main group metals to further develop applications in both catalysis and materials chemistry.<sup>2,3,4</sup>

The formation of metallosalen complexes can be achieved by simply mixing the ligand with a metal ion after its conversion to the corresponding phenoxide ion derivative or under basic conditions, Figure 4.1. Most metal ions can form salen complexes, with the exception of alkali, alkaline-earth and some of the rare-earth metals.<sup>5</sup>

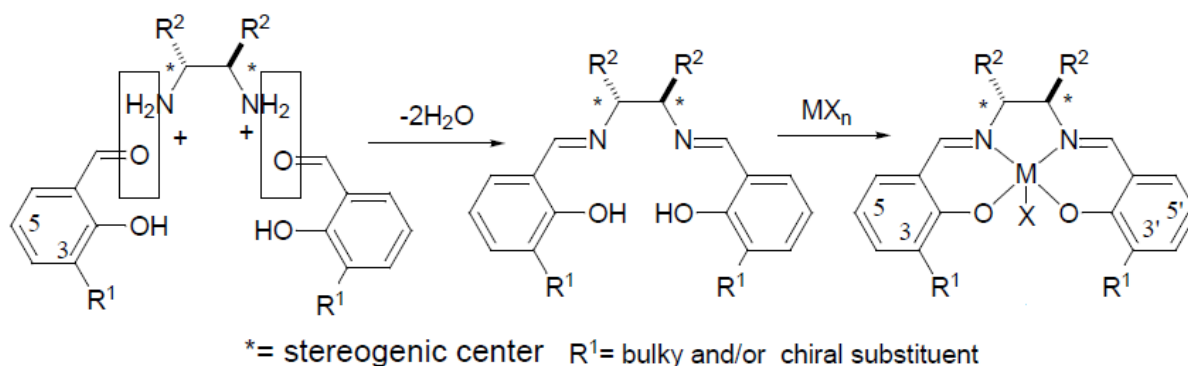


**Figure 4.1** Synthetic scheme for metallosalen complex.

## 4.2 Synthesis

The ligand (*R,R*)-**20** was metallated with zinc chloride to afford the mononuclear complex (*R,R*)-**25**. The complex, (*R,R*)-**25** is afforded as a pale yellow colored precipitate and is of high purity, as was indicated by <sup>1</sup>H/<sup>13</sup>C NMR. The high solubility of the ligand versus the high insolubility of the complex in toluene allows for facile purification by washing with solvent.

Similarly, the complex (*R,R*)-**26** is also synthesized using manganese(II) chloride. Four equivalents of sodium methoxide were added into the reaction mixture. The role of NaOMe is to deprotonate the two phenolic oxygens from the salen ligand to facilitate the metallation. The by-product, methanol, can be easily removed by vacuum drying. Dioxygen gas was bubbled through the pale brown suspension for 2 h to oxidize Mn(II) to higher oxidation states. Dark green was obtained upon Soxhlet extraction in CH<sub>2</sub>Cl<sub>2</sub> in moderate yields.

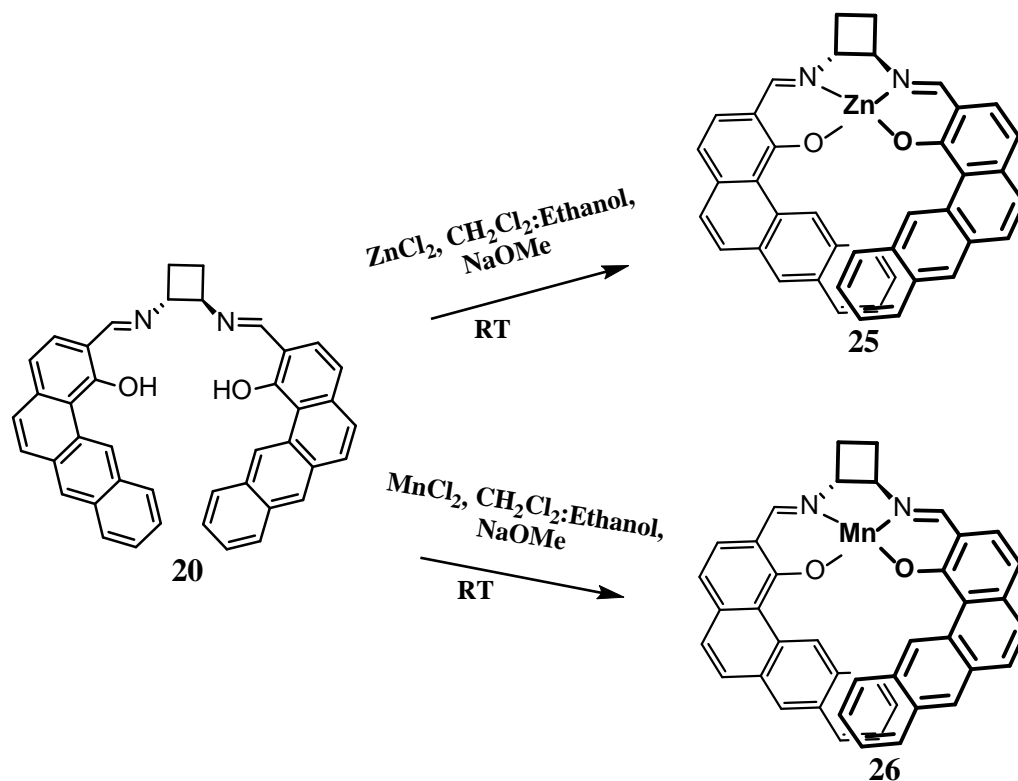


**Figure 4.2** Synthetic scheme for complex (*R,R*)-**25** and (*R,R*)-**26**.

Similarly, the ligand (*R,R*)-**21** was metallated with zinc(II) chloride in the presence of the base sodium methoxide to afford the mononuclear complex (*R,R*)-**27**. The complex, (*R,R*)-**27** is afforded as a greenish yellow colored precipitate and analyzed by <sup>1</sup>H NMR. (*R,R*)-**27** showed low solubility in most NMR solvents, making <sup>13</sup>C NMR analysis difficult. The complex (*R,R*)-**28** is also synthesized using iron chloride. The metalation gave a brown colored product. The paramagnetic nature of complex (*R,R*)-**28** doesn't allow detailed NMR analysis.

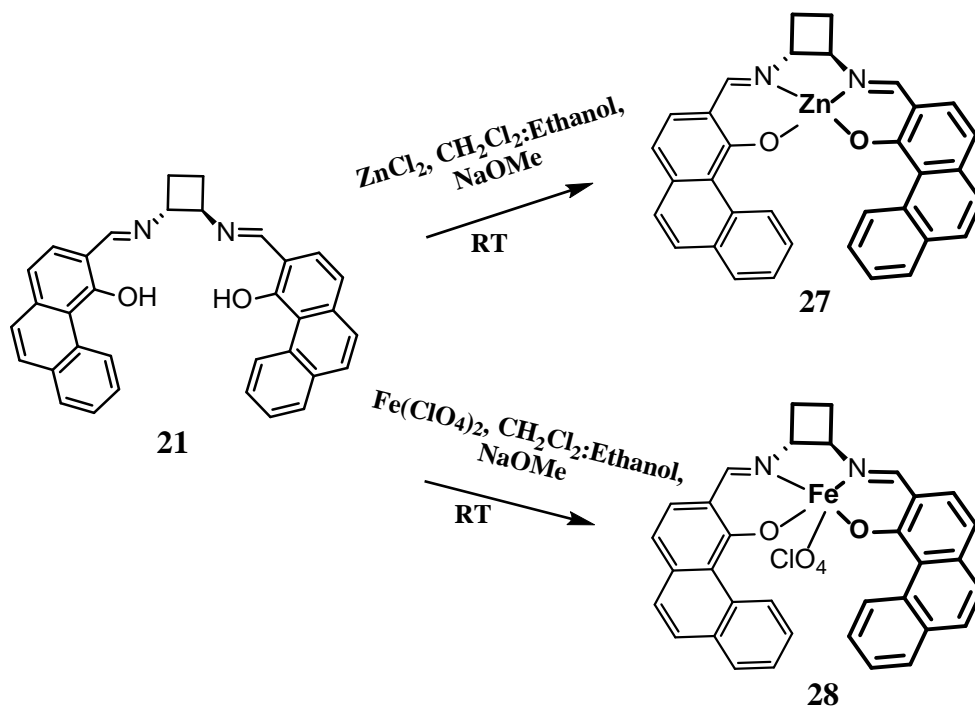


**Figure 4.3** Synthetic scheme for complex (R,R)-27 and (R,R)-28.

Acid-functionalized salen ligands such as ligand (R,R)-24 have a great potential as versatile ligands that can produce a variety of coordination environments for metal ions. Their two metal binding pockets have significantly different binding abilities; the salen pocket, consisting of two imine-nitrogen donors and two phenoxide donors, can be activated by the addition of a mild base while the phenoxide/carboxylate pocket requires a stronger base for deprotonation. Both binding pockets are suitable for coordinating to transition metals of different geometries. In further studies, ligand (R,R)-24 was metallated with nickel(II) acetate, to afford dinuclear complex, but instead, we obtained mononuclear complex (R,R)-29. Nickel complex (R,R)-29 was afforded in moderate yields, and <sup>1</sup>H NMR spectra the indicated paramagnetic nature of the complex. The reaction of ligands (R,R)-24 with different metal salts such as nickel perchlorate also gave the mononuclear nickel complex. Previously our research group mentioned that using strong base in reaction with acid functionalized ligand can give dinuclear complexes but in case of ligand (R,R)-24 only mononuclear complexes obtained.

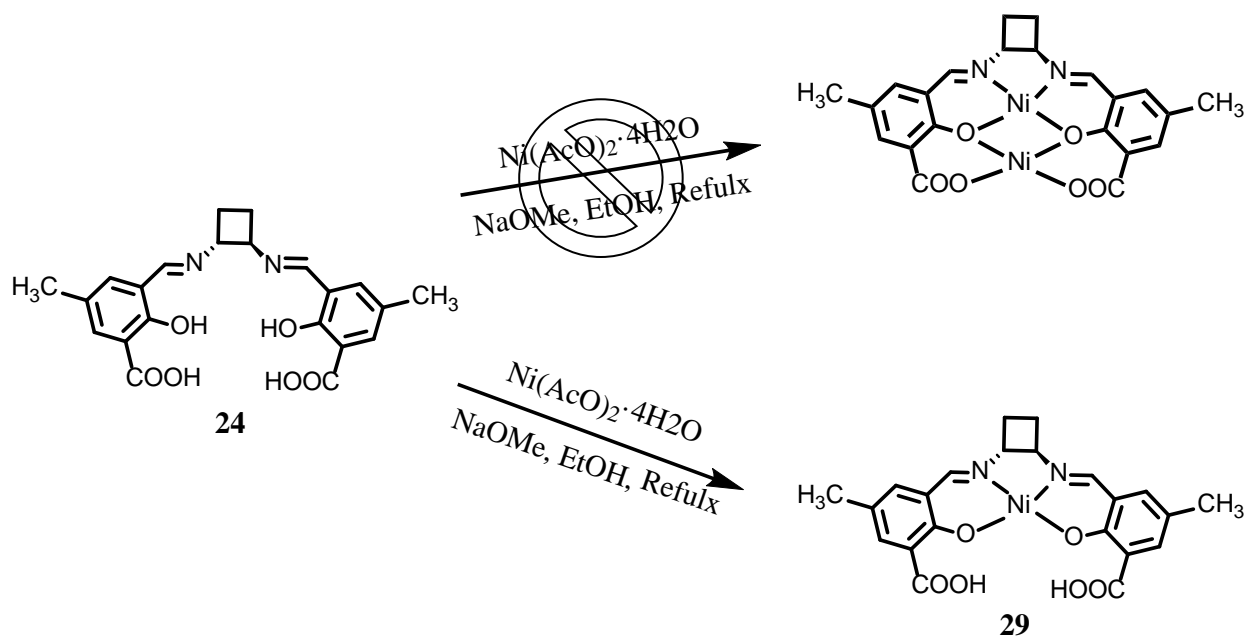


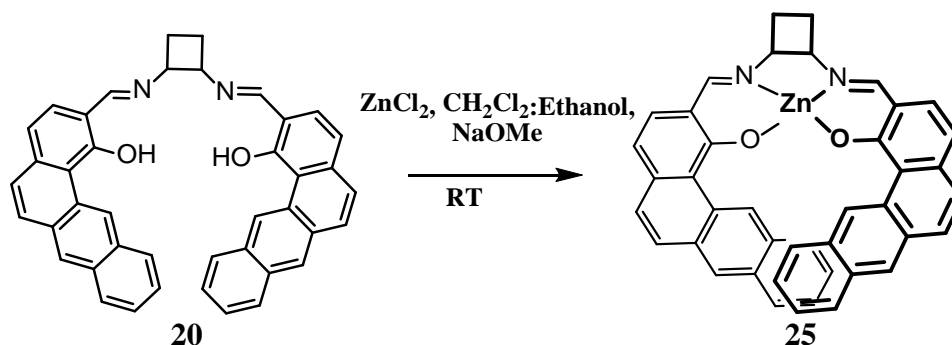
**Figure 4.4** Synthetic scheme for nickel complex (*R,R*)-29.

## 4.2 Experimental

### 4.2.1 Synthesis

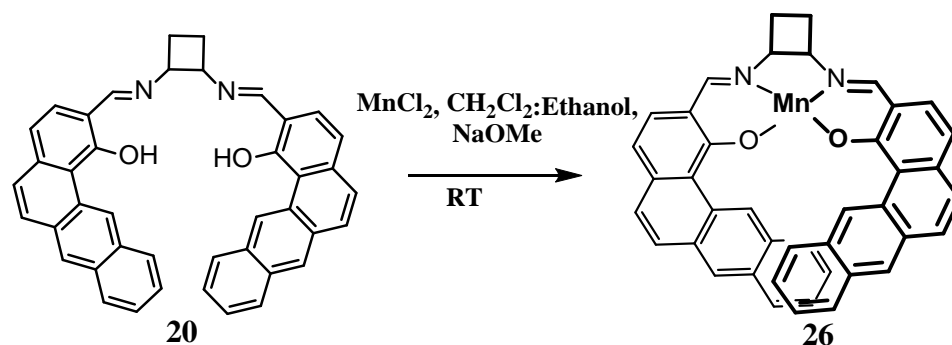
$^1\text{H}$  and  $^{13}\text{C}$  NMR spectra were recorded on a Varian Unity plus 400 MHz or 200 MHz spectrometer in  $\text{CDCl}_3$  or  $\text{DMSO}-d_6$ . Data is expressed in parts per million (ppm) downfield shift from tetramethylsilane or residual protiosolvent as internal reference and are reported as position (in ppm), multiplicity (s = singlet, d = doublet, t = triplet, m = multiplet), coupling constant ( $J$  in Hz) and integration (number of protons). IR spectra were collected on a Nicolet 380 FT-IR (Thermo Scientific, Madison MN) at room temperature. UV-Vis spectra were obtained on a Varian Cary 500 scan UV-Vis-NIR spectrophotometer (Agilent Technologies) in tetrahydrofuran (THF). The solution samples for UV-Vis were prepared at room temperature, with the concentrations ranged between  $1.5$  and  $2.5 \times 10^{-5}\text{M}$ . A 1.00 cm path length quartz cell was employed for analyses. HR-ESI-Mass spectra were collected by electrospray ionization and acquired on a LCT Premier (Waters Corp., Milford MA) time of flight mass spectrometer.

#### 4.2.1.1 Zn(II)-(*R,R*)-20-complex, ((*R,R*)-25)



Zinc chloride (0.079 g, 0.58 mmol), sodium methoxide (0.093 g, 1.73 mmol) and ligand (*R,R*)-**20** (0.345g, 0.58 mmol) were suspended into a 2:1 mixture of methylene chloride/ethanol (15 mL). After stirring overnight the reaction mixture was concentrated to a yellow solid that was dissolved into THF (20 mL). The solution was carefully filtered to remove fine insoluble solids, and the clear filtrate was diluted with ethanol (40 mL). Stirring for 3 h resulted in the gradual formation of a yellow precipitate. The precipitate was collected and consecutively washed with methylene chloride (5 mL) and ethanol (5 mL) to afford (*R,R*)-**53** (0.37 g, 98% yield). <sup>1</sup>H NMR (400 MHz, CDCl<sub>3</sub>) δ 2.20–2.18 (m, 2 H, CH), 2.43–2.42 (m, 2 H, CH), 4.59–4.57 (m, 2 H, CH), 6.93 (d, 2H, CH), 7.07 (d, 2 H, CH), 7.37–7.34 (t, 2 H, CH), 7.45–7.41 (t, 2 H, CH), 7.59 (d, 2 H, CH), 7.79 (d, 2 H, CH), 7.96–7.93 (m, 4 H, CH), 8.14 (s, 2 H, CH), 8.33 (s, 2 H, CH), 10.98 (s, 2 H, CH). <sup>13</sup>C NMR (100 MHz, CDCl<sub>3</sub>) δ 172.98, 170.55, 139.42, 134.44, 132.79, 131.94, 130.99, 130.51, 129.54, 128.15, 127.43, 126.52, 125.64, 125.37, 123.07, 116.36, 116.06, 68.21, 30.18, 26.08..

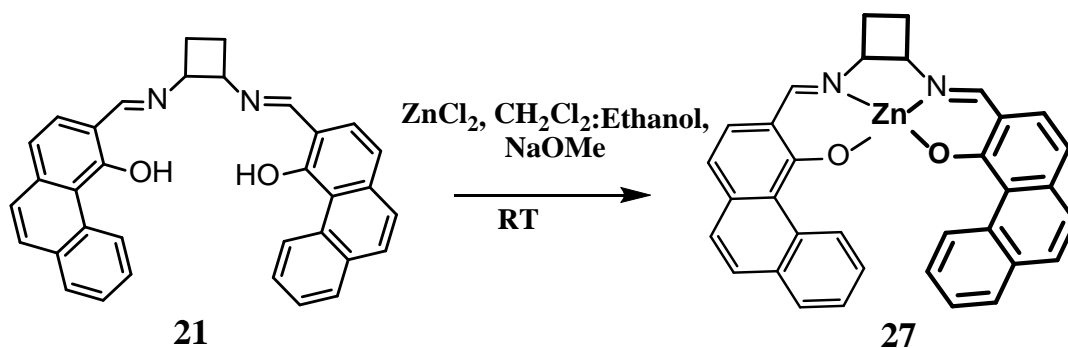
#### 4.2.1.2 Mn(IV)-(*R,R*)-20-complex, ((*R,R*)-26)



Manganese(II) chloride (0.12 g, 0.96 mmol), sodium methoxide (0.10 g, 1.9 mmol) and ligand (*R,R*)-**20** (0.30 g, 0.502 mmol) were suspended into a 2:1 mixture of

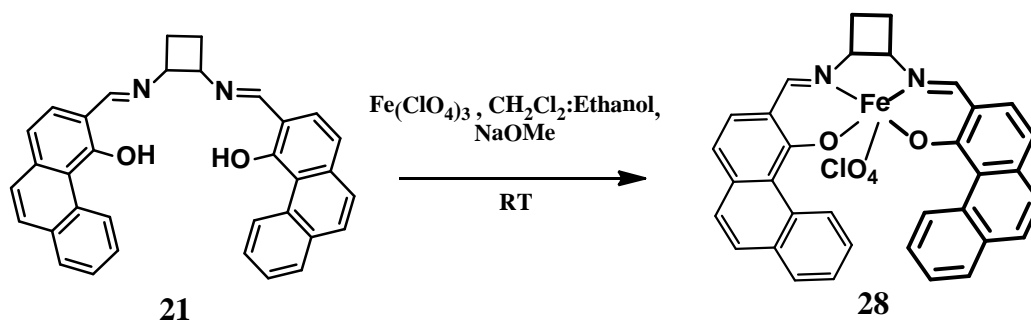
dichloromethane/ethanol (15 mL) and stirred overnight. The reaction mixture was oxidized by oxygen gas for 2 hours followed by soxhlet extraction in dichloromethane (100 mL). The filtrate was concentrated to yield a dark green powder (0.13 g, 41 %).

#### 4.2.1.3 Zn(II)-(*R,R*)-21-complex, ((*R,R*)-27)



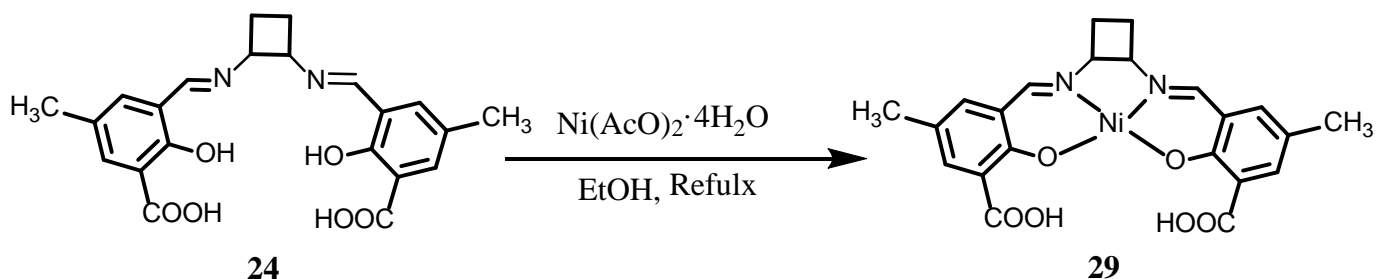
Zinc chloride (0.079 g, 0.58 mmol), sodium methoxide (0.093 g, 1.73 mmol) and ligand (*R,R*)-**21** (0.286 g, 0.58 mmol) were suspended into a 2:1 mixture of methylene chloride/ethanol (15 mL). After stirring overnight the reaction mixture was concentrated to a yellow solid that was dissolved into THF (20 mL). The solution was carefully filtered to remove fine insoluble solids, and the clear filtrate diluted with ethanol (40 mL). Stirring for 3 h resulted in the gradual formation of a yellow precipitate. The precipitate was collected and consecutively washed with methylene chloride (5 mL) and ethanol (5 mL) to afford (*R,R*)-**27** (0.307 g, 95% yield). <sup>1</sup>H NMR (400 MHz, DMSO) δ 2.18–2.16 (m, 2 H, CH), 4.76–4.54 (m, 2 H, CH), 6.98 (d, 2 H, CH), 7.23 (d, 2 H, CH), 7.56–7.52 (m, 2H, CH), 7.64–7.61 (m, 4 H, CH), 7.84 (d, 2 H, CH), 7.90 (d, 2 H, CH), 8.52 (s, 2 H, N=CH), 10.38 (d, 2 H, CH). One backbone signal overlaps with the solvent peaks.

#### 4.2.1.4 Fe(III)-(R,R)-21-complex, ((R,R)-28)



Iron (II) perchorate (0.168g, 0.480 mmol), sodium methoxide (0.078 g, 1.450 mmol) and ligand (R,R)-21 (0.237 g, 0.48 mmol) were suspended into a 2:1 mixture of methylene chloride/ethanol (15 mL). After stirring overnight the reaction mixture was concentrated to a solid that was dissolved into THF (15 mL). The solution was filtered to remove fine insoluble solids, and the clear filtrate diluted with ethanol (15 mL). Upon stirring for 30 minutes a black precipitate formed, and this was collected to afford (R,R)-28 (0.211 g, 68% yield).

#### 4.2.1.5 Ni(II)-(R,R)-24-complex, ((R,R)-29)



To a solution of Schiff base ligand (R,R)-24 (820 mg, 2.0 mmol) in EtOH (10 mL), was added  $\text{Ni}(\text{OAc})_2 \cdot 6\text{H}_2\text{O}$  (995 mg, 4.0 mmol), and the mixture was stirred for 12 h under reflux. After cooling down to room temperature, the precipitate (Ni<sup>2+</sup>/Schiff base complex) was collected by filtration. Then, the solid was washed with H<sub>2</sub>O (x 3), EtOH (x 3), and Et<sub>2</sub>O. The solid was dried under reduced pressure to afford the Ni<sup>2+</sup>-Schiff base (R,R)-29 complex (860 mg, 92 %) as a blue green solid.

## 4.3 Results and discussion

### 4.3.1 NMR spectroscopy

After completion of synthetic steps,  $^1\text{H}$  spectroscopy were employed to characterize the prepared zinc(II) complexes. Table 4.1, includes the  $^1\text{H}$  NMR chemical shifts of the ligands and diamagnetic zinc(II) complexes. Absolute assignment of all signals was not attempted due to the intricacy of the spectra, although those readily identifiable were assigned. For both complexes, a single set of proton resonances was observed, suggesting the existence of only one discrete species in solution, and the absence of dinuclear complexes (helicates) in the case of the zinc salens. The number of resonances was half that possible in total, as is expected for  $C_2$  symmetric molecules.

**Table 4.1** Ligand and Zn(II) complex  $^1\text{H}$  NMR chemical shifts.

	Imine C–H	O··H··N	Aliphatic C–H	Aromatic C–H
Ligand ( <i>R,R</i> )- <b>20</b>	8.42	15.72	2.27–2.26 (m, 2 H, CH), 2.48–2.47 (m, 2 H, CH), 3.34–3.32 (m, 2 H, CH).	7.24 (d, 2 H, CH), 7.38 (d, 2H, CH), 7.52 (d, 2 H, CH), 7.57–7.55 (m, 4 H, CH), 7.90 (d, 2 H, CH), 8.05–8.02 (m, 2 H, CH), 8.25–8.23 (m, 2 H, CH), 8.36 (s, 2 H, CH), 10.66 (s, 2 H, CH).
Complex( <i>R,R</i> )- <b>25</b>	8.33		2.20–2.18 (m, 2 H, CH), 2.43–2.42 (m, 2 H, CH), 4.59–4.57 (m, 2 H, CH).	6.93 (d, 2H, CH), 7.07 (d, 2 H, CH), 7.37–7.34 (t, 2 H, CH), 7.45–7.41 (t, 2 H, CH), 7.59 (d, 2 H, CH), 7.79 (d, 2 H, CH), 7.96–7.93 (m, 4 H, CH), 8.14 (s, 2 H, CH), 10.98 (s, 2 H, CH).
Ligand ( <i>R,R</i> )- <b>21</b>	8.33	15.45	2.22–2.21 (m, 2 H, CH), 2.46–2.45 (m, 2 H, CH), 4.28–4.26	7.22 (d, 2 H, CH), 7.31 (d, 2 H,CH), 7.63–7.56 (m, 4 H, CH), 7.73–7.69 (m, 2 H, CH), 7.87 (d, 2 H, CH), 7.89 (dd, 2 H, CH), 10.11 (d, 2 H, CH).
Complex ( <i>R,R</i> )- <b>27</b>	8.52		2.18–2.16 (m, 2 H, CH), 4.76–4.54 (m, 2 H, CH) (One backbone signal	6.98 (d, 2 H, CH), 7.23 (d, 2 H, CH), 7.56–7.52 (m, 2H, CH), 7.64–7.61 (m, 4

			overlap with solvent peak).	H, CH), 7.84 (d, 2 H, CH), 7.90 (d, 2 H, CH),
--	--	--	-----------------------------	---

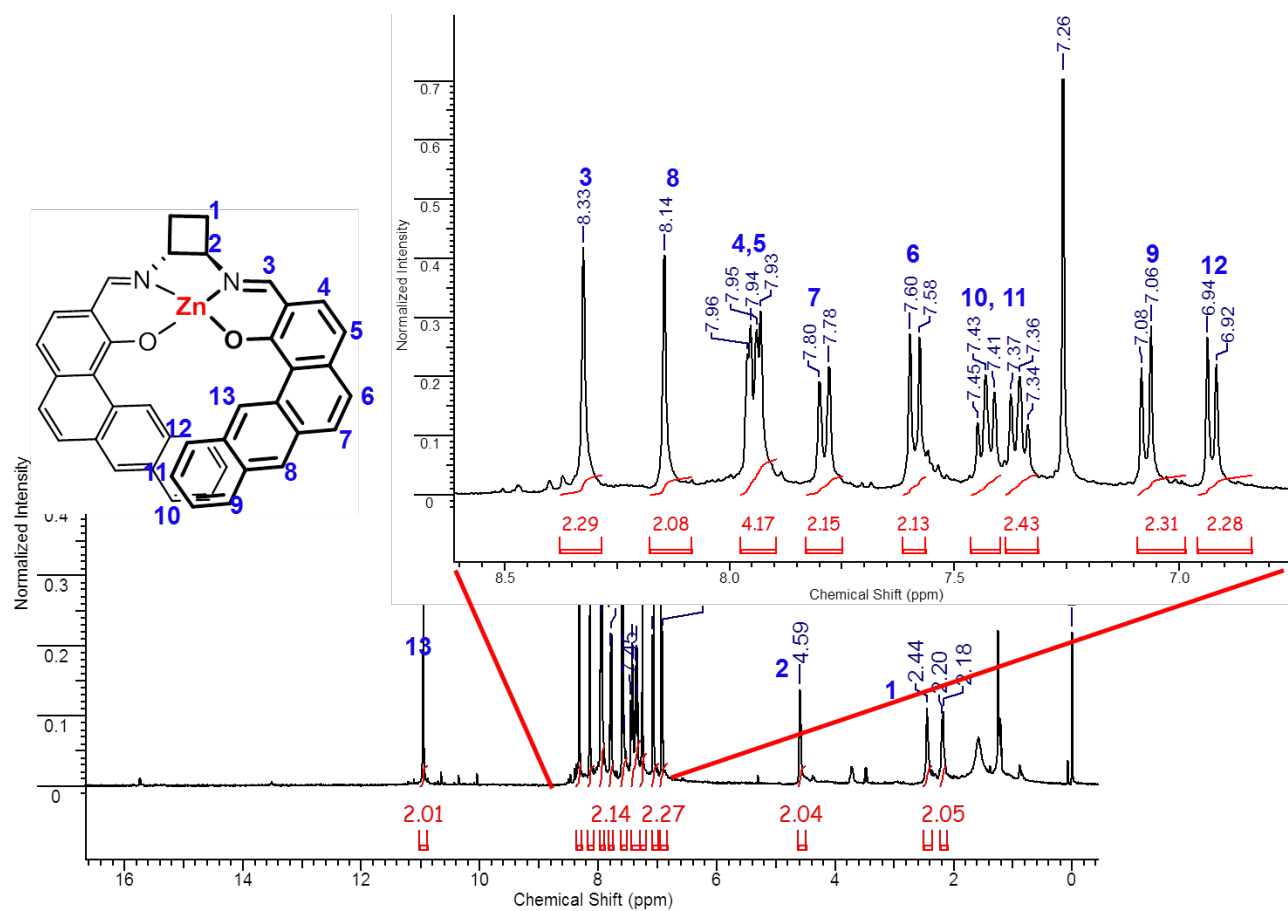


**Figure 4.5** The <sup>1</sup>H NMR spectrum of complex (R,R)-25 with specific assignments.

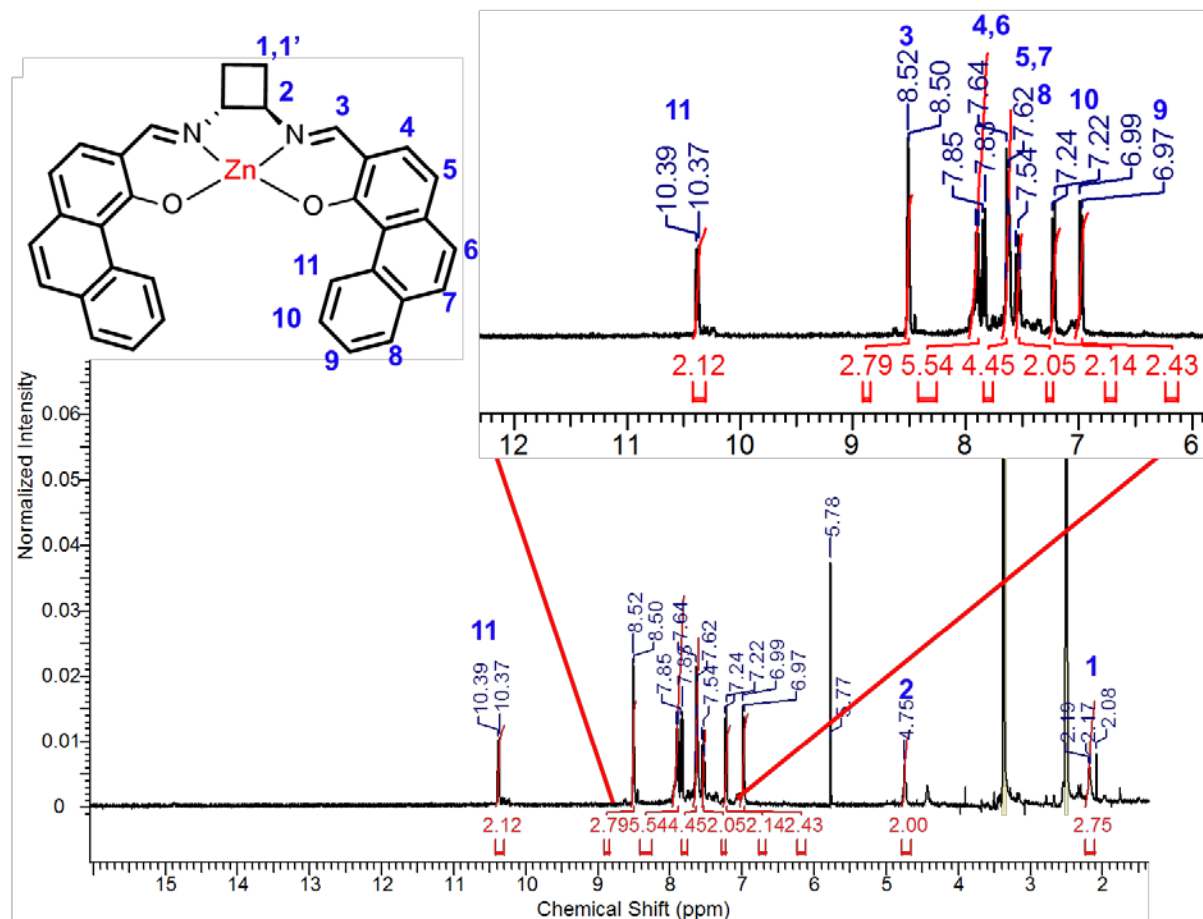


**Figure 4.6** The  $^1\text{H}$  NMR spectrum of complex  $(R,R)$ -27 with specific assignments.

### 4.3.2 Electronic and infrared spectra

The characteristic IR bands of complexes are summarized in Table 3.2. Compared to the free ligands Zn(II) salen complexes showed a red shift in the position of  $\nu(\text{C}=\text{N})$  in the corresponding complexes indicating the coordination of imine N to the metal ion, Figure 4.7 to Figure 4.10. Furthermore, the phenoxo  $\nu(\text{C}-\text{O})$  bands are blue shifted in the corresponding complexes, which indicates the coordination of phenol O to the metal center. The characteristic bands derived from the aromatic region in the salen ligand and in the complex are very complicated, and most are in the fingerprint region and very hard to assign. The IR spectra of the Ni complex a shows a sharp  $\nu(-\text{COOH})$  band near  $2918\text{cm}^{-1}$  which specifies the absence of hydrogen bonding between carboxylic acid and hydroxyl groups. Also, this shows that the metal ion attached through the hydroxyl group.

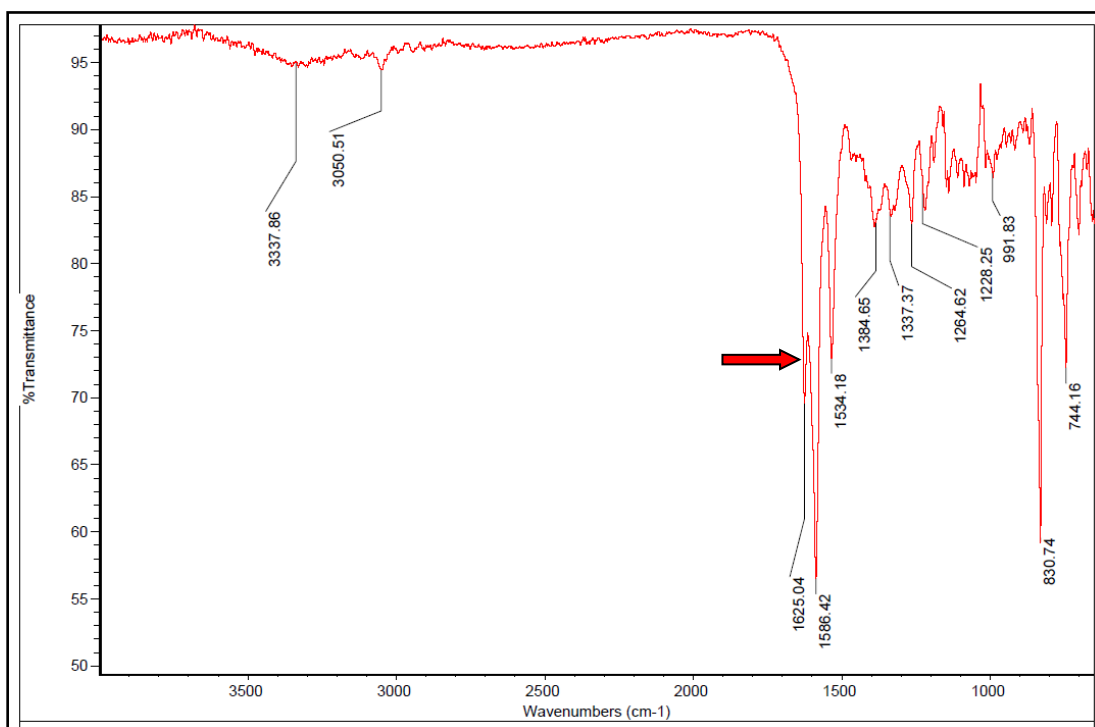


**Figure 4.7** The IR spectra of ligand (*R,R*)-20.

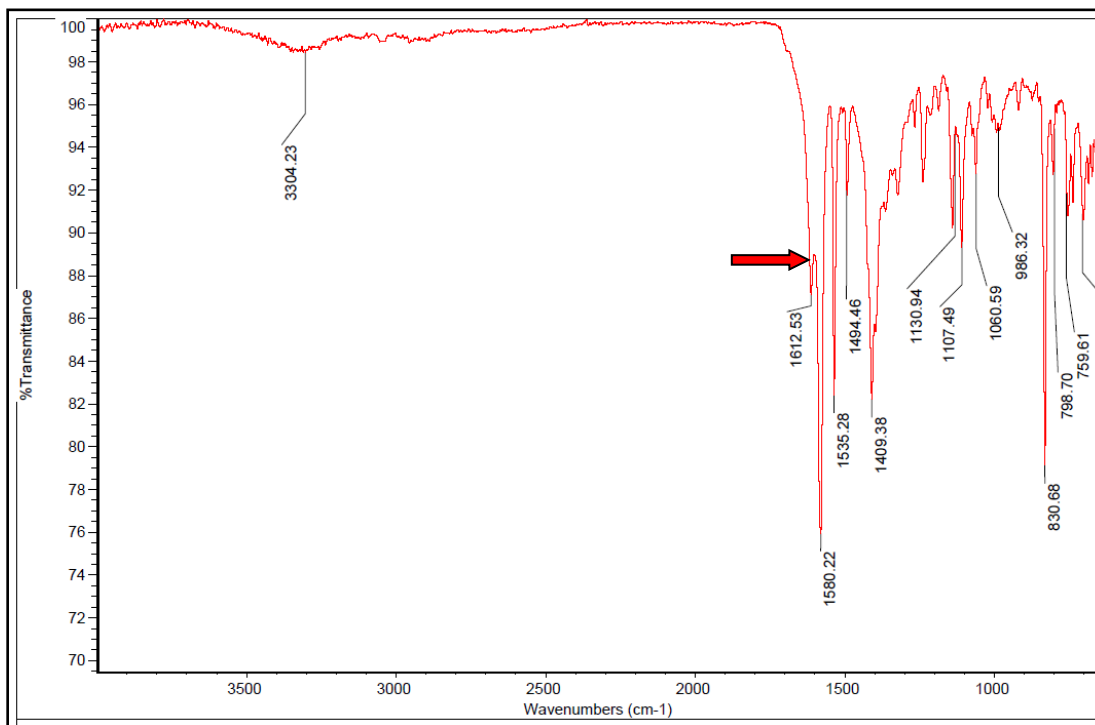


**Figure 4.8** The IR spectra of Zn complex (*R,R*)-25.

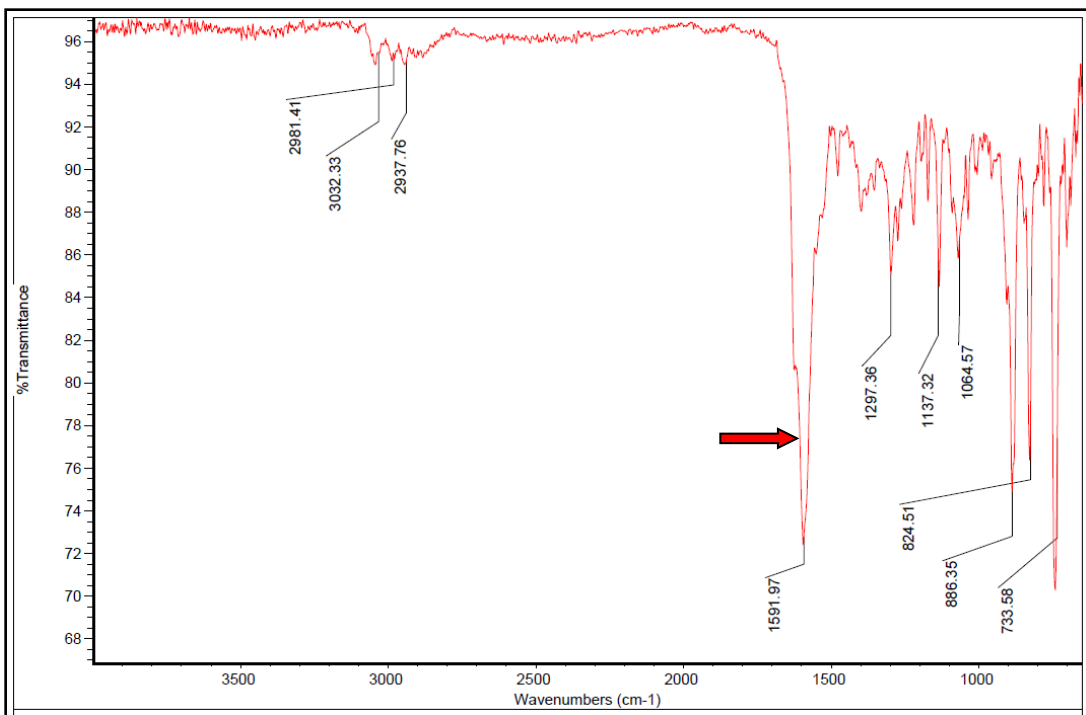


**Figure 4.9** The IR spectra of ligand (*R,R*)-21.

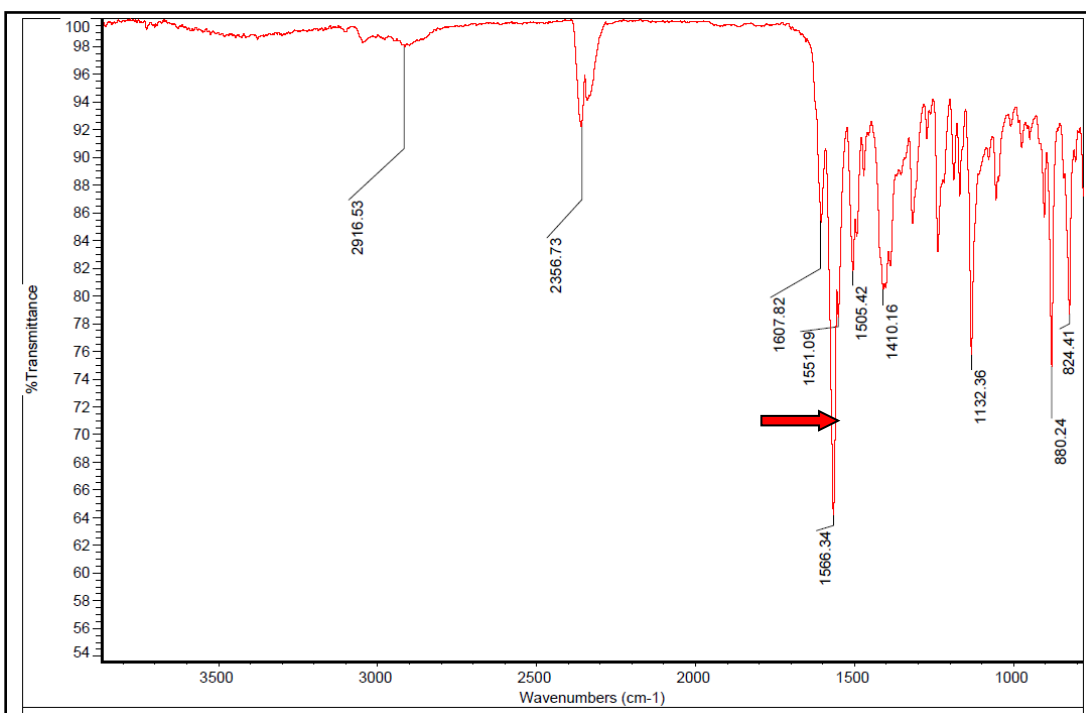


**Figure 4.10** The IR spectra of Zn complex (*R,R*)-27.

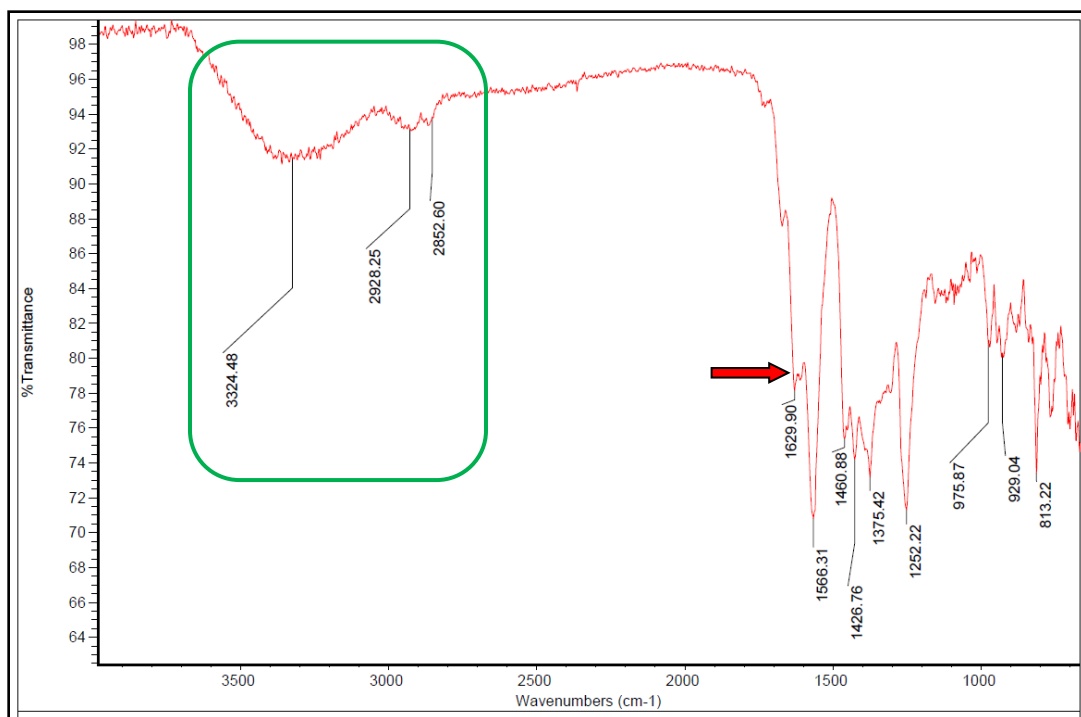


**Figure 4.11** The IR spectra of ligand (*R,R*)-24a.

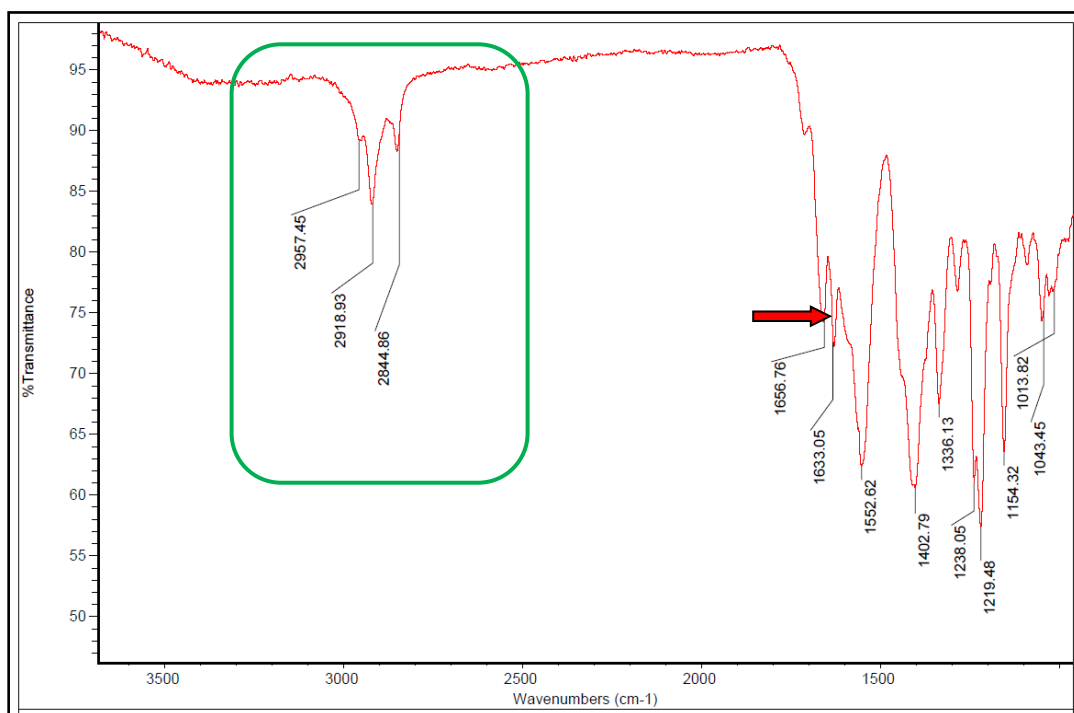


**Figure 4.12** The IR spectra of Ni complex (*R,R*)-27.

### 4.3.3 Mass spectra analysis

Mass spectroscopy can directly measure the molecular weight of a molecular ion/fragment derived from a complex. In addition, the isotopic pattern may be quite distinct which can help to identify the compositions of species in solution.

The mass data of **25-29** were collected in methanol by HR-ESI-MS. The Zn complex (*R,R*)-**25** and (*R,R*)-**27** showed molecular ion peak with one mole of molecular water. The Ni complex (*R,R*)-**29** formed doubly charged species indicated by peak near 465amu and also shows absence of dinuclear complexes.

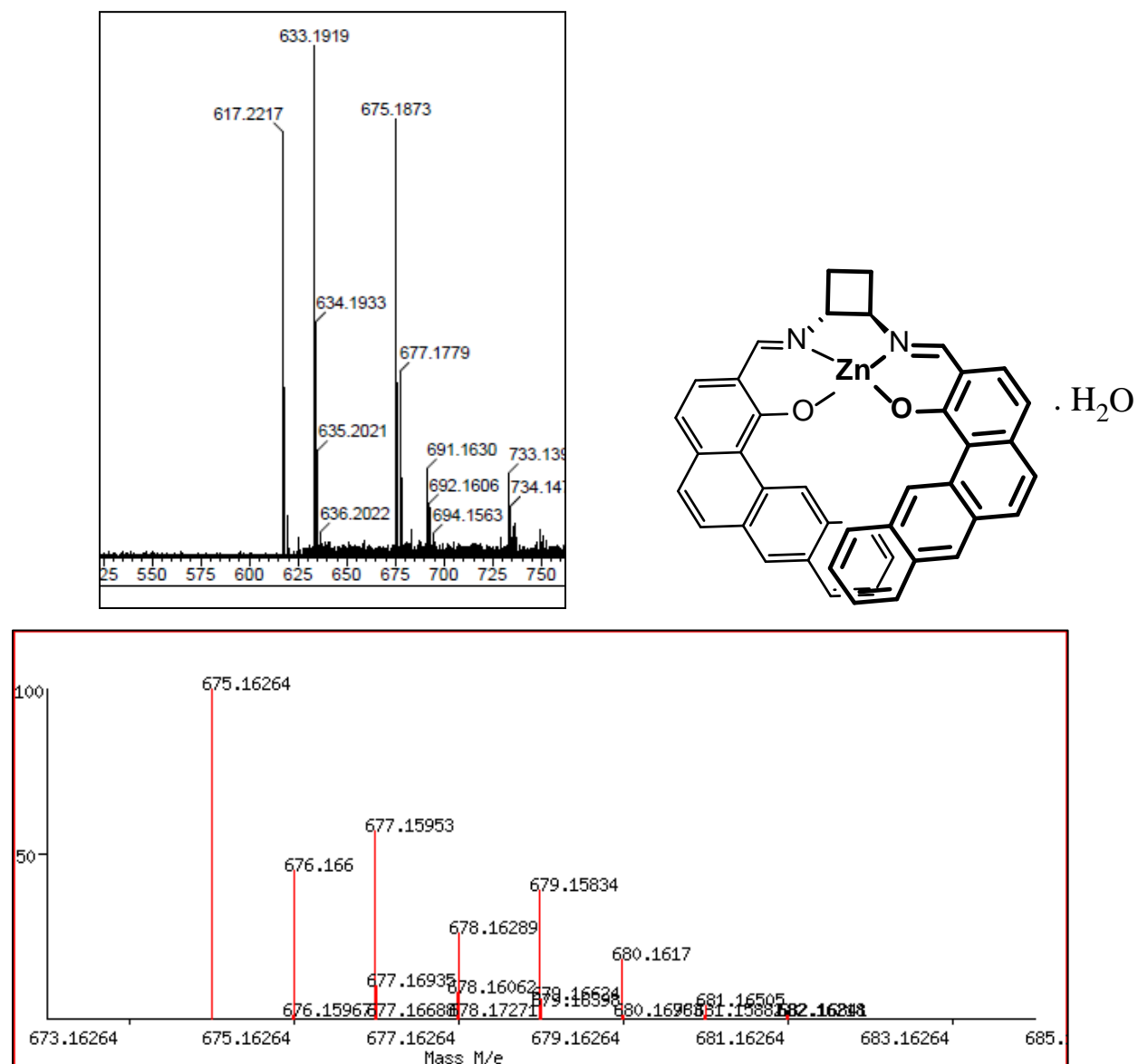


**Figure 4.13** Observed mass spectrum (top) for Zn salen complex (*R,R*)-**25** with simulated isotopic pattern (bottom).

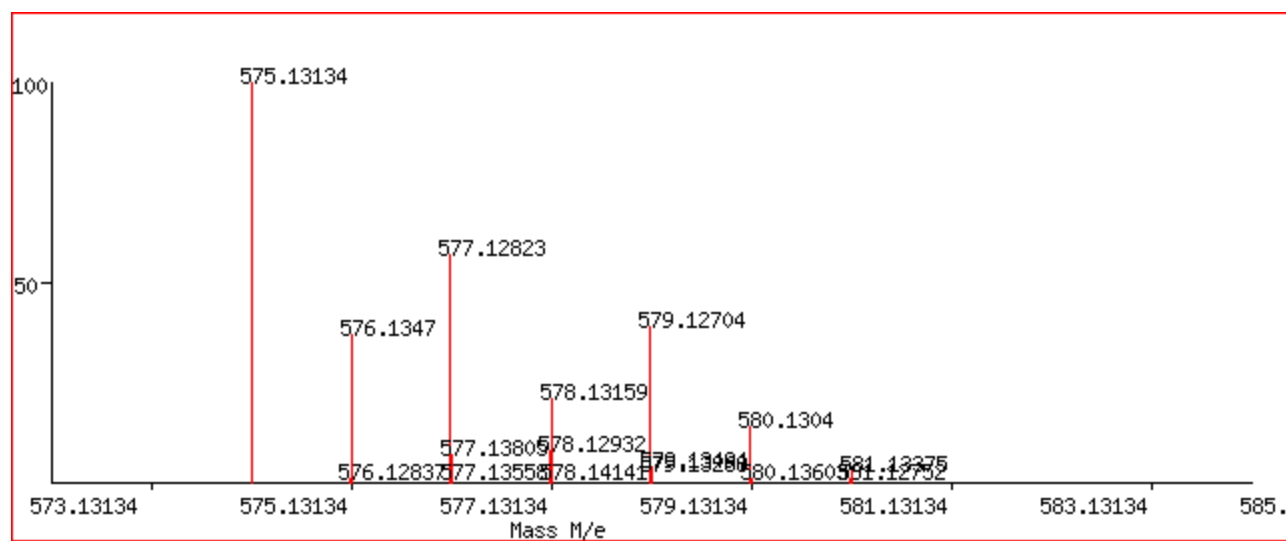
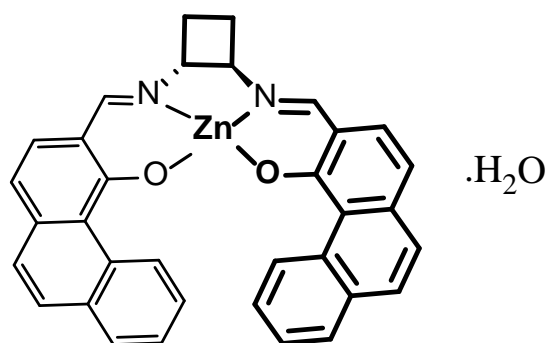
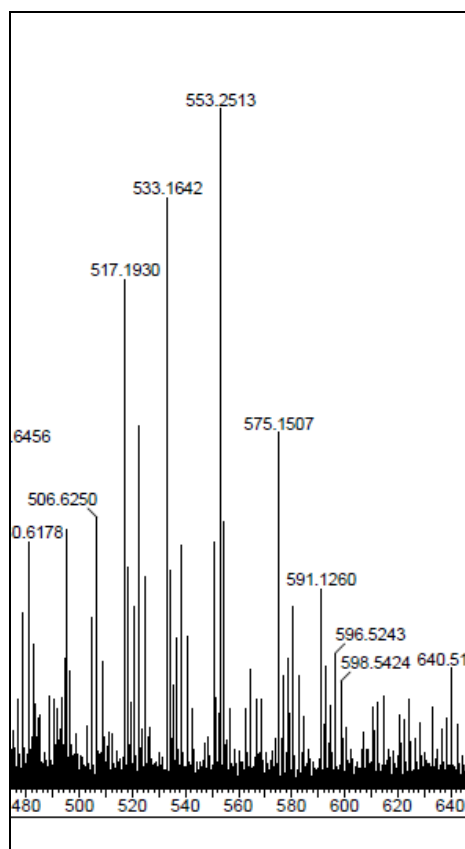
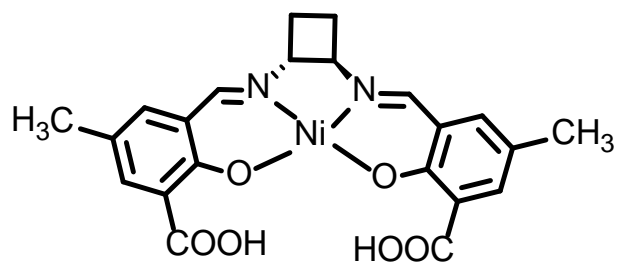
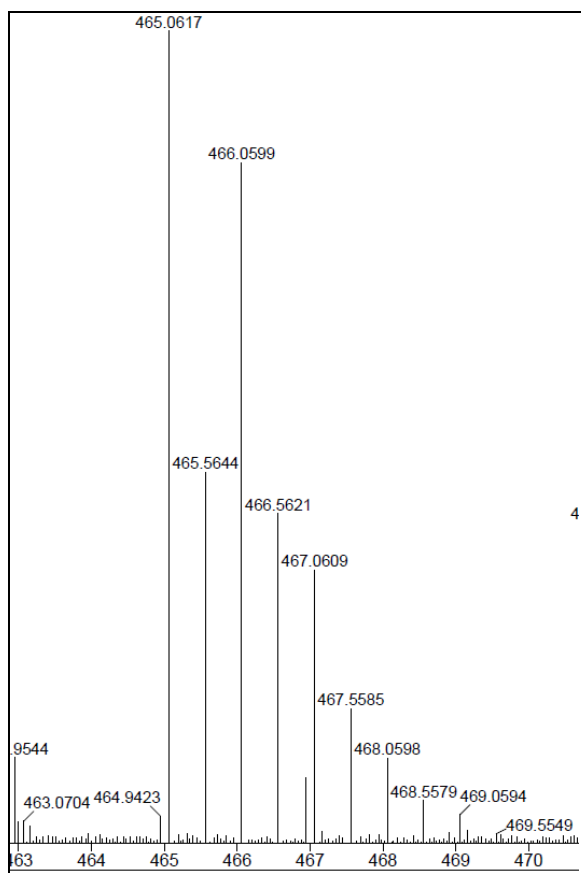


**Figure 4.14** Observed mass spectrum (top) for Zn salen complex (*R,R*)-**27** with simulated isotopic pattern (bottom).



Chemical Formula:  $C_{22}H_{20}N_2NiO_6$   
 Exact Mass: 466.0675

**Figure 4.15** Observed mass spectrum for Ni salen complex (*R,R*)-**29** by negative ESI.

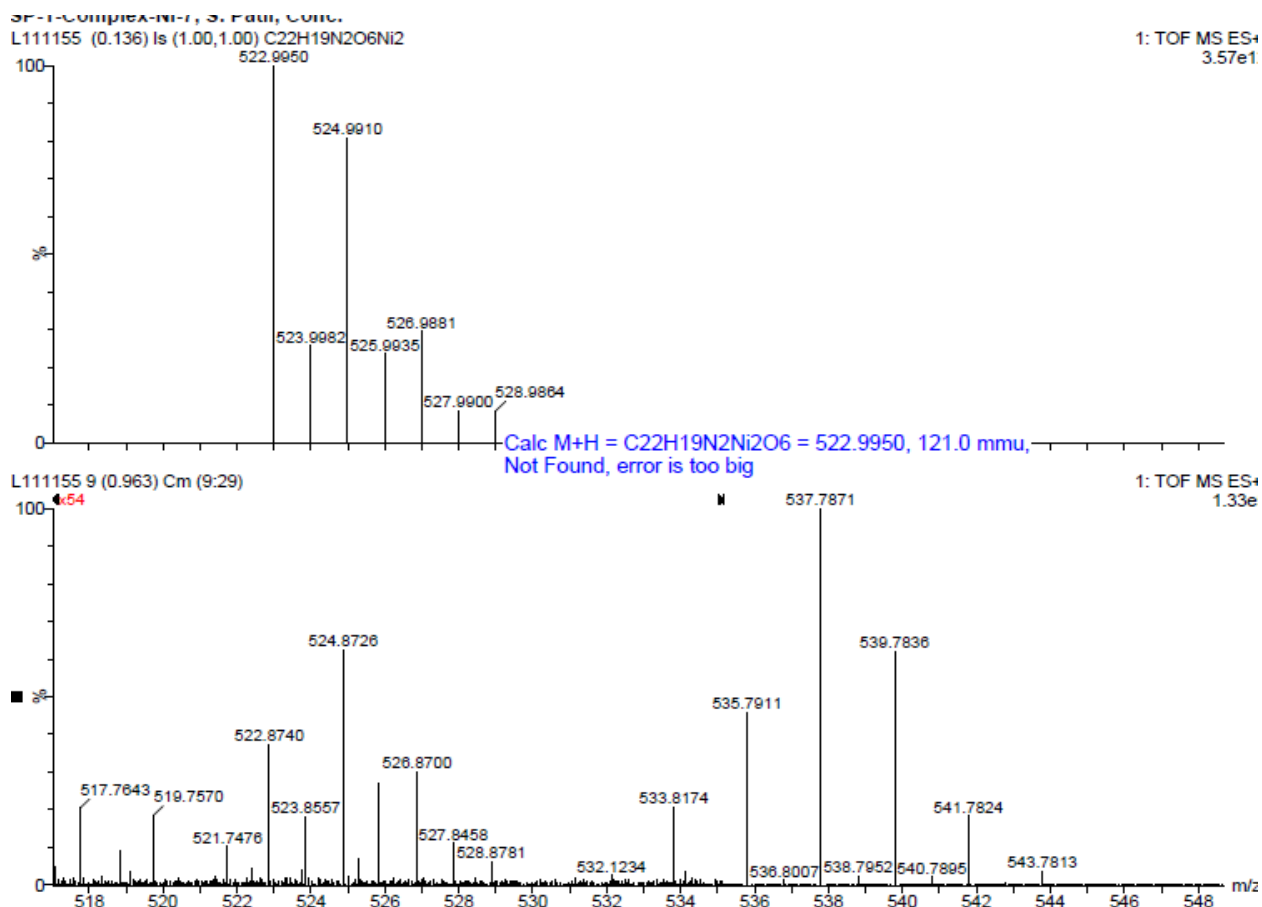


**Figure 4.16** Observed mass spectrum for Ni salen complex (*R,R*)-**29** indicating absence of dinuclear complex.

## 4.4 Conclusion

The salen complexes with chiral cyclobutyl backbone have been synthesized and characterized. ESI-MS reveals the presence mononuclear complexes. <sup>1</sup>H NMR studies showed that Zn complexes have *C*<sub>2</sub> symmetry. The IR spectrum of these solids contained the characteristic imine stretch. However, the electrospray mass spectrum indicated the Zn complexes have molecular water attached. The manganese and iron complexes are not readily identifiable from their mass spectrum or IR spectrum. This indicates that manganese and iron metal are not suitable to form metal complexes with highly twist cyclobutyl backbone.

## References

---

- <sup>1</sup> Canali, L.; Sherrington, D. *Chem. Soc. Rev.* **1999**, 28, 85-93.
- <sup>2</sup> Bohle, D.; Zafar, A.; Goodson, P.; Jaeger, D. *Inorg. Chem.* **2000**, 39, 712-718.
- <sup>3</sup> Singer, A.; Atwood, D. *Inorg. Chim. Acta* **1998**, 277, 157-162.
- <sup>4</sup> Morris, G.; Zhou, H.; Stern, C.; Nguyen S. *Inorg. Chem.* **2001**, 40, 3222-322.
- <sup>5</sup> Katsuki, T. *Fascination of metallosalen complexes: Diverse catalytic performances and high asymmetry-inducing ability.*

## Chapter 5 - Catalytic study of complexes with cyclobutyl backbone

### 5.1 Introduction

Enantioselective synthesis is also called chiral synthesis or asymmetric synthesis. This enantioselective synthesis is generally defined as a chemical reaction (or reaction sequence) in which one or more new elements of chirality are formed in a substrate molecule and which produces the enantiomeric or diastereoisomeric products in unequal amounts. More simply, it is the synthesis of a compound by a method that favors the formation of a specific enantiomer or diastereomer.<sup>1,2</sup>

Enantioselective synthesis is a key process in modern chemistry and is particularly important in the field of pharmaceuticals, as the different enantiomers or diastereomers of a molecule often have different biological activity. As an example Figure 5.1, shows enantiomers of the chiral drug Thalidomide.<sup>3</sup>

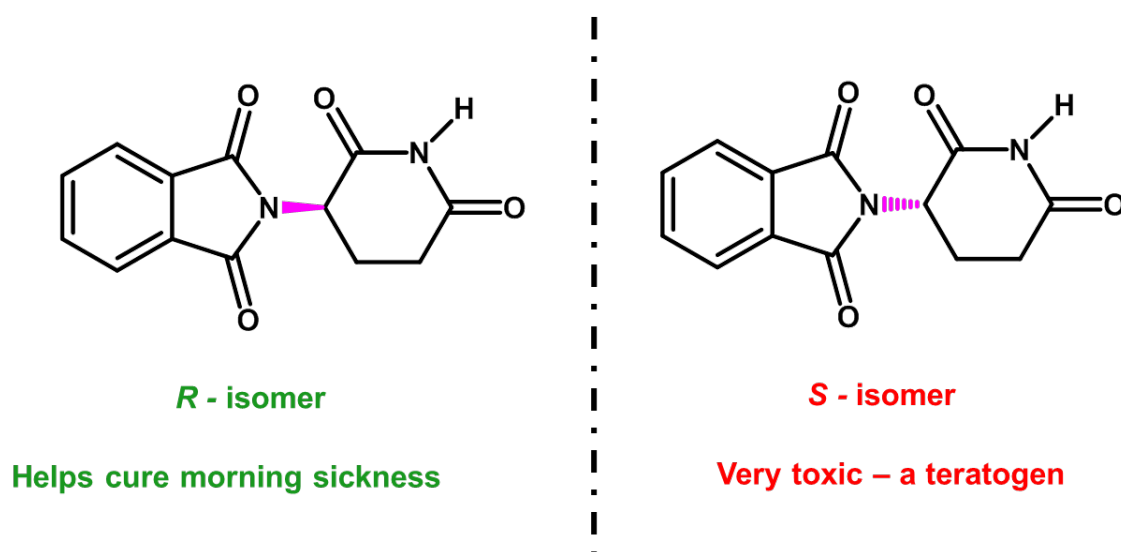


Figure 5.1 Enantiomers of chiral drug Thalidomide.

## 5.1.2 Catalysis

In considering the properties of catalysts and their commercial importance, we have chosen Diels-Alder and Mannich-type reactions to illustrate the catalytic activity of our catalyst systems.

### 5.1.2.1 Diels-Alder reaction

Diels-Alder reactions<sup>1</sup> have been one of the most powerful organic synthetic methods for the construction of 6-membered cyclic compounds.<sup>4</sup> In particular, asymmetric catalytic variants of Diels-Alder reactions have received special attention due to their potential ability to rapidly provide enantiomerically pure and complex compounds from simple substrates.<sup>5</sup> Chiral Lewis acid catalysts have played an important role in these Lewis acid-promoted reactions. From a practical point of view, developing highly efficient chiral Lewis acids with low catalyst loading and minimal deactivation by moisture is one of the most important objectives in organic synthesis. Diels-Alder reactions of cyclopentadiene with 3-alkenyl-2-oxazolidinones have also been used as model systems for developing new chiral Lewis acid catalysts and testing the degree of asymmetric induction.<sup>5</sup>

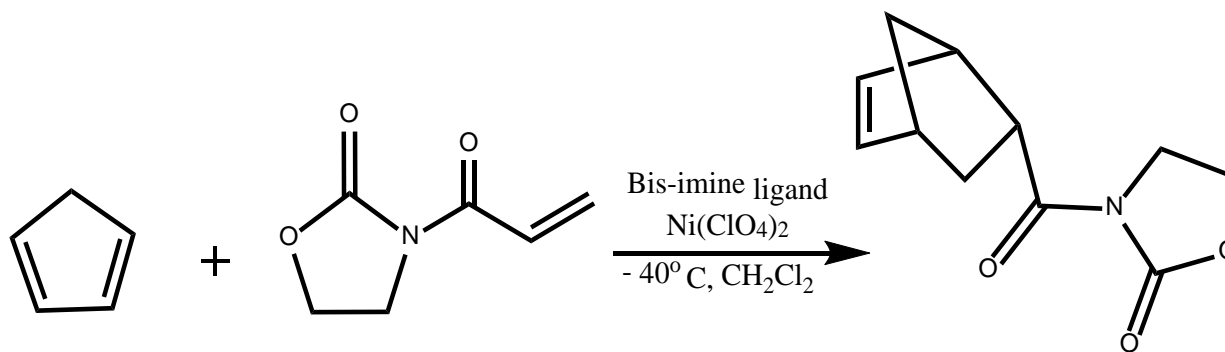


**Figure 5.2** Diels-Alder reactions of cyclopentadiene with 3-alkenyl-2-oxazolidinones.

### 5.1.2.1 Mannich-type reaction

Chiral  $\alpha,\beta$ -diamino acids are crucial structural components in various biologically active compounds.<sup>6</sup> Among possible routes for their synthesis, asymmetric synthesis via direct Mannich-type reactions of a glycine Schiff base are one of the most effective and straight forward route for producing chiral syn- $\alpha,\beta$ -diamino acids.<sup>7,8</sup> Considering the importance of  $\alpha,\alpha$ -disubstituted  $\alpha$ -amino acids as chiral building blocks for pharmaceuticals and artificial peptides,

a new catalyst for chiral  $\alpha$ -tetrasubstituted  $\alpha,\beta$ -diamino acid synthesis with a broad substrate scope is in high demand.<sup>9,10</sup>

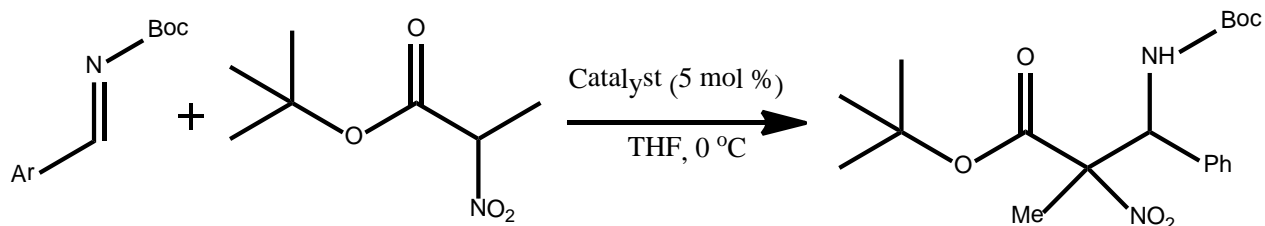


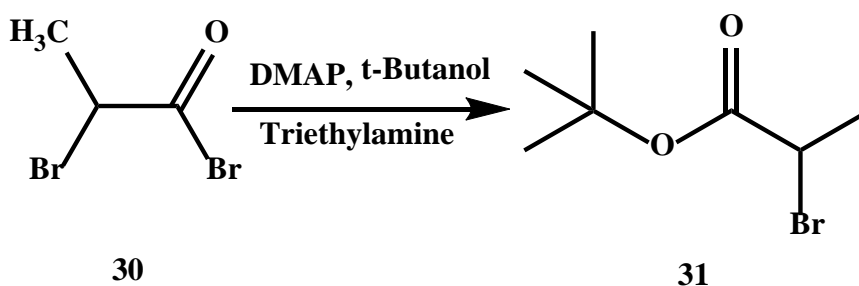
**Figure 5.3** Mannich-type reactions of *N*-Boc imines and  $\alpha$ -substituted nitroacetates.

## 5.2 Experimental

### 5.2.1 Synthesis

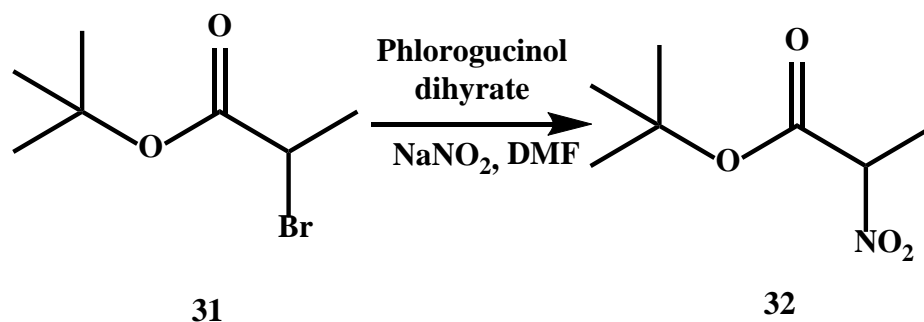
$^1\text{H}$  and  $^{13}\text{C}$  NMR spectra were recorded on a Varian Unity plus 400 MHz or 200 MHz spectrometer in  $\text{CDCl}_3$  or DMSO. Data is expressed in parts per million (ppm) downfield shift from tetramethylsilane or residual protiosolvent as internal reference and are reported as position (in ppm), multiplicity (s = singlet, d = doublet, t = triplet, m = multiplet), coupling constant ( $J$  in Hz) and integration (number of protons). IR spectra were collected on a Nicolet 380 FT-IR (Thermo Scientific, Madison MN) at room temperature. UV-Vis spectra were obtained on a Varian Cary 500 scan UV-Vis-NIR spectrophotometer (Agilent Technologies) in tetrahydrofuran (THF). The solution samples for UV-Vis were prepared at room temperature, with the concentrations ranging between 1.5 and  $2.5 \times 10^{-5}\text{M}$ . A 1.00 cm path length quartz cell was employed for analyses.

#### 5.2.1.1 *t*-butyl 2-bromo-propanoate, 31



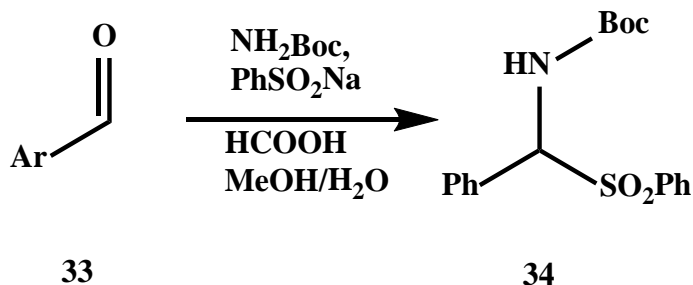
2-Bromopropionyl bromide **30** (2.00 g, 9.26 mmol) was dissolved in dichloromethane (10 mL) followed by the addition of *t*-butanol (1.03 g, 13.9 mmol), triethylamine (0.94 g, 9.3 mmol) and DMAP (20 mg). After stirring for 16 hours the solution was washed with 10% HBr and saturated solution of NaHCO<sub>3</sub>, dried over anhydrous MgSO<sub>4</sub>, and concentrated under reduced pressure, yielding a tan oil **31** (1.42g, 73% yield). <sup>1</sup>H NMR δ 4.23 (q, 1H,CH), 1.71 (d, 3H, CH), 1.43 (s, 9H, 3CH<sub>3</sub>); <sup>13</sup>C NMR δ 169.4, 82.3, 42.1, 27.8, 21.7.

#### 5.2.1.2 *t*-butyl 2-nitro-propanoate, **32**



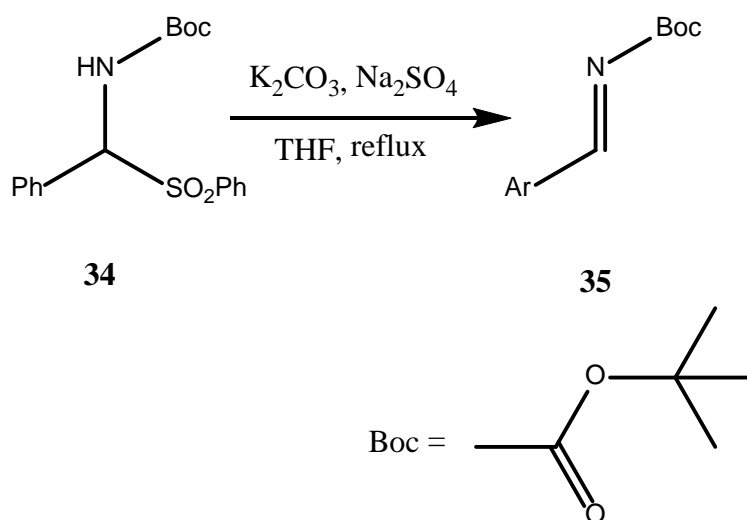
Tertiary-butyl 2-bromo-propanoate **31** (400mg, 1.91 mmol) was dissolved in 5 mL dimethyl formamide along with phloroglucinol dihydrate (310 mg, 1.91 mmol) and sodium nitrite (145 mg, 2.10 mmol). After stirring for two hours, the solution was separated between diethyl ether and water. The organic layer was washed with brine, dried over MgSO<sub>4</sub>, and concentrated to dryness under reduce pressure. The resulting brown solid was purified by flash chromatography using dichloromethane as the eluent, yielding **32** (93 mg, 28%) of a clear oil. <sup>1</sup>H NMR 5.10 (q, 1H, CH), 1.75 (d, 3H, CH), 1.50 (s, 9H, 3CH<sub>3</sub>); <sup>13</sup>C NMR (400 MHz, CDCl<sub>3</sub>) δ 164.18, 84.40, 84.07, 27.63, 15.65.

#### 5.2.1.3 *α*-sulfonyl amine, **34**



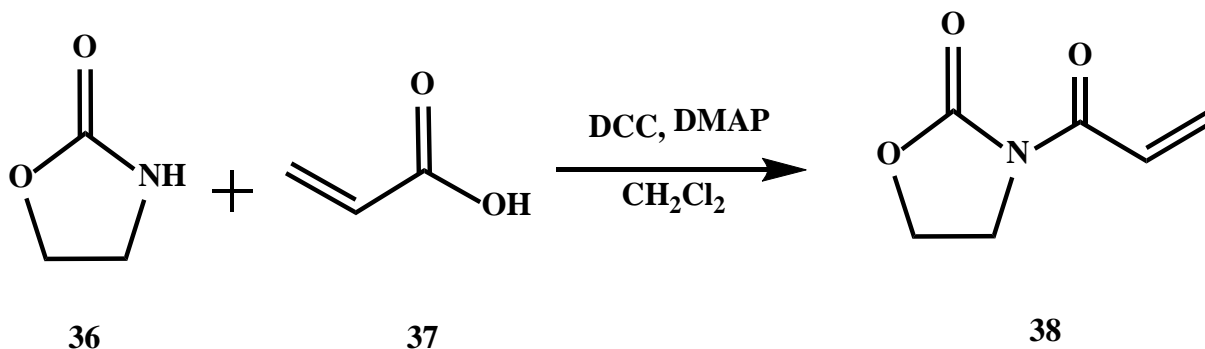
A mixture of benzaldehyde 33 (2.10 mL, 20.0 mmol), *tert*-butyl carbamate (1.17 g, 10.0 mmol), benzenesulfinic acid sodium salt (4.11 g, 25.0 mmol) and formic acid (0.760 mL, 20.0 mmol) in methanol (10 mL) and water (20 mL) was stirred at room temperature for 24 h. The resulting precipitate was filtered and washed well with diethyl ether. After drying under reduce pressure, the product 34 was obtained as a white solid (2.61 g, 75%). <sup>1</sup>H NMR (CDCl<sub>3</sub>, 400 MHz) δ 1.24 (s, 9H, 3CH<sub>3</sub>), 5.73 (d, 1H, CH), 5.90 (d, 1H, NH), 7.43-7.40 (m, 5H, Ar-H), 7.54-7.51 (m, 2H, Ar-H), 7.62-7.64 (m, 1H, Ar-H), 7.89 (d, 2H, ArH); <sup>13</sup>C NMR (CDCl<sub>3</sub>, 400 MHz) δ 27.96, 73.90, 81.16, 128.72, 128.90, 129.00, 129.44, 129.80, 129.91, 133.89, 136.93, 153.46.

#### 5.2.1.4 *N*-Boc imine, 35



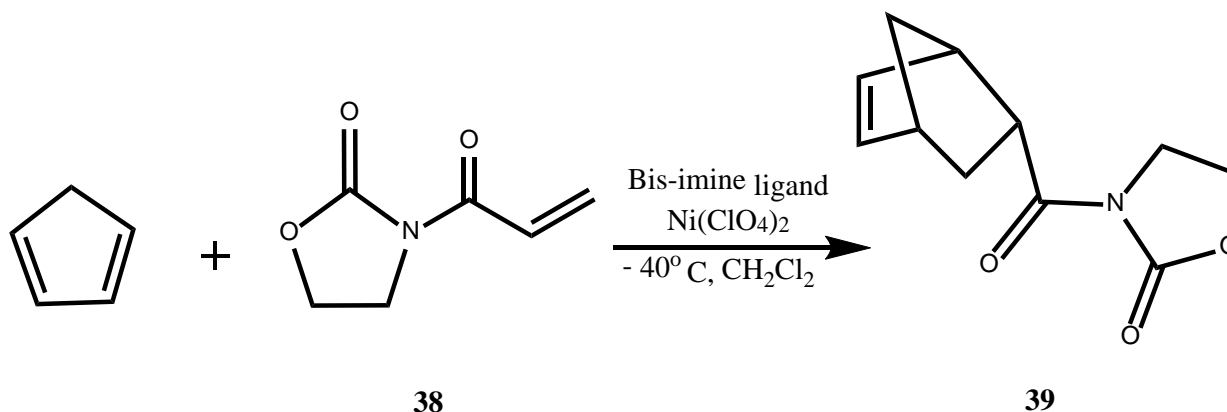
A 100 mL round bottom flask with potassium carbonate (4.14 g, 30.0 mmol) and sodium sulfate (4.97 g, 35.0 mmol) was dried in oven at 200 °C. After the flask was cooled down to room temperature under N<sub>2</sub>, sulfonamide 34 (1.74 g, 5.00 mmol) was added along with dry THF (20 mL). The mixture was refluxed under N<sub>2</sub> for 18 h. It was then allowed to cool to room temperature, filtered through Celite, and the filtrate was concentrated to give the imine 35 as a colorless oil (1.00 g, 5.00 mmol, 99%) which was used without further purification for the catalysis reaction. <sup>1</sup>H NMR (CDCl<sub>3</sub>, 400 MHz) δ 1.47 (s, 9H, 3CH<sub>3</sub>), 7.46-7.33 (m, 3H, Ar-H), 7.81-7.78 (m, 2H, Ar-H), 8.75 (s, 1H, CHN); <sup>13</sup>C NMR (CDCl<sub>3</sub>, 400 MHz) δ 27.93, 82.28, 128.85, 130.19, 133.49, 134.10, 162.64, 169.64.

### 5.2.1.5 3-acryl-2-oxazolidinone, 38



To a suspension of oxazolidinone (1.13 mmol), DMAP (0.15 mmol) and acrylic acid (1.47 mmol) in  $\text{CH}_2\text{Cl}_2$  (1.5 mL) at 0 °C, under an argon atmosphere, was added DCC in one portion (1.47 mmol). After 10 min the temperature was raised to r.t. and stirring was continued until no starting material has left, as confirmed by TLC. The dicyclohexylurea formed was filtered and the precipitate washed with  $\text{CH}_2\text{Cl}_2$  (10 mL). The filtrate was washed with saturated  $\text{NaHCO}_3$  (10 mL), dried with anhydrous  $\text{Na}_2\text{SO}_4$  and concentrated at reduced pressure to furnish the crude product, which was purified by silica gel chromatography (30% EtOAc in hexanes).  $^1\text{H}$  NMR ( $\text{CDCl}_3$ , 400 MHz)  $\delta$  4.10 (t, 2H, CH), 5.92 (d, 1H, CH), 6.58 (d, 1H, CH), 7.50 (q, 1H, CH).  $^{13}\text{C}$  NMR (400 MHz,  $\text{CDCl}_3$ )  $\delta$  165.19, 153.52, 131.95, 127.11, 62.29, 42.76.

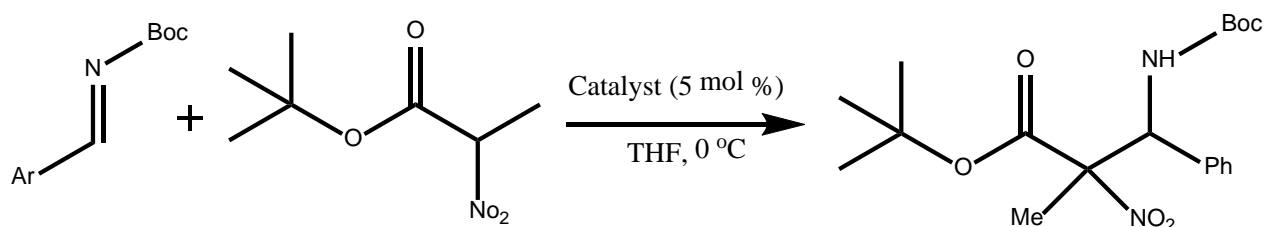
### 5.2.1.6 3-(Bicyclo[2.2.1]hept-5-en-2-ylcarbonyl)-2-oxazolidinone, 39



To a mixture of  $\text{Ni}(\text{ClO}_4)_2 \cdot 6\text{H}_2\text{O}$  (18 mg, 0.05 mmol) and powdered molecular sieves ( $4\text{\AA}$ , 0.125 g) was added a solution of (*R,R*)-**22** (23 mg, 0.05 mmol) in  $\text{CH}_2\text{Cl}_2$  (2 mL); the

mixture was then stirred at room temperature for 6 h. To the above mixture was added a solution of 3-acryloyl-2-oxazolidinone **38** (72 mg, 0.50 mmol) in CH<sub>2</sub>Cl<sub>2</sub> (1 mL). After cooling to -40 °C, the mixture was allowed to react with cyclopentadiene (0.33 g, 5.0 mmol) for 17 h. The reaction mixture was quenched with a saturated NH<sub>4</sub>Cl solution (3 mL) and then filtered. The filtrate was extracted with CH<sub>2</sub>Cl<sub>2</sub> (5 mL × 3). The combined extracts were dried over anhydrous MgSO<sub>4</sub> and evaporated in vacuo. The residue was chromatographed on silica gel with hexane–diethyl ether (7:3 v/v) to give cycloadduct **39** (0.098 g, 92%). <sup>1</sup>H NMR (CDCl<sub>3</sub>, 400 MHz) 1.36–1.48 (3H, m), 1.89–1.96 (1H, m), 2.91 (1H, m), 3.28 (1H, m), 3.87–4.03 (3H, m), 4.32–4.42 (2H, m), 5.84 (1H, dd), 6.21 (1H, dd).

### 5.2.1.7 *tert*-Butyl 3-(*tert*-Butoxycarbonylamino)-2-methyl-2-nitro-3-phenylacrylate, **40**



Powdered molecular sieves (4Å, 75 mg), the Ni catalyst **29** (7.0 mg, 0.015 mmol) and THF (750 μL) were added to a 50 mL flask under argon. To the mixture at 25 °C was added nitroacetate (57.8 mg, 0.33 mmol) and the mixture was cooled down to 0 °C. After stirring for 15 min at 0 °C, *N*-Boc-imine (61.6 mg, 0.3 mmol) was added. The reaction mixture was stirred for 12 h at 0 °C. The reaction mixture was evaporated under reduced pressure, and the crude product **40** was analyzed by <sup>1</sup>H NMR. The yield was very low; therefore product was not able to be satisfactorily purified.

## 5.3 Results & Discussion

### 5.3.1 Diels–Alder reactions with bis-imine catalyst

Initially, an uncatalysed Diels–Alder reaction of cyclopentadiene with 3-acryloyl-2-oxazolidinone was conducted in CH<sub>2</sub>Cl<sub>2</sub> at room temperature for 1 hour. The obtained product NMR spectrum is as shown in Figure 5.4 which indicated ≤ 56% conversion as reported previously.<sup>11</sup>

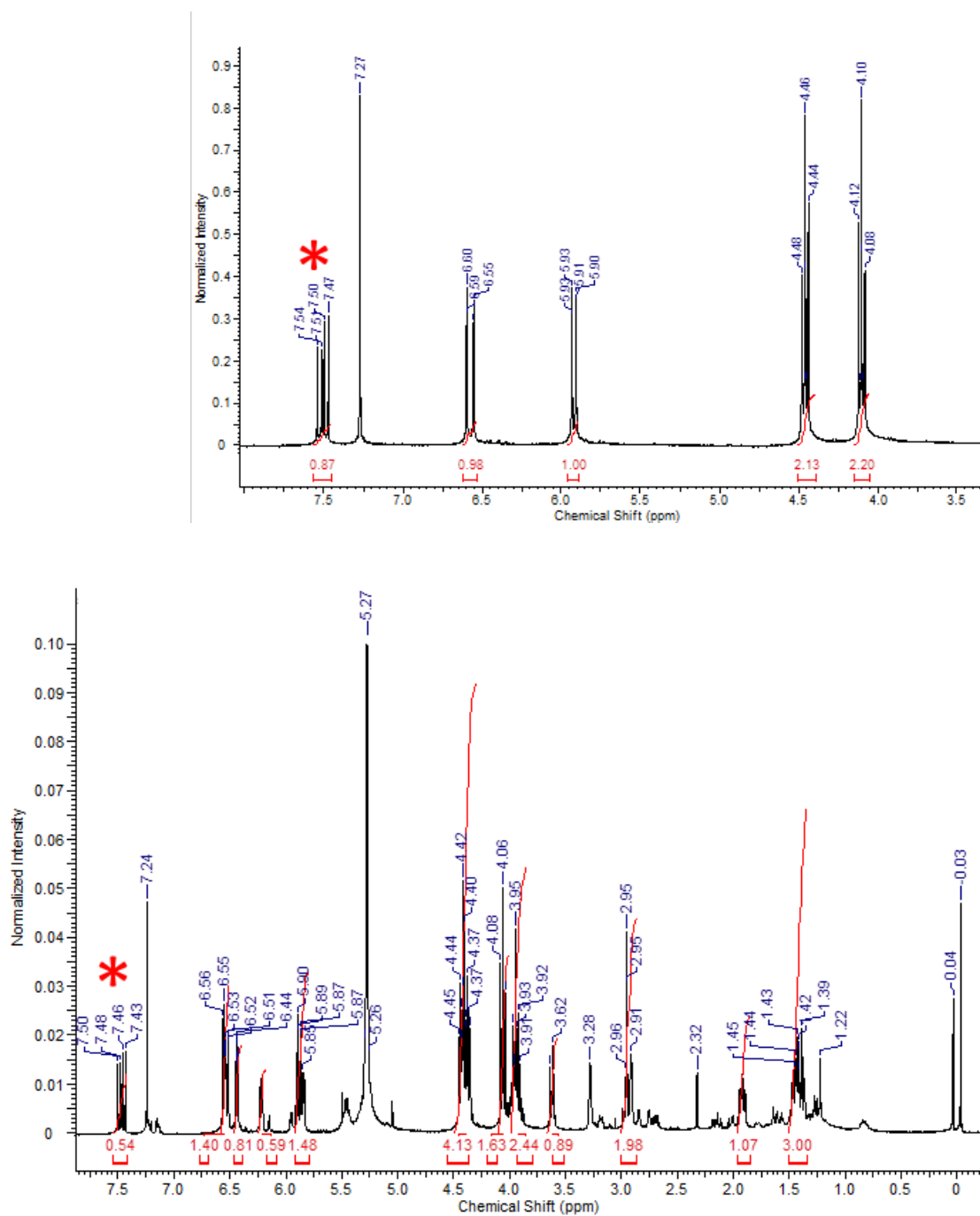


**Figure 5.4**  $^1\text{H-NMR}$  spectra of 3-alkenyl-2-oxazolidinones (top) and  $^1\text{H-NMR}$  spectra of Diels–Alder reactions of cyclopentadiene with 3-alkenyl-2-oxazolidinones without catalyst. (\* shows peak indicating conversion)

Diels–Alder reaction of cyclopentadiene with 3-acryloyl-2-oxazolidinone proceeded smoothly (yield = 92%) with 10 mol% of chiral bis(iminoquinoline)-Ni(II) catalyst with diastereomer ratio (endo:exo = 99:1). For this reaction, we have done *in situ* catalyst preparation by using ligand (*R,R*)-22 and Ni metal salt.

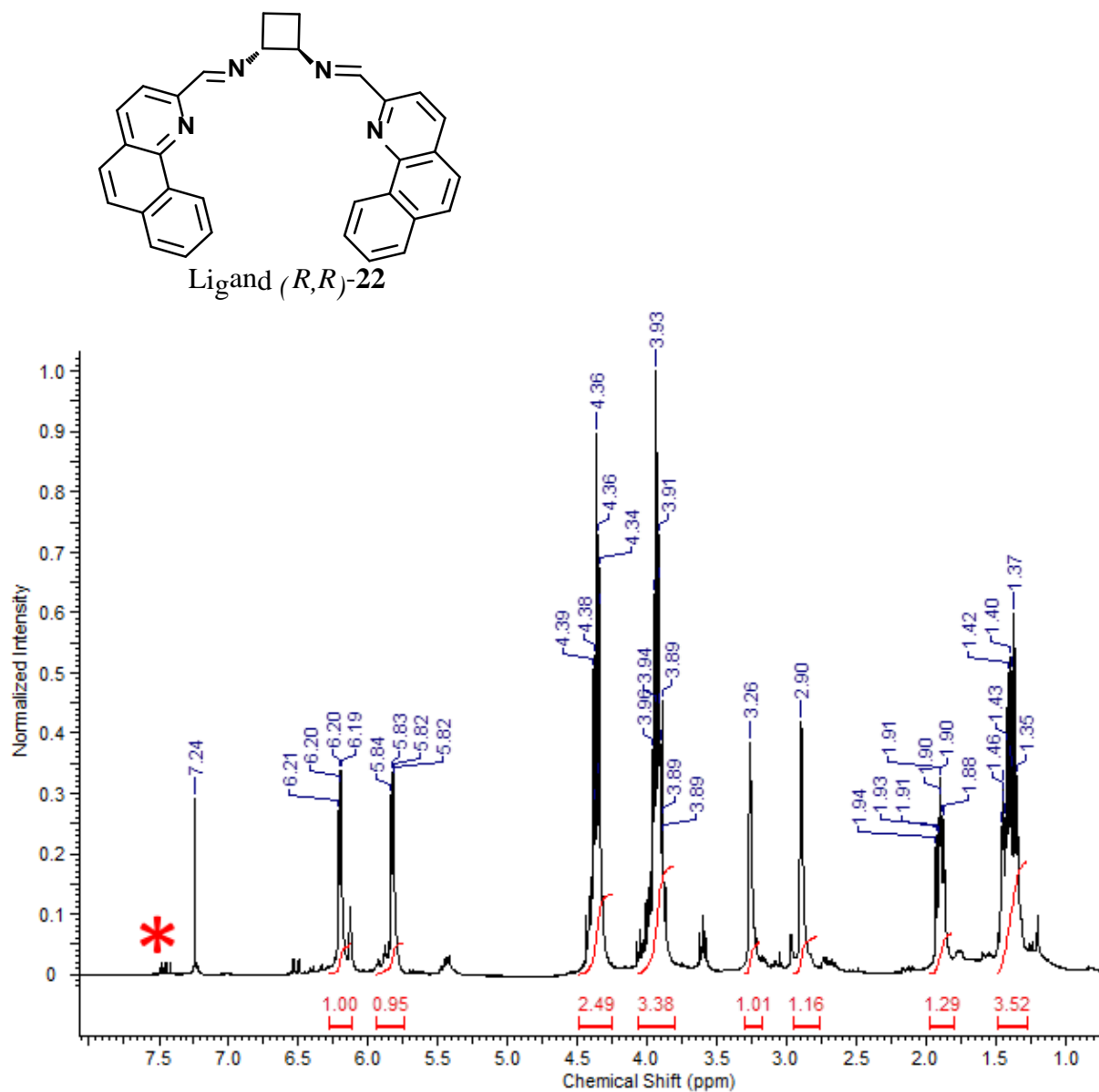


**Figure 5.5** Ligand used in catalyst preparation (top) and <sup>1</sup>H-NMR spectra of Diels–Alder reactions of cyclopentadiene with 3-alkenoyl-2-oxazolidinones with catalyst. (\* shows peak indicating conversion)

### 5.3.2 Mannich-type reactions with acid fictionalized catalyst

Controlled Mannich-type reactions of *N*-Boc imines and  $\alpha$ -substituted nitroacetates showed that mononuclear salen Ni-complex are not effective for the present reaction catalysis and gave poor reactivity, Figure 5.6. This suggests that binuclear Ni-complexes are important for achieving high yields. As previously explained by the Shibasaki group, we need to have binuclear Ni-complex salen to accomplish our goal of high yields and enantioselectivity.

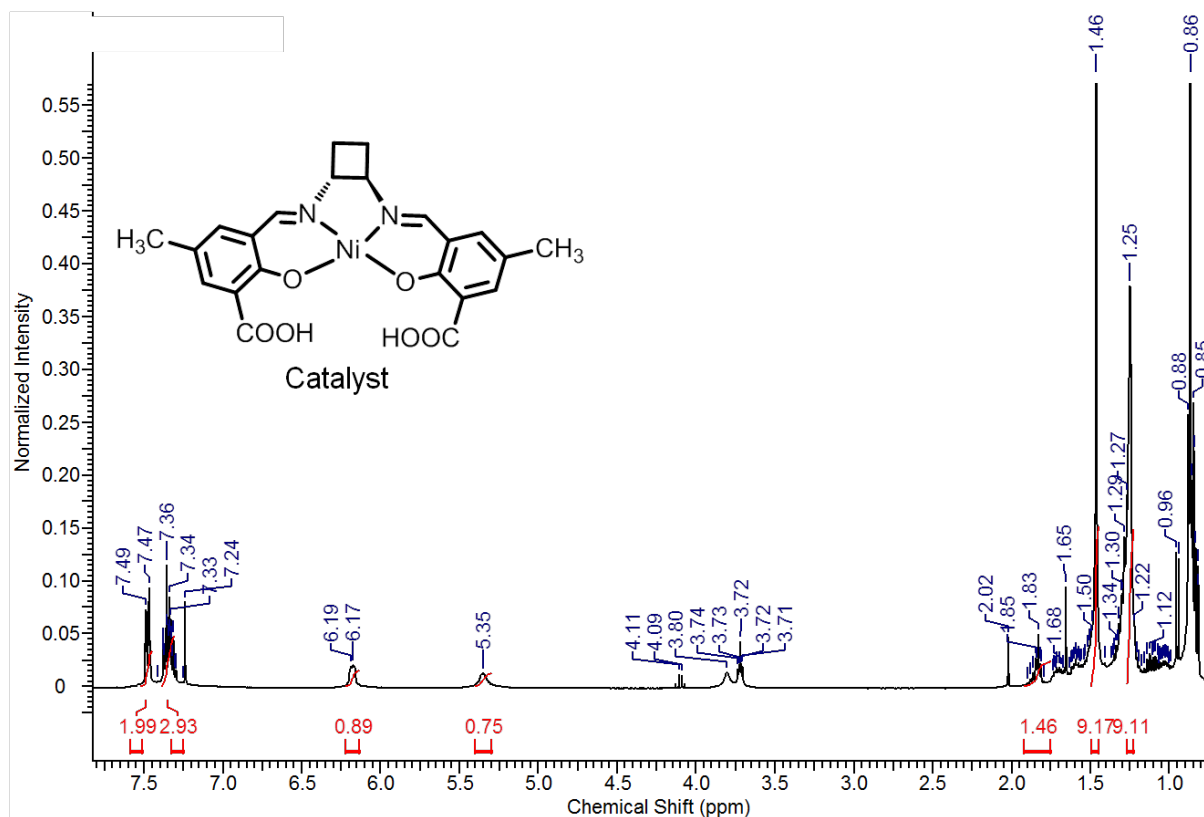


**Figure 5.6** <sup>1</sup>H-NMR spectra of Mannich-type reactions of *N*-Boc imines and  $\alpha$ -substituted nitroacetates.

## 5.4 Conclusion

A chiral bis(iminoquinoline) Ni(II) complex, was prepared from the chiral ligand and Ni(ClO<sub>4</sub>)<sub>2</sub>·6H<sub>2</sub>O in the presence of powdered 4Å molecular sieves in CH<sub>2</sub>Cl<sub>2</sub>. This was an efficient chiral Lewis acid catalyst for the asymmetric Diels–Alder reaction of cyclopentadiene with several 3-acryloyl-2-oxazolidinones, which yielded greater than 99% endo-cycloadduct. In the case of Mannich-type reactions with acid-functionalized catalyst, we assume that cooperative functions of the two Ni metal centers in the catalytic complex would be important for achieving high stereoselectivity as well as reactivity.

## References

- 
- <sup>1</sup> IUPAC, *Compendium of Chemical Terminology*, 2nd ed. (the "Gold Book") (1997).
  - <sup>2</sup> IUPAC, *Compendium of Chemical Terminology*, 2nd ed. (the "Gold Book") (1997).
  - <sup>3</sup> Verheul, H.; Panigrahy, D.; Yuan, J.; d'Amato, R. *Br J Cancer*. **1999**, *79*, 114–118.
  - <sup>4</sup> Diels O.; Alder, K. *Justus Liebigs Ann. Chem.* **1928**, *460*, 98.
  - <sup>5</sup> Kagan H.; Riant, O. *Chem. Rev.* **1992**, *92*, 1007.
  - <sup>6</sup> Viso, A.; Ferná'ndez de la Pradilla, R.; Garcí'a, A.; Flores, A. *Chem. Rev.* **2005**, *105*, 3167.
  - <sup>7</sup> Marques, M. *Angew. Chem., Int. Ed.* **2006**, *45*, 348.
  - <sup>8</sup> Shibasaki, M.; Matsunaga, S. *J. Organomet. Chem.* **2006**, *691*, 2089.
  - <sup>9</sup> Cativiela, C.; Diaz-de-Villegas, M. *Tetrahedron: Asymmetry* **1998**, *9*, 3517.
  - <sup>10</sup> Ohfuné, Y.; Shinada, T. *Bull. Chem. Soc. Jpn.* **2003**, *76*, 1115.
  - <sup>11</sup> Goodrich, P.; Hardacre, C. *Adv. Synth. Catal.* **2011**, *353*, 995 – 1004

## Chapter 6 - Overall conclusion and future work

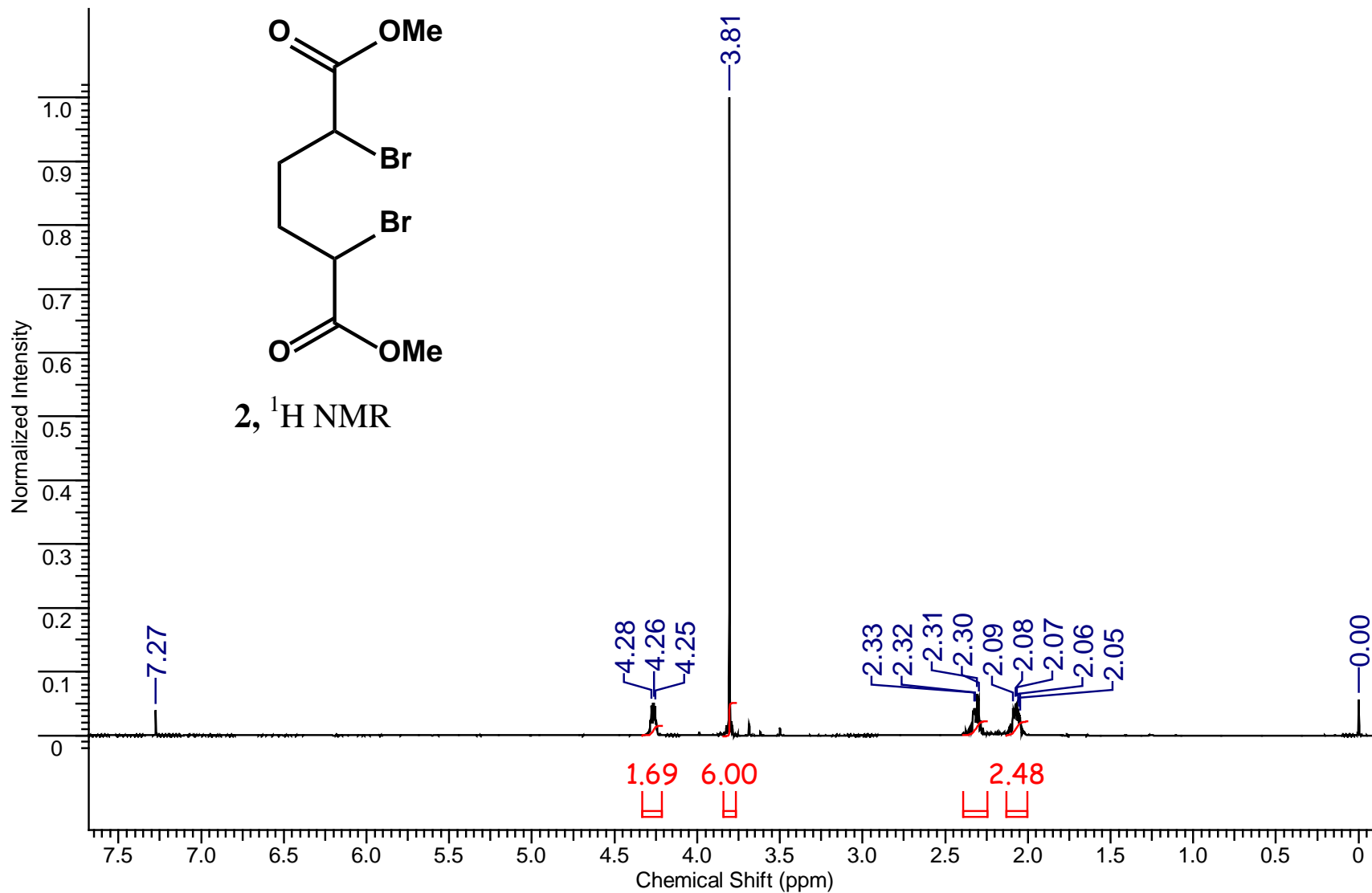
In order to produce Schiff base, a chiral C<sub>2</sub>-symmetric diamine can be employed: the ligands are prepared by condensation reactions with these backbones. For our study, we have selected the cyclobutyl backbone. Since the smaller ring diamines might lead to more enantioselective catalysts by increasing the N-C-C-N dihedral angle and thus altering the ligand conformation in a favourable manner. Also, the computational studies suggest that the (1*R*,2*R*)-cyclobutyldiamine unit can produce highly twisted salen complexes with a large energy difference between the *M* and *P* helical forms. It has alkyl substituents on the amine groups, making them relatively basic. This will result in stronger imine or amide donors in the ligands produced after condensation. The electron rich nature of the imine groups of Schiff bases with this backbone make them relatively inert to hydrolysis.

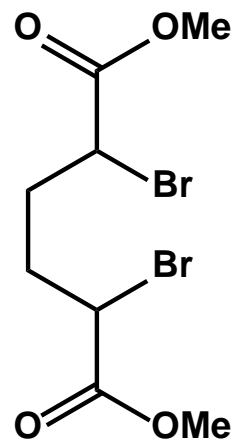
Some novel ligands using chiral cyclobutyl backbone were prepared and consequently metallated with Zn(II), Ni(II), Mn (II) and Fe(II). The greener solvent assisted grinding method was introduced in synthesis of bis-imine ligands. The synthesized mononuclear complexes were characterized with different techniques. It was hoped these ligands would consistently form monohelimeric complexes but due to lower solubility of formed complexes we were unable to get crystallographic data. The asymmetric catalysis reaction using bis-imine cyclobutyl ligand with Ni metal showed great potential. It will be interesting to study more catalysis reaction with different component using bis- imine cyclobutyl ligand. The acid fictionalized mononuclear complexes showed lack in reactivity in Mannich-type reactions which can be improve in future by incorporating second metal.

The goal of this project was to synthesize metal complexes that would act as catalysts for asymmetric reactions. As we have had some success in catalysis of Diels-alder reaction, in future our group will explore other aspects of reaction such as,

1. Investigate the catalysis mechanism
2. Examine different substrate
3. Optimize the reaction conditions

## Appendix A – $^1\text{H}$ and $^{13}\text{C}$ NMR





— 169.69

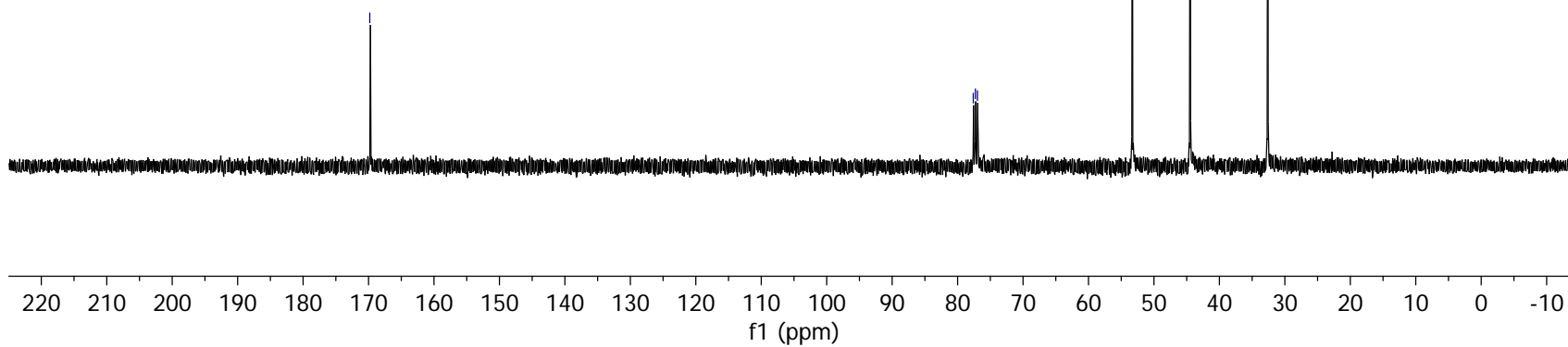
77.48  
77.16  
76.84

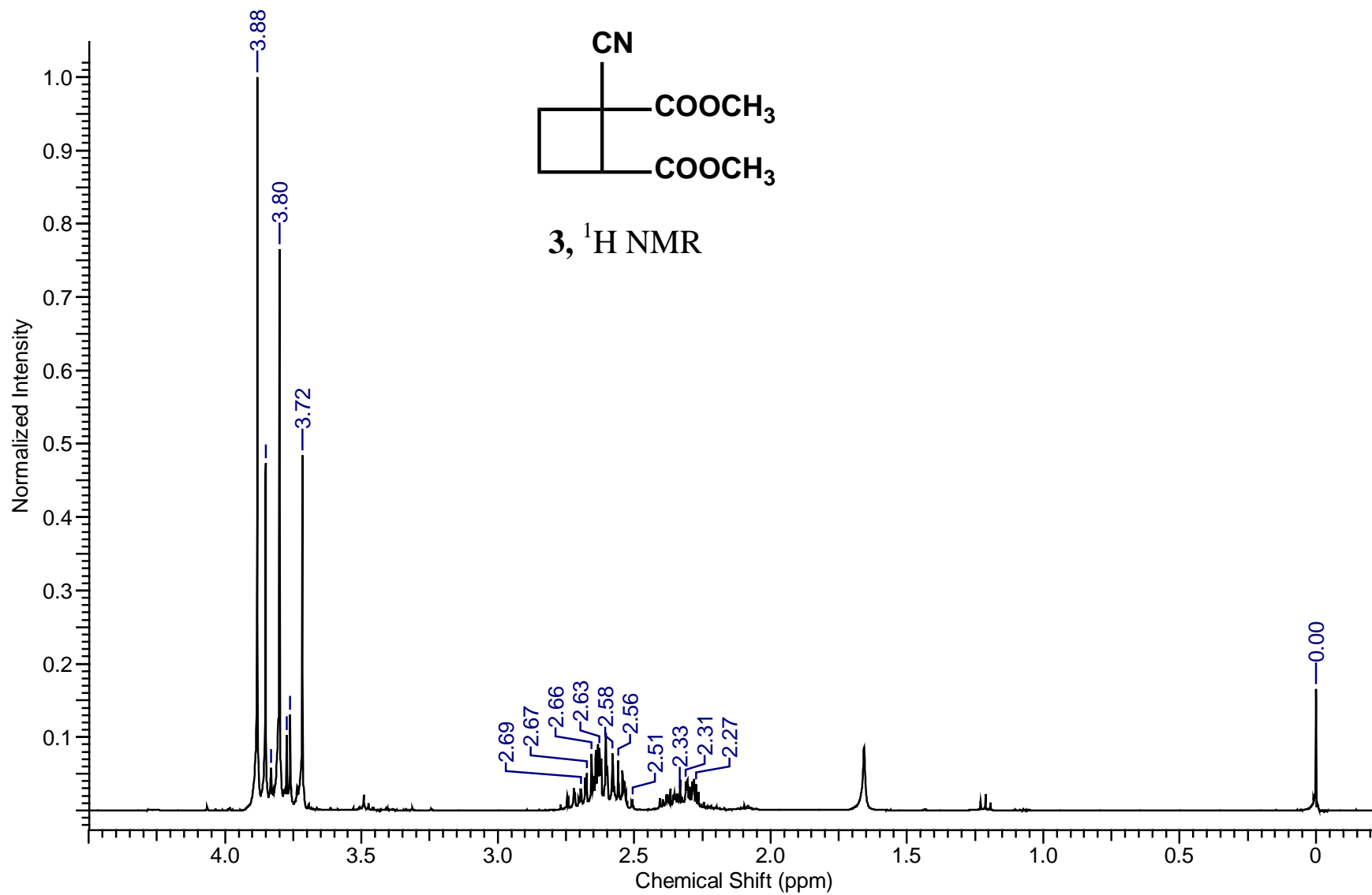
— 53.21

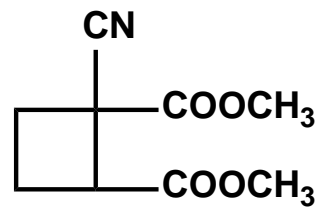
— 44.34

— 32.49

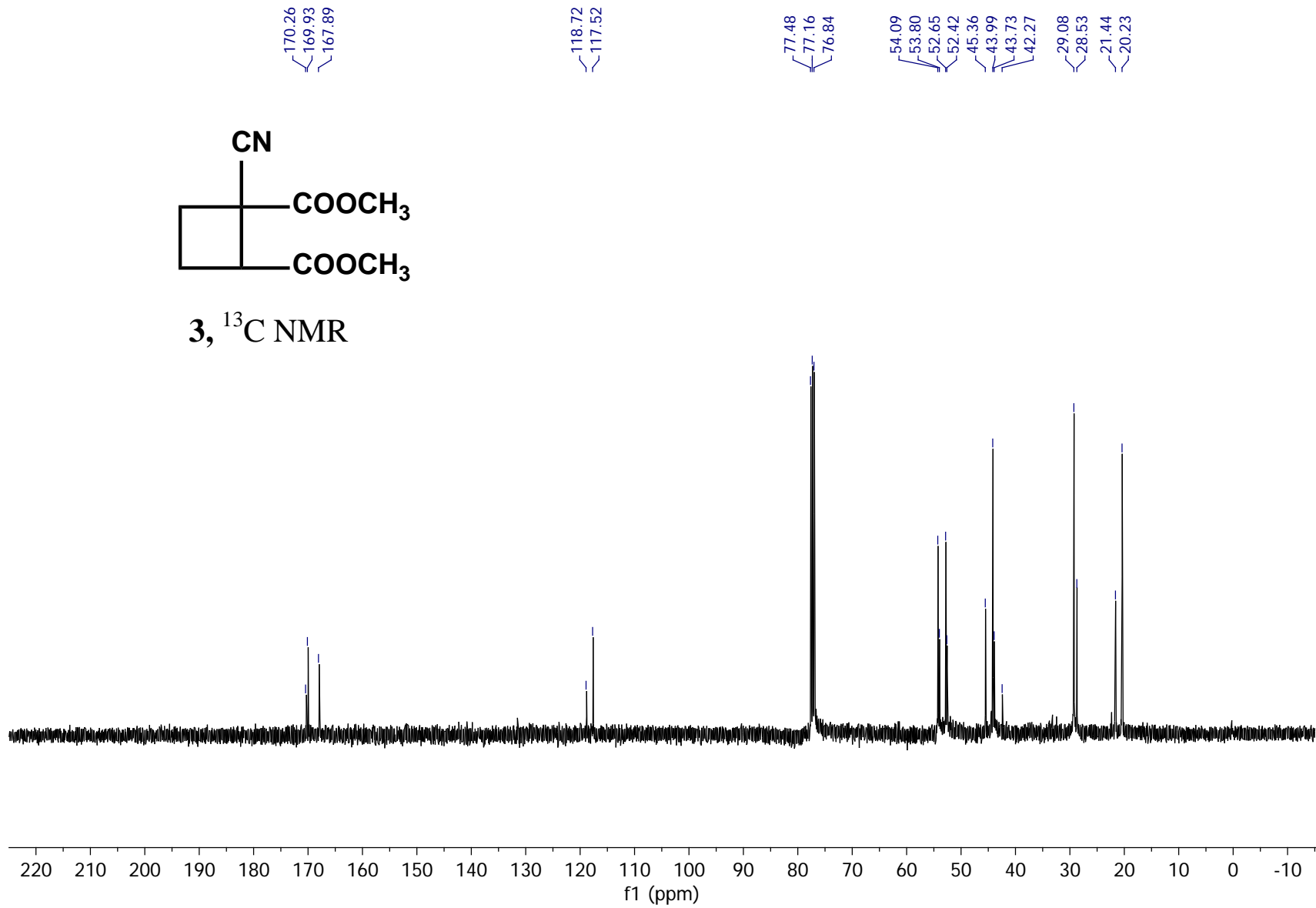
2, <sup>13</sup>C NMR

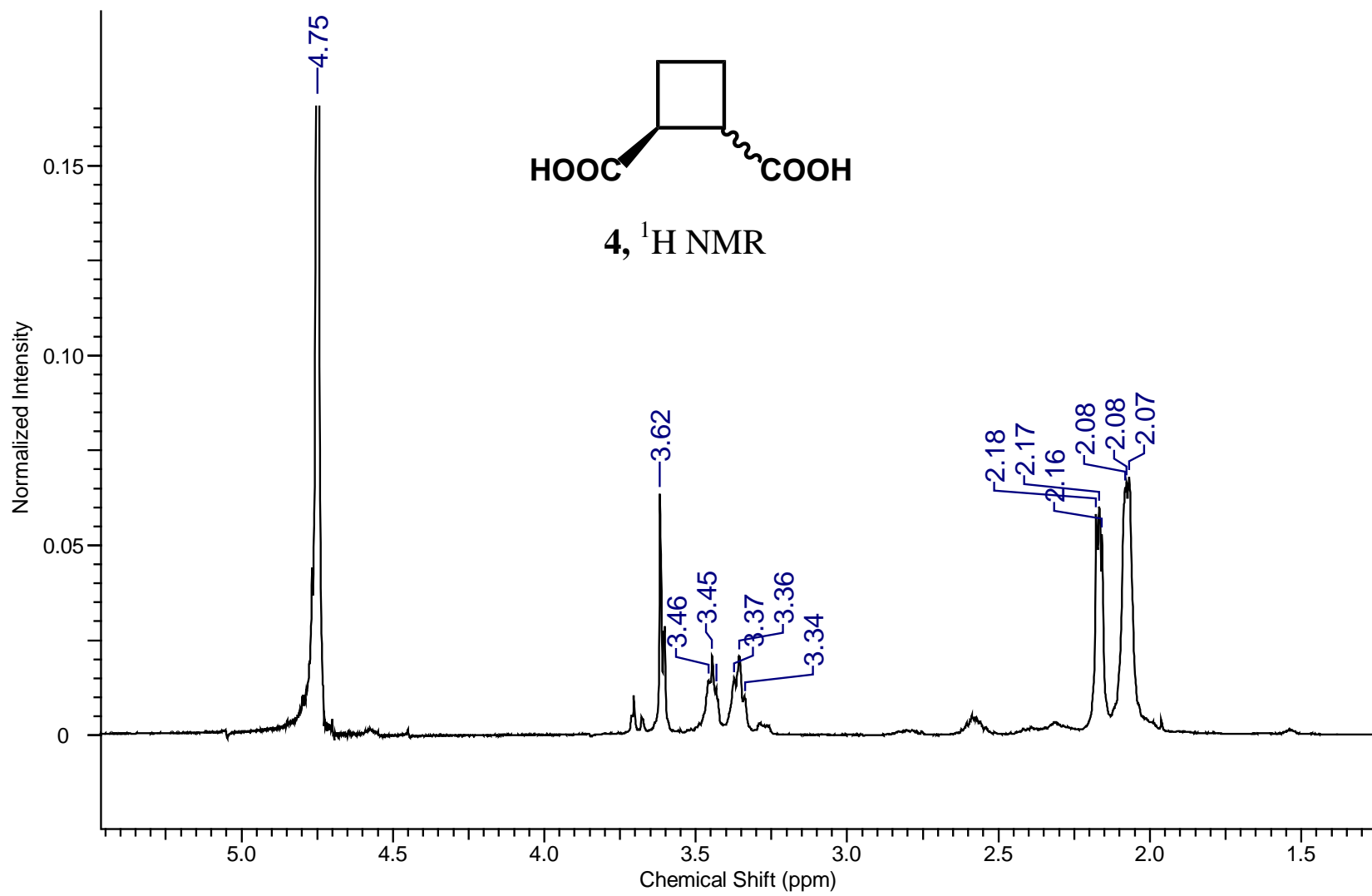


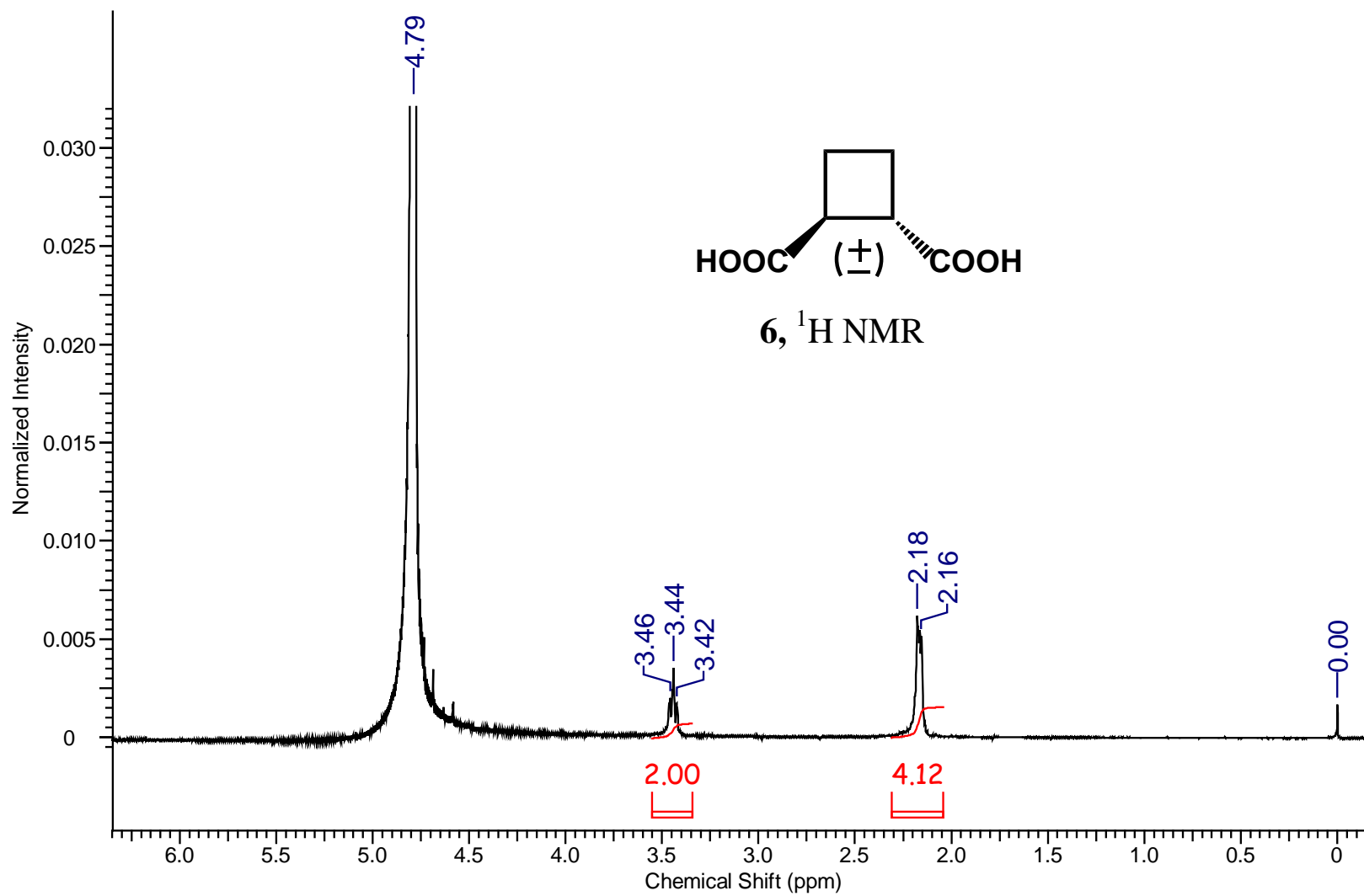


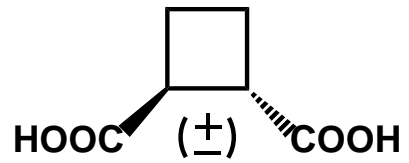


3, <sup>13</sup>C NMR

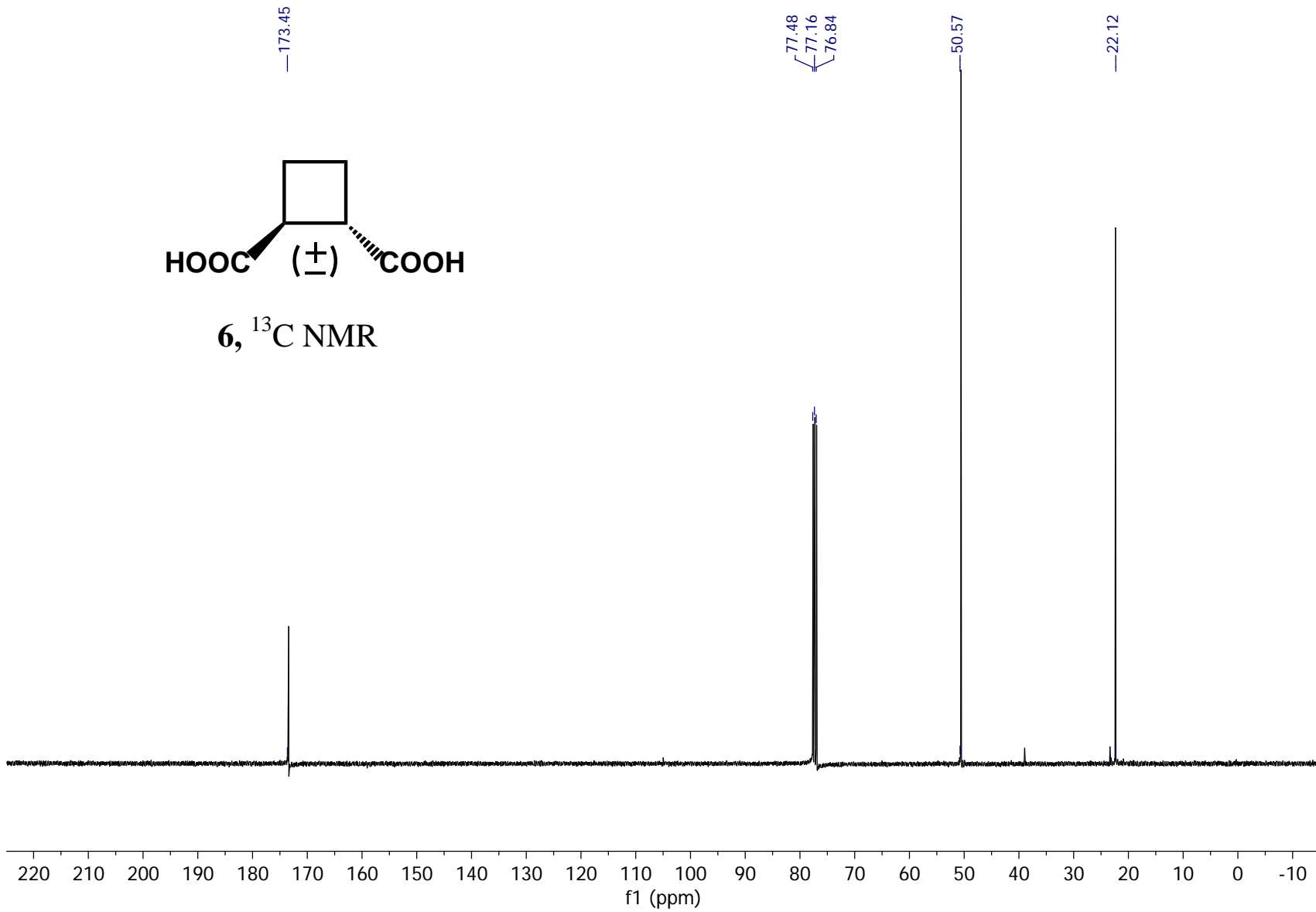


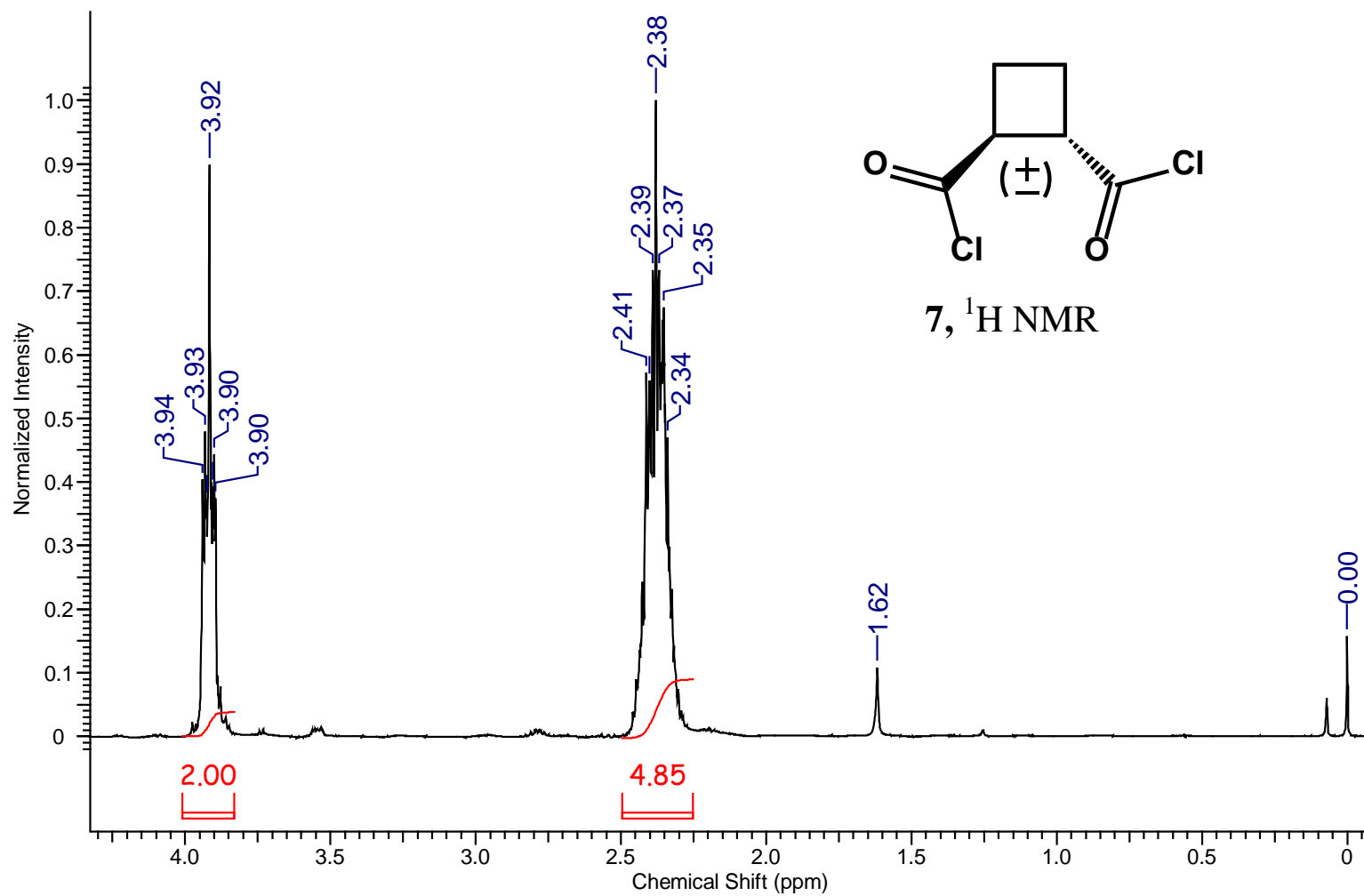


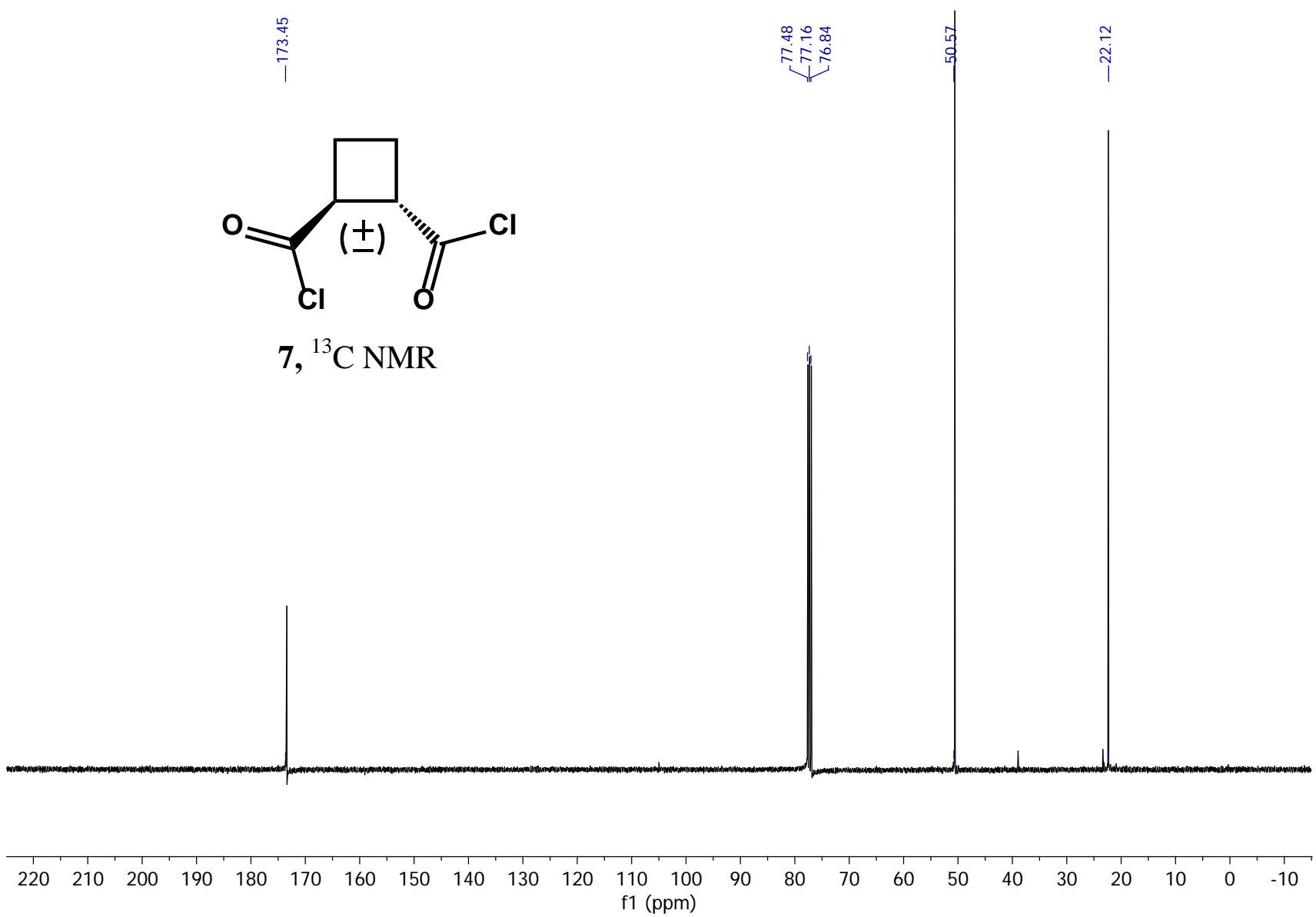
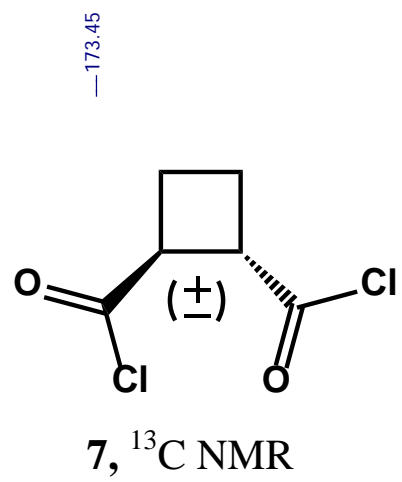


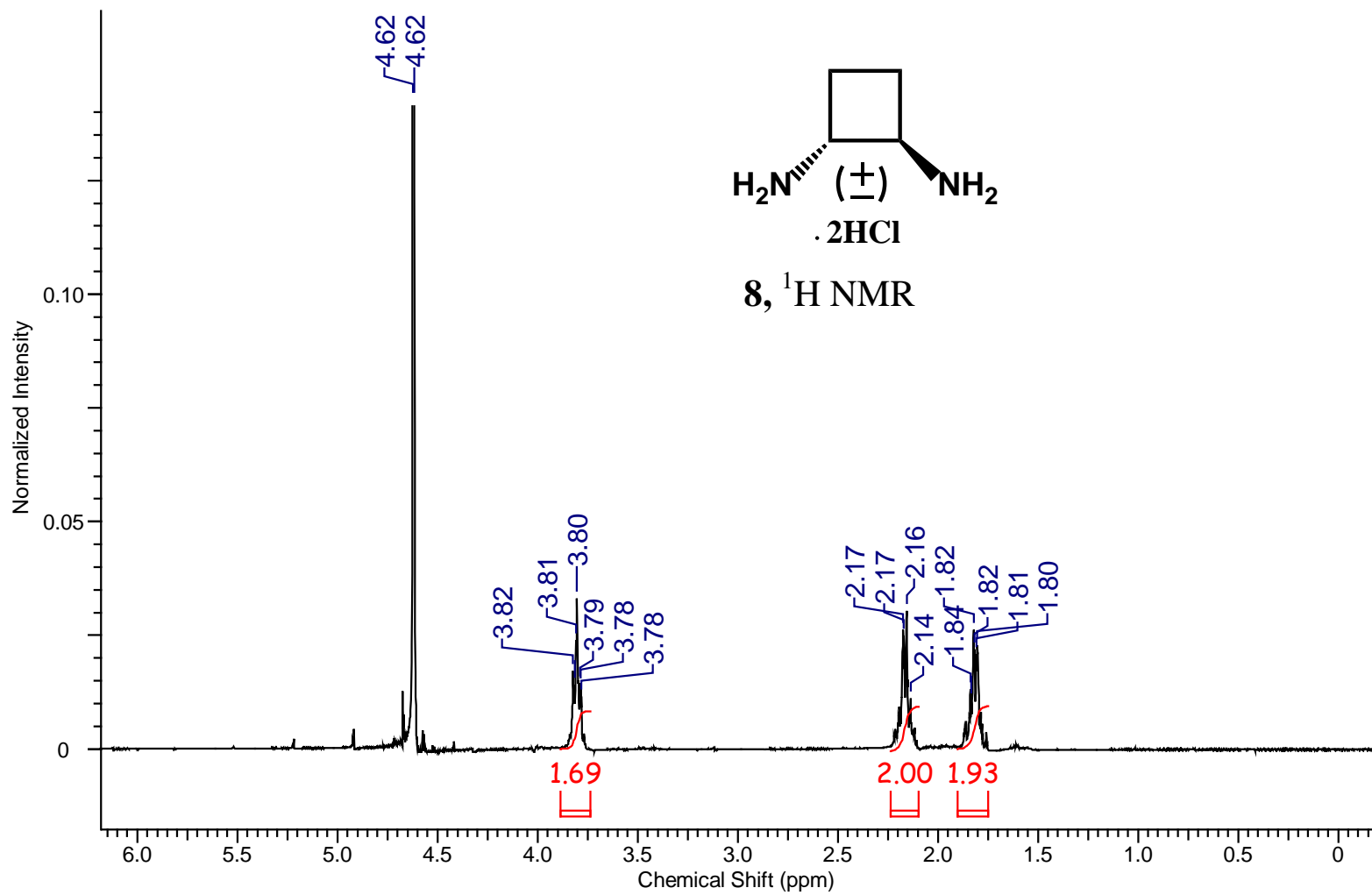


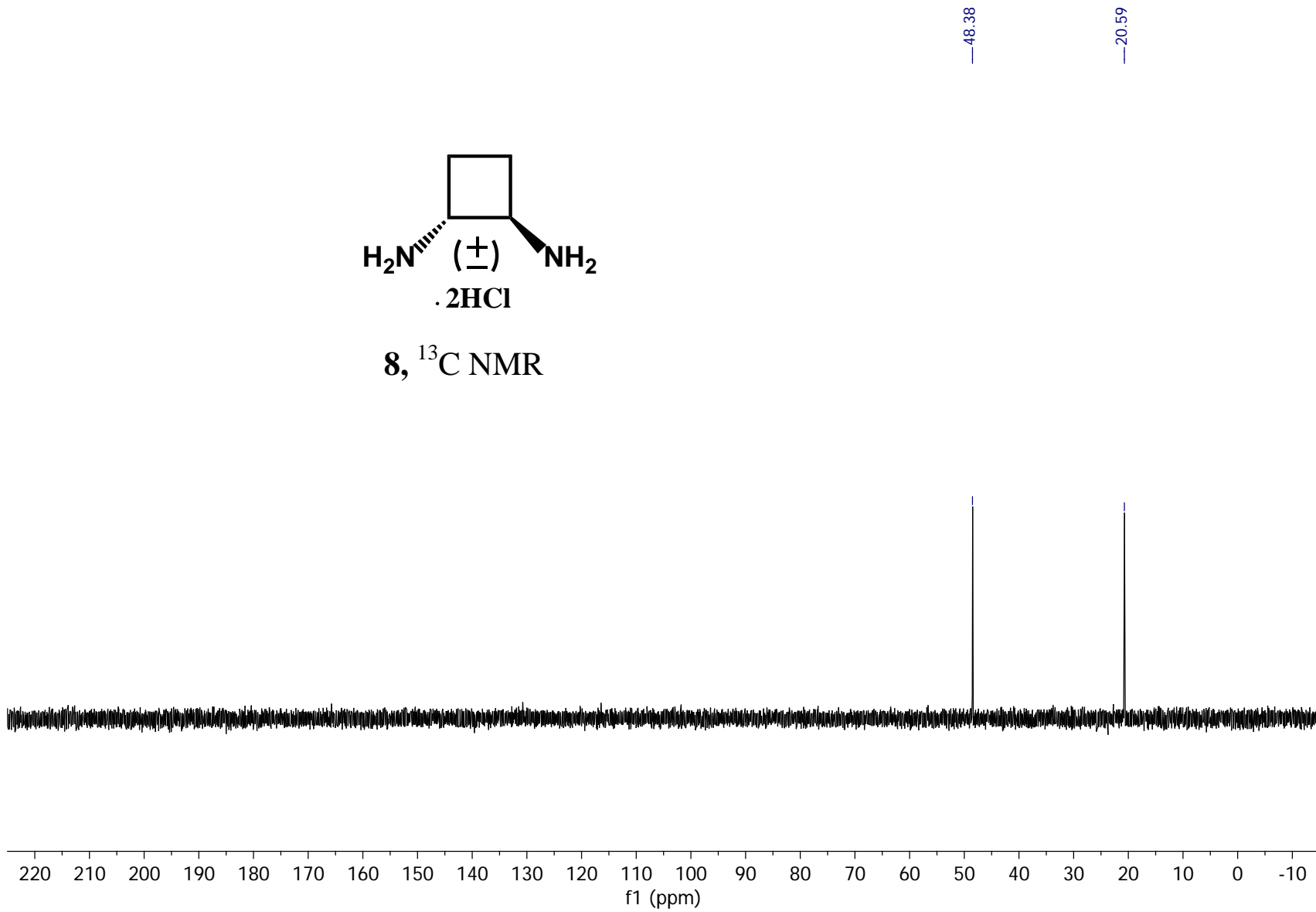
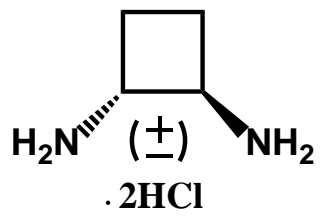
6,  $^{13}\text{C}$  NMR

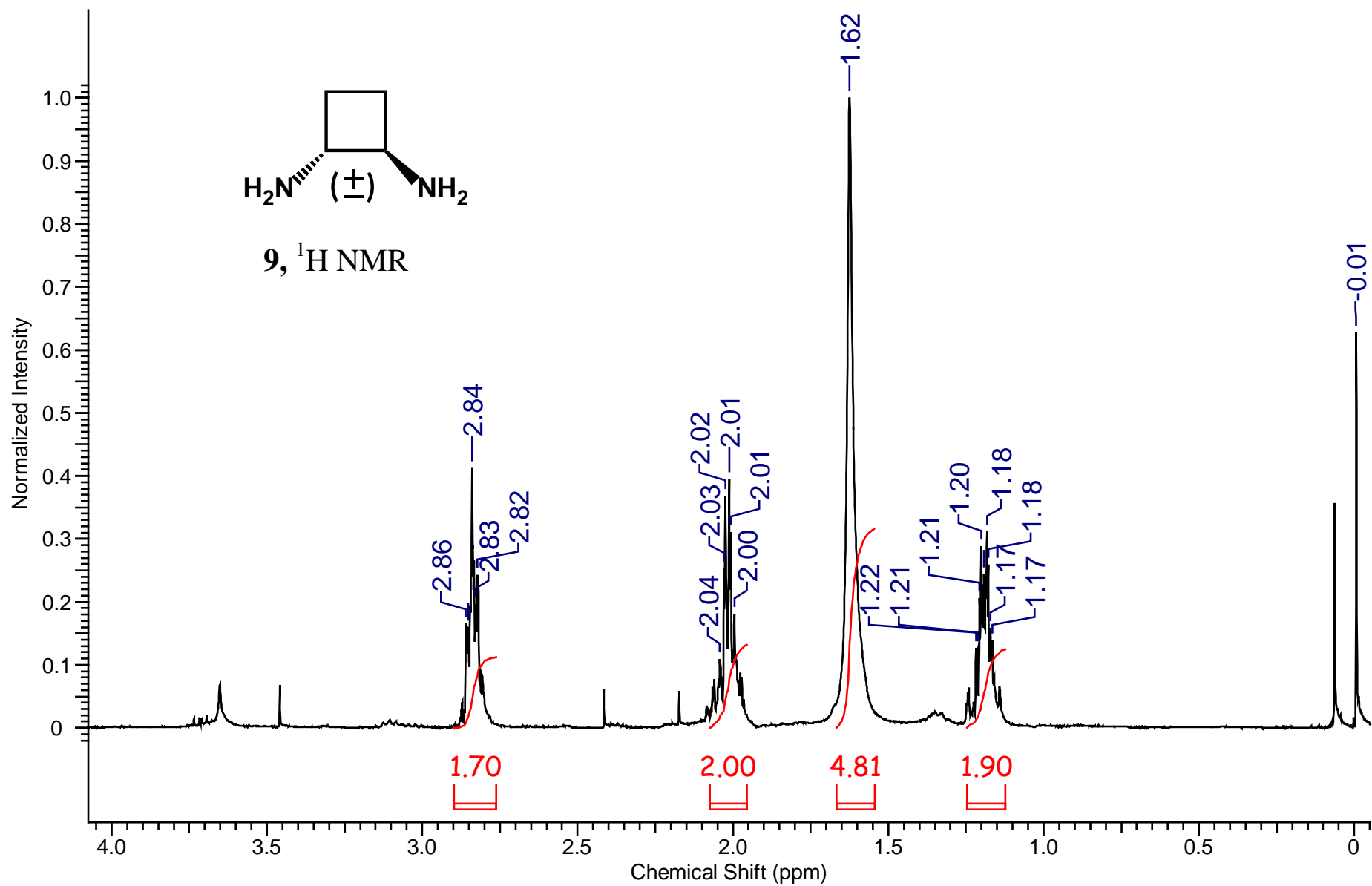


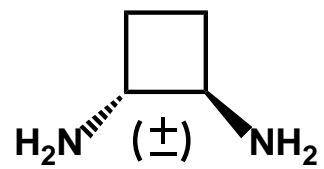




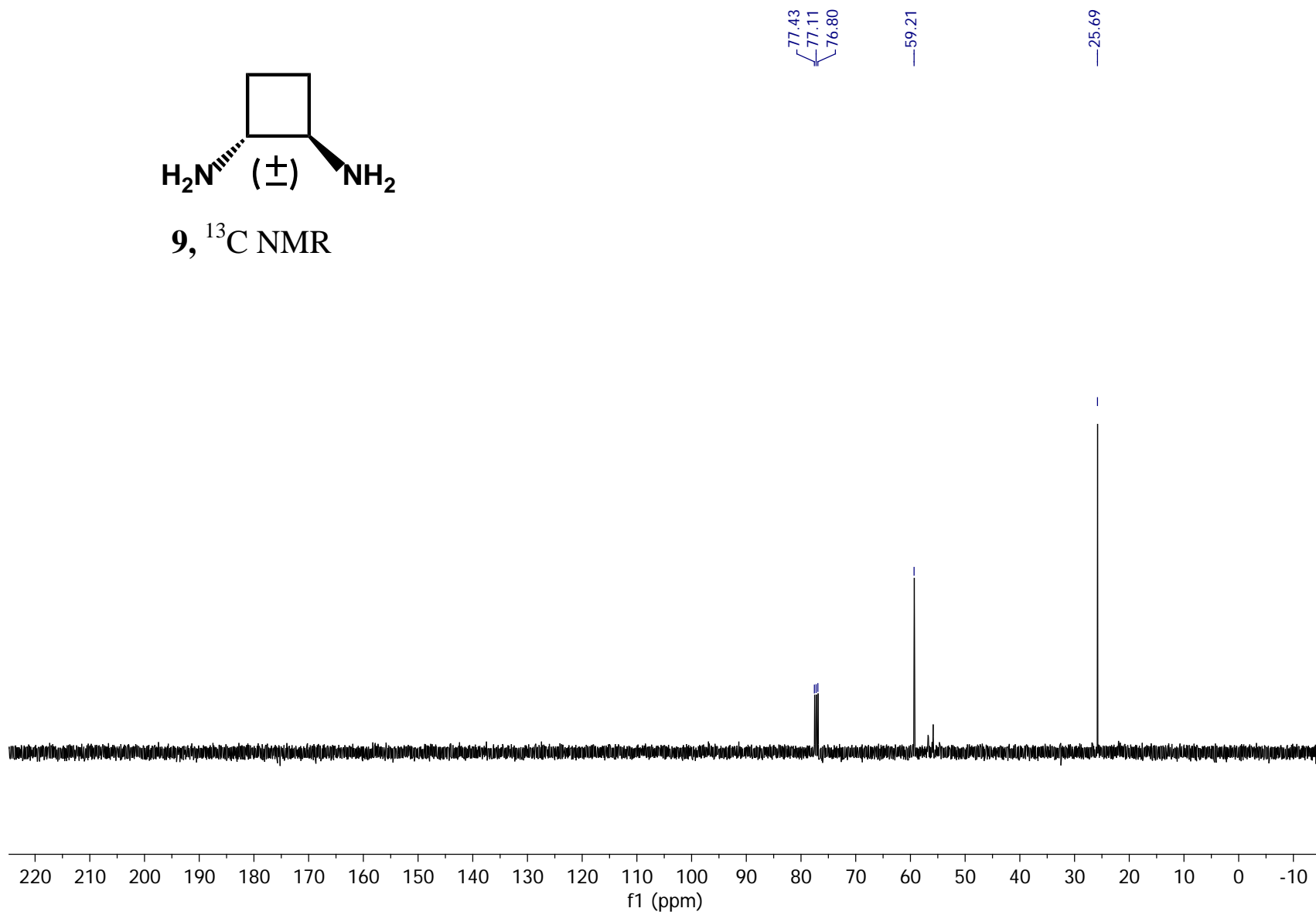


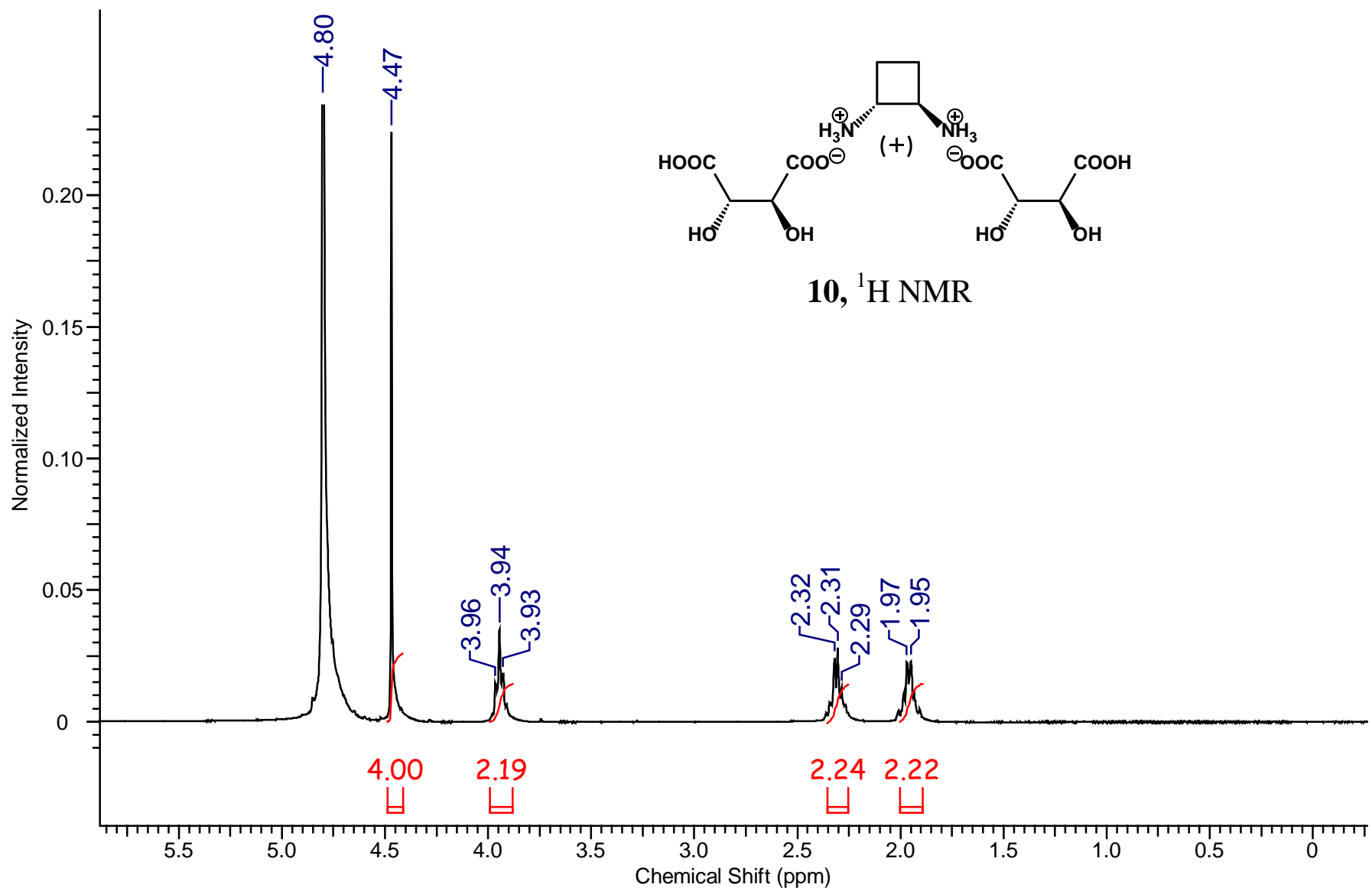


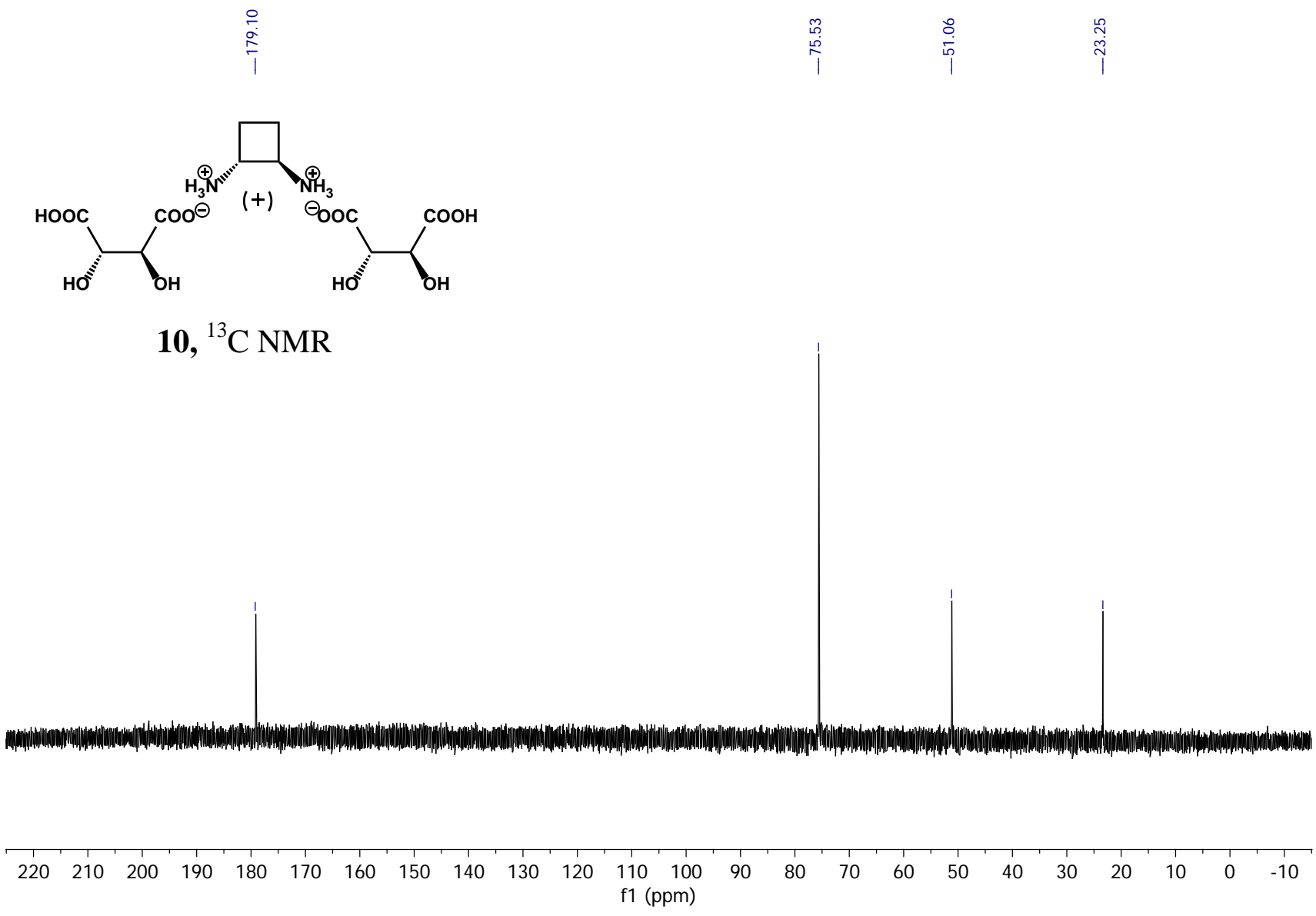
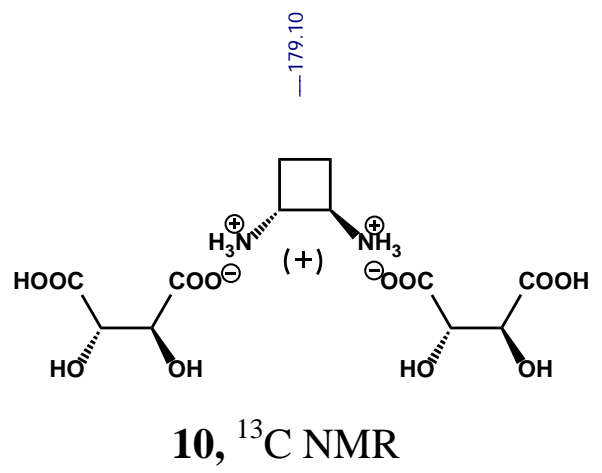


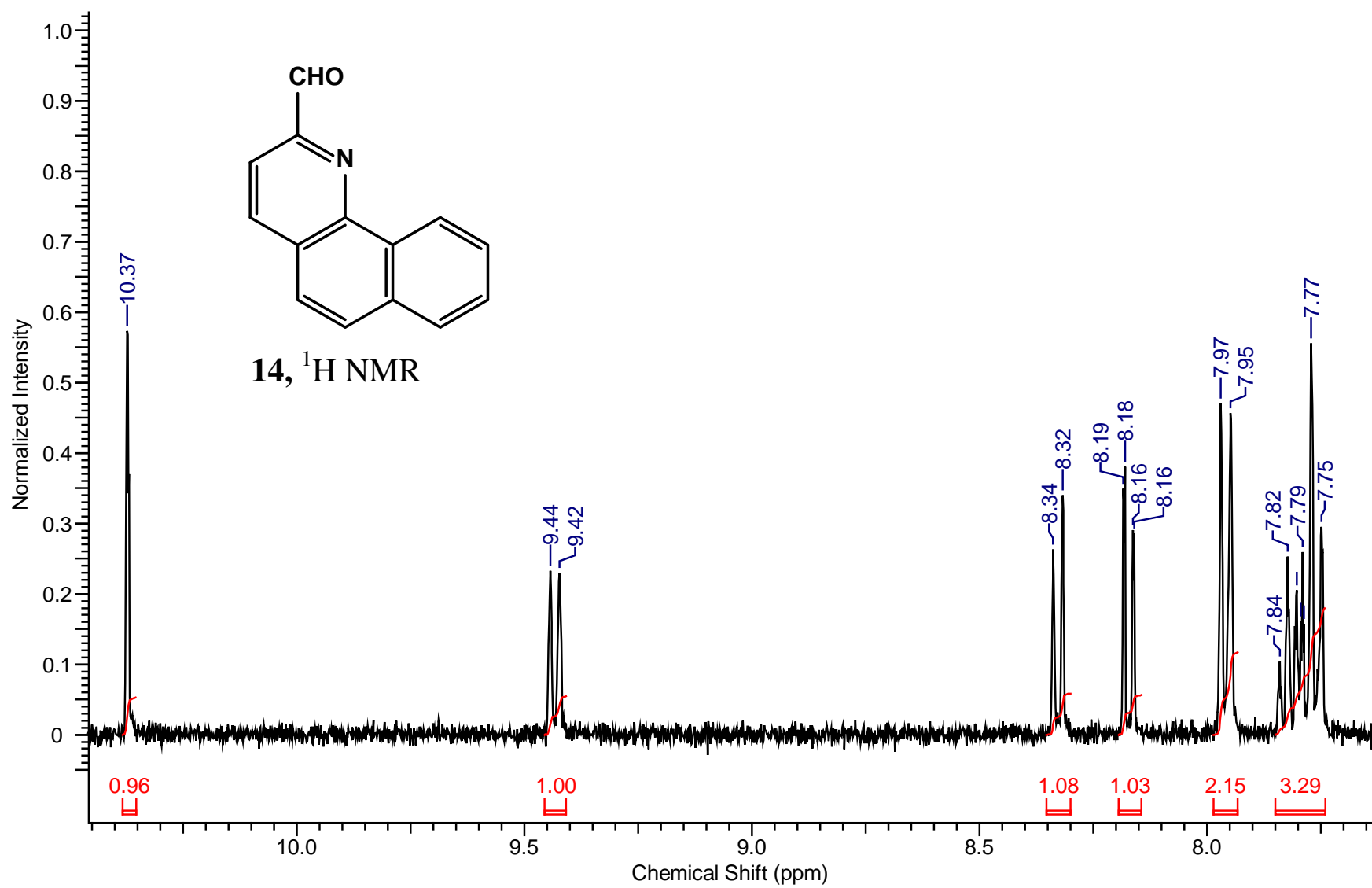


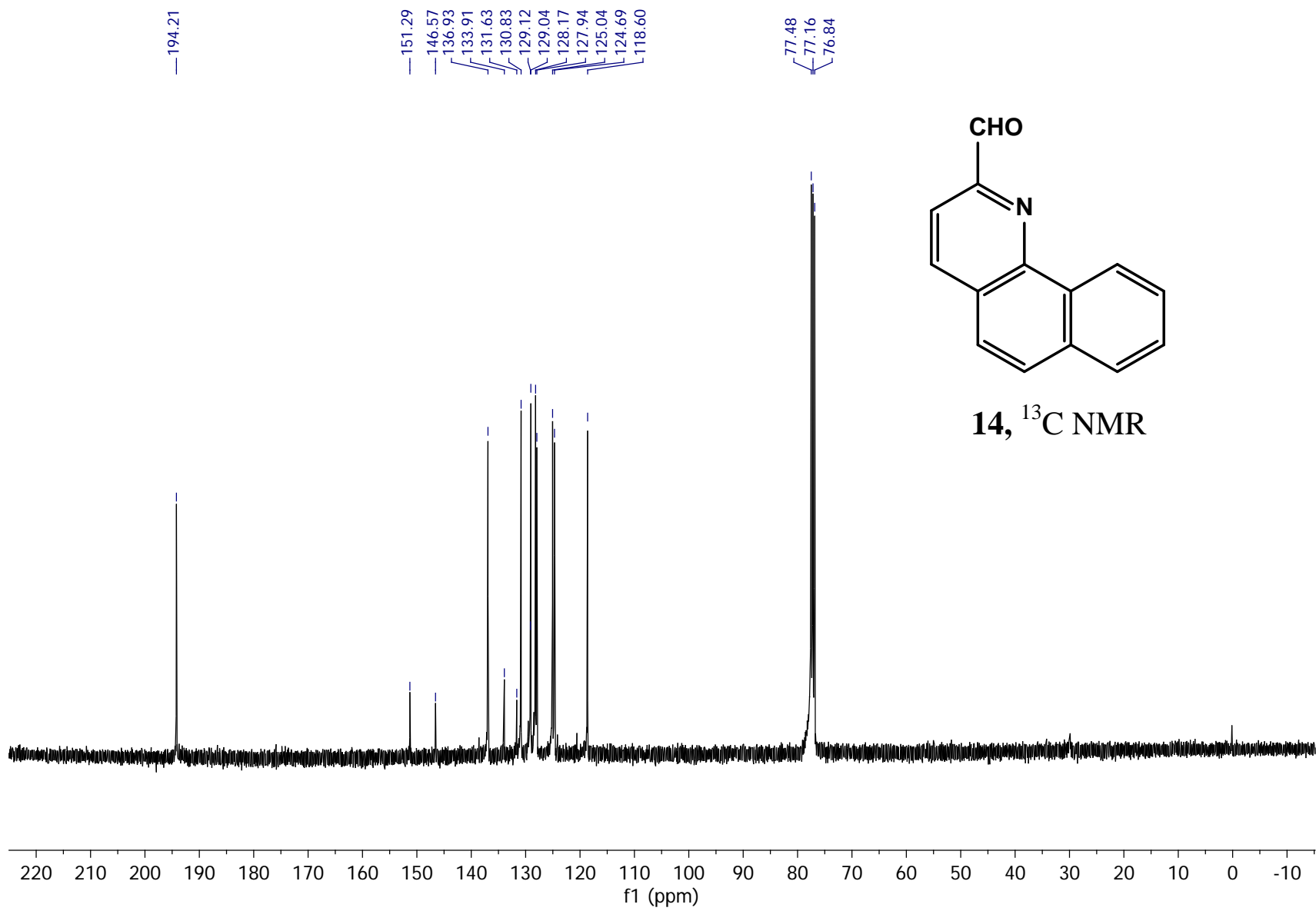
9,  $^{13}\text{C}$  NMR

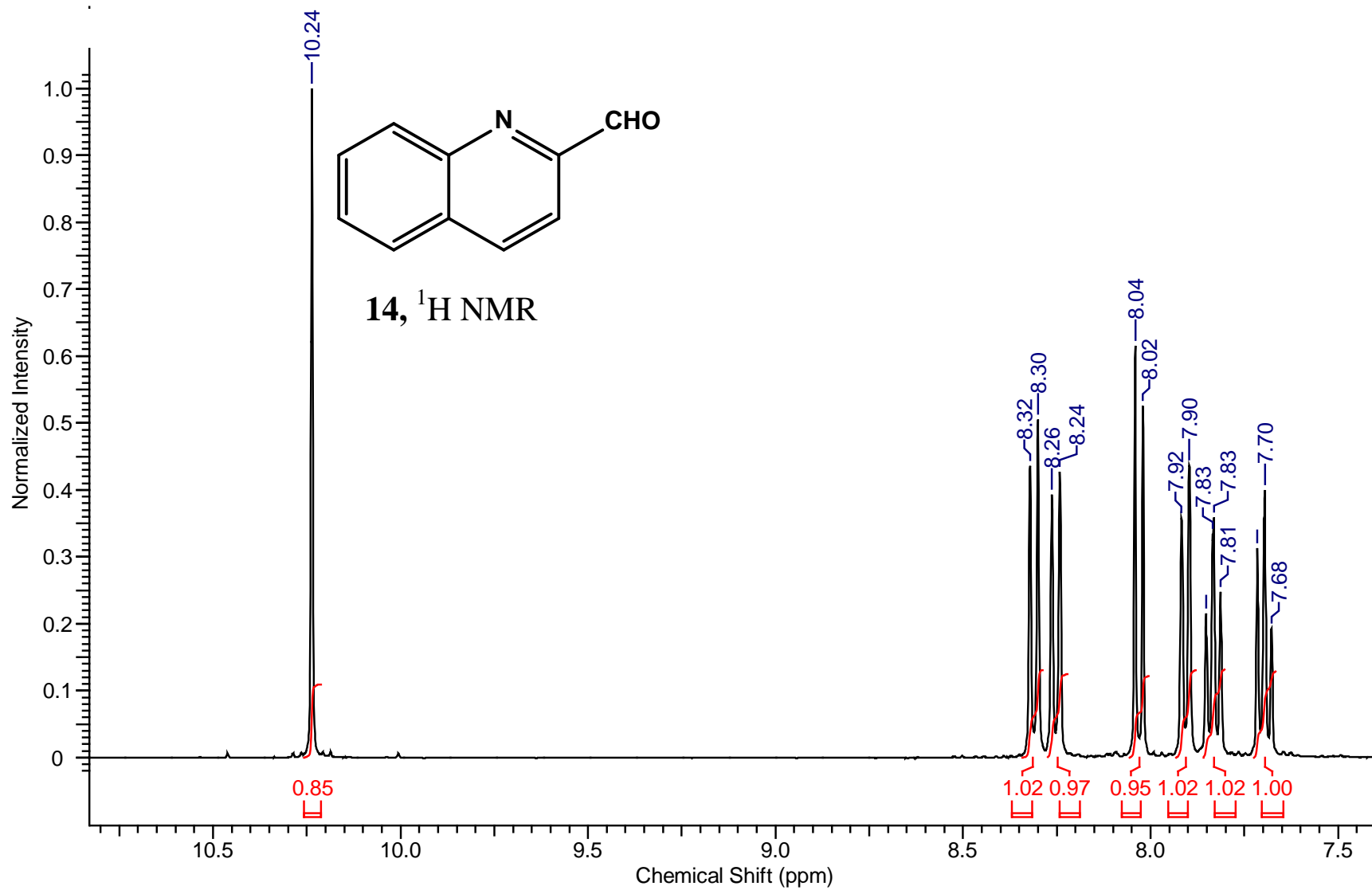


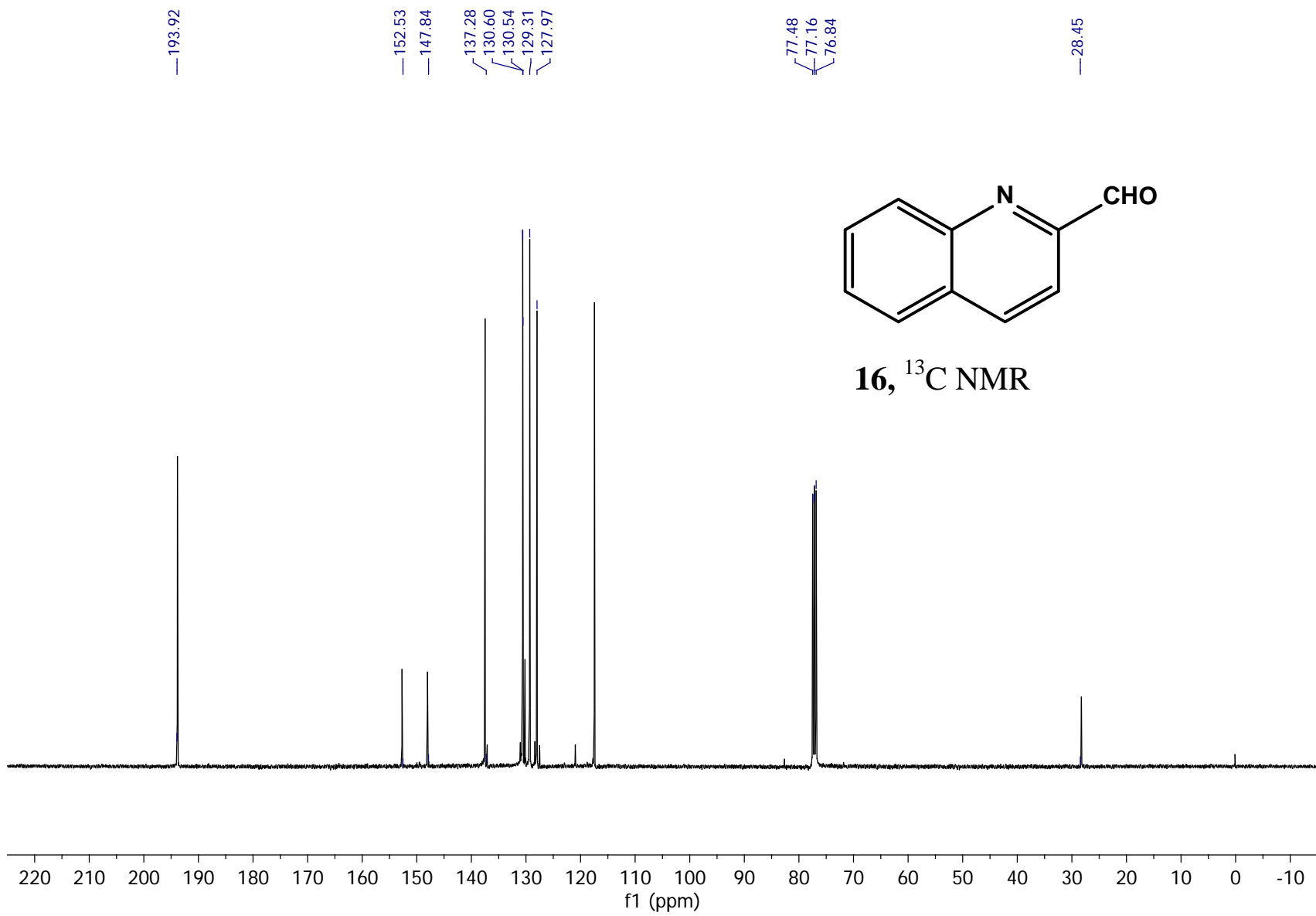


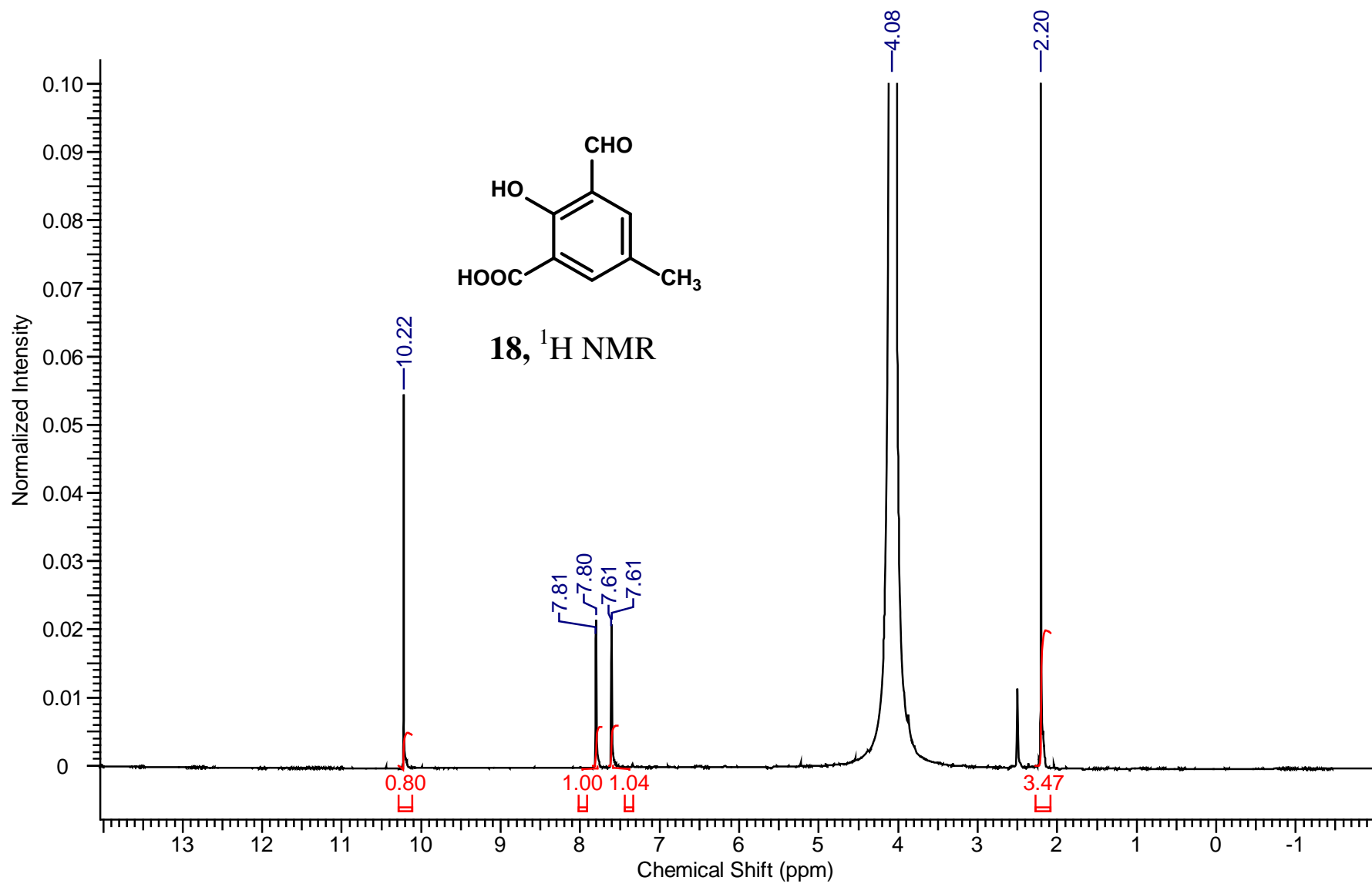


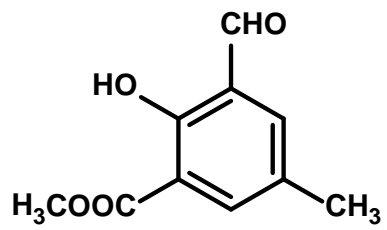




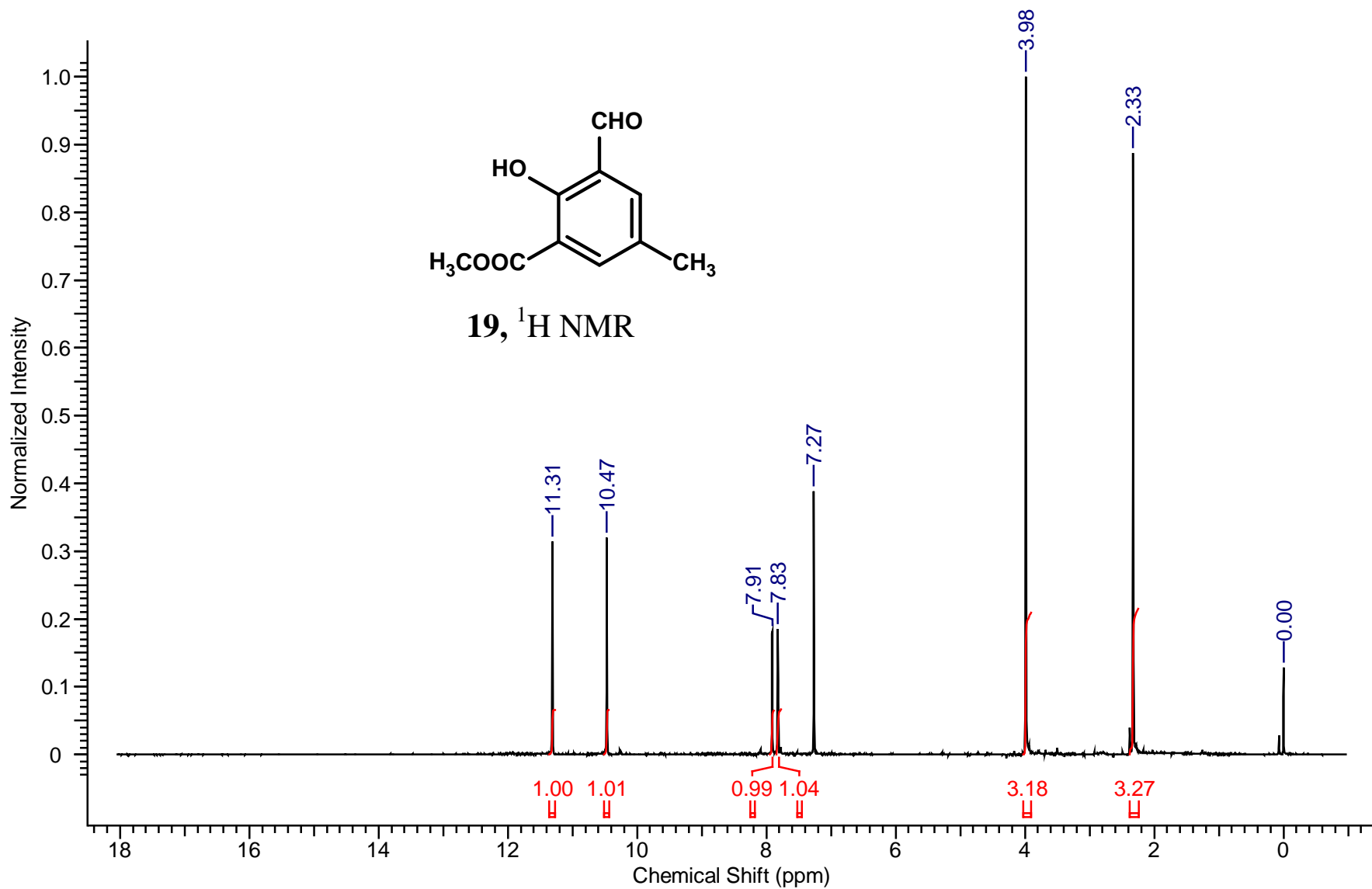


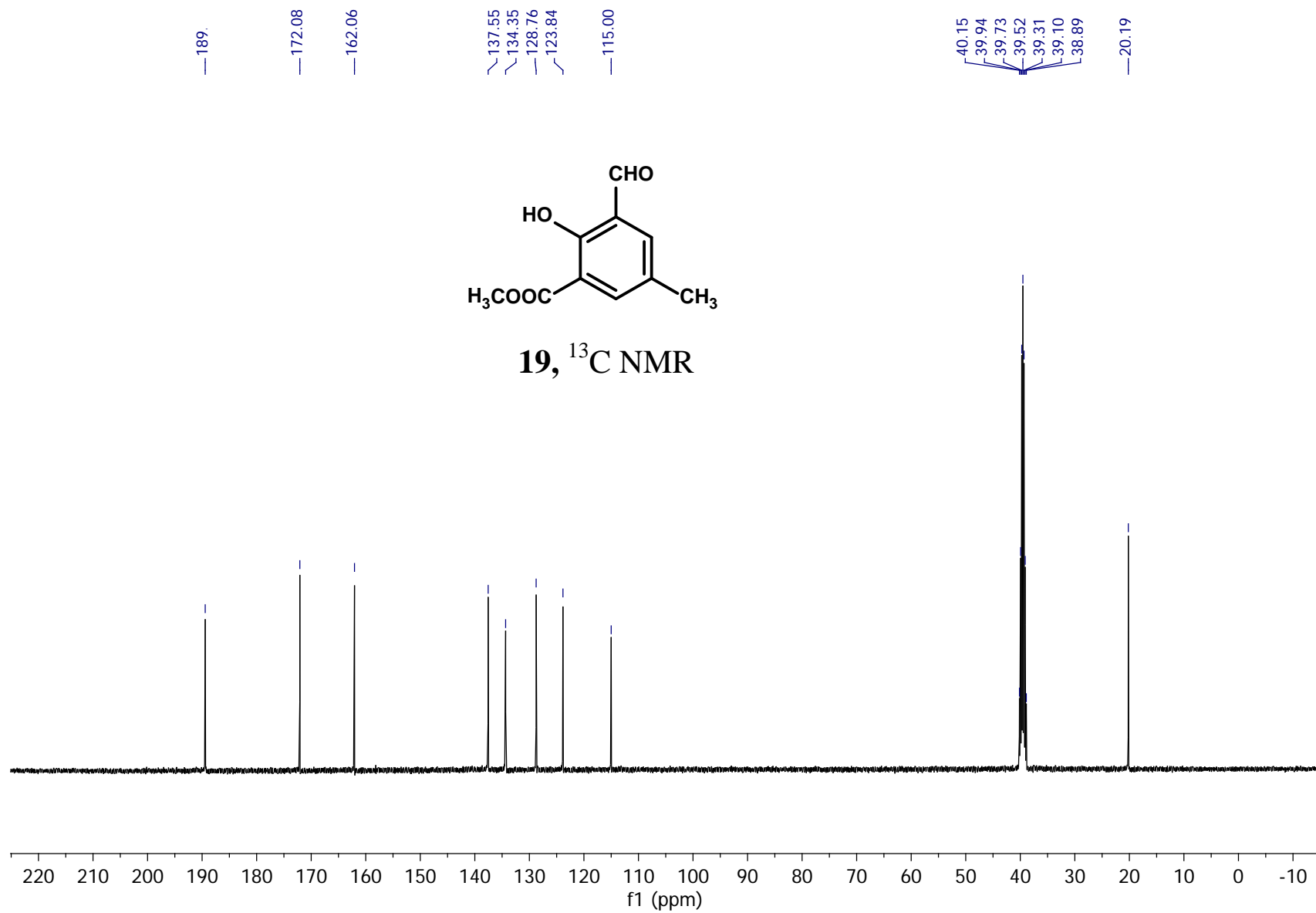


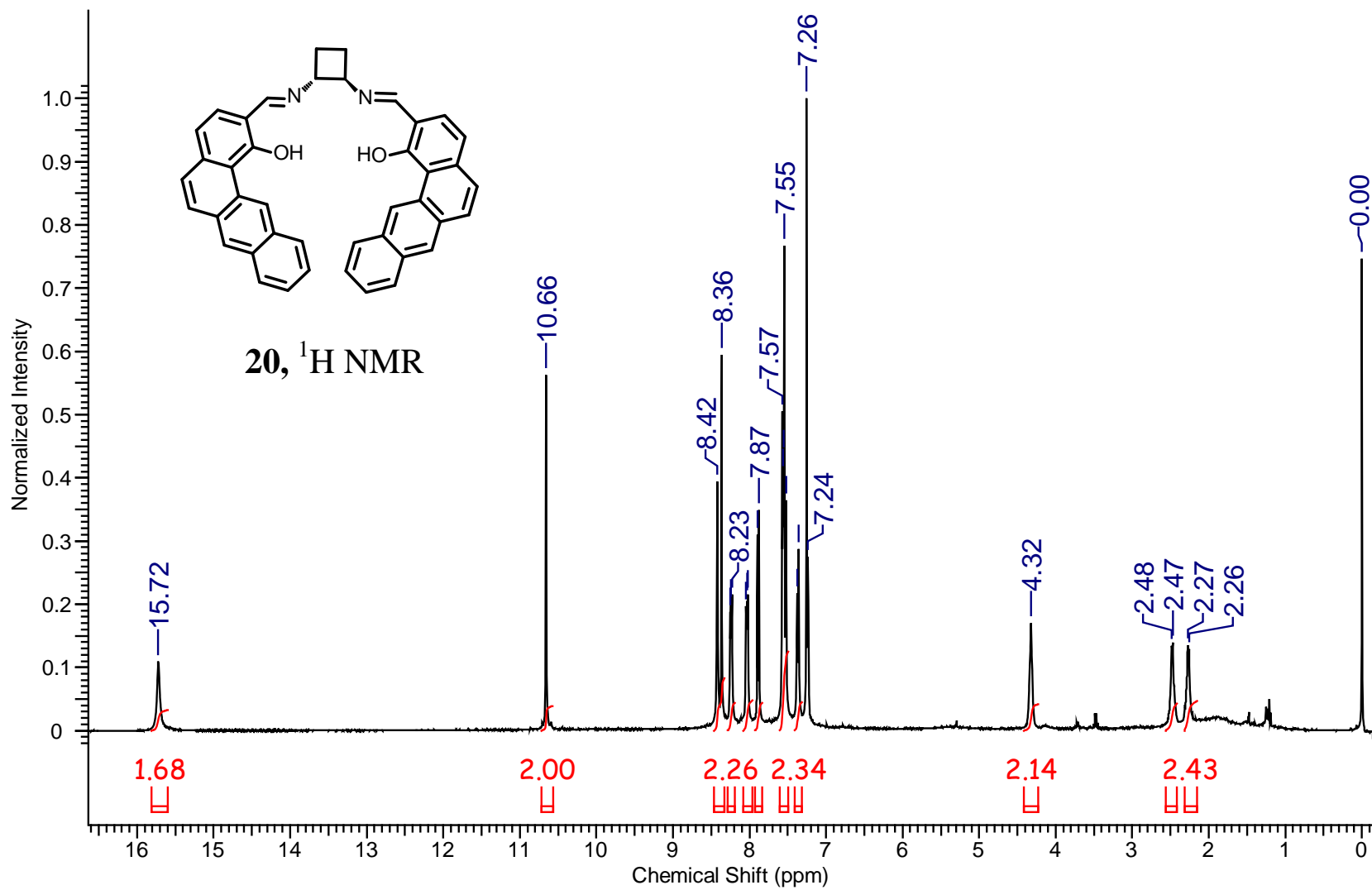


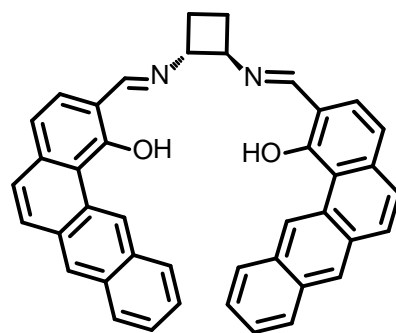


**19**, <sup>1</sup>H NMR

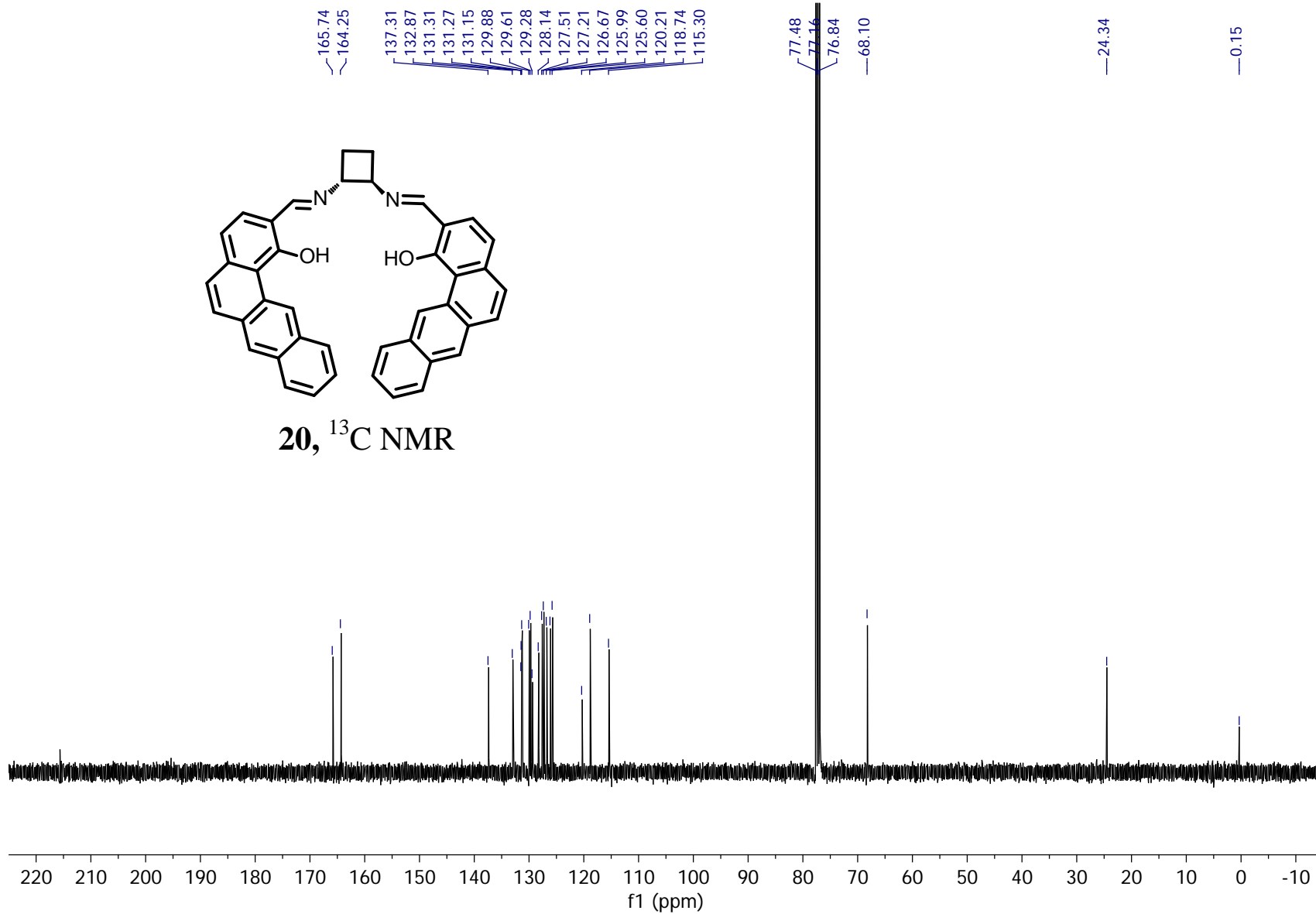


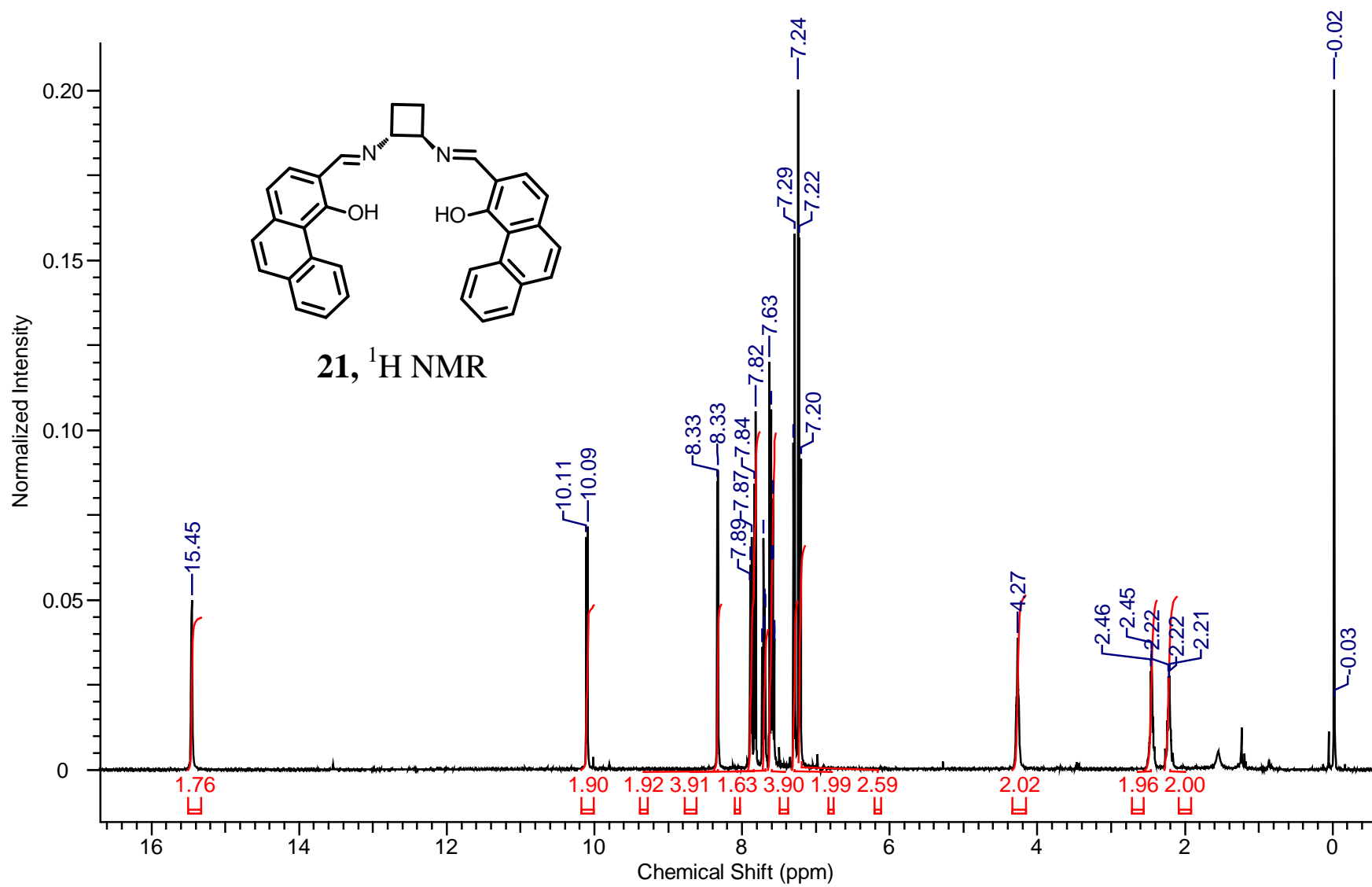


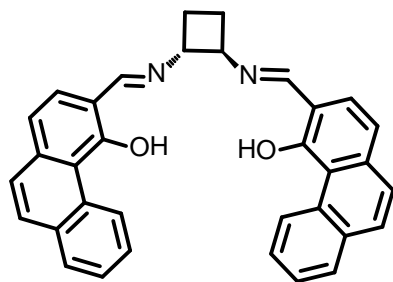




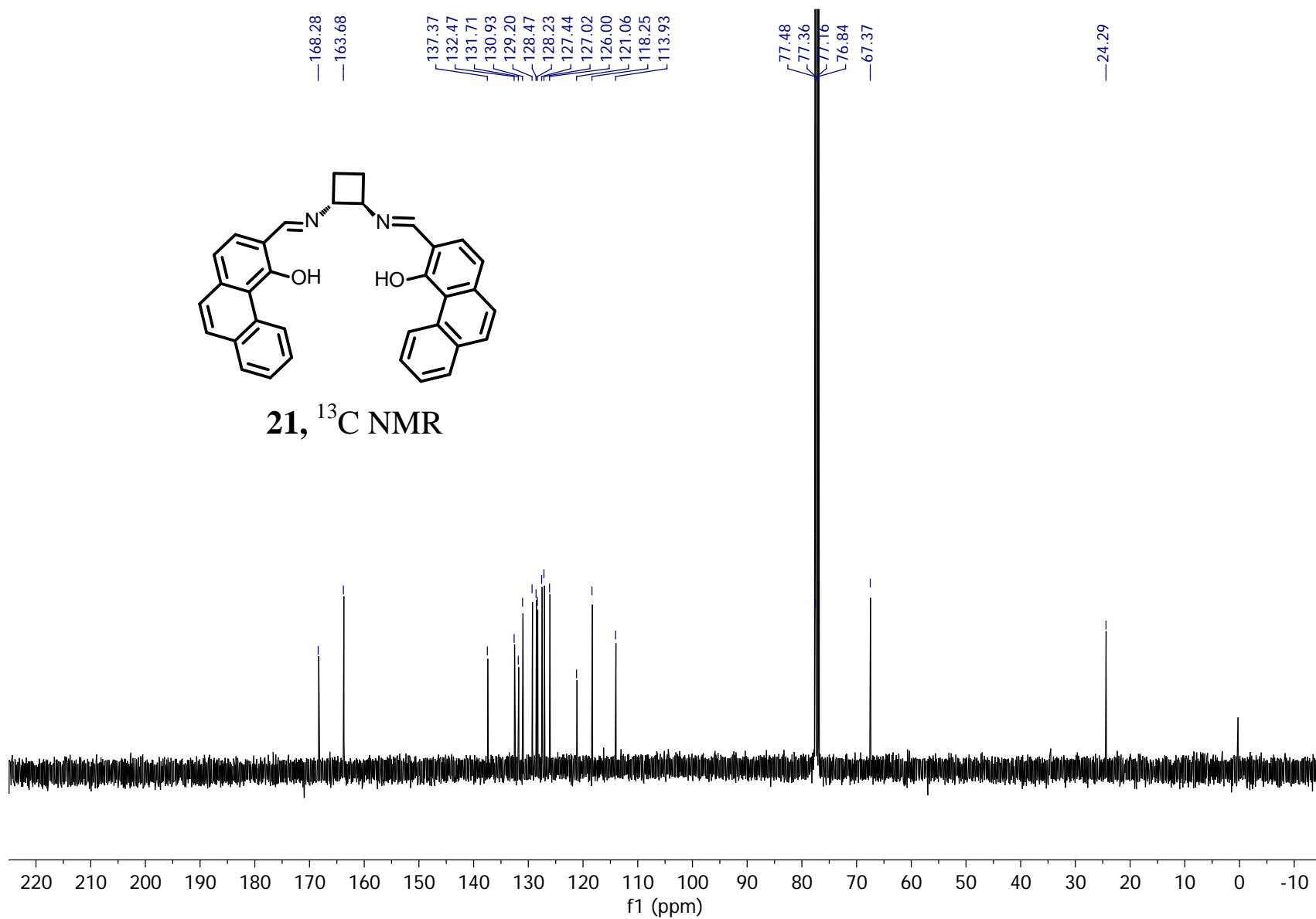
20,  $^{13}\text{C}$  NMR

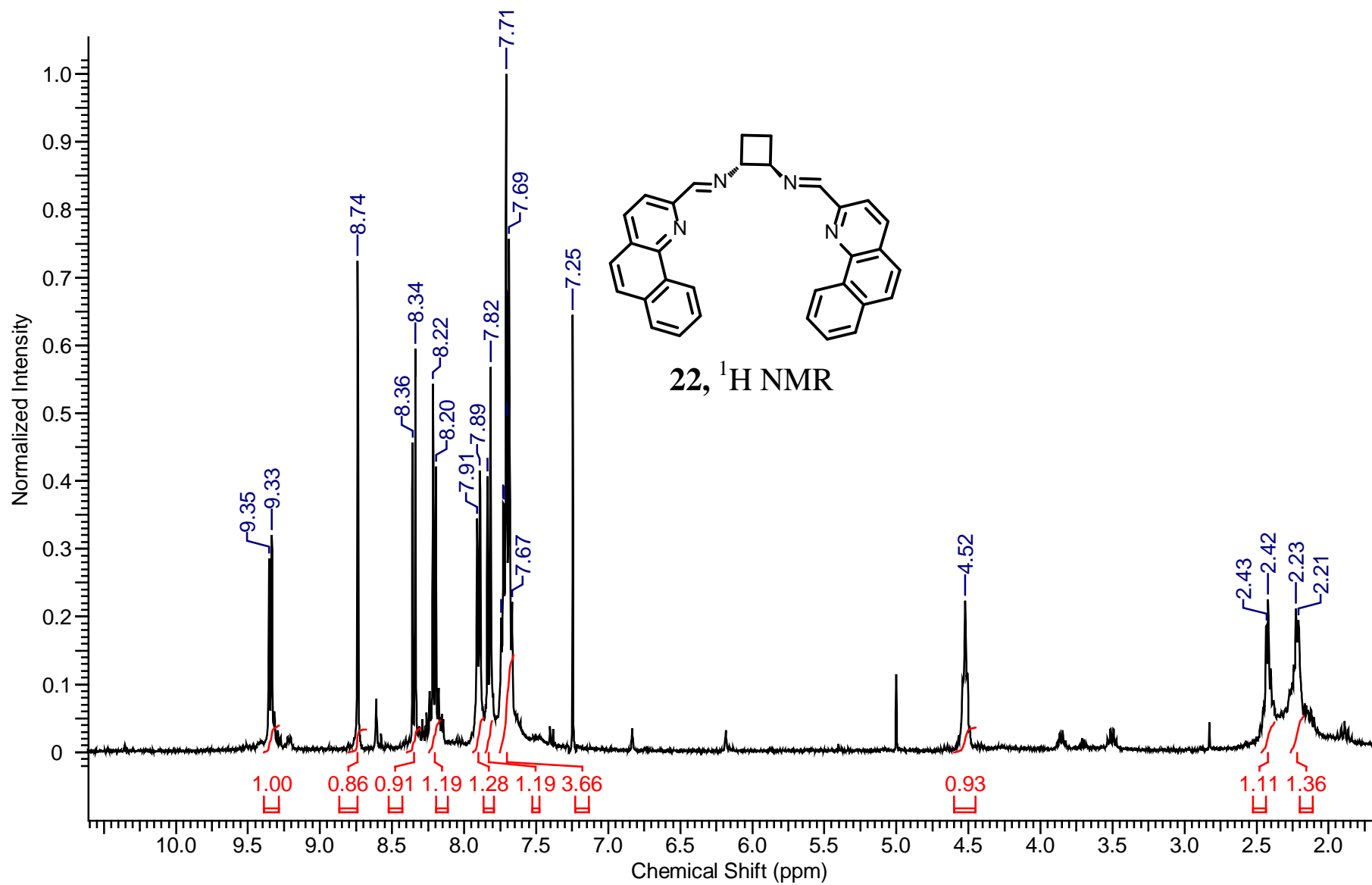


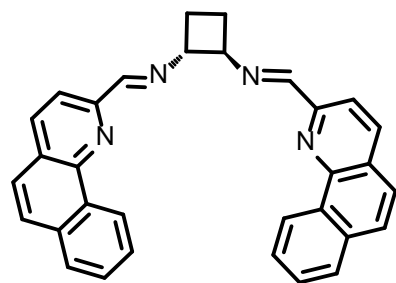




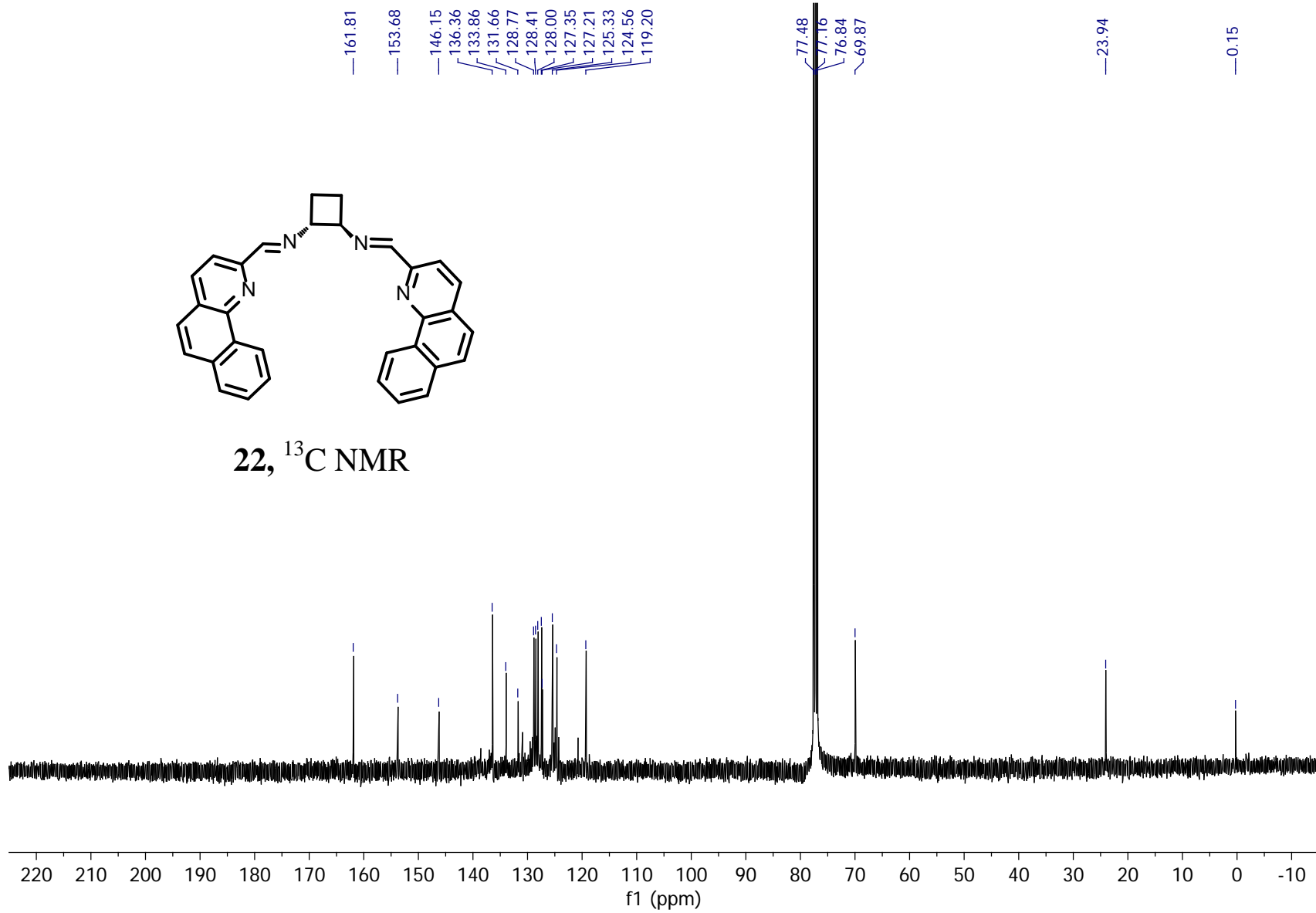
**21**,  $^{13}\text{C}$  NMR

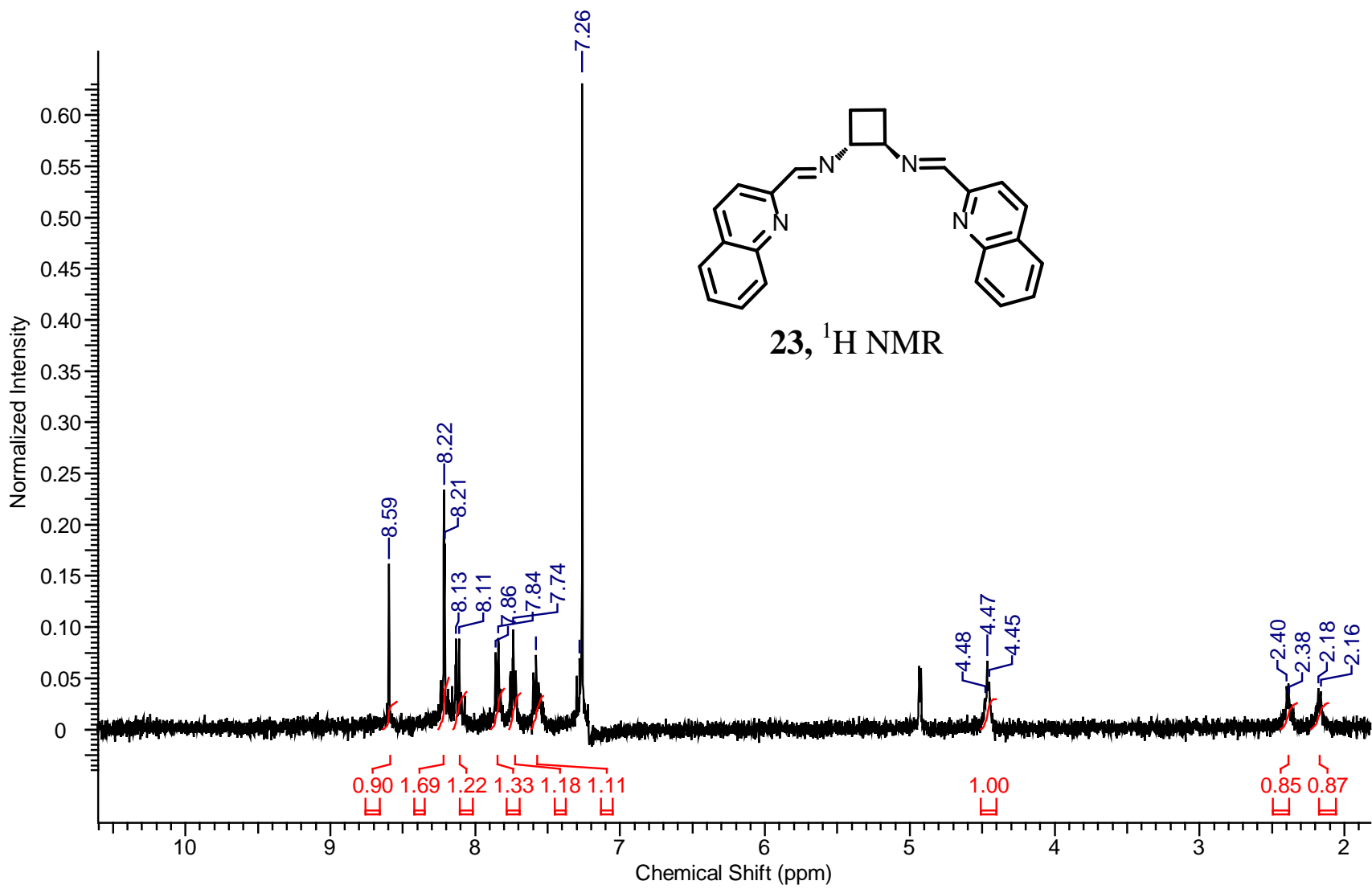


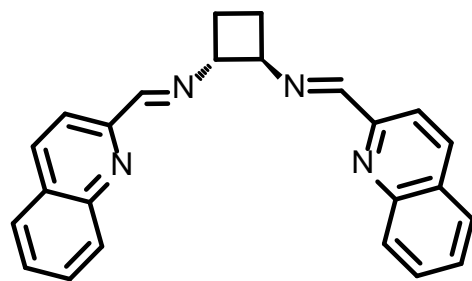




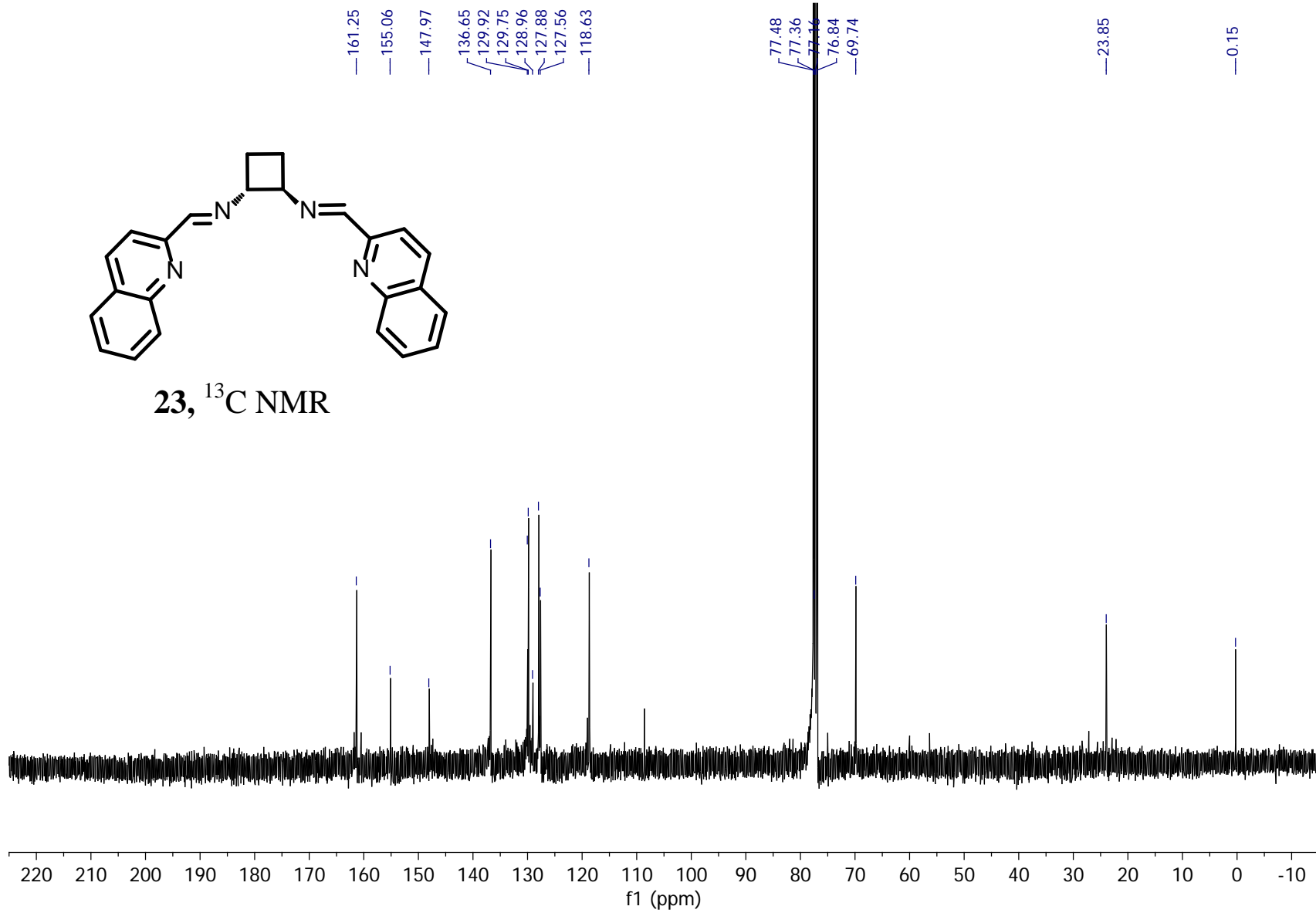
22,  $^{13}\text{C}$  NMR

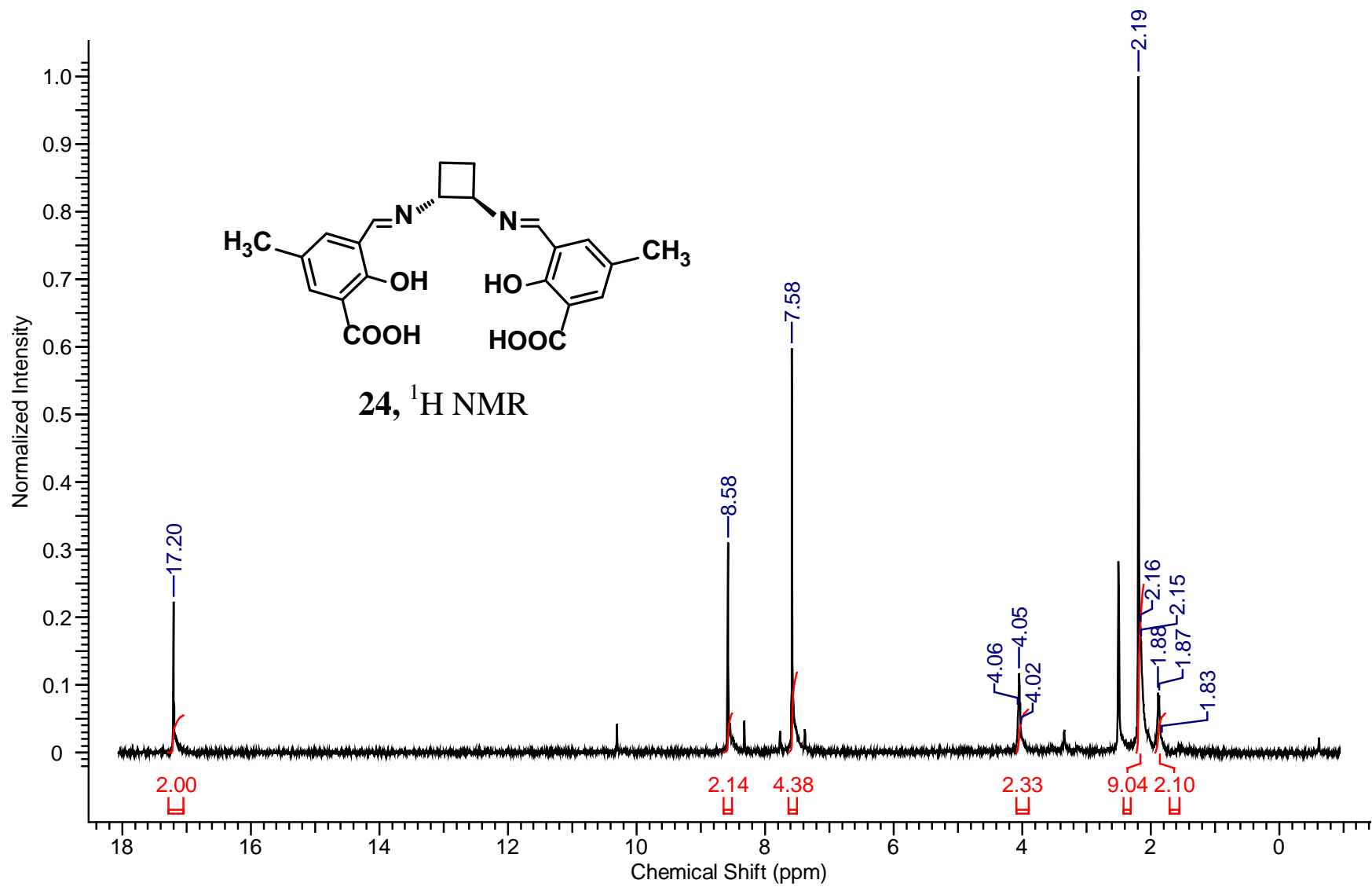


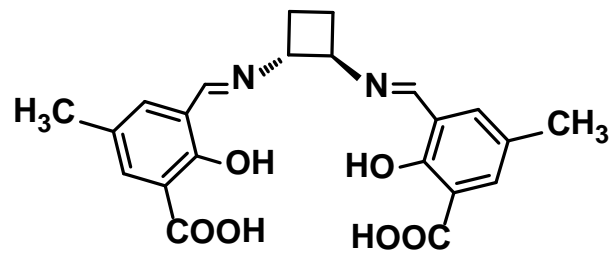




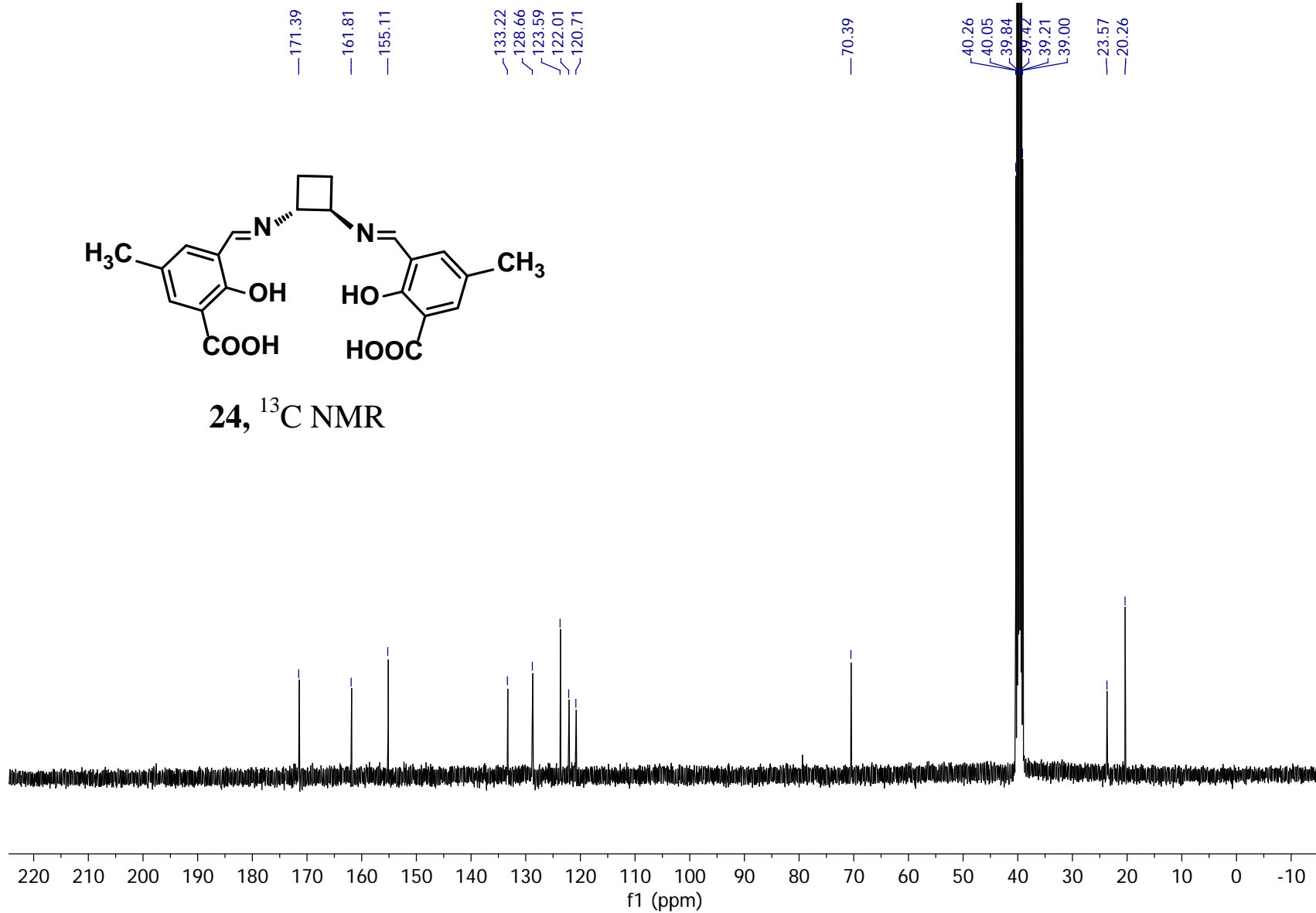
23,  $^{13}\text{C}$  NMR

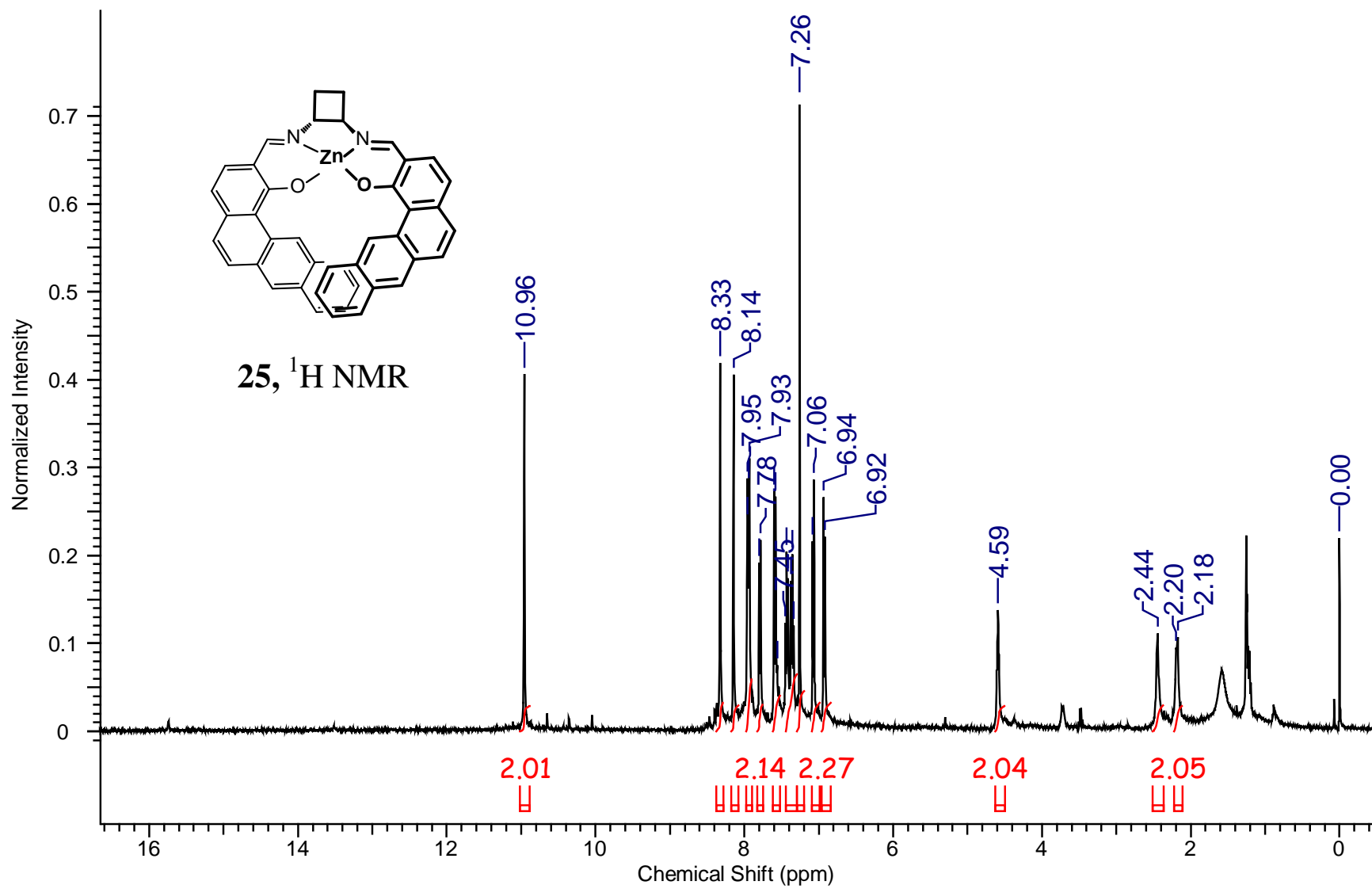




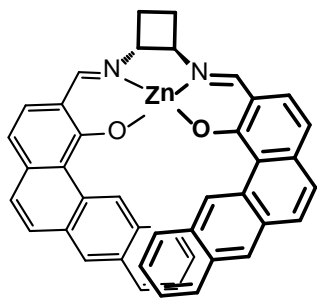


24, <sup>13</sup>C NMR

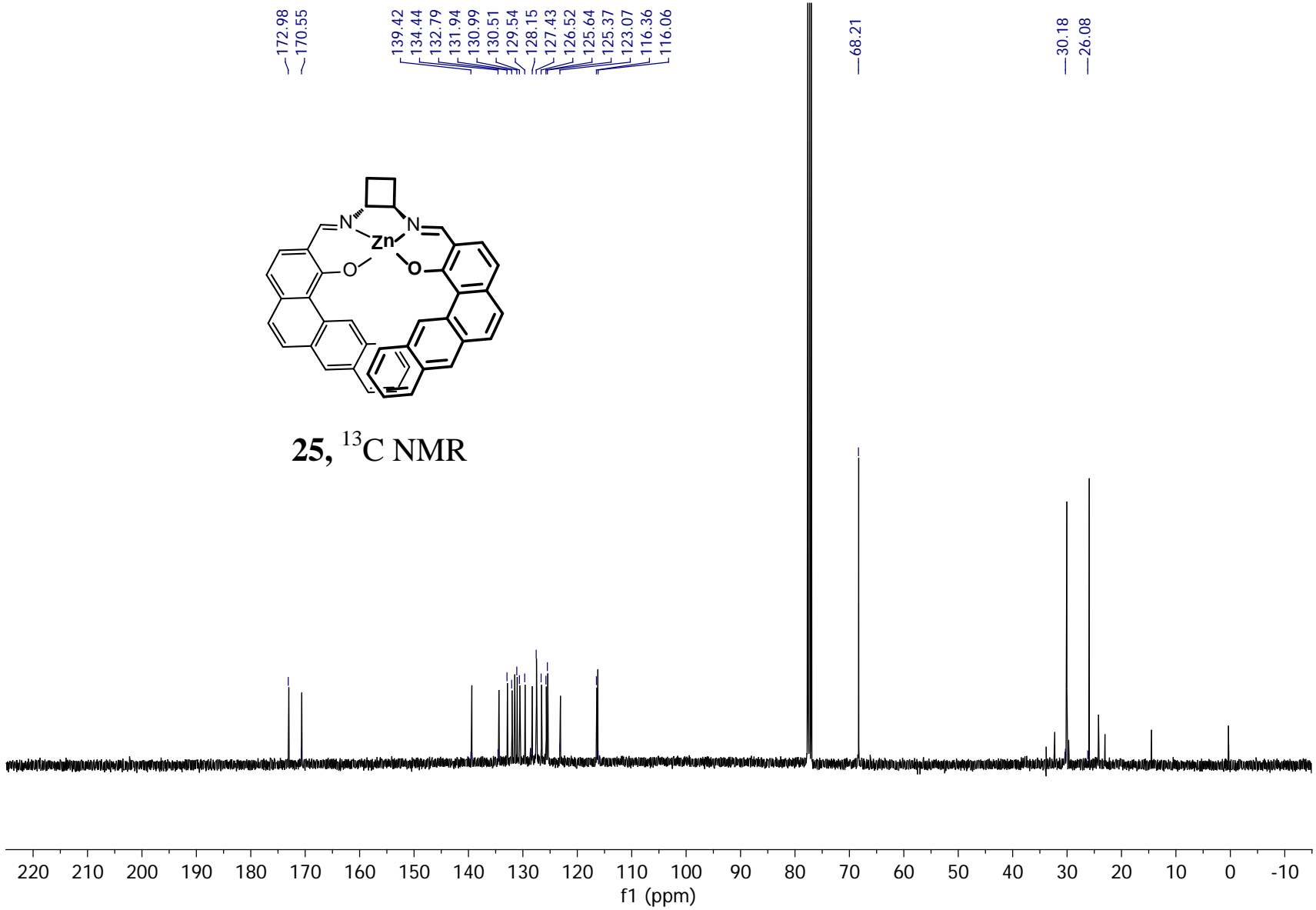


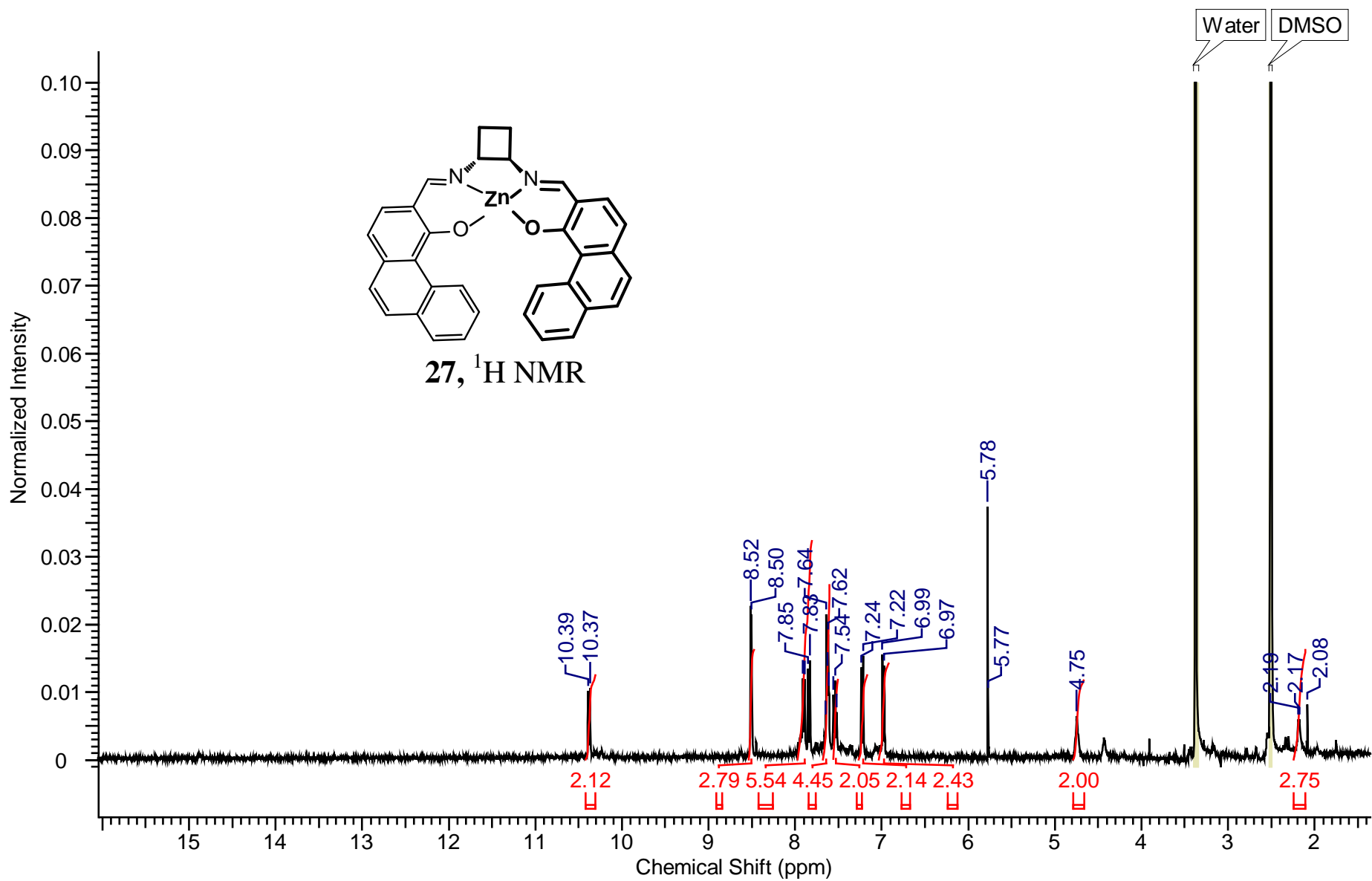


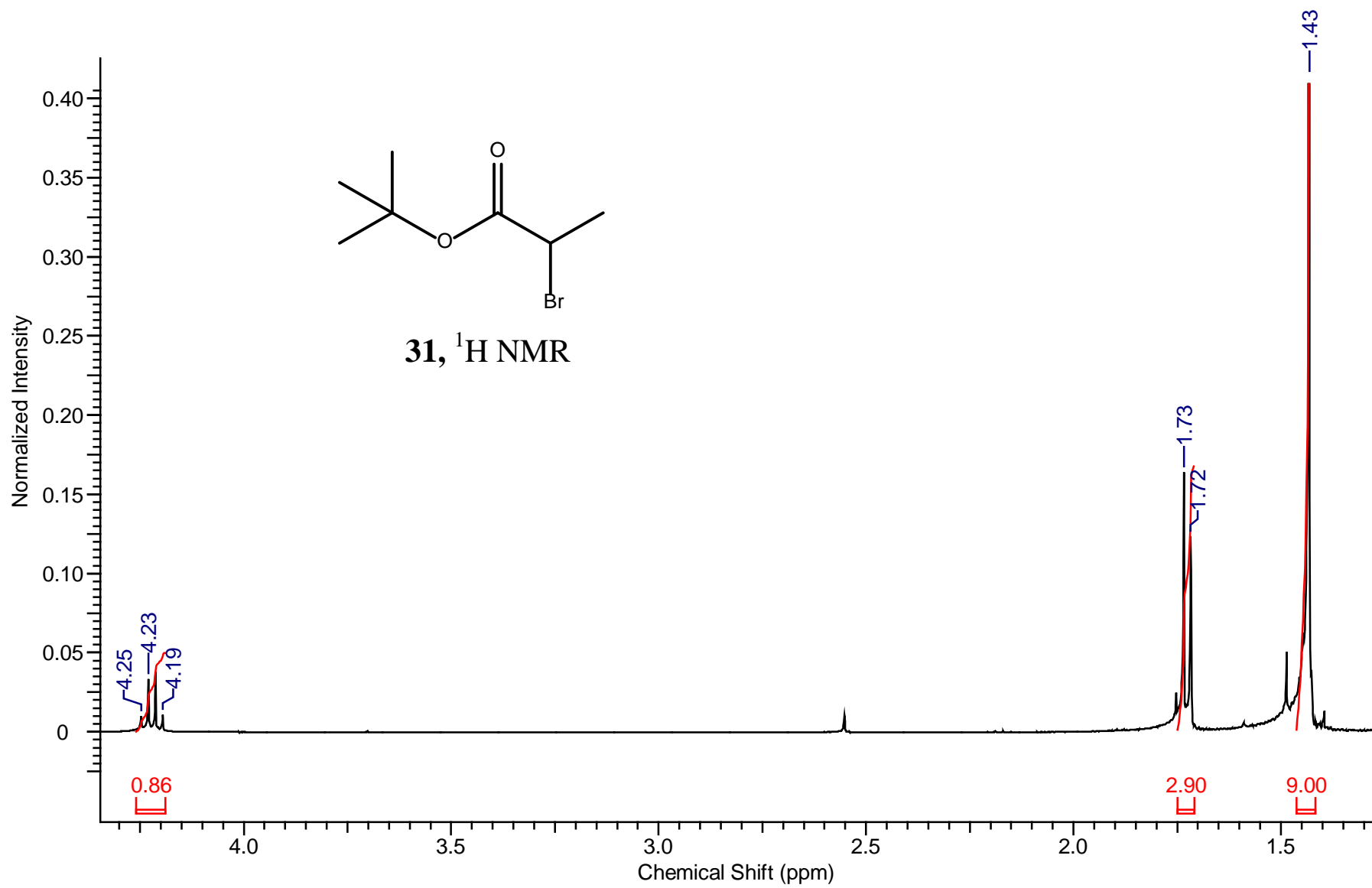
172.98  
 170.55  
 139.42  
 134.44  
 132.79  
 131.94  
 130.99  
 130.51  
 129.54  
 128.15  
 127.43  
 126.52  
 125.64  
 125.37  
 123.07  
 116.36  
 116.06

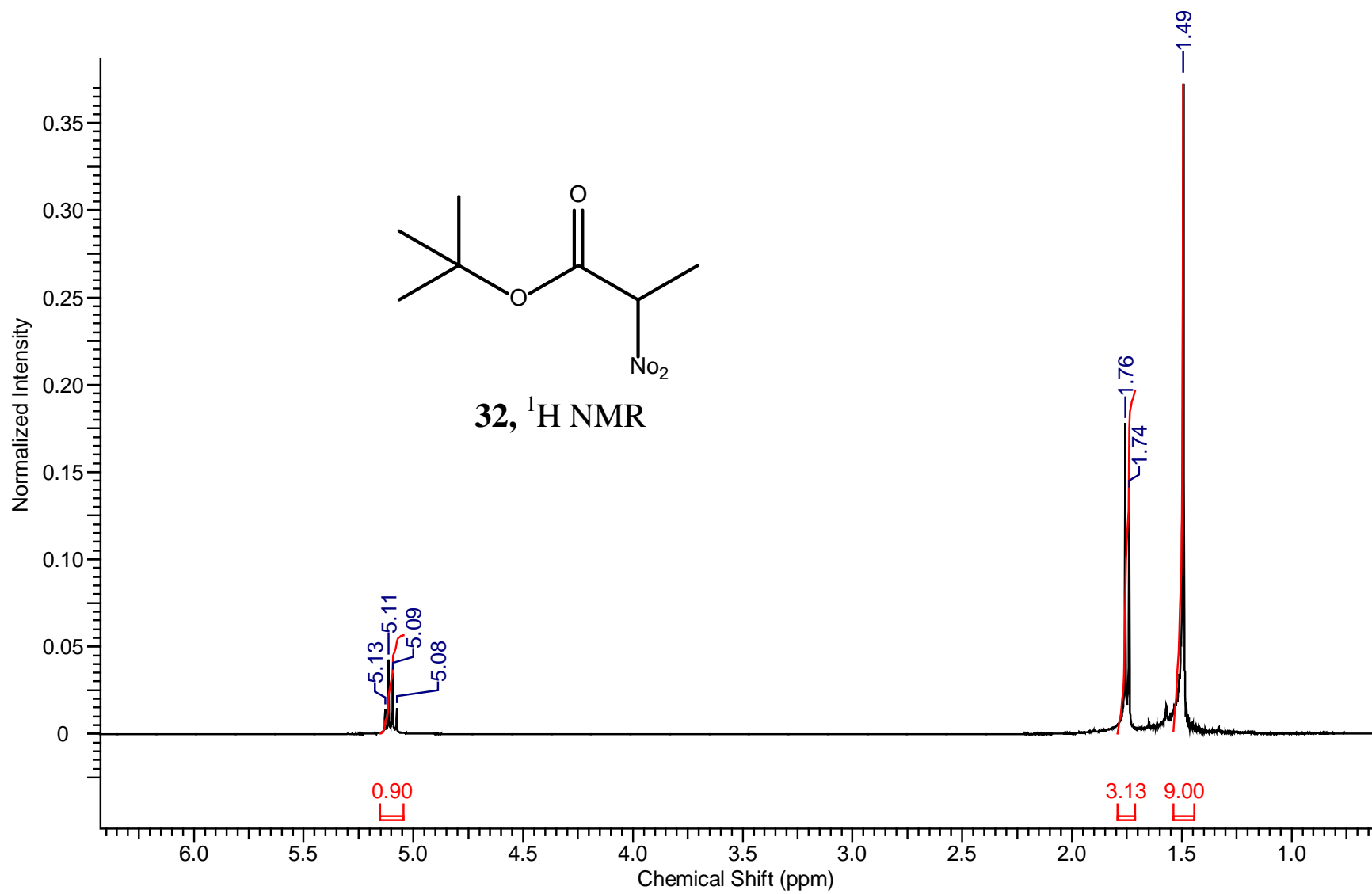


25, <sup>13</sup>C NMR

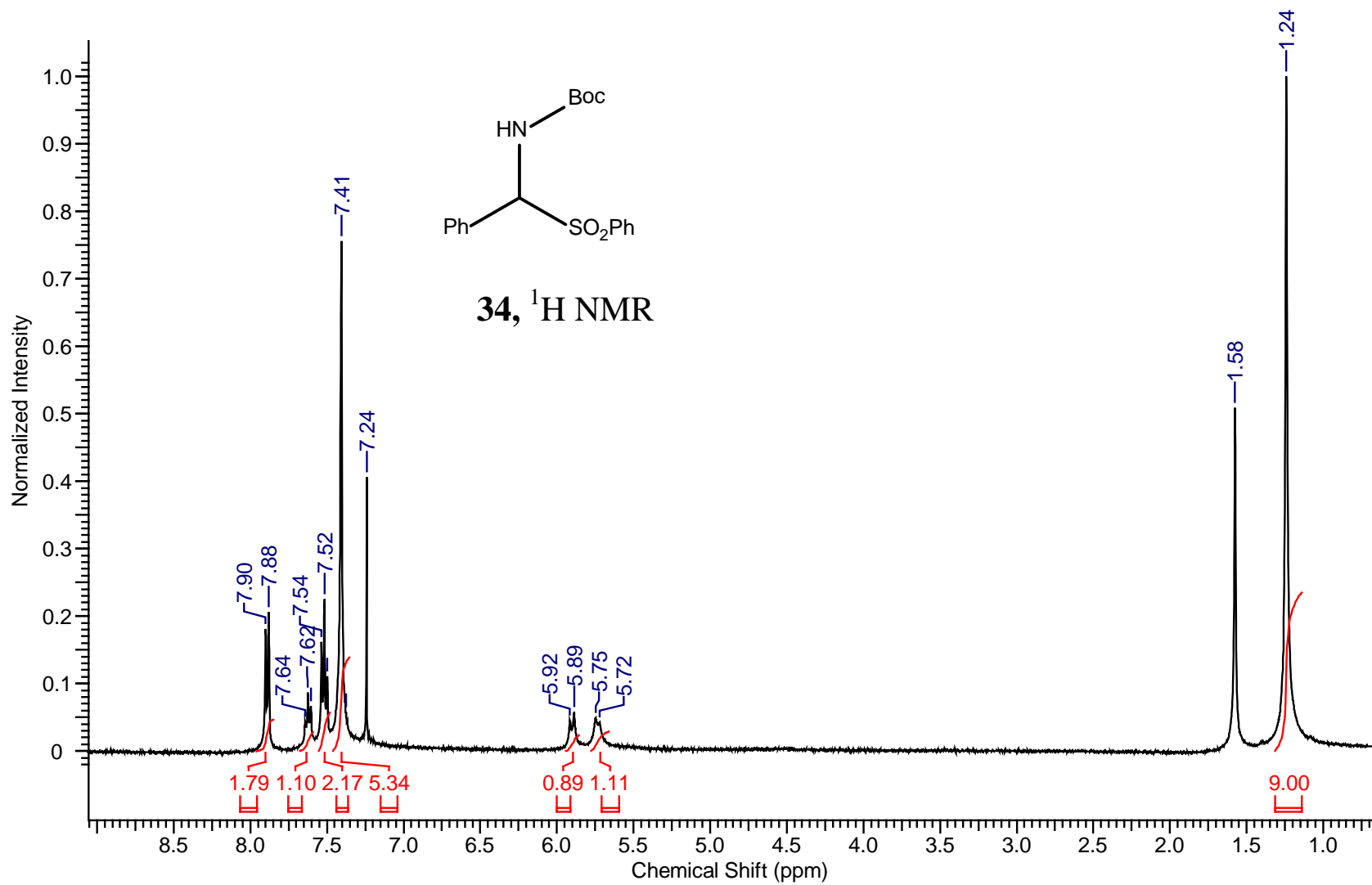


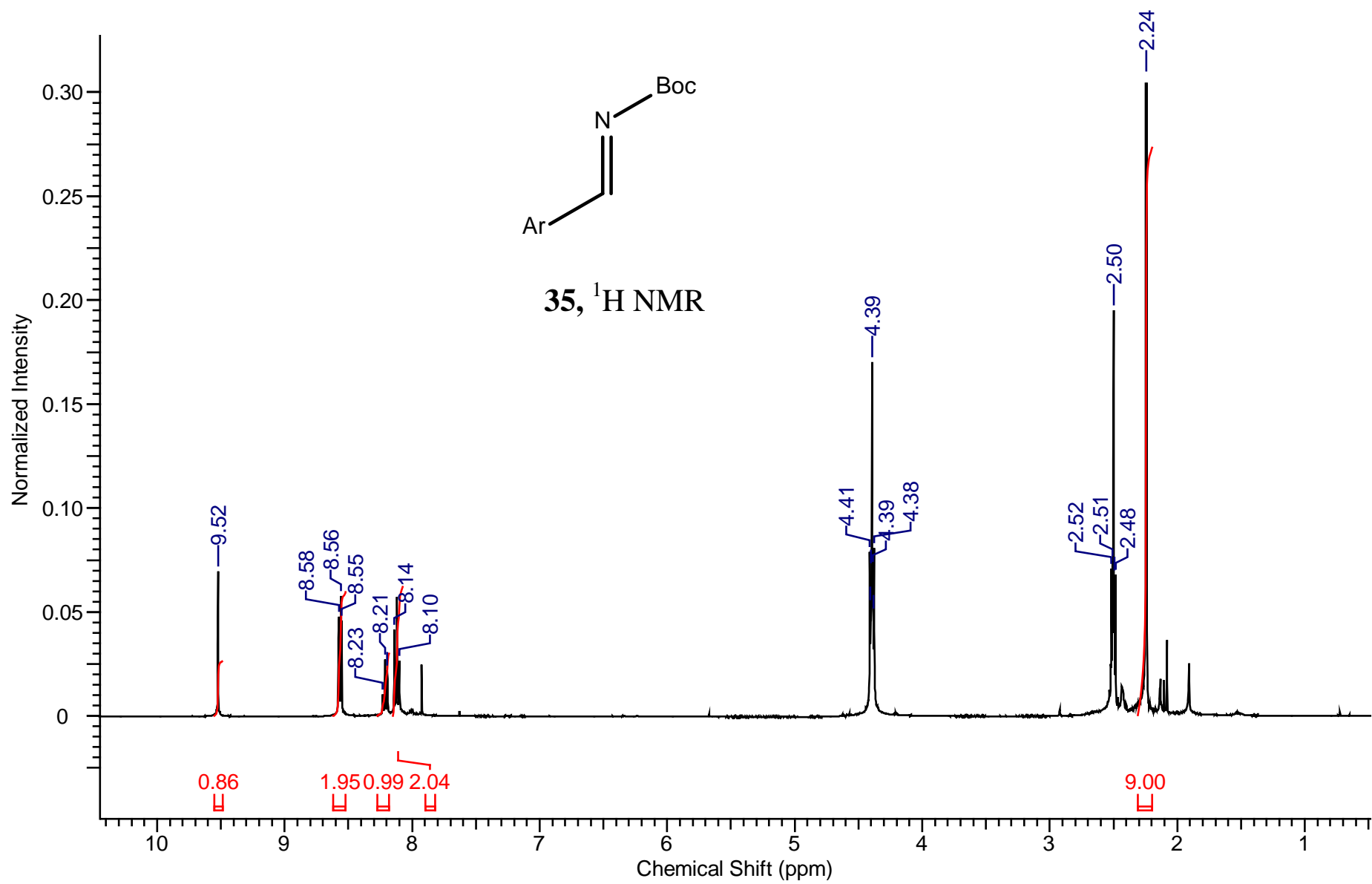


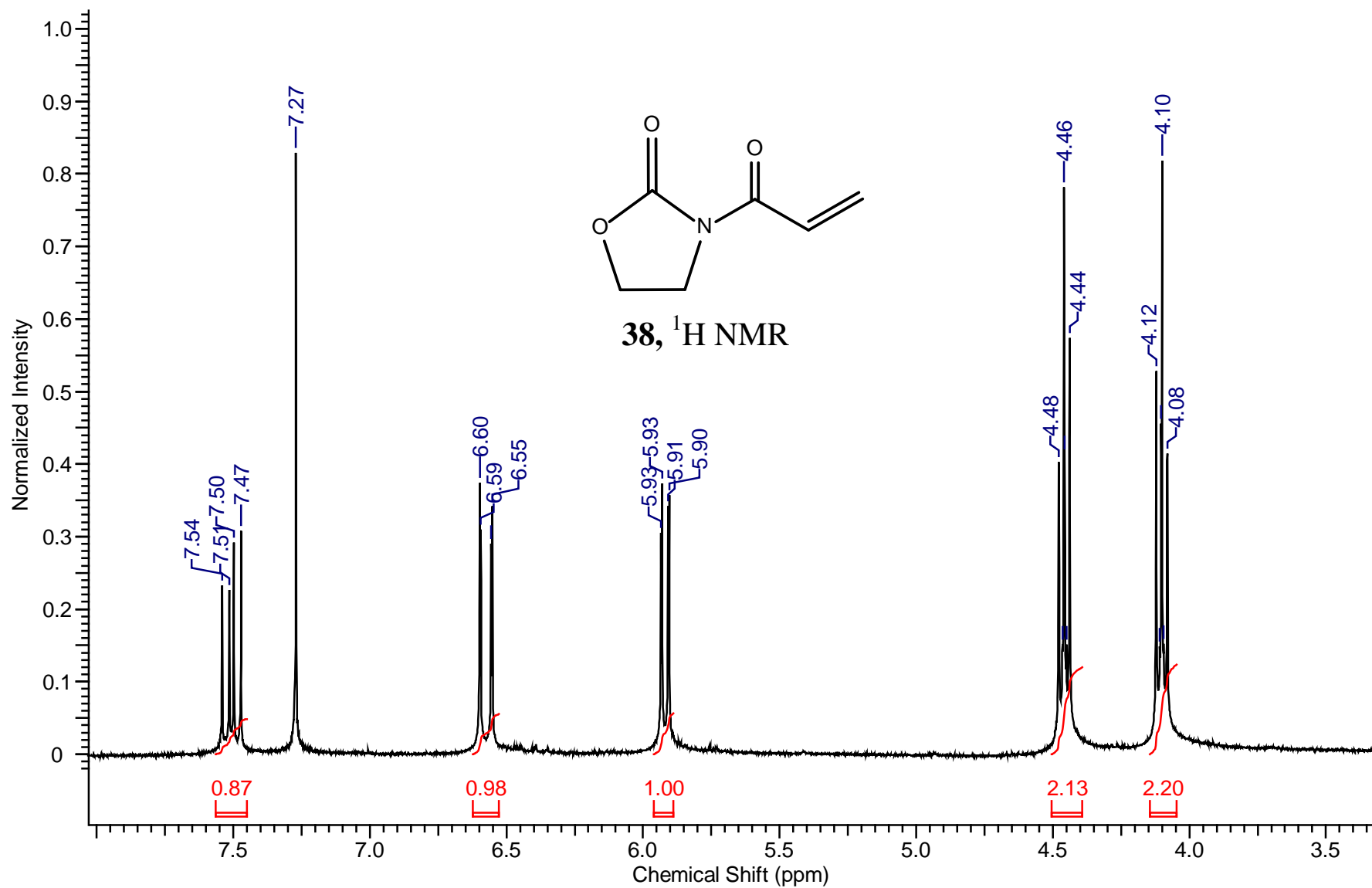


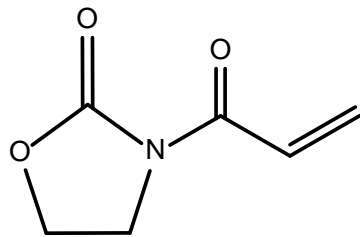












**38**,  $^{13}\text{C}$  NMR

